Analysis of the functional role of synaptic adhesion molecules in mouse neurons

Inaugural-Dissertation

zur Erlangung des Doktorgrades
der Mathematisch-Naturwissenschaftlichen Fakultät
der Heinrich-Heine-Universität Düsseldorf

vorgelegt von

Kim Nadine Pielarski
aus Essen

Düsseldorf, Oktober 2010

aus dem Institut für Neuro- und Sinnesphysiologie

der Heinrich-Heine-Universität Düsseldorf

Gedruckt mit der Genehmigung der

Mathematisch-Naturwissenschaftlichen Fakultät der

Heinrich-Heine-Universität Düsseldorf

Referent: Prof. Dr. K. Gottmann

Koreferent: Prof. Dr. C. Rose

Tag der mündlichen Prüfung:

Abstract

Sophisticated information processing in the brain requires highly specified neuronal circuits. Besides selective synapse formation, the specific elimination of inappropriate synapses is crucial for the complex wiring of unique networks. Based on its homophilic binding properties, matching pre- and postsynaptic N-cadherin is proposed to be a key player in synaptic recognition. Accordingly, the asymmetric expression of N-cadherin might be pivotal in the selective elimination of synapses. To experimentally address this hypothesis, single ES cell-derived neurons deficient for N-cadherin (Ncad-/-) were transfected with N-cadherin, leading to its expression postsynaptically. All presynaptic neurons still lacked N-cadherin, thus enabling the analysis of the effect of an asymmetric N-cadherin expression. Recordings of AMPA receptor-mediated miniature postsynaptic currents (mEPSCs) 48h after transfection revealed a significant defect in synaptic transmission, which could be demonstrated to be caused by disturbed presynaptic vesicle release. Putative candidate molecules for heterophilic interaction with N-cadherin are other classical cadherins. To study a cooperation with the postsynaptically expressed N-cadherin, antagonistic peptides specifically binding to the cadherin binding motif were applied. No effects of the peptides were observed in recordings of AMPA receptor-mediated mEPSCs, making an involvement of classical cadherins in the signaling pathway unlikely. In contrast, the addition of BDNF was shown to reverse impairment of synaptic transmission. Moreover, a dependence of BDNF-induced potentiation of synaptic activity on N-cadherin was found. However, using biochemical approaches (coimmunoprecipitation) no direct interaction between N-cadherin and the BDNF receptors TrkB or p75^{NTR} could be detected. As an impaired synaptic function may be a potential trigger for later synapse disassembly, immunocytochemical stainings for the vesicle protein VAMP2 were performed 8 days after transfection, revealing a reduced number of synapses. A detailed analysis including the distinction of synapses and autapses at later maturational stages was done by combining stainings (VAMP2) and cotransfections (PSD-GFP, N-cadherin, DsRed2-VAMP2), confirming in fact an elimination of synapses. Moreover, this elimination appeared to be accompanied by axon and dendrite retraction as shown by conditional N-cadherin knockout. Additionally, a cooperation of N-cadherin and neuroligin1 in modulating synaptic function was revealed via electrophysiological recordings of AMPA- and NMDA receptor-mediated currents.

Zusammenfassung

Für komplexe Hirnleistungen ist ein spezifisch verschaltetes neuronales Netzwerk essentiell. Dabei ist neben der selektiven Synapsenbildung insbesondere die spezifische Synapsenelimination unpassender synaptischer Partner ein wichtiger Faktor. Aufgrund der starken homophilen Bindung von prä- und postsynaptischen N-Cadherin Molekülen, wird N-Cadherin eine wichtige Rolle in der synaptischen Erkennung zugeschrieben. Folglich könnte die asymmetrische Expression von N-Cadherin eine ebenso entscheidende Funktion in der Elimination von Synapsen haben. Um dies zu überprüfen, wurden in der vorliegenden Arbeit einzelne N-Cadherin defiziente Neurone mit N-Cadherin transfiziert (postsynaptische Expression), während die präsynaptischen Zellen weiterhin kein N-Cadherin exprimierten. Somit war es möglich, die asymmetrische Expression von N-Cadherin hinsichtlich ihrer Auswirkung auf die Synapsenstabilität zu untersuchen. Die nach 48 Stunden gemessenen AMPA Rezeptor-vermittelten Miniatur-EPSCs bestätigten, dass in der Tat die synaptische Funktion beträchtlich eingeschränkt war. Als Ursache hierfür konnten Defekte in der präsynaptischen Vesikelfreisetzung festgestellt werden. Um zu überprüfen, ob andere klassische Cadherine als Kandidaten für eine Interaktion mit dem postsynaptischen N-Cadherin in Frage kommen, wurden Peptide, welche spezifisch an die Cadherin-Bindungsstelle von N-Cadherin binden, appliziert. Da diese Peptide keinen Einfluss auf die Beeinträchtigung der synaptischen Transmission hatten, konnten klassische Cadherine als Kooperationspartner ausgeschlossen werden. Im Gegensatz dazu bewirkte die Zugabe von BDNF, dass sich die synaptische Aktivität normalisierte. Überdies wurde eine Abhängigkeit der BDNF induzierten Potenzierung synaptischer Transmission von N-Cadherin festgestellt. Eine direkte Interaktion mit den BDNF Rezeptoren TrkB oder p75[NTR] konnte allerdings mittels biochemischer Methoden (Co-Immunopräzipitation) nicht bestätigt werden. Störungen in der synaptischen Transmission können ein Hinweis auf bevorstehende Synapsenelimination sein. Entsprechend zeigten Färbungen für das synaptische Vesikelprotein VAMP2 8 Tagen nach der Transfektion eine deutliche Reduktion der Synapsen. Eine detaillierte Analyse, welche eine Unterscheidung von Autapsen und Synapsen ermöglichte, bestätigte eine Synapsenelimination. Darüber hinaus konnte nach konditionalem Knockout von N-cadherin in einzelnen Neuronen eine Retraktion des Axon und der Dendriten festgestellt werden. Zusätzlich konnte eine Kooperation von N-cadherin und Neuroligin1 in der Regulation synaptischer Aktivität auf funktioneller Ebene durch die Analyse AMPA- und NMDA Rezeptor-vermittelter Ströme bestätigt werden.

Contents

1. Introduction

Nerve cells (neurons) of the central nervous system (CNS) serve as assimilation and propagation units for information. The CNS of mammals comprises $\sim10^{11}$ neurons, of which each exhibits $\sim10^{4}$ connections (synapses) to other neurons. Due to this networking system neurons are able not only to process information but also to send it throughout the entire organism. On the basis of different propagation associated with different morphologies a rough classification into electrical and chemical synapses can be made. While at electrical synapses the information in form of potential shifts can be spread bidirectional between two neurons, chemical synapses transmit unidirectional by presynaptic release of chemical messengers (neurotransmitters) and resulting postsynaptic responses in form of electrical signals. The wiring of neurons in the brain is very complex. Every neuron is specifically connected to other neurons propagating the information to the desired final location. Thus, the CNS is not made up of one network connecting all neurons, but rather of many smaller networks wired together for a special purpose. Hence, for developing connections neurons have to recognize other neurons as appropriate synaptic partners. For this target recognition cell adhesion molecules (CAMs), interconnecting two neurons, are suggested to be key players. Whether a synapse gets formed and subsequently stabilized or eliminated is regulated by the trans-synaptic CAMs, possibly by interplaying with neurotrophins.

1.1 Organization of chemical synapses

The signaling system of neurons consists of three different structures. Dendrites serving as postsynaptic elements receive the information and guide it to the soma of the cell. At the initial segment of the axon these signals account for the generation of action potentials subsequently conducted along the axon to its end, the presynaptic terminal, and thus to downstream connected neurons. The synaptic cleft between pre- and postsynaptic compartments plays an important role as many proteins ere embedded in the extracellular matrix filling the cleft. A synapse can be made in principle not only between axon and dendrite (axo-dendritic), which is the most common connection, but also between axon and soma (axo-somatic) and axon and axon (axo-axonic). The structure of a chemical synapse comprises the presynaptic terminal, the synaptic cleft (20-40nm width) and the postsynaptic density. Dependent on their morphology chemical synapses are divided into two different types. Excitatory, mainly glutamatergic, synapses comprise the Gray-type I synapses. This

type is especially characterized through more expanded structures in comparison to the second type, Gray-type II. The synaptic cleft is about 30 nm in width and the active zone, representing the site of presynaptic vesicle release, comprises ~1-2 μm^2. Likewise the "postsynaptic density" with a large number of scaffolding proteins is especially distinctive. In contrast Gray-type II synapses, comprising mainly inhibitory synapses, display synaptic clefts with a width of ~20 nm and active zones smaller than 1 μm^2.

1.1.1 The presynaptic terminal

Presynaptic boutons are expansions of the axon terminals and comprehend besides various proteins also mitochondria and vesicular structures containing the neurotransmitters. If an action potential reaches the presynaptic terminal it gets depolarized. Voltage-gated Ca^{2+}-channels open and lead to an inward directed Ca^{2+} flow into the terminal, thus increasing the intracellular Ca^{2+} concentration (Augustine et al., 1987). This increase is especially characterized by so called Ca^{2+}-microdomains that come up close to Ca^{2+}- channels on the cytoplasmatic side (10-200μM Ca^{2+} instead of values within the range of nm).

Based on this shift in Ca^{2+} concentration the entire signaling machinery resulting in the release of neurotransmitters from presynaptic vesicles into the synaptic cleft gets initiated. Presynaptic vesicles (~200; Schikorski and Stevens, 1997) can be divided into 3 groups characterized by their state of release ability and their location (Rizzoli and Betz, 2005). Docked at the active zone are the vesicles of the "readily releasable pool" (RRP), while vesicles of the "reserve pool" and the "resting pool" form clusters away from the active zone (Garner et al., 2000, Südhof, 2000). In mammalian central synapses the number of vesicles belonging to the RRP is quite limited (4-10 vesicles per active zone; Schikorski and Stevens, 2001; Rizzoli and Betz, 2005; Ryan and Smith, 1995; Harata et al., 2001). It was shown that this pool is able to fully recycle in less than 30 s (Ashton and Ushkaryov, 2005) dependent on the maximal steady-state rate for synaptic transmission, which involves the ability to retrieve used vesicles from the cell surface (Gandhi and Stevens, 2003). As the size of the RRP is not sufficient to maintain synaptic transmission under enhanced activity, the RRP can also be replenished by vesicles of the reserve pool, although the readily releasable vesicles can undergo multiple cycles of release without mobilization of the reserve pool (Ashton and Ushkaryov, 2005). Thus, both pools are active participants in the vesicle cycle (Südhof, 2000). The resting pool is normally not mobilized by synaptic activity and its role is not fully understood by now. Recent studies implicate a function in spontaneous release (Ben Fredj and Burrone, 2009) as was shown by demonstrating that vesicles retrieved for spontaneous and

activity-dependent release originate from distinct pools with limited cross-talk with each other (Yildirim et al., 2005).

The release of presynaptic vesicles is divided into several steps, called the synaptic vesicle cycle. Due to the binding of 5 Ca^{2+}-ions per (Schneggenburger and Neher, 2000; Bollmann et al., 2000; Wolfel and Schneggenburger, 2003) translocated vesicles dock at the plasma membrane of the active zone, which is the least understood mechanisms in the cycle ("docking"). After the "priming" step the vesicles fuse with the plasma membrane and release their content into the synaptic cleft. Synaptotagmin I, a vesicle-associated transmembrane protein is supposed to serve as activating Ca^{2+}-sensor (The C2A domain binds two Ca^{2+} ions, the C2B domain binds three Ca^{2+} ions; Urbach et al., 1998; Fernandez et al., 2001; Südhof, 2004; Geppert et al., 1997; Chapman, 2002). A change in the conformation of Synaptotagmin I results in activation of the so called SNARE-complex ("soluble N-ethylmaleimide-sensitive-factor [NSF]-attachment-protein-receptor-complex", core-complex), a complex made of various vesicle-associated proteins (Sabatini und Regehr, 1999; Fernandez-Chacon et al., 2001; Südhof, 1995; Hanson et al., 1997; Geppert et al., 1994; Bock und Scheller, 1999). It drives the approach of the vesicles into close apposition to the plasma membrane promoting lipid mixing finally leading to vesicle fusion (Hanson et al., 1997). The SNARE-complex is a 4 α-helices bundle of SNARE-proteins consisting of two proteins resident on the plasma membrane (syntaxin, SNAP-25; t-SNARE proteins) and one protein on the vesicle membrane (VAMP, vesicle-associated membrane protein, Synaptobrevin; v-SNARE). The formation occurs during priming of the vesicles (Chen and Scheller, 2001; Lonart und Südhof, 2000). An important role thereby fulfills nSec1/Munc-18/rbSec1 as Munc-18 binds to Syntaxin, another vesicle-associated protein, and leads to a blockage of the complexing. By phophorylation of Munc-18 via the proteinkinase C (PKC) activated by Munc-13 the Munc-18/syntaxin-complex gets disrupted, the configuration of Syntaxin I gets modified into an open configuration and the formation of the SNARE-complex is enabled (Betz et al., 1997; Fujita et al., 1995; Brose et al., 2000; Yang et al., 2000).

In addition to the above mentioned proteins there are much more involved in the regulation of vesicular trafficking. Until now there are nine families of proteins known. Rab3 for instance is suggested to be essentiell in vesicular docking by interacting with the plasma membrane-associated protein RIM1 (Rab3 interacting molecule 1; Rosenmund et al., 2003; Martelli et al, 2000). Synapsin I is present at almost every presynaptic terminal (DeCamilli et al., 1983; Huttner et al., 1983). It is suggested to cluster the vesicles of the reserve pool via an interaction with elements of the cytoskeleton (neurofilaments, actinfilament, microtubuli)

when being dephosphorylated. A phosphorylation by CaM Kinase II might accordingly lead to the mobilization of the vesicles towards the active zone and involvement in the active vesicle cycle (Bähler und Greengard, 1987; Llinas et al., 1991). The role of Synaptophysin I is also not clear by now. It could be shown to interact with VAMP in promoting its binding to SNARE partners at the plasma membrane. Thus it might be important for the fast recruitment of VAMP under enhanced synaptic activity. Another putative function is the regulating of activity dependent synapse formation (Tarsa and Goda, 2001).

After the vesicles have fused to the plasma membrane the membrane needs to be retrieved enabling a vesicular recycling. For this, dissolving of the SNARE-complex is required, which happens via the binding of NSF (N-ethylmaleimide sensitive factor) by dint of SNAPs (soluble NSF attachment-proteins) under ATP consumption (Whiteheart et al., 1994). Three modes of vesicle recycling are under discussion. The most controversial is called the "kiss-and-run"-fusion (Pyle et al., 2000; Stevens und Williams, 2000; Harata et al., 2006). Thereby the vesicles do not fuse completely with the plasma membrane, but rather a fusion pore is forming and subsequently closing after releasing the neurotransmitters. This mode of vesicle turnover is very rapid, because the vesicles are ready for another round just after reacidification via V-type ATPases and replenishment with new transmitters. The second mode is a much slower one in which the vesicles fuse completely with the plasma membrane. The recycling occurs by "clathrin-mediated endocytosis". The GTPase dynamin is thereby a key player. After binding of the vesicle membrane to the clathrin-structure (mediated by AP2 and AP180; Wakeham et al., 2000; Zhou et al., 1992) dynamin activates the GTP hydrolysis leading to a pinch-off of the clathrin-coated vesicles into the cytoplasm of the presynaptic terminal. Actin was shown to have a similar function as dynamin (Kochubey et al., 2006). After reacifidication, endosom fusion, budding and replenishment with neurotransmitters the vesicles are transported back to the active zone (Südhof et. al., 1995). It could be observed, that at synapses with a low release probability primarily the kiss-and-run mode is used, while at synapse with a high release probability the clathrin-mediated endocytosis dominates (Gandhi and Stevens, 2003). Recently it was proposed that function of dynamin in the fission of clathrin-coated vesicles might be restricted to high frequency events (Ferguson et al., 2007). The third possible way to recycle vesicles is "bulk endocytosis" appearing during high frequency stimulation (rewieved in Clayton et al., 2007). A large area of plasma membrane is endocytosed independently from clathrin-mediated endocytosis. Endosomes develop from which synaptic vesicles bud and remain attached to the plasma membrane until another pulse

is initiating the reintegration (Gad et al., 1998; Stevens und Gandhi, 2003). Subsequent to the closure of the fusion pore an immediate replenishment of transmitters could be observed (Pyle et al.; 2000, Stevens und Williams, 2000; Südhof, 2000).
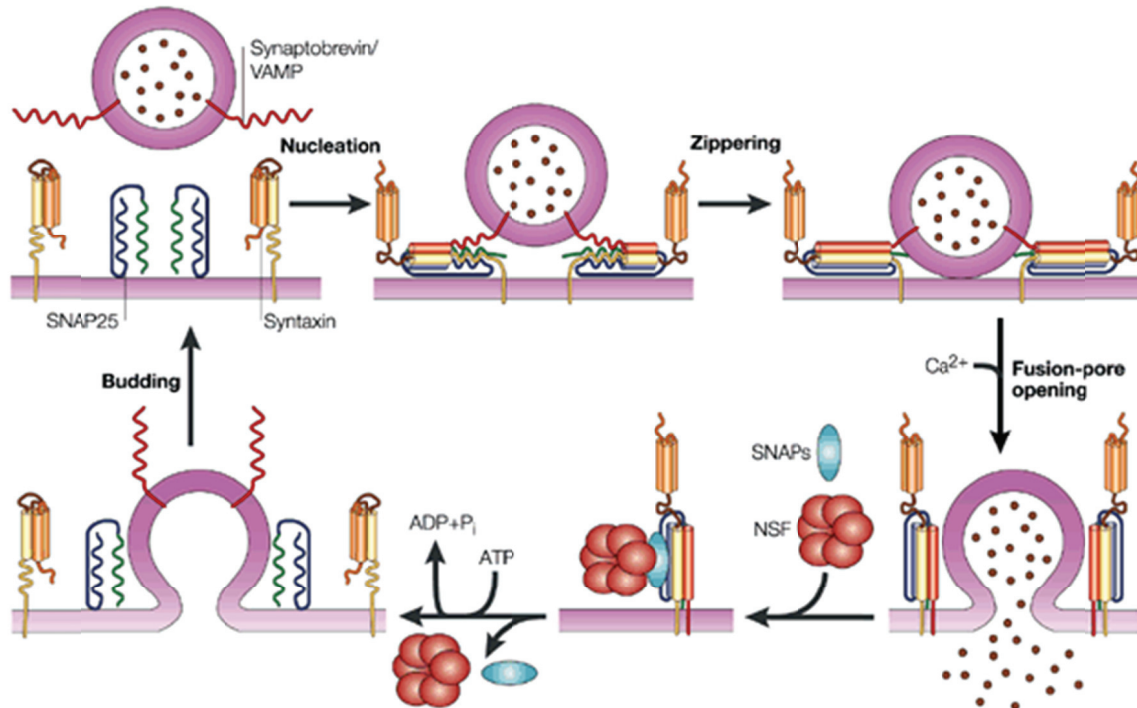
Fig.1.1 The synaptic vesicle cycle.
(after Rizo and Südhof, 2002) Schematic illustration of the synaptic vesicle cycle. A change in the conformational state of Syntaxin allows priming of the vesicles and subsequent assembly of the SNARE-complex, consisting of Syntaxin, SNAP25 and Synaptobrevin/VAMP. After fusion N-ethylmaleimide-sensitive fusion protein (NSF) and soluble NSF-attachment proteins (SNAPs) mediate disassembling of the complex.

1.1.2 Postsynaptic specializations

The postsynaptic site is precisely apposed to the presynaptic terminal. It is characterized by the postsynaptic density, a large protein network composed of ion-channels, receptors, adhesion molecules, filamentous proteins, signaling molecules and enzymes sticked together by scaffolding proteins like PSD-95 (postsynaptic density protein 95 kDa) and SynGaP (synaptic GTPase activating protein) (Kornau et al., 1995; Sheng, 1997).

After being released in the synaptic cleft the neurotransmitters bind specifically at the transmitter receptors integrated in the postsynaptic membrane. Ionotropic receptors (ligand-gated ion channels) are coupled directly to an ion channel, which opens as response to the binding of neurotransmitters and subsequently mediates an ion flow over the membrane. Dependent on the properties of the channel this results in a depolarizing (EPSP, excitatory

postsynaptic potential) or hyperpolarizing (IPSP, inhibitoriy postsynaptic potential) potential in the postsynaptic cell. The important ionotropic receptors are the glutamate receptors, the GABA$_A$-receptor and the nicotinic acetylcholine receptor. Metabotropic receptors are not coupled directly to an ion channel, but they modulate other proteins in a stimulating or inhibiting way. Due to G-protein (GTP-binding protein) activation they are able to initiate intracellular signaling cascades triggering numerous activities (Gasic und Hollmann, 1992; Nakanishi, 1994).

Interestingly, the modulation property through receptor binding occurs not restricted to the postsynaptic neuron. Via transsynaptic signaling several morphogenetic or functional changes (e.g. vesicle release probability) at the presynapse can be retrogradely initiated in the postsynaptic compartment. These transsynaptic modulations can be triggered by secreted factors or directly through mediators like CAMs. An interaction between an AMPA receptor subunit (GRIA2) and the cell adhesion molecule N-cadherin for instance was observed to stimulate presynaptic development and dendritic spine formation (Saglietti et al., 2007). The extracellular domain of Neuroligin expressed postsynaptically was also demonstrated to modulate the presynaptic site by interacting with presynaptically expressed β-neurexin (Comoletti et al., 2007). An increase in synaptic response occurred, which was likewise associated with a potentiated ratio of NMDA/AMPA receptors (Chubykin, 2007). As postsynaptic scaffolding proteins are able to interact with and affect receptors or CAMs (PSD-95/NMDAR Niethammer et al., 1996; S-SCAM/Neuroligin Stan et al., 2010) they serve not only for keeping the PSD together, but they are rather shown to be a major player in modulating synaptic function.

1.2 Organization of glutamatergic synapses

As fast excitation is almost exclusively mediated by ionotropic glutamate receptors (Kristensen et. al., 2006) one of the most important excitatory neurotransmitter is L-glutamate. Glutamate is not only part of the neuronal system, but also involves the glia cells in close proximity. Specific glutamate transporters take it up from the synaptic cleft and convert it to glutamine under ATP-consumption. Back in the presynaptic terminal this gets converted to glutamate again.

1.2.1 Ionotropic glutamate receptors

The ion channel opening after activation of ionotropic glutamate receptors is selective for kations (Hollmann und Heinemann, 1994; Dingledine et al., 1999) thus resulting in an EPSC. 18 different receptor subunits could be found composing three different types of glutamate receptors (Hollmann und Heinemann, 1994): AMPA (α-amino-3-hydroxy-5-methyl-4-isoxazolpropionat-) receptors permeable for K^+ and Na^+, kainite receptors permeable for K^+ and Na^+ and NMDA (N-methyl-D-Aspartat-) receptors permeable for K^+, Na^+ and Ca^{2+} (Lodge and Johnson, 1990; Watkins et al., 1990). 4 identical or diverse subunits form tetramers with 3 transmembrane and 1 hydrophobic domain each (Hollmann et al., 1994). The AMPA receptors are composed of GRIA1-4, kainate- receptors are made up of GRIA5-7 and GRIK4-5 and NMDA receptors form tetramers of GRIN1 and GRIN2A-D subunits (Hollmann und Heinemann, 1994). Recent studies demonstrate distinct opening mechanism for different types of glutamate-receptors (Kristensen et al., 2006).

AMPA and NMDA receptors are found to be mainly localized at cortical synapses (Bekkers und Stevens, 1989; McBain und Dingledine, 1992). The most striking property of AMPA receptors is their fast kinetics. The rise time takes just a few ms in contrast to the rise time of NMDA receptors (10-20ms). The decay time is likewise much faster with 8-10 ms in contrast to more than 100 ms for NMDA receptors (Forsythe und Westbrook, 1988; Sanson und Usherwood, 1990; Bekkers und Stevens, 1989; Edmonds et al., 1995). The number and targeting of AMPA receptors seems to be regulated by the expression level of certain scaffolding proteins (Stein et al., 2003; Ehrlich and Malinow, 2004; Elias and Nicoll, 2007). The protein stargazin was shown to be a linker interacting with AMPA receptors and with a PDZ-domain of PSD-95 (Chen et al., 2000; Schnell et al., 2002; Bats et al., 2007). Other neuronal cell types express homologous of stargazing, referred to as transmembrane AMPA receptor regulatory proteins (TARPs).

NMDA receptors play a crucial role in synaptic plasticity. As the ion channel connected with these receptors is also permeable for Ca^{2+}, Ca^{2+} ions flow into the cell when the channel is opened. This influx initiates signaling cascades mediating some forms of synaptic plasticity (long-term-potentiation LTP, long-term-depression LTD) to modulate synaptic connections permanently (Bliss und Collingridge, 1993; Malenka und Nicoll, 1993). Due to a blockade of the channel pore at negative potentials (~ - 65 mV) with Mg^{2+}, NMDA-receptors can only be activated during simultaneous activity at the presynaptic cell and depolarization of the postsynaptic cell. A postsynaptic depolarization subsequently entails the electrostatic

repulsion of Mg^{2+} ions clearing the channel and enabling an ion flow when being activated by transmitter binding to the receptor. Because of this special feature NMDA receptors are called "coincidence detectors".

Another form of synaptic plasticity at the mossy fibers of the CA3 region of the hippocampus has been shown to be independent from NMDA-receptors. Here kainite receptors seem to be the regulation unit. Additionally a function in the direct modulation of excitatory and inhibitory transmission could be demonstrated (Bortoletto et al., 1999, Watkins und Jane, 2006), as shown for CA3>CA1 synapses. Interestingly, via direct presynaptic action kainite receptors are supposed to depress excitatory synaptic transmission (Freking et al., 2001). However, a metabotropic action was also proposed to be involved.

1.2.2 Metabotropic glutamate receptors

The main function of metabotropic glutamate receptors was found in modulation processes and synaptic plasticity. Structurally the metabotropic glutamate receptors are made up of 7 transmembrane domains. Three groups of metabotropic glutamate receptors can be classified (Conn und Pinn, 1997). Group I consists of the receptors GRM1 A-D and GRM5 A-B, Group II comprises GRM2 and GRM3 and Group III involves GRM4A-B, GRM6, GRM7A-B and GRM8 A-B (Schoepp et al., 1999; Watkins und Jane, 2006). Group I was found mainly at excitatory synapses, both other groups depress glutamate release and therefore inhibit the synaptic response (Watkins und Jane, 2006). Through latter, both excitatory and inhibitory postsynaptic potentials are reduced (Chu and Hablitz, 2000).

The binding of glutamate has no direct effect on synaptic potentials. Instead, the metabotropic glutamate receptors are coupled to a heterotrimeric G-protein initiating numerous signaling cascades, which involves the regulation of second messenger levels. Subsequently to binding and under conversion of GDP to GTP the α-subunit of the receptor-coupled G-protein dissolves from β- and γ-subunits and activates or inhibits, respectively, a primary effector enzyme like phospholipase C (group I) or adenylatecyclase (group II and III). In this way a regulation of second messenger levels like inositol 1,4,5-triphosphate (IP_3; group I) or cyclic adenosine monophosphate (cAMP; group II and III) takes place affecting the modulation and modification of various proteins. $InsP_3$ for instance stimulates the release of Ca^{2+} from intracellular stores (endoplasmatic reticulum and/or mitochondria), which activates the PKC catalyzing the phosphorylation of numerous target proteins.

1.3 Synaptic cell adhesion molecules

The proper assembly of synapses is essential for efficient synaptic transmission. Neuronal cell adhesion molecules are transmembrane proteins expressed on both sites of the synaptic cleft that connect two associated neurons through the direct interaction of their extracellular domains. Thereby the stability of the synapse gets improved, thus enhancing interactions between proteins of the extracellular matrix among each other or with CAMs. But the CAMs do not only mechanically link pre- and postsynaptic membrane, but rather serve as molecular bridge between both cells regulating pre- and postsynaptic functions.

One of the most important functions is the target recognition of appropriate synaptic partners, where adhesion molecules are supposed to constitute a molecular code on the cell surface representing its properties. The selective wiring of specific neurons enables the formation of distinct neuronal subpopulations as well as targeted synapse formation like axo-dendritic spine synapses. Important functions were likewise found in the regulation of pre- and postsynaptic differentiation after initial contact of two neurons, in the modulation of synaptic function, cell motility and other aspects of synaptogenesis (Yamagata et al., 2003; Washbourne et al., 2004).

Based on morphological and functional properties the CAMs are divided into numerous families that have a multitude of diverse members. The superfamily of cadherins, which includes classical cadherins, protocadherins and cadherin related neuronal receptors (CNR) is characterized by the presence of one or more cadherin repeats in their extracellular domains and their mediated Ca^{2+}-dependent adhesion. Other important CAMs are members of the Immunoglobulin-superfamily or the intergins (Yamagata et. al., 2003). The Neuroligin-family is restricted to the postsynaptic site and was found to modulate pre- and postsynaptic processes by its ligand neurexin at the presynaptic site.

1.3.1 Neural (N)-cadherin

Neural (N)-cadherin is the most prominently expressed member of the classic cadherins in the brain representing a type I cadherin. It is characterized through 5 extracellular tandemly repeated domains (EC1-EC5) consisting of 110 amino acids each, anchored via a single-pass transmembrane domain in the plasma membrane and a cytoplasmatic tail (100 amino acids). The extracellular domains serve for distinct roles. The first two domains were suggested to be responsible for adhesion activity, while the role of the other domains is supposed to be found in promoting adhesive efficiency by positioning the essential domains relatively far from the

cell surface (Shan et al., 2004). The extracellular repeats are separated by Ca^{2+}-binding sites, coordinated via interdomain linker and flanking residues (Nagar et al., 1996; Patel et al., 2006; Fig. 1.2).

For proper transsynaptic adhesion with another molecule at the opposite plasma membrane a cis-dimerization of two adjacent N-cadherin molecules has to take place (Brieher et al., 1996). This dimerization is Ca^{2+}-dependent and is carried out between EC1 and EC2 (Pokuttka and Weiss, 2007). Two cis-dimerized molecules then interact to form transsynaptic associations involving only EC1 domains (Tomschy et al., 1996; Koch et al., 1996; Koch et al., 1997, Pertz et al., 1999; Patel et al., 2003). Key structure for both cis- and trans-interaction is putatively the HAV motif within the EC1 domain (Shapiro et al., 1995; Tamura et al., 1998). The binding motif as well as the amino acids immediately flanking, including the INP motif, are supposed to be unique for every cadherin and therefore define its specificity (Nose et al., 1990; Williams et al., 2000). N-cadherin is especially characterized through strong transsynaptic homophilic binding, although heterophilc cis-interactions with R (retinal)-cadherin (Shan et al., 2000) as well as the possible heterophilic binding with E (epithelial)-cadherin or C-cadherin (Prakasam, 2006) could be shown. However, cell aggregation experiments demonstrated aggregations of cells with the same cadherin expression, while cells expressing distinct cadherins separated from each other (Nose et al., 1990; Duguay et al., 2003).

A　　　　　　　　　　　　　　　　　　　　**B**
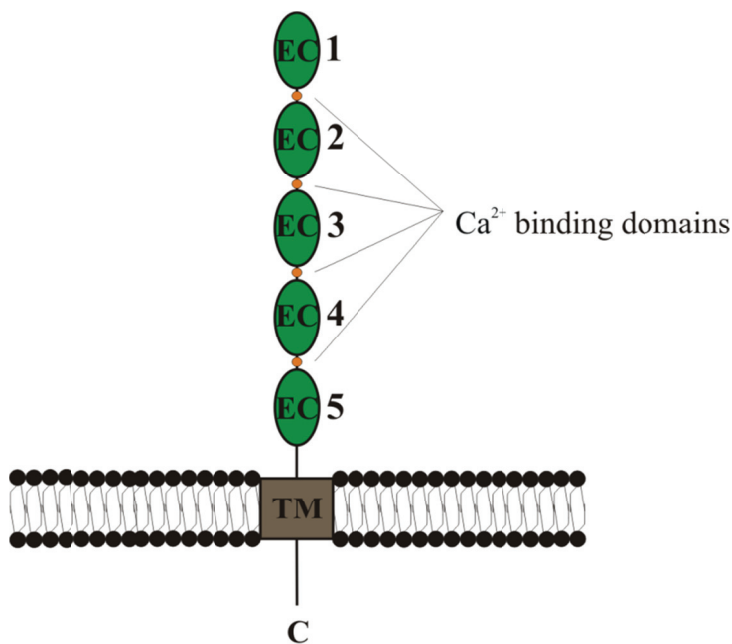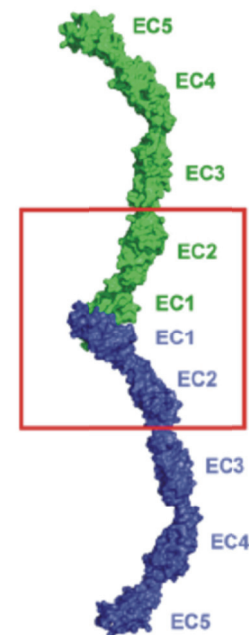
Figure 1.2 Schematic illustration of N-cadherin and its homophilic binding to other N-cadherin molecules
A Ilustration of N-cadherin: C: cytoplasmatic domain; TM: transmembrane domain; EC: extracellular domain **B** (after Katsamba et al., 2009) Pre-and postsynaptically localized N-cadherin molecules are connected through a strong homophilic binding carried out by their EC1 domains. Cis-dimerization involves EC1 and EC2 domains.

In addition to the unique extracellular domain of N-cadherin there is a highly conserved cytoplasmatic tail. It contains binding sites for catenins, which provide an indirect link to the actin and intermediate cytoskeleton (Kemler and Ozawa 1989; Sappert and Kemler, 1994; Takeichi, 1990; Aberle et al., 1994; Barth et al., 1997; Halbleib and Nelson, 2006). N-cadherin is directly interacting with β-catenin/γ-catenin (plakoglobin), which forms a complex with α-catenin, the linkage to actin. These interactions are not static bridges. When β-catenin is dephosphorylated by the protein-tyrosine phosphatase PTP-1B an interaction with N-cadherin is taking place. In its phosphorylated form β-catenin was shown to play a crucial role in the wnt-signaling. Wnts are secreted glycoproteins, which signal through their frizzled (fz) receptors. For the wnt canonical pathway it could be shown that by G-protein activation a signaling cascade is initiated, which results in the translocation of β-catenin to the nucleus, where it activates the transcription of certain target genes (for review see Ciani and Salinas, 2005). Also the binding of α-cateinin is not as static as believed. The monomeric form binds β-catenin, while when being in a dimeric state F-actin is the preferred interaction partner, thus regulating the actin stabilization very dynamically (Balsamo et al., 1998; Yamada et al., 2005; Drees et al., 2005). An indirect linkage via α-catenin binding to the actin-binding protein eplin is discussed (Abe and Takeichi, 2008). p120-catenin is another protein associated with N-cadherin proximal to the β-catenin binding site and suggested to stabilize N-cadherin at the cell surface by regulating proteins of the Rho family of GTPases and the maintenance of β-catenin through recruitment of a protein tyrosine phosphatase, dephosphorylating β-catenin. (Reynolds and Carnahan, 2004, Xu et al., 2004). δ-catenin, restricted to the postsynaptic area, has additional implications for N-cadherin function, as it binds to PDZ-domain proteins in the scaffolding web of the postsynaptic density (Kosik et al., 2005). It was shown to interact with presenillin-1 (PS-1), suggested to play a role in the trafficking of N-cadherin to the plasma membrane (Uemura et al., 2003).

N-cadherin is synthesized from a precursor molecule (Pro-N-cadherin; Ozawa and Kemler 1990). Whether the cleavage that activates the adhesive function occurs already in the rough endoplasmatic reticulum (Koch et al., 2004) or after the transport to the cell surface (Fields, 2006) is still discussed. An inactive N-cadherin at the cell surface might act as dominant-

negative form, suppressing N-cadherin-mediated adhesion during early development and therefore regulating the kinetics of synaptogenesis (Latefi et al., 2009).

N-cadherin expression was shown to occur in specific patterns, supporting the theory of serving as adhesive code for axon guidance and selective formation of neuronal circuits (Redies et al., 1993; Obst-Pernberg et al., 2001). N- and E-cadherin for instance were found to be expressed at hippocampal synapses in an exclusive manner (Fannon and Coleman, 1996). Thereby N-cadherin was shown to be expressed initially at all synaptic sites, whereas in later maturational stages it gets restricted to excitatory synapses (Benson and Tanaka, 1998). On the level of individual synapses N-cadherin was also shown to be differentially expressed with maturational stage. At early development it was found evenly distributed throughout the active zone, while at later stages it appeared clustered perisynaptically bordering the active zone and the PSD (Benson and Tanaka, 1998; Elste and Benson, 2006). At the same time the expression level seems to be rather dynamic (Thoumine et al., 2006). Especially β-catenin and p120-catenin are supposed to be key players thereby. A retrieval of cadherins from the plasma membrane due to for instance growth factor signaling and subsequent endocytosis affects the adhesive state of synapses and might regulates aspects of cell motility, cell fate, tissue morphogenesis and tumorigenesis (for review see Delva and Kowalczyk, 2009). NMDA receptor activity seems to be another decisive aspect for N-cadherin endocytosis (Tai et al., 2007).

The regulatory processes N-cadherin is involved in are very widespread. In knock-out studies N-cadherin mutant embryos died around embryonic day 10 because of dramatic abnormalities in the development of myocardial tissue (Radice et al, 1997). A conditional knock-out of N-cadherin in the cerebral cortex was found to completely randomize the organization of the cytoarchitecture (Kadowaki et al., 2007). One of the most important functions is proposed to be proper axon targeting enabling selective connections with appropriate synaptic partners. Especially the strong homophilic binding seems to be crucial for this. It could be demonstrated that when N-cadherin is blocked by specific antibodies, the thalamic fibers that physiologically grow into the cortical layer IV of the somatosensoric cortex fail to terminate there and instead grow further until layer II (Huntley and Benson, 1999). In earlier maturational stages the ingrowth itself could be attenuated by using N-cadherin blocking agents (Poskanzer et al., 2003). Although this experiments demonstrate a decisive role in synaptogenesis, the persistence of N-cadherin expression in later maturational stages led to the proposal that an importance in remodeling of the synaptic structure cannot be excluded. In

fact it was shown that N-cadherin (in cooperation with β-catenin) is crucial for the organization of presynaptic specializations, like presynaptic vesicle clustering (Togashi et al., 2002; Murase et al., 2002; Bamji et al., 2003; Bozdagi et al., 2004; Stan et al., 2010). N-cadherin is likewise important in postsynaptic processes. In numerous experiments a pivotal role in spine formation and spine morphogenesis could be demonstrated. The knockdown of N-cadherin resulted in filopodia-like dendritic spines, which at the same time was accompanied by a decreased density (Togashi et al., 2002; Saglietti et al, 2007). Stable dendritic spine enlargements in mature stages as well require N-cadherin function (Bozdagi et al., 2010). N-cadherin/β-catenin recruitment to synapses which was suggested to be associated with the recruitment of AMPA receptors may thereby affect spine morphology (Nuriya and Huganir, 2006). N-cadherin-mediated dendrite growth and maintenance of dendritic arbors was proposed to require the association with the actin cytoskeleton (Tan et al., 2010), which is supposed to be regulated by α- and p120-catenin via modulation of Rho-family GTPases (Reynolds, 2007).

Another important role has been suggested in synaptic plasticity. In N-cadherin deletion experiments the short-term plasticity of glutamatergic synapses was dramatically altered (Jüngling et al., 2006). Similary the persistence of LTP at CA1 synapses in the hippocampus is dependent on N-cadherin expression (Bozdagi et al., 2010).

1.3.2 Neuroligin

The neuroligin family of cell adhesion molecules is characterized through a large extracellular domain, a single-pass transmembrane domain and a cytoplasmatic tail. The extracellular domain, responsible for adhesion, consists of several domains, like a cleaved signal peptide, a cholinesterase-like domain and a carbohydrate attachment region. Contrary to cholinesterases neuroligins lack an active serine site, making them catalytically inactive (Ichtchenko et al., 1995). Instead this domain is thought to support the receptor/ligand like adhesion by mediating the required dimerization of two adjacent neuroligin molecules (for review see Lisé and El-Husseini, 2006). The cytoplasmatic tail contains a PDZ-binding motif, enabling the interaction with molecules made up of class I PDZ-domains like PSD-95. The intracellular region is less conserved compared to the transmembrane or extracellular domain, thus suggesting that it might be responsible for localization and/or function of the distinct neuroligins (Ichtchenko et al., 1996). Neuroligin1 and neuroligin2 are the best characterized members of the neuroligin family. While neuroligin1 is specifically localized at excitatory

synapses, neuroligin2 is expressed at inhibitory synapses (Song et al., 1999; Varoqueaux et al., 2004)

The expression of neuroligins is restricted to the postsynaptic site. The members of the neurexin-family expressed in the presynaptic membrane serve as heterophilic adhesion partners. Through alternative splicing numerous isoforms of neurexins are expressed, divided into two classes: α- and β-neurexins. The N-terminal region contains a unique sequence, while transmembrane and cytoplasmatic domains are common to α- and β-neurexins (Missler et al., 1998). The cytoplasmatic region of neurexins contains similar to neuroligins a PDZ-binding motif for class II PDZ-domains. Neuroligin-1 binds to β-neurexins, but only if they lack an insert in a specific splice site (Ichtchenko et al., 1995). A heterotetramer results made up of two β-neurexin monomers binding to two identical sites on the opposite face of one neuroligin-1 dimer (Araç et al., 2007). The complex probably occurs in the center of the synaptic cleft.

First experiments showed that neuroligins expressed in non-neuronal cells were able to induce presynaptic specializations in contacting axons of co-cultured neurons (Scheiffele et al., 2000). A role for Neuroligin1 in the maturation of presynaptic terminals was likewise demonstrated (Wittenmayer et al., 2009). Similarly, the neuroligin/neurexin system was shown to induce postsynaptic specializations (Graf et al., 2004; Chih et al., 2005). A closer look gave rise to a proposed pivotal role in synaptic transmission rather than in initial synapse formation. Knock-out mice for neuroligin1-3 are lethal because of impaired synaptic transmission, whereas synapse numbers remained unaltered (Varoqueaux et al., 2006). In specifying and validating synapses via an activity-dependent mechanism different neuroligins were found to act on distinct types of synapses (Chubykin et al., 2007).

An interaction through the PDZ-binding domain of both neuroligin and neurexin with numerous intracellular proteins is thereby decisive. Presynaptically, the interaction of neurexin with CASK is important (Mukherjee et al., 2008) and enables the nucleation of actin to neurexin (Biederer and Südhof, 2001). CASK was found to be coupled with multiple other proteins like MINT and Veli or CASPRs indicating a putative function in propagating the signals transmitted transsynaptically via neuroligin/neurexin to regulate presynaptic actions like the release machinery (Butz et al., 1998). Postsynaptically, PSD-95 is one of the most important proteins for communicating with the neuroligin/neurexin complex. The expression of both was shown to regulate the ratio of excitatory-to-inhibitory synapses (Prange et al., 2004). Furthermore this interaction might be involved in the recruitment of various proteins like AMPA/NMDA receptors, K$^+$-channels and signaling proteins (Irie et al., 1997).

Neuroligin1 was very recently found to be accumulated by N-cadherin via a linkage through the scaffolding molecule S-SCAM leading to presynaptic vesicle clustering (Stan et al., 2010). Besides neurexin-dependent functions also neurexin-independent functions of neuroligin1 for synapse induction were discussed (Ko et al., 2009).

1.4 Neurotrophins

The secreted neurotrophins (NTFs) consist of four structurally distinct factors: nerve growth factor (NGF), brain-derived neurotrophic factor (BDNF), neurotrophin-3 (NT-3) and neurotrophin-4 (NT-4). All neurotrophins are synthesized as large proneurotrophins (30-34kDa) that associate as homodimers (Radziejewski et al., 1992; Kohlbeck et al., 1994). By proteolysis homodimeric neurotrophins are generated. Interestingly, also regulatory processes in which proneurotrophins are involved were found.

Neurotrophins interact with two distinct receptor types: $p75^{NTR}$ and Trk (tropomyosin receptor kinases), from which three Trks (TrkA, TrkB, TrkC) can be distinguished (for review see Frade and Barde, 1998; Rodriguez et al., 1998; Huang and Reichardt 2003; Reichhardt, 2006). All Trk proteins share a common conserved subdomain organization inclusive two immunoglobulin like domains in the extracellular region and a tyrosine kinase domain in the cytoplasmatic region. Alternative splicing encodes additionally for truncated isoforms of Trk receptors. Although these truncated forms lack a large part of the cytoplasmatic tail, including the tyrosine kinase domain, they are putatively involved in various signaling cascades. The interaction of proneurotrophins is restricted to $p75^{NTR}$, while mature neurotrophins are generally able to bind both types, but exhibit a higher affinity for the interaction with the three Trk receptors. Moreover, each mature neurotrophin features a specific affinity for one of these. During binding of mature neurotrophins Trk receptors dimerize, resulting in activation through transphosporylation of the kinase in their cytoplasmatic domain. By this means the attachment of small adaptor proteins that activate multiple signal cascades is enabled. Contrary p75 receptors get not dimerized and catalytic activity is missing. A direct interaction with other molecules activates several cascades (for review see Reichhardt, 2006, Kaplan and Miller, 2000).

Neurotrophins participate in numerous processes. According to their affiliation to the family of growth factors mature neurotrophins were shown to be key players in promoting neuronal survival, differentiation and neurogenesis. Furthermore a pivotal role in axon outgrowth and synaptic plasticity could be demonstrated (Lessmann et al., 1994; Levine et al., 1995; Lewin

and Barde, 1996; Wang and Poo, 1997; Li et al., 1998). Proneurotrophins/p75^{NTR} signaling was found to have effects that oppose those of mature neurotrophins.

1.4.1 The BDNF/TrkB/p75^{NTR} system

The activity dependent transcription of BDNF gets activated due to cytoplasmatic Ca^{2+}-dependent kinase cascades (Tao et al., 1998; Tao et al., 2002; Chen et al., 2003). TrkB serves as receptor for mature BDNF, whereat proBDNF binds to p75^{NTR}. Both receptors were found to be pre- and postsynaptically located. Recent studies implicate a release from mature neurons of both, proBDNF and BDNF (Yang et al., 2009).

BDNF has various important functions in neuronal physiology. For instance, it is a decisive player in synaptic plasticity. Mature BDNF was shown to promote hippocampal LTP through TrkB, while proBDNF triggered the enhancement of hippocampal LTD through p75^{NTR} (for review see Reichhardt, 2006). In addition, experiments confirmed a crucial role in the regulation of neuronal survival (Lee et al., 2002). BDNF/TrkB supports the survival of neurons and BDNF/p75^{NTR} induces apoptosis when Trk signaling is absent (Casaccia-Bonnefil et al., 1996; Frade et al., 1996; Bamji et al., 1998). Furthermore, other studies revealed an important function in the modulation of synaptic transmission. The application of BDNF to hippocampal cultures induced the formation of excitatory and inhibitory synapse and enhanced synaptic activity (Lessmann et al, 1994; Levine et al., 1995; Vicario-Abejon et al., 1998; Li et al., 1998; Kafitz et al., 1999; Schuman, 1999). Moreover, the maturation of pre-and postsynapse is dependent on BDNF (Bolton et al., 2000; Marty et al., 2000). The BDNF-mediated potentiation was demonstrated to rely on presynaptic modulations (Li et al., 1998). More recent results also suggested a ligand-independent signaling through full length-TrkB receptors that are able to negatively influence glutamatergic synaptic strength, if the ratio of BDNF/TrkB is not balanced (Klau et al., 2001). Furthermore, BDNF has been found to enhance neurogenesis (for review see Binder and Scharfman, 2004).

Truncated TrkB receptors were shown to have a dominant negative effect on BDNF signaling (Eide et al., 1996). The truncated isoform TrkB.T1 for instance was shown to control Ca^{2+} release from intracellular stores required for BDNF transcription via G-protein activation in astrocytes (IP3 pathway, Rose et al., 2003). A regulation of the formation of dendritic filopodia in hippocampal cultures by the same truncated isoform could be shown (Hartmann et al., 2004).

A monodirectional interference is discussed when p75^{NTR} and TrkB are coexpressed. Experiments showed that p75^{NTR} is able to suppress ubiquitination of TrkB, therefore

delaying its internalization and degradation and promoting TrkB signaling. A contrary paper demonstrated a p75^{NTR} driven support of TrkB endocytosis (for review see Reichhardt, 2006). Furthermore a reduction of TrkB autophosphorylation initiated by p75^{NTR} was reported (Vesa et al., 2000).

Although p75^{NTR} is suggested to induce apoptosis of neurons, it was also shown to promote axon elongation in mice carrying a mutation in the p75 gene. Furthermore, these opposite effects were shown be mediated by activation of RhoA when being unliganded and by inactivation of RhoA by BDNF binding (Yamashita et al., 1999).

1.5 Selective synapse assembly and elimination

Signaling among all neurons in the CNS without pattern and selectivity would end up in a chaotic state. To constitute functional neuronal circuits unique sets of neurons have to be wired together with appropriate synaptic partners. Therefore neurons should be enabled to precisely send their axons into remote target areas and even select particular domains on the postsynaptic cell to form a synapse. Axon pathfinding events depend on multiple mechanisms, including labeling of synaptic partners, coordinated axon and dendrite guidance cues and elimination of inappropriate synapses. But not only the cell-cell-contact has to be defined, moreover synaptogenesis is ascertained by the induction of pre- and postsynaptic differentiation and maturation. It should be mentioned that also dendritic growth cones were observed to initiate synaptic contact (Sabo et al., 2006), but this will not be further discussed here.

In order to sense guidance cues the tip of the axons is specialized by means of exhibiting a growth cone, able to receive and process signals. Two mechanisms were described acting from close or remote origin. The first happens via contact of receptors in or on the membrane of the growth cone with ligands on other neurons or extracellular matrix proteins. Secondly, secreted molecules from remote areas are able to serve as cues by binding to receptors on the growth cone membrane. Both mechanisms affect axon guidance by supporting the elongation via attraction of the growth cone or sending repulsive signals (for review see Tessier-Lavigne and Goodman, 1996). Elongation of the axon is enabled through actin-based motility. The growth cone is composed of two distinct populations of F-actin-filaments: parallel, long and bundled filaments radiated from and into filopodia and branching short filaments filling the volume between dorsal and ventral membrane surfaces (lamellipodia), both of them differentially orientated in polarity (Lewis and Bridgman, 1992). The bundled filaments are in

the proximal portion of the growth cone associated with microtubules growing along the filopodia (Tanaka and Sabry, 1995; Schäfer et al., 2002). Guidance cue initiated actin polymerization at the leading edge or depolymerization in proximal regions of individual filopodia in specific areas of the growth cone as well as the rate of F-actin flow define extension, stabilization or retraction of the axon and therefore the direction of elongation and repulsion, respectively. Similarly, cues that stabilize or capture microtubule ends are involved in this process.

Individual guidance cues can serve as attractants and repellants. Important secreted cues are the Netrins. They were shown to attract axons from interneurons in the spinal cord to the floor plate if the growth cone is expressing a specific receptor (DCC-receptor; deleted-in-colorectal-cancer). However, at the same time, when being complexed within the cytoplasmatic domain with another receptor (UNC-5), netrins mediate repulsion (Hong et al., 1999; Huber et al., 2003). Conformational changes enabling the complexion might be initiated by netrin binding.

Similar multifunctional cues are the members of the Slit family (Brose et al., 1999; Li et al., 1999; Wang et al., 1999). Their receptors belong to the Roundabout (Robo) family of receptors (Huber et al., 2003).

The semaphorins represent another major group of guidance cues. Some members are secreted; others are cell-membrane bound. Most of the semaphorins have repulsive effects on axons, but also attractant mechanisms were observed (Bagnard et al., 1998; Wong et al., 1999; Cheng et al., 2001). As receptors serve plexins and neuropilins, able to complex when liganded by distinct semaphorins (semaphorins class 3; plexin A; neuropilin-1 and-2; He and Tessier-Lavigne 1997, Kolodkin et al. 1997, Takahashi et al. 1999, Tamagnone et al. 1999). Neuropilins seem to have only co-receptor function, as they do not appear to propagate signaling (Dickson et al., 2002). Other proteins were shown to constitute to the plexin receptor complexes, such as the adhesion molecule L1 and the receptor tyrosine kinases Met and OTK (drosophila) (Dickson et al., 2002; Huber et al., 2003).

Although still discussed neurotrophins are suggested to serve among other functions as guidance cues. Signaling through both receptor types (Trk, $p75^{NTR}$) was observed to interfere with transduction pathways mediating axon attraction and repulsion. Furthermore, neurotrophins were shown to modulate the responsiveness of growth cones to other guidance cues. NGF and semaphorin 3A for instance seem to indirectly interact in regulating sensory growth cone motility (Dontchev and Letourneau, 2002). Another interconnection was observed as neuronal cultures growing in the presence of BDNF are more sensitive to

semaphorine3A (Tuttle and O`Leary, 1998; Hubert et al., 2003). Moreover, in recent studies it was suggested that the cooperation between semaphorin3A and the neurotrophins regulate the balance between apoptosis and survival (Zvi et al., 2006).

The ephrins are membrane-attached and therefore are a group of contact-dependent guidance cues (Cheng et al., 1995; Drescher et al., 1995). Their receptors, the eph tyrosine kinases, are divided into two subclasses: EphA and Eph B, each responsible for the binding of ephrin-As and -Bs, respectively (Huber et al., 2003). In the visual system EphA/ephrins-A were found to have repulsive effects on axons (anterior-posterior), while EphB/ephrins-B attract them (dorso-ventral) (Hindges et al., 2002). Interestingly, EpH/ephrin complexes were found to transduce the signal bidirectional, known as "forward" and "reverse" signaling (Huber et al., 2003).

Furthermore, contact-dependent cell adhesion molecules have been discussed to be important in navigating the growth cone in a contact-dependent manner. Three major groups, the immunoglobulins, integrins and cadherins, seem to guide axons through their specific hetero- or homophilic interactions with ligands in the extracellular matrix or on adjacent cells.

The downstream signaling mechanisms for axon guidance remain unclear by now, but the modulation of Rho-GTPases and associated second messengers like cAMP putatively play a key role (Song and Poo, 1999). For example, decreased levels of cAMP were found to promote repulsive effects. Targets for the signaling pathways might be molecules such as Arp2/3 (to nucleate new actin filaments), Ena/VASP proteins (to promote filament elongation), adhesion molecules (to couple actin filaments to the substrate) and myosins (to regulate the retrograde flow of actin filaments) (Dickson et al., 2002).

Once axons reach the target area contacts between growth cone and dendritic filopodia occur, from which some are selectively stabilized, while many are just short-lived. Molecular matching seems to be decisive. By molecular labeling of the postsynaptic cell, extrinsic cues, such as glial fibers, and repellent molecules not only the contact is defined, but also the localization of the later synapse (Axo-axonic, axo-dendritic, axo-somatic). In case a synapse is stabilized ingrowing axons secrete morphogens that coordinate growth and phenotypic specificity of the synapse (Sanes and Yamagata, 2009). Neuroligins were likewise shown to contribute in specifying excitatory and inhibitory synapses, respectively (Cubykin et al., 2007, see 1.3). Subsequently the growth cone converts into an immature presynaptic terminal and pre- as well as postsynaptic differentiation begins. Communication between pre- and postsynaptic cell through cell adhesion or secreted molecules initiates the accumulation of

pre– and postsynaptic specific proteins like active zone elements or neurotransmitter receptors to the nascent synapse. It is suggested that the presynaptic components are transported together along developing axons in dynamic and specific vesicular packages, called precursor vesicles (Ahmari et al., 2000; Zhai et al., 2001; Ziv and Garner 2004). These were observed to move bidirectional, to split into smaller units or to fuse into larger ones (Ziv and Garner 2004). With temporal delay postsynaptic components accumulate, likewise transported in discrete packages (Washbourne et al., 2002; Washbourne et al., 2004; Ziv and Garner 2004). Shortly after assembly of synaptic elements, synaptic transmission could be observed (Ziv and Garner 2004). With increasing amounts of pre- and postsynaptic proteins the synapses grow larger. Especially the postsynaptic site undergoes huge structural changes, as glutamatergic synapses initially form on filopodia or dendrite shafts that develop into dendritic spines (Waites et al., 2005). This dendritic spine morphogenesis is essential for proper synaptic function and is regulated amongst others by N-cadherin (for review see Tada and Sheng, 2006). Mature spines can have differential shapes, from which the mushroom type is the most common. The functional maturation is accompanied by the enlargement of presynaptic vesicle pools and an increase in vesicle release probability. Additionally developmental changes in the composition of postsynaptic receptor subunits are settled, determining the properties of the synapse such as kinetics of synaptic responses.
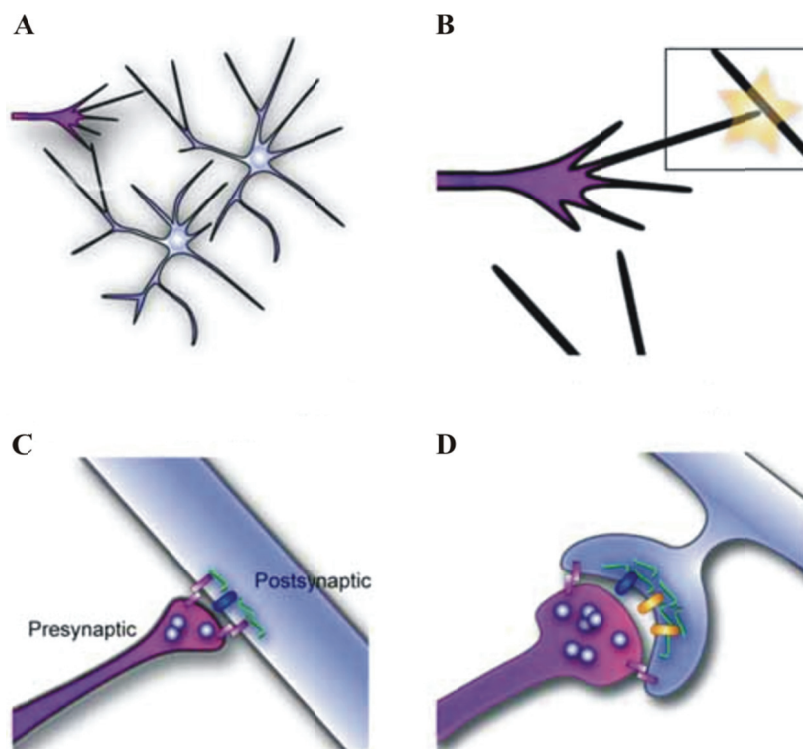
Figure 1.3 The assembly of synapses.
(after Gerrow and El-Husseini, 2006) **A-B** Axon guidance cues and target selection iniate initial contact between axons and dendrites. **C** Pre- and postsynaptic proteins are recruited to the nascent synapses. **D** With maturation of the synapse the spine undergoes indispensable morphological changes.

Most synapses are formed during development, but due to modification and fine-tuning of synaptic systems individual synapses can be formed or eliminated over the entire life. Sometimes the elimination of synapses serves the purpose of quantitative matching of input and target populations, other cases have shown a qualitative improvement of synaptic strength by selectively removing inappropriate connections in a competitive manner (for review see Sanes and Yamagata, 2009). Evoked and spontaneous rewiring of microcircuits is suggested to be also involved in learning and memory processes (Bailey and Kandel, 1993; Le-Bé and Markram, 2006). The elimination is either restricted to single synaptic sites (synapse disassembly) or all synapses between two neurons are degraded (input elimination) (Eaton and Davis, 2003). Experiments showed that as the connection between two neurons is lost not all of the synaptic input on the target neuron is vanished, thus indicating an independent character of synapse elimination (Lichtman and Colman, 2000). However, as the morphological shape of the postsynaptic site is converted as soon as the axon retracts, this dendritic location is not retaining connections with other axons anymore (Balice-Gordon and Lichtman, 1993; Lichtman and Colman, 2000). This observation and an experiment showing that before elimination the content and efficiency of quantal responses became progressively weaker led to the conclusion that the postsynaptic site may be the initiator for the removal (Colman et al., 1997; Lichtman and Colman, 2000).

Little is known about the entire molecular machinery or the precise mechanism of synapse elimination. Following an oversimplified postulate introduced by Donald Hebb in 1949 that declares "cells that fire together, wire together", synaptic activity patterns are probably responsible for the specific elimination (Knott et al., 2002; Trachtenberg et al., 2002; Goda and Davis 2003), although not being the only factor. Thereby not the activity per se seems to be important, but rather the pattern of activity from one set of synapses of a single axon. Asynchronous firing patterns are believed to support the removal of synapses (for review see Lichtman and Colman, 2000). Moreover, a combination of patterned neuronal activity and molecular cues, such as ephrins or the ubiquitin-mediated protein degradation, is proposed to define more precisely connectivity maps (Ding et al., 2007; Cang et al., 2008; Sebeo et al., 2009). Both, intra- and intersynaptic signaling that allows active synapses to destabilize inactive synapses is discussed (Lichtman and Colman, 2000). Retrograde or anterograde

signaling through recognition molecules like N-cadherin or retrograde trophic factors such as BDNF might play a leading role. Furthermore, local acting proteases that degrade cell adhesion molecules were observed to be involved (Zoubine et al., 1996).

1.6 Aims of the study

Members of the classical cadherins are proposed to play key roles in essential synaptic processes. Especially due to selective and strong homophilic binding, N-cadherin has been suggested to be pivotal for the recognition of appropriate synaptic partners during the definition of synaptic circuits. In addition to selective synapse formation, the specific elimination of inappropriate synapses is supposed to be a critical step in wiring processes. Accordingly, an asymmetric expression of N-cadherin at individual synapses might lead to an impairment of synaptic transmission and ultimately to an elimination of these mis-matched synapses. While a role of N-cadherin in synaptic recognition was often in the focus of discussion, no study raised the question for a specific role of asymmetrically expressed N-cadherin in synapse elimination, thus making the verification of the preceding hypothesis the leading aim of this work.

To enable the analysis of asymmetric N-cadherin expression on the level of individual synapses, a need for allowing synaptic interplay between neurons lacking N-cadherin and neurons expressing N-cadherin in common networks was given. As knockout mice for N-cadherin are lethal in a very early embryonic stage and conditional knock-out mice have initially not been available, N-cadherin knockout neurons derived from embryonic stem (ES) cells have been used for this purpose. In order to create a N-cadherin mis-match situation these neurons were transfected with a very low efficiency (due to the use of the Lipofectamine technique) with N-cadherin (for visualization cotransfected with EGFP). This resulted in only few transfected neurons expressing N-cadherin postsynaptically, while the surrounding presynaptic neurons did not express N-cadherin. The concept for this approach was instigated by previous work (Jüngling et al., 2006), indicating that no strong alterations occur when N-cadherin was absent only postsynaptically.

In the first part of this study a morphological characterization of the N-cadherin transfected knockout neurons as well as putative functional alterations in the N-cadherin mis-match system have been in the focus of analysis using immunocytochemical stainings (N-cadherin, VAMP2) and electrophysiological recordings of spontaneous miniature excitatory postsynaptic currents (mEPSCs), respectively. As intrinsic control autaptic connections of N-

cadherin transfected neurons were examined by electrophysiological recordings of evoked autaptic responses. Similarly the necessity for a qualitative mis-match was studied by N-cadherin overexpression in wildtype neurons.

To some degree the molecular background of alterations was illuminated in a second part. The application of various peptides (N-cadherin blocking agents; BDNF) and their effect on functional alterations was analyzed using electrophysiological recordings of mEPSCS in the N-cadherin mis-match situation. Moreover, biochemical approaches (co-immunoprecipitation) were applied to find a molecular binding partner of postsynaptically expressed N-cadherin.

The third part of this work was aimed at the investigation of the consequences of functional alterations, analyzed in the first part, i.e. the induction of a synapse elimination process. Immunocytochemical stainings against a synaptic marker (VAMP2) in combination with transfections, enabling additionally the visualization of specific synaptic markers (PSD-95; VAMP2) were applied in the N-cadherin mis-match situation and used for the description of effects on synaptic density. In order to investigate a retraction of axonal processes the mis-match situation was created in a different way. Cultured neurons from N-cadherin floxed mice were transfected with Cre-recombinase using the Lipofectamine technique, which resulted in few transfected neurons lacking N-cadherin, while the surrounding neurons expressed the molecule. In this situation the degree of axonal and dendritic retractions due to asymmetric N-cadherin expression could be analyzed.

The fourth part of this work dealt with the cooperation of the N-cadherin and the neuroligin systems. It was part of a project (Stan et al., 2010), investigating a necessity for the interaction of both cell adhesion systems in regulating presynaptic vesicle accumulation. In this study the functional aspects of the cooperation were analyzed. By means of electrophysiological recordings of AMPA receptor-mediated mEPSCs and the progressive block of NMDA receptor-mediated EPSCs by MK801 regulatory properties of overexpressed neuroligin1 were studied in the presence or absence of N-cadherin.

2. Materials and Methods

2.1. Solutions and chemicals

DNA purification kits were purchased from Qiagen, Western blot equipment was obtained from Bio-Rad.

2.1.1 Cell culture medium

(all solutions were obtained from Invitrogen if not stated otherwise)

EF ("embryonic feeder" cells) medium

DMEM	500 ml	Gibco; Cat. No. 21969
Fetal Calf Serum (FCS;heat-inactivated)	50 ml	Gibco; Cat. No. 10500-064
L-Glutamin 200mM	5 ml	Gibco; Cat. No. 15140-122
Penicillin-Streptomycin solution 100X	5 ml	Gibco; Cat. No. 15140-122

KO ES (knock out embryonic stem cell) medium

Knock out DMEM	425 ml	
FCS (heat-inactivated)	75 ml	Gibco; Cat. No. 10500-064
MEM Non Essential Amino-acids	5 ml	Gibco; Cat. No. 11146
Penicillin-Streptomycin solution 100X	5 ml	Gibco; Cat. No. 15140-122
2-mercaptoethanol 50 mM	0.5 ml	Gibco; Cat. No. 31350-10
LIF (fresh added)	0.7 μl/5 ml	Esgro; Cat. No. ESG1107

SR ("serum replacement") medium

DMEM	425 ml	Gibco; Cat. No. 21969
Serum Replacement	75 ml	Gibco; Cat. No. 10828
L-Glutamin 200 mM	5 ml	Gibco; Cat. No. 15140-122
2-mercaptoethanol 50 mM	0.5 ml	Gibco; Cat. No. 31350-10
Penicillin-Streptomycin solution 100X	5 ml	Gibco; Cat. No. 15140-122

[26]

Differentiation medium

DMEM	200 ml	Gibco; Cat. No. 21969
FCS (heat-inactivated;10 %)	50 ml	Gibco; Cat. No. 10500-064
L-Glutamin 200 mM	2,5 ml	Gibco; Cat. No. 15140-122
MEM non-essential Aminoacid-Solution	2.5 ml	Gibco; Cat. No. 11146
β-Mercaptoethanol solution*	2.5 ml	Serva
Penicillin-Streptomycin solution 100X	2.5 ml	Gibco; Cat. No. 15140-122
Retinoic acid solution** fresh added	5 ul/ml	Sigma; Cat. No. A4544

* β-Mercaptoethanol solution: 3.4 ul β-Mercaptoethanol in 10 ml DMEM

** Retinoic acid solution: 3mg retinoic acid (Serva) in 10 ml; 1:9 dilution in differentiation media

Neurobasal (NB) medium I

Gibco; Cat. No. 21103-049

addition of:

B27-Supplement 50 X	10 ml	Gibco; Cat. No. 17504-044
GlutaMAX-I Supplement	2.5 ml	Gibco; Cat. No. 35050-038
Penicillin-Streptomycin solution 100X	5 ml	Gibco; Cat. No. 15140-122

Neurobasal (NB) medium II

Gibco; Cat. No. 21103-049

addition of:

GlutaMAX-I Supplement	2.5 ml	Gibco; Cat. No. 35050-038
Penicillin-Streptomycin solution 100X	5 ml	Gibco; Cat. No. 15140-122
NS21 (after Chen et al., 2008)	10 ml	
Bovine Albinum	37μM	Sigma; Cat. No. A4919
Catalase	0,01 μM	Sigma; Cat. No. C40
Glutathione (red.)	3,2 μM	Sigma; Cat. No. G6013
Insulin	0,6 μM	Sigma; Cat. No. I1882
Superoxidase dismutase	0,077 μM	Sigma; Cat. No. S5395
Holo-transferrin	0,062 μM	Calbiochem; Cat. No. 616424

T3 (triiodo-L-thyronine)	0,0026 µM	Sigma; Cat. No. T6397
L- Carnitine	12 µM	Sigma; Cat. No. C7518
Ethanolamine	16 µM	Sigma; Cat. No. E9508
D(+)-Galactose	83 µM	Sigma; Cat. No. G0625
Putrescine	183 µM	Sigma; Cat. No. P5780
Sodium selenite	0.083 µM	Sigma; Cat. No. S9133
Corticosterone	0,058 µM	Sigma; Cat. No. C2505
Linoleic acid	3,5 µM	Sigma; Cat. No. L1012
Linolenic acid	3,5 µM	Sigma; Cat. No. L2376
Lipoic acid (thioctic acid)	0,2 µM	Sigma; Cat. No. T1395
Progesterone	0,02 µM	Sigma; Cat. No. P8783
Retinol acetate	0,2 µM	Sigma; Cat. No. R7882
Retinol, all trans	0,3 µM	Sigma; Cat. No. 95144
D,L- alpha-Tocopherol	2,3 µM	Sigma; Cat. No. 95240
D,L- alpha-Tocopherol acetate	2,1 µM	Sigma; Cat. No. T3001

BME medium   Gibco; Cat. No. 21370-028

addition of:

FCS (heat-inactivated)	50 ml	Gibco; Cat. No. 10500-064
L-Glutamin 200 mM	5ml	Gibco; Cat. No. 25030-024
Glucose (40%) 20 mM	3ml	J.T. Baker; Cat. No. 0114
Insulin-Transferrin-Selenium solution	5 ml	Gibco; Cat. No. 5130-044
Penicillin-Streptomycin solution	5 ml	Gibco; Cat. No. 15140-122

Following solutions were used as well in cell culturing:

1x Trypsin- EDTA 0,05%	Gibco; Cat. No. 25300-054
Trypsin 0,25%	Gibco; Cat. No. 25050-014
PBS Dulbecco`s phosphatebuffered Saline	Gibco; Cat. No. 14040-091
PBS Dulbecco`s phosphatebuffered Saline without Ca $^{2+}$ and Mg^{2+}, Natriumbicarbonat (PBS $^{-/-}$)	Gibco; Cat. No. 14190-094
Cytosin-β-D-Arabinofuranosidhydrochloride	

(ARA-C)	10μM	Sigma-Aldrich; Cat. No. C-6645
Poly-L-Ornithine	1 mg/mgl	Sigma-Aldrich; Cat. No. P-3655
Boric acid	0,15M	Sigma-Aldrich; Cat.No. 083K0055
Xylen		
abs. Ethanol		
Aceton		
Lipofectamine 2000		Invitrogen; Cat. No. 11668-027
LIF (Leukemia inhibitory factor)		Sigma; Cat. No.L5158
Mitomycin C (from Streptomyces caespitosus)		Sigma; Cat. No. M4287
Papain		Worthington; Cat. No.31266
Trypsin inhibitor (Ovomucoid)		Roche; Cat. No. 10109878001
TRIS-HCL	50mM	Promega; Cat. No. H5123

2.1.2 Media for growing bacteria

(Media were autoclaved for 20 min/antibiotics were supplemented prior to use)

LB-medium

Bacto-tryptone, pH 7.5	10 g/l	Sigma; Cat. No. T9410
NaCl	5 g/l	J.T. Baker; Cat. No. 0278
Yeast extract	5 g/l	Sigma, Cat. No. Y1625
Glucose (w/v)	2 %	Merck; Cat. No. 108337
$MgSO_4$	1 mM	Sigma; Cat. No. M2643

LB/Amp-medium

(same for LB/Kan-medium)

Ampicillin in LB-medium	100 mg/l

LB/Amp-plates

(same for LB/Kan-plates)

Agar in LB-medium	20 g/l	Sigma; Cat. No. A5306
Amplicillin	100 mg/l	

[29]

2.1.3 Solutions for electrophysiological recordings

Recordings of spontaneous postsynaptic miniature currents (mEPSCs)

Extracellular solution I:

NaCl	130 mM	J.T. Baker; Cat. No. 0278
KCl	5 mM	Sigma-Aldrich; Cat. No. 31248
$MgCl_2$	1 mM	J.T. Baker; Cat. No. 0163
$CaCl_2$	2,5 mM	Sigma-Aldrich; Cat. No.12074
HEPES	20 mM	AppliChem ; Cat. No.7365-45-9

adjusted to pH 7,3 with NaOH

Intracellular solution I:

KCl	110 mM	Sigma-Aldrich; Cat. No. 31248
$CaCl_2$	0,25 mM	Sigma-Aldrich; Cat. No. 12074
EGTA	10 mM	Serva; Cat. No. 11290
HEPES	20 mM	AppliChem; Cat. No. 7365-45-9

adjusted to pH 7,3 with KOH

Recordings of evoked postsynaptic currents (PSCs):

Extracellular solution II :

NaCl	130 mM	J.T. Baker; Cat. No. 0278
KCl	5 mM	Sigma-Aldrich; Cat. No. 31248
$CaCl_2$	2,5 mM	Sigma-Aldrich; Cat. No.12074
HEPES	20 mM	AppliChem ; Cat. No.7365-45-9
Glycine	10 µM	Sigma; Cat. No. G8898

adjusted to pH 7,3 with NaOH

Extracellular solution III :

NaCl	130 mM	J.T. Baker; Cat. No. 0278
KCl	5 mM	Sigma-Aldrich; Cat. No. 31248
$MgCl_2$	1 mM	J.T. Baker; Cat. No. 0163
$CaCl_2$	5 mM	Sigma-Aldrich; Cat. No.12074
HEPES	20 mM	AppliChem ; Cat. No.7365-45-9

adjusted to pH 7,3 with NaOH

Intracellular solution II:

Cesium methanesulfonate	110 mM	Sigma; Cat. No. C1426
$CaCl_2$	0,25 mM	Sigma-Aldrich; Cat. No.12074
TEA	20 mM	Sigma; Cat. No. T2265
EGTA	10 mM	Serva; Cat. No. 11290
HEPES	20 mM	AppliChem; Cat. No. 7365-45-9

adjusted to pH 7,3 with KOH

neurotoxins: DNQX 10µM, GABAzine 10 µM, TTX 1µM, MK-801 20 µM

2.1.4 Solutions for immuncytochemical stainings

Blocking buffer I:

PBS (Dulbecco`s Phosphatgepufferte Saline)	82,7%	Gibco; Cat. No. 14040-091
Triton-X-100	0,3%	Sigma-Aldrich; Cat. No.X-100
BSA/ Albumine Bovine Fraction V ≥96%	2%	Riedel de Haen; Cat. No. 2329362
Succhrose	5%	J.T.Baker; Cat. No. 0334
FCS (heat-inactivated)	10%	

Blocking buffer II appropriate to blocking buffer I but without addition of FCS

Additionally used:

Paraformaldehyd	4%	Riedel de Haen

2.1.5 Solutions for coimmunoprecipitations and Western blots

Solutions for coimmunoprecipitations

Homogenization buffer, pH7.4

HEPES; pH7,4	20mM	AppliChem ; Cat. No.7365-45-9
$CaCl_2$	1mM	Sigma-Aldrich; Cat. No.12074
$MgCl_2$	1mM	J.T. Baker; Cat. No. 0163
PMSF (Phenylmethylsulfonylfluorid)	100µM	Sigma; Cat. No. P7626
Complete EDTA-free		
Protease inhibitor cocktail	1x	Roche; Cat. No. 11873580001
Leupeptin	10µg/ml	Roche; Cat. No. 11017101001
Aprotenin	1µg/ml	Roche; Cat. No. 10236624001
DAPT	1µM	Calbiochem; Cat. No. 565784
GM6001	20µM	Calbiochem; Cat. No. 364205

RIPA buffer, pH7,4

(modified after Du et al., 2009)

HEPES; pH7,4	20mM	AppliChem ; Cat. No.7365-45-9
NaCl	100mM	J.T. Baker; Cat. No. 0278
Na_3VO_4	1mM	Aldrich; Cat. No. 450243
NaF	50mM	Sigma; Cat. No. 57920
NP-40 (Igepal CA-630)	1%	Sigma; Cat. No. I3021
Deoxycholate acid	1%	Sigma; Cat. No. D6750
SDS (sodium dodecyl sulfate)	0,1%	Sigma; Cat. No. 75746
PMSF	100µM	Sigma; Cat. No. P7626
Complete, EDTA-free		
Protease inhibitor cocktail	1x	Roche; Cat. No. 11873580001
Leupeptin	10µg/ml	Roche; Cat. No. 11017101001
Aprotenin	1µg/ml	Roche; Cat. No. 10236624001
DAPT	1µM	Calbiochem; Cat. No. 565784
GM6001	20µM	Calbiochem; Cat. No. 364205

Additionally used:

A/G-agarose beads	25µl	Santa cruz; Cat. No. sc-2003
BSA/ Albumine Bovine Fraction V ≥96%	2mg/ml	Riedel de Haen; Cat. No. 2329362
BCA protein assay kit		Thermo Scientific; Cat. No. 23221

Solutions for Western blots:

SDS (sodium dodecyl sulfate)-PAGE:

8%:

Aqua dest.	2,79 ml	
1M TRIS pH 8,8	3 ml	Sigma; Cat. No.T1378
10% SDS (sodium dodecyl sulfate)	80 µl	Sigma; Cat. No. 75746
30% Acrylamid/ 0,8%Bisacrylamid	2,14 ml	Applichem; Cat. No. A3857
10% APS (Ammoniumpersulfat)	16 µl	Applichem; Cat. No. A0834
TEMED (Tetramethylethylendiamin)	8 µl	Applichem; Cat. No. A1148

10%:

Aqua dest.	2,25 ml	
1M TRIS pH 8,8	3 ml	Sigma; Cat. No.T1378
10% SDS (sodium dodecyl sulfate)	80 µl	Sigma; Cat. No. 75746
30% Acrylamid/ 0,8%Bisacrylamid	2,67 ml	Applichem; Cat. No. A3857
10% APS (Ammoniumpersulfat)	16 µl	Applichem; Cat. No. A0834
TEMED (Tetramethylethylendiamin)	8 µl	Applichem; Cat. No. A1148

12 %:

Aqua dest.	1,72 ml	
1M TRIS pH 8,8	3 ml	Sigma; Cat. No.T1378
10% SDS (sodium dodecyl sulfate)	80 µl	Sigma; Cat. No. 75746
30% Acrylamid/ 0,8%Bisacrylamid	3,2 ml	Applichem; Cat. No. A3857

[33]

| 10% APS (Ammoniumpersulfat) | 16 µl | Applichem; Cat. No. A0834 |
| TEMED (Tetramethylethylendiamin) | 8 µl | Applichem; Cat. No. A1148 |

Stacking gel:

Aqua dest.	2,1 ml	
1M TRIS pH 6,8	380 µl	Sigma; Cat. No.T1378
10% SDS (sodium dodecyl sulfate)	40 µl	Sigma; Cat. No. 75746
30% Acrylamid/ 0,8%Bisacrylamid	500 µl	Applichem; Cat. No. A3857
10% APS (Ammoniumpersulfat)	15 µl	Applichem; Cat. No. A0834
TEMED (Tetramethylethylendiamin)	6 µl	Applichem; Cat. No. A1148

Running buffer (1x):

TRIS	25 mM	Sigma; Cat. No.T1378
Glycine	192 mM	Sigma; Cat. No. G8898
SDS (sodium dodecyl sulfate)	0,1 %	Sigma; Cat. No. 75746

Transfer buffer (1x):

TRIS	25 mM	Sigma; Cat. No.T1378
Glycine	192 mM	Sigma; Cat. No. G8898
SDS (sodium dodecyl sulfate)	0,001%	Sigma; Cat. No. 75746
Methanol	20 %	Merck

TBS-T Washing buffer:

TRIS	10 mM	Sigma; Cat. No.T1378
NaCl	150 mM	J.T. Baker; Cat. No. 0278
Tween 20	0,1 %	Serva; Cat. No. 37470

Laemmli-buffer (5x):

| Aqua dest. | 22 % | |

1M TRIS; pH 6,8	125 mM	Sigma; Cat. No.T1378
Glycerol	20 %	Sigma ; Cat. No. G8773
10 % SDS (sodium dodecyl sulfate)	10 %	Sigma; Cat. No. 75746
0,5 % bromphenolblue (in a.d.)	0,1 %	Sigma; Cat. No. 2040862

Freshly added: β-mercaptoethanol 5% to 2x Laemmli

Additionally used:

Precision Plus protein all blue standards   Bio-Rad; Cat. No. 1610373

2.1.6 Plasmids

pEGFP-N1 Clontech. Kanamycin resistence

pMS 149.1 Full murine N-cadherin. Ampicillin resistance. Gift from Dr. R. Kemler, MPI Freiburg, Germany

N-cad ΔE N-cadherin from Xenopus laevis lacking most of the extracellular domain inserted into pCS2+ vector (University of Michigan). Ampicillin resistance. Gift from Dr. C. Holt, University of Cambridge, UK

DsRed2-VAMP2 VAMP2 (Synatobrevin II) from Rattus norvegicus inserted into MCS of pDsRed2-C1 (Clontech). Kanamycin resistance. Gift from Dr. V. Lessmann, University of Mainz, Germany

PSD95-GFP PSD95 from Rattus norvegicus inserted into GW1 vector (British Biotechnology). Ampicillin resistance. Gift from Dr. V. Lessmann, University of Mainz, Germany

Neuroligin1-GFP Neuroligin1 from Rattus norvegicus inserted into MCS of pEGFP-N1 (Clontech). Kanamycin resistance. Gift from Dr. T. Dresbach, University of Heidelberg, Germany

pBS598 EF1alpha-EGFPcre Cre recombinase fused to EGFP inserted into pBS598 vector (addgene). Ampicillin resistance.

2.1.7 Peptides

16mer peptide "HAV" (Poskanzer et al., 2003) in 0,1 % acetic acid

HLRA<u>HAV</u>DINGNQVEN (peptide)   200μg/ml   Mimotopes

ARLQHDVNANVHEING (scrambled)   200μg/ml   Mimotopes

7mer peptide "INP" (Williams et al., 2000) in 0,1 % acetic acid

<u>INP</u>ISGQ-NH$_2$ (peptide)   100μg/ml   neoMPS

LVRIRS-NH$_2$ (scrambled)   100μg/ml   neoMPS

BDNF

in 0,1% BSA (peptide)   100 ng/ml   Sigma; Cat. No. B3795

0,1 % BSA (vehicle)   Riedel de Haen; Cat. No. 2329362

2.1.8 Antibodies

Antibodies for L1-immunoisolation

Goat anti-rat (1,3 mg/ml)   1:125   Jackson Labs; Cat. No. 112005167

L1   14 ml/cell culture dish

Antibodies for immunocytochemical staining

Primary antibodies:

Mouse anti-VAMP2 (Synaptobrevin2)   1:1000   Synaptic Systems;Cat. No. 104211

Rabbit anti-N-cadherin   1:1666   Abcam; Cat. No. ab18203

Secondary antibodies:

Goat anti-Mouse IgG Cy3	1:1000	Chemicon; Cat. No. AP124C
Goat anti-Rabbit Oregon green	1:500	Invitrogen; Cat. No. O6381
Goat anti-mouse Alexa Flour 350	1:12,5	Invitrogen; Cat. No. A21120

Antibodies for coimmunoprecipitations

Rabbit anti-N-cadherin	7µg/ml	Abcam; Cat. No. ab18203
Rabbit IgG preimmuneserum	5µg/ml	Santa Cruz; Cat. No. sc-66931
TrkB/Fc "receptor body" in 0,1% BSA	1µg/ml	R&D systems; Cat. No. 688TK100

Antibodies for Western blot:

Primary antibodies (addition of NaN$_3$ 10µl/ml*)*

Rabbit anti-N-cadherin	1:1000	Abcam; Cat. No.ab
Rabbit anti-pan Trk	1: 500	Santa Cruz; Cat. No. sc-11 (C-14)
Rabbit anti-p75	1:1000	Covance; Cat. No. PRB-602C

Secondary antibodies:

IRDye goat anti-rabbit 800 CW	1:10 000	Odyssey; Cat. No. 92632211

2.2 Cell culture

2.2.1 Proliferation and differentiation of mouse embryonic stem (ES) cells

To analyze a gene`s function knocking it out is a commonly used method. As N-cadherin knockout mice are lethal in a very early embryonic stage, mainly due to dramatic defects in cardiac tissue development (Radice et al., 1997), the majority of experiments in this work has been done on ES-cell derived neurons deficient for N-cadherin.

2.2.1.1 N-cadherin deficient mouse ES cell lines

(Moore et al., 1999)

All ES cell lines used in this work were provided by Prof. Kemler (MPI of Immunobiology, Freiburg). The inactivation of the N-cadherin gene followed the principles of homologous recombination, where a targeting vector with special features and the wild-type allel get recombined. The generation of the targeting vector (figure 2.1) included the insertion of a neomycin phosphotransferase expression cassette (neo) into a unique *Sal*I site of the exon 10 of the N-cadherin gene disrupting the open reading frame of the N-cadherin gene. Serving as promoter a flanking herpes simplex virus thymidine kinase expression cassette (HSV tk) was inserted. The construct was linearized and electroporated into D3 ES cells. Colonies were selected by the G418 and ganciclovir resistance of the neo cassette. The correct integration and exon 10 replacement by the neo cassette was analyzed using Southern blot (*SmaI-HindIII* digest). Postive clones were injected into blastocysts of C57Bl/6 mice, which were brought into the uteri of pseudopregnant females. The mice were genotyped by Southern blot or PCR. To obtain N-cad -/- ES cells heterozygous mice were breeded with each other. At embryonic day 2,5 (E2,5) the blastocysts were isolated and their inner cell mass was proliferated in vitro. The genotype was verified by Southern blot (Radice et al., 1997, Moore et al., 1999).
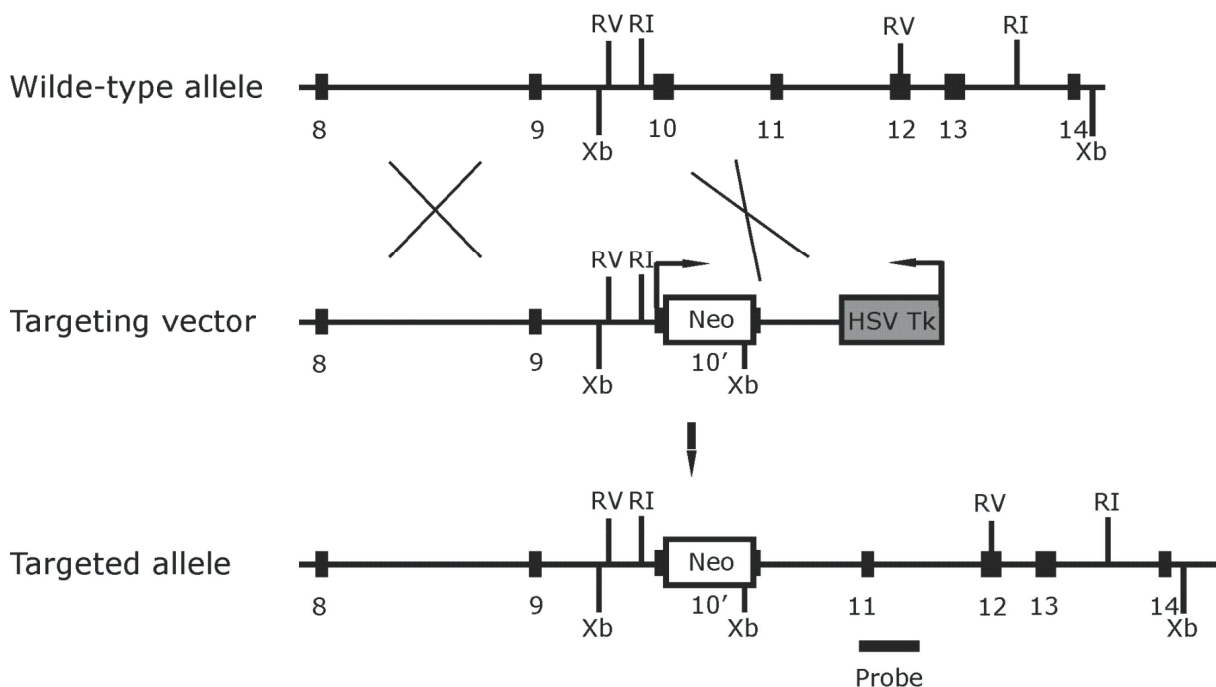

Figure 2.1. Schematic illustration of the targeted N-cadherin gene replacement
(after Radice et al., 1997)

Representation of the targeting vector with inserted neo cassette, HSV tk promoter and several restriction sites. Homologous recombination results in the targeted allel, in which exon 10 of the N-cadherin genome is replaced by the neo casette.

2.2.1.2 Preparation and proliferation of embryonic mouse fibroblasts feeder (EF) cells

To ensure giving the ES cells every needed metabolite, the proliferation of ES cells was carried out on confluent layers of mouse embryonic feeder (EF) cells taken from the dermal- and myotissue of E13 (13th day of pregnancy) mouse embryos. After sacrificing a pregnant C57BL/6 mouse via CO_2 gassing the embryos were exempted from the uteri and washed in sterile PBS. After decapitation and removal of intestines, spinal cord and interior organs the remaining tissue was chopped with a scalpel and subsequently incubated in 5 ml Trypsin/EDTA at 37°C and 5 % CO_2 for 5 minutes to dissolve the cells out of their tissue. After the incubation time, the enzymatic reaction was stopped by washing with 5 ml of FCS containing EF medium. The incoherent pieces of tissue were further mechanically dissociated by pipetting with 1000 µl and 200µl pipettes and transferred into a (175 cm2) tissue culture flask containing 40 ml EF medium. By changing the media every 24 h and incubating at 37°C, 5 % CO_2 and 95% humidity the cells proliferate until a confluent layer was grown. Before detaching the cells by addition of 5 ml Trypsin/EDTA for 5 minutes first all disturbing ions were removed by washing them with PBS$^{-/-}$. 5 ml EF medium stopped all proteolytic effects, so that the cells could be transferred into 15 ml Falcon tube and centrifuged at 800 rpm for 5 minutes. After resuspension in EF medium the cells could be used either for further cultivation by splitting them on 0,1%-gelatine coated culture flasks or, on purpose to mount them, for freezing. For freezing in liquid nitrogen 0,5 ml cell suspension was filled together with 0,5 ml freezing medium (60% EF medium, 20% FCS, 20% DMSO) into cryovials. After 24h at -80 °C the cells were conveyed into the liquid nitrogen for long time storage. The EF cells which have been splitted on gelatine coated flasks could be used further after growing confluent. To avoid an overgrowing of the later added ES cells by the EF cells it was necessary to block the proliferation of the latter. Therefore the EF cells were incubated in EF-medium containing the cytostatic acting Mitomycin C (1mg/5ml Mitomycin C in PBS per 200 ml EF medium) for 2h at 37°C/5% CO_2. After removal of Mitomycin C, several washing steps with PBS and 24 h incubation time the EF cells could be used for ES cell culturing.

2.2.1.3 Culturing and in vitro differentiation of mouse ES cells

As the proliferation of the EF cells was inactivated they have been ready to serve as basal layer for ES cells. For that purpose $1x10^6$ ES cells were plated in 5 ml ES medium on monolayers of EF cells and incubated at 37°C, 5 % CO_2 and 95 % humidity (Fig. 2.2A). Addition of the Leukemia inhibitory factor (LIF), which inhibits spontaneous differentiation, preserved the pluripotent character of the ES cells until they have been proliferated to an adequate mass, size and effectual maturation stage. The medium was changed every 24 h until a considerable formation of cell aggregates had occured. To ensure having as less EF cells as possible in the later differentiation stages the ES cells were then detached from the culture flasks as described in chapter 2.2.1.2 and splitted on each of two 0,1%-gelatine coated culture flasks without feeders. After reaching the desired size and mass (2-3 days later) the ES cells were again relieved from the culture flasks, with the difference that 5 ml SR medium instead of 5 ml ES medium served as blocker of proteolytic effects. In order to further reduce the amount of EF cells the suspension was placed twice for 20 minutes each on adherent bacterial culture dishes (100 mm diameter; Sarstedt Inc. Newton, NC). As EF cells have a higher affinity to attach on culture plates it is supposed that the ES cells remain in suspension, while most of the EF cells attach to the ground. The suspension (~$0,75x10^6$ ES cells) was further cultivated in 10 ml SRM medium on non-adherent bacterial culture dishes (Fig. 2.2B; 92 mm diameter; Sarstedt, Germany). In these floating cultures embryoid bodies (EBs), which are macroscopically visible cell aggregates, formed. After 6 days the EBs were collected in 4 small culture dishes (35 mm; Falcon) containing 2 ml differentiation medium (Fig. 2.2C). The addition of retinoic acid ($5x10^{-7}$, Serva) supported the differentiation to neurons as described in the literature. 2 days later the EBs could be redistributed in adherent bacterial culture dishes coated with Poly-L-Ornithine and containing 10 ml NB medium II (content of 2 Falcon dishes in 1 bacterial dish). The EBs attached and were allowed to maturate and differentiate for 1-2 weeks. During this time period the EBs started to develop outgrowing fibers shown in figure 2.2D.
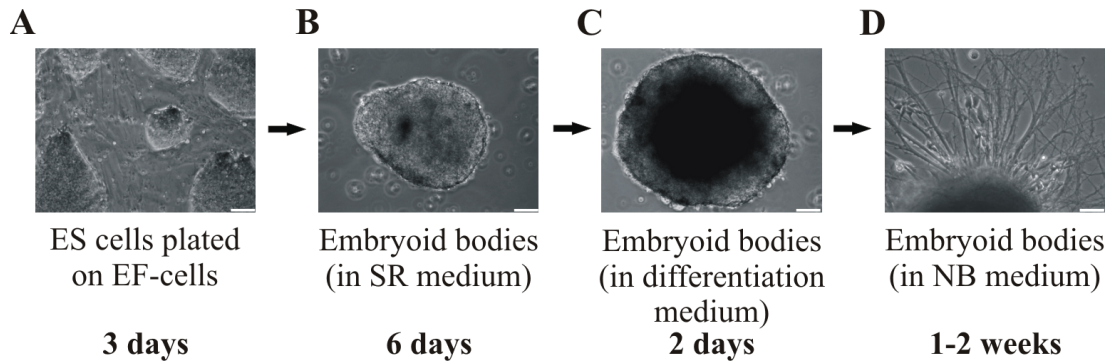
Figure 2.2. The ES cell differentiation protocol to neurons.
A-B ES cells cultured on EF cells (A) were after EF cell deprivation transferred to SR medium, in which embryoid bodies aggregated for 6 days (B). **C** EBs were transferred in differentiation medium in the presence of RA. **D** After 2 days they got redistributed in NB medium and kept in culture for 1-2 weeks. (Scale bars: 200 µm).

2.2.1.4 Dissociation of embryoid bodies

In order to get suspensions of single cells out of the embryoid bodies, they had to be dissociated. For this the EBs were collected in 15 ml Falcon tubes containing 10 ml EBSS medium with addition of 1,5 mM $CaCl_2$, 1mM EDTA, 1mM $MgCl_2$, 120 µl papain (77,8 units; Worthington) and 200 µl Desoxyribonuclease I (1mg/ml stock solution; Sigma, Germany) and incubated for 50 minutes at 37°C, 5 % CO_2 and 95 % humidity. Every 10 minutes the tubes have been turned upside down to ensure a sufficient efficacy of the papain (more gentle protease as for example trypsin). After smoothly centrifuging the tube the suspension could be neglected and the proteolytic effect of papain was stopped by addition of 4 ml 0,15 % ovomucoid solution (in $PBS^{+/+}$ + DNaseI solution; Trypsin inhibitor; Roche, Germany). After a second short centrifugation step the EBs were stepwise mechanically dissociated in 0,15% ovomucoid solution using a 1 ml pipette. Following another centrifugation step (2000rpm, 1 minute) the dissociated EBs were washed in 6 ml 1% ovomucoid solution and subsequently centrifuged. The washed cells were resuspended in 10 ml 0,02% BSA and 0,25 %FCS (in $PBS^{+/+}$) and ready to be used for the following L1-immunoisolation.

2.2.1.5 L1-immunoisolation of ES cell-derived neurons

Although, due to factors such as retinoic acid, prefentially neuronal cell types have been differentiated also other cell types as e.g. muscle cells were derived by the protocol. In order to achieve a pure population of neurons an immunoisolation of the ES-cell derived neurons

has to be done based on the neuron specific expression of the adhesion molecule L1 (Jüngling et al., 2003; Fig. 2.3).
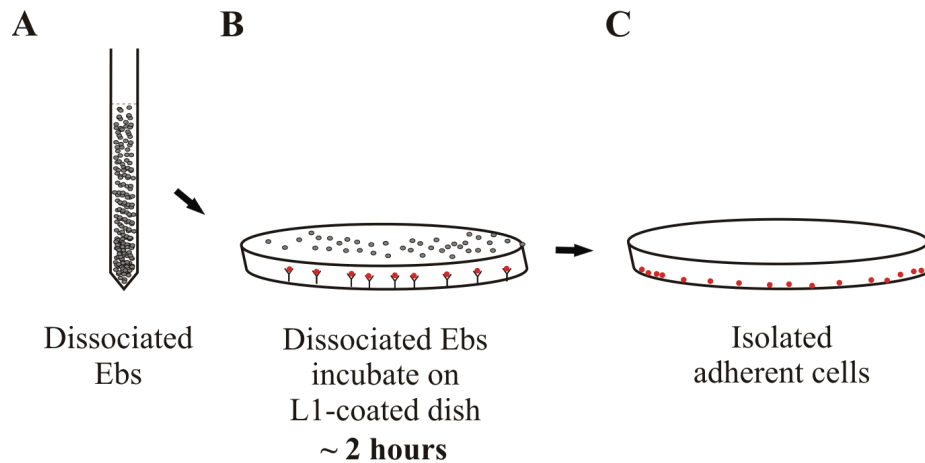

Figure 2.3. Schematic representation of the L1-immunoisolation.
A-B Dissociated EBs (A) were plated on L1 antibody-coated non-adherent dishes and left for incubation for ~ 2 hours (B). **C** Neurons got isolated due to binding to L1 antibody.

Therefore a non-adherent bacterial culture dish was coated overnight at 4°C with 80 µl goat anti-rat IgG in 10 ml TRIS-HCL buffer (pH 9,4) specific for the later added primary antibody against L1. After washing thrice with 5 ml PBS$^{+/+}$ each, 14 ml of L1 antibody, made up of the supernatant of a hybridoma cell culture, was applied and incubated either overnight at 4 °C or for at least 1,5 hours at 37°C, 5 % CO_2 and 95 % humidity. Rinsing the culture dish thrice with 5 ml PBS$^{+/+}$ removed non-attached antibody after incubation so that the previously dissociated EBs could be plated. As L1 is specifically expressed by neurons all neuronal cell types bound during the following 1,5 – 2 hours incubation time at room temperature to the L1 antibody and in this way attached to the culture dish. Every 15 minutes the culture dish was shaked in order to redistribute unbound neurons making more of them bind to L1 antibodies. All other cell types were not able to bind, so that these could be washed away after the incubation time in 6-10 washing steps with 5 ml PBS $^{+/+}$. In order to detach the neurons from the culture dish, they were incubated for 2,5 minutes in 4 ml Trypsin/EDTA at 37°C, 5 % CO_2 and 95 % humidity. Proteolytic effects were stopped via the addition of 4 ml 20% FCS in PBS$^{+/+}$ twice and all neurons could be washed from the culture dish into a 15 ml falcon tube. After centrifugation for 1 minute at 2000 g the neurons were resuspended in glia conditioned BME medium and added to glial microislands. The applied density of 30 000 - 40 000 cells/ coverslip (~ 2x10^5/culture dish with 5 coverslips) resulted in small networks of 10-20 neurons per glial microislands. The cultures were treated with glia-conditioned medium (GCM) in

order to support the survival of the neurons. GCM was obtained from purified confluent grown glia cell cultures incubated with NB medium I or II for 5 days. Collected GCM was applied to neuronal cultures every second day in a ratio 1:1,5 with fresh media (Pfrieger and Barres, 1997). Neuroligin experiments required more mass culture-like conditions, so that the cells were plated on nearly confluent glia layers.

2.2.2 The N-cadherin conditional knockout mouse

(Kostetskii et al., 2005)

In order to analyze a retraction of axons as an important step of eliminating synapses, part of this work was made using neurons from N-cadherin floxed mice (Ncad-flox) instead of ES-cell derived neurons deficient for N-cadherin. The N-cadherin floxed mice were made by Kostetskii et al. and obtained from Jackson Labs. A first step to knock out the N-cadherin gene was the homologous recombination of the wild-type allele and a targeting vector featuring special insertions leading to the replacement of a specific gene locus. For generating an appropriate targeting vector, 2 genomic clones from a genomic library screen corresponding to the first exon of N-cadherin were used. As shown in figure 2.4 the targeting vector contained two Lox-P sites flanking exon 1 from the N-cadherin gene and a neomycin phosphotransferase expression cassette (neo) flanked by two FRT sites for later excision by Flp recombinase also inserted into the intron. Additionally an *Eco*RI site was inserted near the distal Lox-P-site. The targeting vector was linearized with ClaI and electroporated into TL ES cells. Due to the integrations a fusion transcript instead of the wild-type transcript gets transcribed when recombined successfully. Positive colonies got selected by the neo–casette resistance to G418. All homologous events were detected by Southern blot (KpnI digest) and subsequently screened for the presence of the distal Lox-P site (*Eco*RI digest) confirming successful insertion. Via the injection of the ES cells into blastocysts from C57Bl/6J mice mutant mice were generated. The floxed mice were genotyped by PCR. To attain the deletion of the N-cadherin gene a Cre-mediated excisive recombination at the inserted Lox-P sites is required. One possibility is to breed Ncad-flox mice together with mice, in which the Cre-recombinase and an appropriate promoter were inserted. Part of the offspring will display both mutations, resulting in the knockout of N-cadherin. In this work the animals were breeded as homozygous Ncad-flox mice. The activation of the knockout was realized by transfecting cultured neurons with CreGFP leading to an expression of the Cre recombinase in the transfected Ncad-flox neurons.
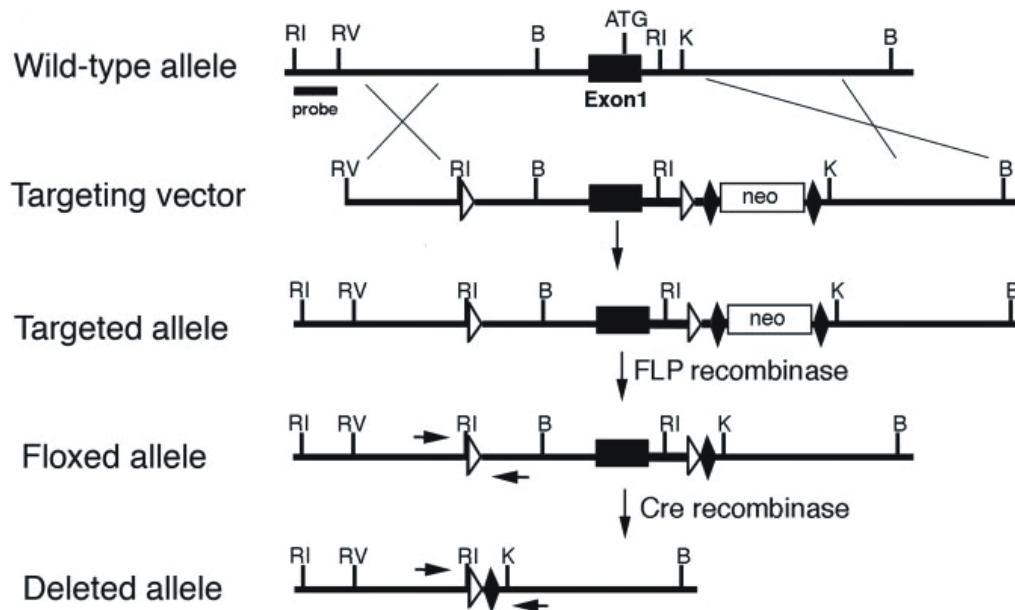
[43]

Figure 2.4. Schematic illustration of the N-cadherin conditional knockout.
(after Kostetskii et al., 2005)
Representation of the wild-type allele, the targeting vector, the targeting allele, the floxed allele and the final resultant deleted allel. The targeted vector includes Lox-P sites (triangles), FRT sites (diamonds) and the neo cassette. Illustrated are also the restriction sites. Homologous recombination results in the targeted allel. After excision of the neo cassette by the FLP recombinase the floxed allel is ready to be modified by cre-mediated recombination resulting in the deleted allele.

2.2.3 Preparation of sterile coverslips

2.2.3.1 Sterilization of coverslips

Neuronal cultures were plated on coverslips (Assitant, 12 mm) either with a layer of glial microislands on the coverslips or directly on the glass coated with Poly-L-Ornithine. Before sterilization the coverslips had to be prepared. Approximately 1000 coverslips were cleaned by exposing to Xylen for at least 3 hours or overnight during constant shaking. Subsequent washing was carried out in several washing steps (3x aceton, 3x abs. ethanol) before the coverslips could be sterilized in the heat sterilizer (3 hours at 180°C). The coverslips were placed with or without previous coating with Poly-L-Ornithine on 35 mm culture dishes (5 per dish; Falcon) or on 24-well plates.

2.2.4.2 Coating of sterile coverlips with Poly-L-Ornithine

To ensure an attachment of neurons on coverslips without the help of a layer of glial microislands, the coverslips had to be coated with Poly-L-Ornithine before adding the neurons. Therefore the coverslips were incubated for 24 hours with 150 µl of Poly-L-Ornithine (1mg/ml in 0,15 M Boratbuffer (pH 8,35)) and subsequently washed thrice with sterile aqua dest.. The coverslips were dried on aluminum foil for another 24 hours, before they were ready to use.

2.2.4 Preparation and dissociation of primary neocortical neurons

To obtain brain tissue from embryonic foetuses (E17) first the mother had to be sacrificed using CO_2 gassing. The medial 4-8 foetuses were exempted out of the uteri and decapitated. To keep the brain cells alive, all steps were taking place on ice. To reach the brain first the skullcap and then the scalp were opened and removed using two forceps (Dumont & Fils). Furthermore the brain was taken out by a micro scoop and transferred into a culture dish (Falcon) containing PBS to avoid drying-out of the tissue.

Using a binocular (20x magnification) both hemispheres of the cortex were isolated from the rest of the brain, cut into smaller pieces and transferred into 1ml PBS. To dissolve single cells out of the tissue, the cortices were incubated in 200µl 0,25% Trypsin for 5 minutes at 37°C. The proteolytic reaction was stopped by removing the Trypsin and washing with 1 ml FCS containing BME medium. To complete the destruction of tissue networks the cells got mechanically crudely dissociated by the use of a 1ml pipette tip and subsequently subtle dissociated with a 200µl pipette tip. As small networks of about 10-20 neurons had to be achieved the dissociated cells were added to glial microisland cultures. Neuroligin experiments involving primary neurons were carried out in mass cultures and therefore the neurons were directly plated on Poly-L-Ornithtine covered culture dishes. Hence, $4x10^4$ neurons were placed in form of a drop into the middle of Poly-L-Ornithine coated coverslips. For 1 hour they were incubated at 37°C/ 5%CO_2/ 95% humidity before 2 ml NB medium I or II was added.

2.2.5 Setting up glial microisland cultures

For retrieving small networks of neurons enabling the analysis of pre – and postsynaptically N-cadherin mis-matched synapses, glial microisland cultures were used. Neocortical tissue from postnatal mice (P0-P3) was prepared and dissociated analogous to 2.2.4. The cell suspension has been subsequently cultivated in a cell culture flask (Nunc, 25 cm^2) containing 5 ml BME medium for approximately 2-3 weeks until all neurons had disappeared and the glial cells were grown as a confluent monolayer. For setting up glial microisland cultures the medium was sucked off and cells were washed with 3 ml PBS$^{-/-}$. Incubation with 5 ml 0,5 % Trypsin/EDTA at 37°C for 5 minutes was dissolving all tissue and was subsequently stopped by addition of 5 ml FCS containing BME medium. After centrifugation (2000 rpm/1minute), abolishment of the supernatant and resuspension in 1ml BME medium the glia cells were cultivated with a density of 50 000 to 60 000 cells/dish (Falcon, 35 mm) on 5 sterile uncoated coverslips per culture dish in 2 ml BME medium or on sterile uncoated coverslips in 24-wells containing 0,5 ml BME medium. When the glial cells were placed on coverslips in Falcon dishes, 2 hours before application of the cells 2 ml of BME was added and incubated at 37°C/5% CO$_2$/ 95% humidity. To establish glia microisland cultures the proliferation of the glial cells was stopped before they could grow to confluency by adding 10 µM ARA-C. 1 day after adding neurons to glial microislands the BME medium was changed to NB medium. Density and size of the glial microislands were chosen to result after plating of neurons in small networks of 10-20 neurons per island.

2.2.6 Preparation of "sandwich" cultures for immunocytochemical stainings for N-cadherin

N-cadherin is not only expressed by neurons, but also by glial cells. As ES cell-derived neurons had to be cultured on glial cells, it was difficult to distinguish the signals from N-cadherin expression in glia and neurons using immunocytochemical staining. Therefore so called "sandwich" cultures were prepared. L1-selected neurons without glia were applied on coverslips coated with PO and incubated for 1 hour at 37°C/5% CO$_2$/ 95% humidity. To ensure that all required metabolites were present during cultivation this coverslips were placed upside-down on a layer of glial microislands. For transfection or immunocytochemical staining/imaging the coverslips were turned over. After incubation time with the transfection reagents they were turned back again.

2.2.7 Isolation and Propagation of plasmid DNA

2.2.7.1 Transformation of bacteria

All vectors used in this study were propagated and maintained in TOP10 competent bacteria (Invitrogen). 1µg of plasmid DNA or 20µl of ligation mixture were applied to 100µl of TOP10 competent bacteria and incubated for 30min on ice. An incubation at 42 °C for 2 minutes and cooling down on ice for 3 minutes followed, before 800µl of LB-medium was added to the bacteria. After 30 minutes at 37ºC cells were centrifuged (10000rpm, 1min, RT), the supernatant removed and the pellet resuspended in 100µl LB medium. The cell suspension was plated on LB plates containing the appropriate antibiotics and incubated at 37ºC overnight (Sambrook and Russell, 2000).

2.2.7.2 Minipreps of plasmid DNA

(Sambrook and Russell, 2000; Amersham Pharmacia Miniprep preparation kit)

To isolate plasmid DNA 3ml LB/Antibiotic-Medium were inoculated with a single colony. After incubation overnight at 37ºC (300rpm agitation), cultures were transferred into 2ml Eppendorf tubes and centrifuged at 12000rpm for 1min. According to the protocol of the preparation kit plasmids were isolated from the bacteria. The DNA was eluted from the columns by addition of 50µl TRIS-HCl (10mM, pH 8.0) with subsequent centrifugation (12000rpm, 2min, RT).

2.2.7.3 Maxipreps of plasmid DNA

(Qiagen Maxiprep kit)

In order to propagate DNA, maxipreps of the plasmid DNA were used. A single colony was inoculated with 2ml LB-Antibiotic medium and left for growth at 37ºC for 8 hours (300rpm constant agitation). The culture was collected in 500 ml LB-Antibiotic medium and incubated at 37 °C overnight (300rpm constant agitation). The next day cells were centrifuged at 6000 rpm for 15 minutes at 4 °C, before the DNA was isolated according to the Quiagen maxiprep protocol. The air-dried DNA pellet was resuspended in 200-400 µl aqua dest. and the DNA concentration was determined using a spectrophotometer.

2.2.8 Transfection of ES cell-derived and neocortical neurons

All transfections were carried out using Lipofectamine 2000. Cationic lipid vesicles binding to DNA vectors form liposomes, which can fuse with the plasma membrane and thereby mediate the transport into the cell, where the DNA gets expressed. 3µl of Lipofectamine and varying dilutions of DNA (1,5 µg-7,5µg) were added separately to two Eppendorf tubes containing 50 µl NB medium I. After 5 minutes incubation time for stabilizing the pH, both tubes were mixed and incubated for another 20 minutes. Subsequently 800 µl of NB medium I was applied serving as incubation medium during transfection time. After collecting all medium from the culture into an Eppendorf tube, the lipofectamine/DNA mix was added to the cells with subsequent gentle shaking for an equal distribution. After incubation for 6-7 hours at 37°C/5% CO_2/ 95% humidity the DNA mix was discarded and 1 ml of fresh NB medium II together with 1 ml of the collected culture medium was added to the cells. Electrophysiological recordings were performed 2 days after transfection, immunocytochemical stainings as well as axonal and dendritic length/branch determination were accomplished 2 or 8 days after transfection. As the efficacy from Lipofectamine technique is very low, only one neuron per glial microisland was transfected making a defined situation of pre- and postsynaptic expression possible.

2.2.9 Peptide experiments

In some experiments N-cadherin antagonistic peptides or BDNF were applied to ES cell-derived N-cad -/- cultures transfected with EGFP or EGFP+N-cadherin in order to analyze their effect. In all cases the peptides/BDNF were added directly after transfection and analyzed 48 hours later.

2.3 Electrophysiological recordings

2.3.1 The "patch-clamp" technique

Developed between 1973 and 1976 by Erwin Neher and Bert Sakmann, the patch clamp technique was a massive improvement compared with all methods used until then in electrophysiological analysis. Due to this technique it was possible to isolate very small areas

of the membrane and record currents mediated by single ion channels in the range of a few pA. One of the other methods used already before the invention of the patch-clamp technique is the voltage-clamp technique, described for the first time in the 1930s by Cole and Curtis. Two microelectrodes are required for the technique, whereat a microelectrode means an Ag/AgCl-electrode connected with an amplifier and ending up in a glass pipette filled with an electrolytic solution. One of them is measuring the difference in the potential between the bath solution (extracellular solution) and the intracellular environment. By comparison of the measured potential and the command potential adjusted at the amplifier, the second electrode injects via a backcoupling mechanism a compensation current into the cell equating the aberration in potential and leading by this means to a constant membrane potential. Thus currents of whole populations of ion channels can be analyzed. Similar recordings are possible by the patch-clamp technique used in this work, whereas the biggest advantage hereby is the use of only one microelectrode.

In this work the glass pipettes were made of 10 cm borosilicate-glass (GB150 ETF 10, science products GmbH with an external diameter of 1,5 mm and an internal diameter of 1,17 mm). Via a DMZ universal puller (Zeitz) these were pulled out in several steps using different temperature and time adjustments resulting in two microelectrodes having a cone end of 1-2 µm diameter. A specific intracellular solution was filled into the pipettes and the cell culture media was changed to an extracellular solution. The pipette was put into a pipette holder including a silver wire coated with chloride and subsequently directed towards the cell using manipulators for crude adjustment. After dipping into the bath solution the pipette resistance could be calculated following Ohm`s law (R=U/I) and varied between 5-8 MΩ. When reaching the neuron with the cone end of the pipette, surface and diffusion potentials were compensated via the amplifier. Hydraulic micromanipulators for the fine adjustment were used to get closer to the cell surface until neuron and tip end were brought in line with each other. By assembling high pressure the solution in the pipette was floating towards the membrane, which could be retraced by a visible deformation of the cell surface. A following quick application of low pressure via air exposure led to an interplay of pipette edge and cell membrane causing the formation of a giga ohm seal resistance ("gigaseal"), thus leading to an isolation of the area which deemed inside the pipette ("patch").
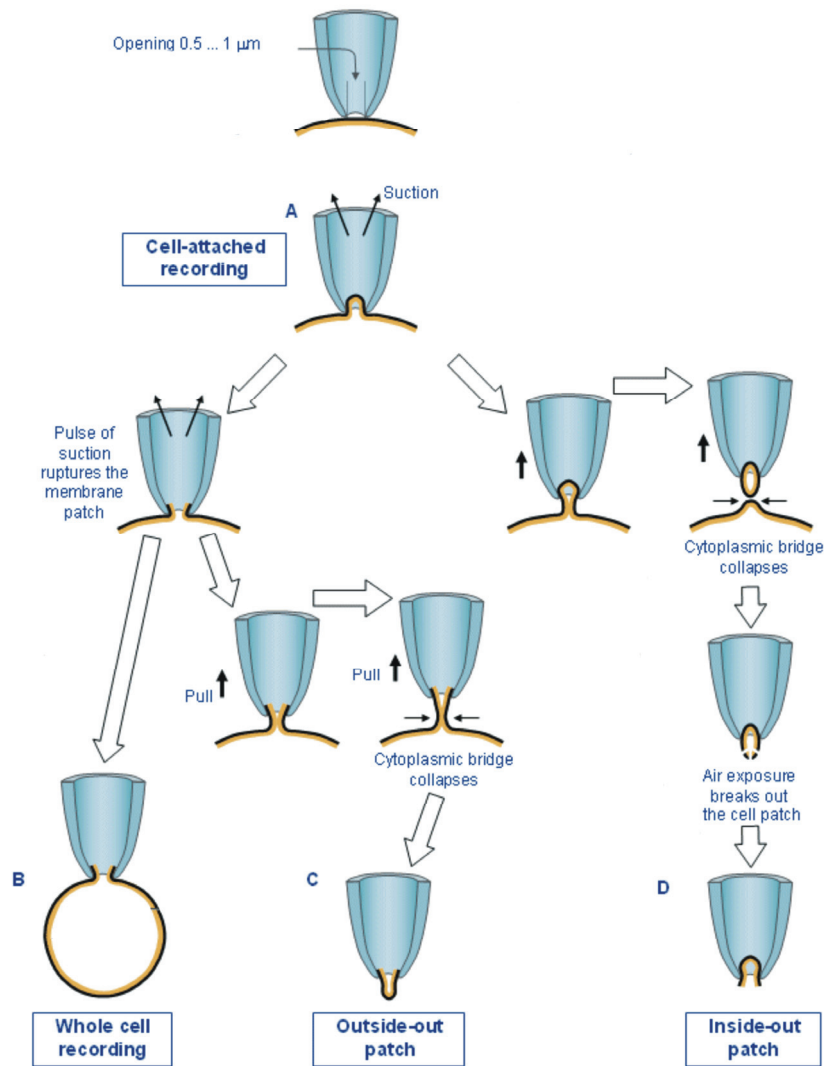
Figure 2.5. Illustration of the possible patch-clamp configurations.
(modified after Malmivou J. and Plonsey R., 1995)

The patch-clamp technique is characterized through the possible use of four different configurations (Figure 2.5).

After obtaining the gigaseal already the so called cell-attached configuration is set up. By retracting the pipette slowly the patch can be removed from the rest of the cell and the inside-out configuration is obtained. Hereby the cytoplasmatic side of the membrane is directed towards the bath solution, while the extracellular side faces the intracellular solution. Consequently the variation of different solutions and pharmaceutics at the cytoplasmatic side can be analyzed. The configuration which was used in this work is the whole-cell configuration. After obtaining the cell-attached configuration an increasing pressure on the patch inside the pipette leads to the disruption of the patch making a recording of whole cell currents possible. In this configuration the pipette solution diffuses into the cell.

[50]

By slowly retracting the pipette starting from the whole cell configuration the patch membrane closes in front of the pipette cone end, which is called the outside-out configuration. The extracellular side of the membrane is directed towards the bath solution and can be affected. All recordings in this work were carried out in the whole-cell configuration.

The use of only one electrode makes it necessary to use an electronic circuit that acts as current-to-voltage converter. The voltages to be compared are applied to both inputs of the operational amplifier (op-amp, figure 2.6).
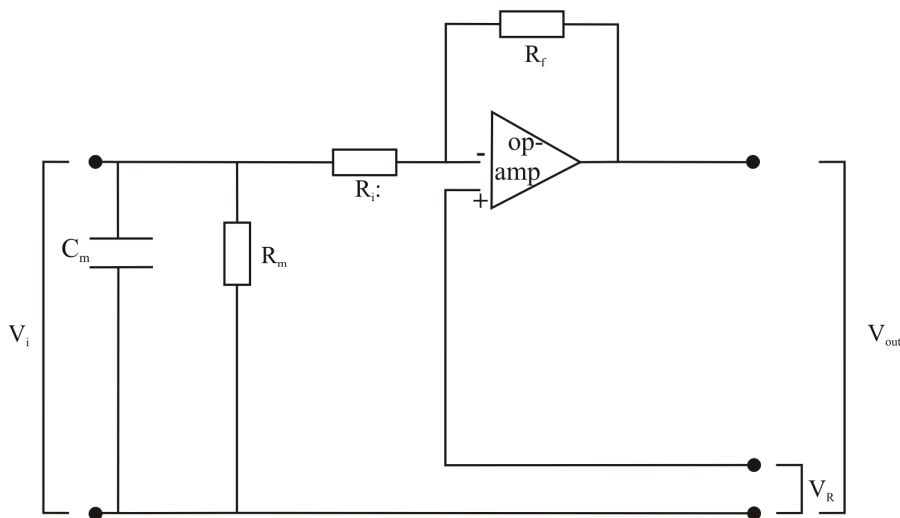

Figure 2.6. Circuit diagram of a patch–clamp recording.
C_m: capacitance of the cell membrane; R_m: resistance of the cell membrane; R_i: input resistance; R_f: feedback resistor; Op-amp: operational amplifier; V_i: difference in the potential between voltage at the reference electrode and effective voltage in the cell lumen; V_R: rated voltage; V_{out}: output voltage, proportional to the ion current flow, quantity to be measured.

The op-amp makes it possible to detect the cell potential (V_i) via the negative input (-), while the rated voltage (V_R) is applied to the positive input (+). This results in an output voltage corresponding to the difference of these two. A backcoupling mechanism allows the compensation of the difference by a current flow over the feedback resistor (R_f), which is connected to the negative input of the op-amp. The outcome of this is an equalized application of the rated voltage to the negative input and for that reason to the cell membrane. By reason of the very high input resistance of the op-amp, which should be ideally infinite and realistically constitutes around 10^{12} Ω, the current detected over the membrane can only flow into the pipette and to the feedback resistor, which causes that the voltage at the output of the op-amp (V_{out}) is after subtraction of V_R proportional to the current flow over the membrane I_m

[51]

($V_{out=}$ V_{R+} I_mx R_f). Thus the output voltage of the op-amp can be used as measured variable for the quantification of this current conduction. An immediate downstream differential amplifier isolates rated voltage and voltage corresponding to the current flow making a registration of it possible. The better the electrical connection between pipette and the cell lumen the lower is the input resistance. This means a better electrical conductance enabling a more precise measurement.

However, due to the destruction of the patch it is likely that small fragments of the membrane reach close to the pipette. This leads to an increase in the impedence, which results in a slower charge reversal of the membrane and therefore to a delayed compensation of the detected voltage and also to a delayed change in conductance. It may happen that the potential of the cell therefore differs to a certain amount from the rated voltage leading to unwanted depolarisations. The patch-clamp amplifier comes up with circuits, that compensate such depolarisations (C-fast, C-slow compensation).

2.3.2 The experimental setup

The most important components of the experimental setup are shown in figure 2.7. Central element was the inverted microscope (Zeiss, Axiovert 35M) encircled by a Faraday cage including two phase contrast objectives (10x: Zeiss, ACHROSTIDMAT; 10x/0,25 Ph1; 32x: Zeiss LD ACHROSTIGMAT 32x/0,40 Ph2) and an UV illumination (Mercury Short Arc Photo optic lamp, HBO 50 W/AC L1; Osram). Adequate filters (Filterset 17 "FITC" BP 485/20, FT 510, BP515-565) were controlled by a shutter (Vincent Associates, Uniblitz, model:VMM-D1). Additionally mounted on the microscope table was a patch electrode holder with appropriate preamplifier, one stimulation electrode and two micromanipulators (Narishige, Japan). To reduce vibration the microscope table was vibration-cushioned. In addition all cables and tubes were fixed at the table via rubber tape. Current flows were detected, amplified and filtered (low pass filter 3 kHz) using a patch-clamp amplifier (L/M-EPC-7; Comp. List, Darmstadt, Axon instruments). Stimulation pulses were given via a stimulator (SD 9, Grass Technologies, West Warwick, RI, USA). An A/D-D/A- converter (DigiData 1322A, Axon Instruments) digitized the data (4-30 kHz) with a digitizing rate of 10 kHz. All signals were displayed by the monitor of a personal computer and an oscilloscope (Tektronix 2212) and saved by the PC (Intel Pentium II, Software Pclamp 9.2, Axon Instruments).
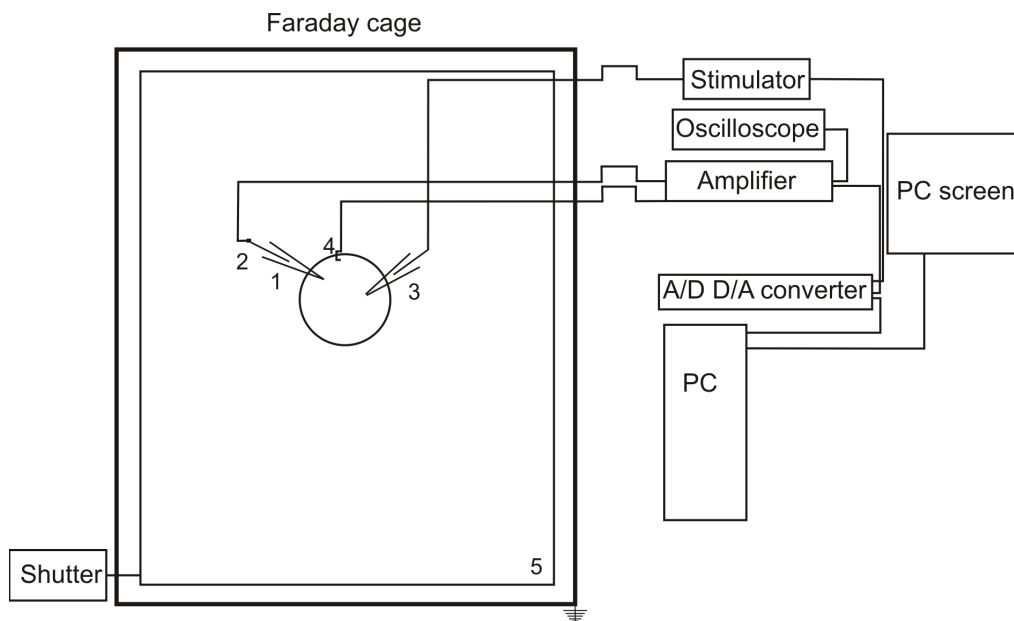
A
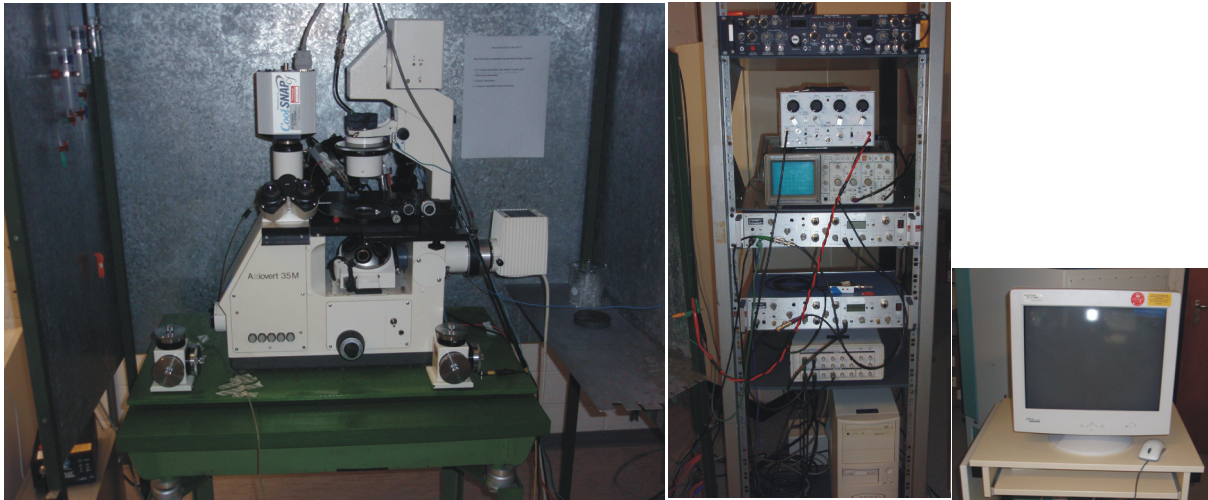
B

Figure 2.7. Illustration of the patch-clamp setup.
A Photos of the patch-clamp setup. **B** Schematic model of the central elements (1) patchpipette, (2) preamplifier, (3) stimulation electrode, (4) reference electrode, (5) microscope with brightfield and UV-illumination

2.3.3 Detection of spontaneous miniature postsynaptic currents (mPSCs)

All analyzed neurons were cultured either on glial microislands (mis-match and Neuroligin experiments) or on Poly-L-Ornithine (Neuroligin experiments, primary neurons) and had approximately the same density of neighboring cells (10-20). The cultures (DIV9-11) were either consisting of ES-cell derived N-cadherin deficient (Ncad-/-) neurons, N-cadherin heterozygous (Ncad+/-) neurons or of primary cortical wildtype neurons. All cultures were

transfected with different kinds of plasmids (EGFP; pMS 149.1; Ncad ΔE; Neuroligin1-GFP) as well as treated with different kinds of additions to the bath solution

The transfected neurons were distinguished from the non-transfected cells via fusion of the expressed proteins with the green-fluorescent protein or cotransfection with it by their fluorescence. In all experiments only the transfected cells were analyzed. A solution with a physiological concentration of sodium and potassium that contained a physiological concentration of magnesium and calcium (extracellular solution I) or a physiological concentration of magnesium but an elevated concentration of calcium (extracellular solution III) served as the bath solution. The elevation of calcium led to an increased vesicle release probability and therefore enhanced synaptic activity.

The pipette was filled with intracellular solution, which was in all cases physiological. To avoid action potential-activity (in order to isolate the miniature currents) 1μM TTX was added to the different extracellular solutions. The pharmacological separation of AMPA receptor-mediated mEPSCs from $GABA_A$-receptor mediated mIPCs was carried out via 10 μM Gabazine (blocking of $GABA_A$-receptor mediated mIPCs). NMDA receptor-mediated mEPSCs were prevented by 1mM $MgCl_2$ in the extracellular solution and the negative holding potential of -60 mV. After ending of each recording the mPSCs were tested by addition of 10 μM DNQX which blocks AMPA receptor-mediated mEPSCs. The duration of recording constituted 65,5 seconds.

2.3.4 Registration of evoked autaptic AMPA receptor-mediated postsynaptic currents (PSCs)

Autaptic AMPA receptor-mediated PSCs were recorded from cultures consisting of N-cad -/- neurons cultured on glial microislands (DIV9-11) and transfected with EGFP or EGFP + N-cadherin. Extracellular solution III served as bath solution. This solution is characterized through increased concentration of Ca^{2+}- ions in order to enhance presynaptic vesicle release making it possible to detect all autaptic currents. As Cs^+-ions reduce the conductance for K^+- ions KCl was replaced by Cesium methanesulfonate in the intracellular solution II. The prevention of $GABA_A$-receptor mediated PSCs was accomplished via 10 μM Gabazine, while NMDA receptor-mediated PSCs were blocked by 1 mM Mg^{2+} and a negative holding potential of -60 mV. The injection of 20 mV pulses (1 ms duration, 10s interval) through the patch pipette led to the generation of an action potential at the axon hillock. Conducted along the axon it reached the presynaptic terminal, where the resulting calcium-inward current

initiated an enhanced fusion of vesicles with the presynaptic membrane. The resultant neurotransmitter release triggered postsynaptic currents, which could be detected by the same patch pipette that injected the pulse in case the presynaptic terminal made a synapse on its own processes. 40 pulses per cell have been recorded and analyzed.

## 2.3.5 Registration of evoked NMDA receptor-mediated excitatory postsynaptic currents (EPSCs)

The registration of evoked NMDA receptor-mediated PSCs was carried out on primary cortical neurons cultivated on PO coated culture dishes (10-12 DIV) and transfected with different kinds of plasmids (EGFP; Neuroligin1-GFP; N-cad ΔE). Extracellular solution II, which contained no magnesium served as bath solution. The lack of magnesium ions, which under physiological conditions block the NMDA receptor channel at negative potentials, made it possible to record NMDA receptor-mediated inward currents at -70mV holding potential. AMPA receptor-mediated and GABA$_A$-receptor mediated PSCs were blocked by addition of 10 µM DNQX and 10µM Gabazine to the bath solution. After detecting a transfected neuron under UV-light a second microelectrode ending up in a glass pipette filled with extracellular solution II and 1M NaCl in a ratio 1:1 was placed near the processes of the cell. The controlled destruction of the glass at the cone end by touching the base of the culture dish resulted in a tip diameter of approximately 10µm. After patching the depicted neuron with the first microelectrode the second electrode was used to extracellularly stimulate the neuron by electrical pulses (20 seconds interstimulus interval, maximal stimulation). The resulting depolarization led to fusions of vesicles at the presynaptic terminals and NMDA receptor-mediated EPSCs. Subsequent addition of 20 µM MK-801 initiated a progressive block of these, which could be recorded and saved on the personal computer. At least 5 control pulses before the blockage were given. The stimulator with adjustable strength was triggered by the A/D D/A converter.

2.4 Imaging experiments

2.4.1 Imaging setup

All images were taken with an inverted axiovert 200M deconvolution microscope (Zeiss) equipped with a 63 x oil-immersion objective (Zeiss, plan apochromat; 63x1,4; 113-106) and a 10 x objective (Zeiss, ACHROSTIDMAT; 10x/0,25 Ph1). Images were captured by a 12-bit monochrome CoolSNAP ES Charged-Coupled-Device (CCD) camera using MetaVue 7.5.6 software (Visitron Systems) demonstrated in figure 2.8.

A

B

Brightfield-shutter

Fluorescence-shutter

PC screen

CCD camera

PC

1

[56]
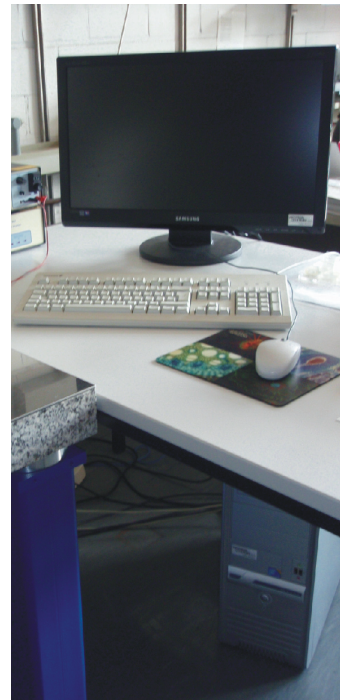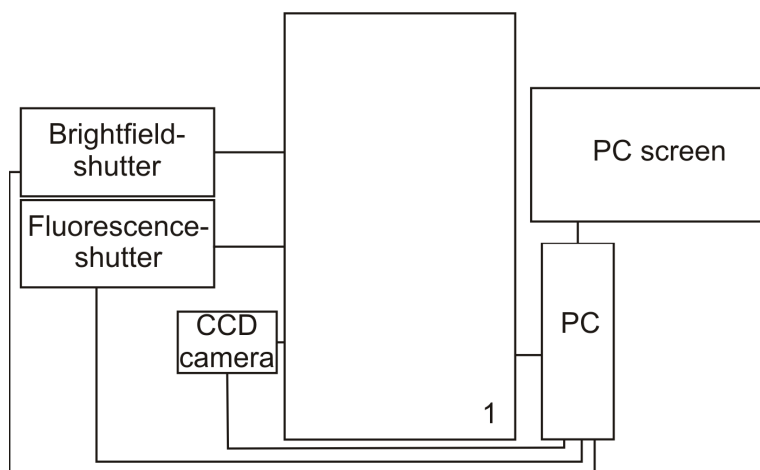
Figure 2.8. Illustration of the imaging setup.
A Photo of the imaging setup. **B** Schematic illustration of the imaging setup (1) microscope with brightfield and UV illumination.

Adequate sets of filters were obtained from Zeiss (Filterset 49 "DAPI" G365, FT395, BP 445/50; Filterset 43 "CY3 " BP 545/25, FT 570, BP605/70; Filterset 17 "FITC" BP 485/20, FT 510, BP515-565). Brightfield and fluorescence illumination was controlled by two appropriate shutters (Vincent Associates, Uniblitz, model: VMM-D1).

2.4.2 Immunocytochemical stainings

Immunocytochemical staining procedures enable the detection of proteins inside cells. For example, accumulations of the presynaptic vesicle-associated protein VAMP2 and the postsynaptic density-associated protein PSD95 can be used as evidence for pre- and postsynaptic terminals (Gottmann et al., 1994). At the same time it is also possible to directly show the expression of specific proteins such as N-cadherin. Through coimmunocytochemical stainings using different fluophores for multiple proteins even the localization of proteins at synaptic sites can be detected. All immunocytochemical stainings were performed at different maturation stages of N-cad-/- neurons cultivated on glial microislands and in most cases transfected with different vectors (N-cadherin, DsRED2-VAMP2, EGFP, PSD-95-GFP). As N-cadherin is also expressed by glial cells the detection of N-cadherin expression was carried out on neurons cultivated in "sandwich" cultures (see 2.2.6).

To get rid of remaining medium and cell debris the cells were washed twice with 2 ml PBS$^{+/+}$ and subsequently fixed in 4% Paraformaldehyd solution for 20 minutes. After thrice washing with 2ml PBS$^{+/+}$ for each 5 minutes the cells were permeabilized by incubation in blocking buffer I containing Triton-X 100 for 30 minutes. In order to saturate unspecific binding sites additionally BSA was applied to this buffer. Subsequently a primary antibody raised against the protein desired to be detected was added (in blocking buffer I; dilutions from 1:500-1:1666) and incubated either overnight at 4°C or for 1 hour at room temperature. Remaining primary antibody was removed by thrice washing with 2 ml PBS$^{+/+}$ for 10 minutes each, before the secondary antibody was applied (tagged to fluorescent dyes; light protected in blocking buffer II; dilutions from 1:12,5-1:1000). Washing thrice more with 2 ml PBS$^{+/+}$ for 10 minutes each abolished leftovers of the secondary antibody, making the cells ready for being imaged via UV-illumination using a 63x oil-immersion objective (2x2 binning, 0,2 –1 s exposure time).

2.4.3 Visualization of axonal and dendritic processes

The analysis of axonal and dendritic arborization in mis-match and control situations were performed on cultures consisting of neurons derived from Ncad-flox mice or C57Bl/6 mice. Ncad-flox or C57Bl/6 neurons were cultured on glial microislands and transfected with pBS598 EF1alpha-EGFPcre (CreGFP). For the purpose of distinguishing transfected neurons the Cre protein was fused to EGFP. As the CreGFP fusion gene product rapidly targeted the nucleus of the cells, a cotransfection with EGFP was necessary to make all processes detectable. At different maturational stages images were taken using a 10x objective, UV-illumination and a corresponding filter set (2x2 binning, 0,5-1 s exposure time).

2.5 Protein biochemistry

All following steps have been carried out on ice unless stated otherwise.

2.5.1 Analyzing protein-protein interactions using coimmunoprecipitation

2.5.1.1 Principle of coimmunoprecipitation

Various biochemical techniques are available for searching molecular interaction partners of proteins. In this work the coimmunoprecipitation technique was used to look for protein interactions with the postsynaptic N-cadherin. Immunoprecipitations are precipitation procedures by which a known antigen, N-cadherin, is pulled down out of a brain homogenate by a specific antibody. In this way not only the antigen gets pulled down, but rather the whole protein complex, with which this protein is connected. Via immunochemical reactions (Western blot) certain proteins assumed to interact with N-cadherin can then be tested for being interaction partners.

2.5.1.2 Preparations before coimmunoprecipitation

2.5.1.2.1 Activation of sodium orthovanadate

Sodium orthovanadate is an essentiell component of the RIPA-buffer, a main buffer used in the coimmunoprecipitation. Activation depolymerizes the vanadate, converting it into a more

potent inhibitor of protein tyrosin phosphatases (Gordon J, 1991). After preparing, a 200 mM sodium orthovanadate solution got adjusted to pH10, which makes it turning yellow. Boiling for 10 minutes removes all color and the cooled down solution got subsequently readjusted to pH10. These steps were repeated until the solution stays colorless and stable in pH.

2.5.1.2.2 Brain homogenization

For coimmunoprecipitation experiments brains of P6 mice were used. Before proteins could be pulled down, these had to be homogenized. After decapitation of the mice, the brain were removed like described in chapter 2.2.4 and immediately homogenized in 0,5 ml homogenization buffer using a homogenizer (Kimble Kontes LLC, Kontes Gerresheimer). By screwing the homogenizer very gently up and down the brains got crushed into a uniform homogenate. 1:50 diluted probes were prepared to estimate protein concentrations (in homogenization buffer). To homogenization buffer and later used RIPA (Lysis-) buffer a general EDTA-free protease inhibitor cocktail, the matrix metalloprotease inhibitor GM 60001, the γ-secretase inhibitor DAPT and specific inhibitors for certain serine and cysteine proteases were added to prevent proteolysis.

2.5.1.2.3 Determination of the protein concentration

The protein concentration was determined using the BCA protein assay kit. Therefore BSA standards from 0,1 mg/ml, 0,2 mg/ml, 0,5 mg/ml, 0,8 mg/ml and 1mg/ml for the calibration curve and samples of the 1:50 diluted brain homogenates were prepared, vortexed and added to a 96-well-plate (Nunc; 10μl each). 200 μl of reagents A and B (50:1) of the BCA kit were applied and after gentle agitation the plate was incubated for 30 minutes at 37°C. Due to this procedure Cu^{2+} protein complexes formed under alkaline conditions and got quickly reduced to Cu^{1+} by several amino acids such as tryptophan. The more protein was present the more Cu^{2+} got reduced. BCA bound to Cu^{1+} turning the color of the formerly green solution into different shades of purple, depending on the amount of reduction of alkaline Cu^{2+} and therefore on the protein concentration. The absorbance of each sample at a maximum of 562 nm measured by a spectrometer (software: Fluostar) mirrored this amount and by the measured values a standard curve of absorbance could be prepared. The protein concentrations of the original sample were determined from the amount protein, volume/sample, and dilution factor via the usage of Microsoft Excel.

2.5.1.2.4 Lysis

After the protein concentration was determined 1 mg of protein was taken for further analysis. The homogenized brain tissue had to be lysed in order to break down the cells and obtain cell lysates comprising the various proteins. Therefore 1 ml of RIPA buffer was applied to the volume of the sample containing 1 mg protein and incubated for 1-2 hours constantly rotating at 4 °C. For releasing adequate amounts of protein the lysis buffer contained non-ionic detergents such as NP-40 and ionic detergents like deoxycholate acid and SDS as main constituents for the disruption of the cell membrane. As proteolysis, dephosphorylation and denaturation began as soon as lysis occurred, previously described inhibitors were added and the procedure was carried out on ice. A centrifugation step of 15 minutes at 15000 g and 4 °C was necessary to remove all uncrushed and unlysed pieces, which were collected in the pellet. The supernatant was used for further coimmunoprecipitation.

2.5.1.3 Coimmunoprecipitation

2.5.1.3.1 Blocking of BDNF-TrkB interaction with TrkB/Fc

To ensure giving N-cadherin and TrkB a chance to interact without BDNF eventually disturbing this, BDNF was sequestered by truncated forms of TrkB (TrkB/Fc) applied to the cell lysates before starting the coimmunoprecipitation. These so called "receptor bodies" are homodimers containing the ligand-binding domain of the TrkB receptor followed by the hinge and Fc$_\gamma$ region of human IgG1 (Glass et al., 1996). BDNF is scavenged by theses false receptors and therefore hindered to bind at endogenously expressed TrkB receptors in a competitive manner. TrkB/Fcs have been shown to be highly specific antagonists to BDNF (Shelton et al., 1995; Binder et al., 1999). 1µg/ml of TrkB/Fc or a vehicle (0,1 % BSA in PBS) was added to the cell lysates and incubated for 3 hours on a rotating wheel at 4°C.

2.5.1.3.2 Pre-clearing of the cell-lysates

Subsequently to the treatment with TrkB/Fc the cell lysates had to be cleared from it. Therefore the cell-lysates were pre-cleared. During this procedure all proteins that bind immunoglobulins unspecifically will be removed, so that additionally the possibility of unspecific binding to the later added antibody is decreased. 25 µl of A/G-agarose beads were

added to the supernatant and incubated for 3 hours on a rotating wheel at 4°C. ProteinA/G is a genetically-engineered gene fusion product expressed in E.coli combining characteristics of protein A and protein G. Both of these proteins find their origin in the cell membrane of bacteria and show strong binding to immunoglobulins with a special affinity to the isotype IgG. Because of the gelling character of agarose, protein A/G and bound immunoglobulins can be easily separated from non-bound immunoglobulins by coupling protein A/G to agarose coated beads. By a centrifugation step (1000g, 5 minutes, 4 °C) the beads and all unspecific bindings could be wasted together with the pellet.

2.5.1.3.3 Antibody binding and pull-down of N-cadherin protein complexes

In order to precipitate N-cadherin 10 µg of an N-cadherin antibody was added to the supernatant. As a control for the specificity of the antibody a preimmune serum (IgG) was added in each experiment to a second sample. During incubation for 24 hours on a rotating wheel at 4 °C the antibody was given time to bind all N-cadherin protein complexes. After this time A/G agarose beads (25 µl) were applied and incubated for 3 hours (rotating wheel, 4°C) this time binding all N-cadherin protein complexes coupled with the IgG antibody/preimmune sera. Followed by a centrifugation step (1000g, 5minutes, 4°C) these could be collected in the pellet. Nevertheless it was necessary to wash the beads in order to decrease the possibility of unspecific binding further. Therefore 1 ml of RIPA buffer was added to the pellet and everything was mixed by turning the eppi 7 times upside-down. After centrifugation (1000g, 5 minutes, 4 °C) the supernatant was removed and the washing procedure repeated until the beads have been washed overall for 5 times. The last washing step was carried out in homogenization buffer to remove detergents interfering with the following steps. To detect the N-cadherin protein complexes the proteins had to be separated from each other, which was done by use of a SDS-polyacrylamide gel electrophoresis (SDS-PAGE).

2.5.1.3.4 Preparation of the protein-coupled beads for SDS-polyacrylamide gel electrophoresis

Before being able to analyze the proteins by SDS-PAGE the beads had to be separated from them. Therefore 45 µl of homogenization buffer and 45 µl of Laemmli buffer/ β-mercaptoethanol were added to the pellet, gently vortexed and shortly spinned down.

Incubation at 100 °C for 5 minutes shaked the proteins up, resulting in a settling down of the beads at the bottom of the Eppendorf tube, while the proteins remained in the supernatant. The presence of Laemmli buffer/ β-mercaptoethanol was one of the essentiell components in preparing the proteins for Western blot. While β-mercaptoethanol breaks down all disulfide bonds of the proteins for a better separation, SDS changed the charge of each positive charged protein to a negative one in proportion to its mass by binding to them in a constant weight ratio of 1.4 g/g of polypeptide. At the same time it denatured the proteins. Thus the proteins could be separated by size. The boiling procedure supported binding to SDS. Glycerol and bromphenolblue were important for enabling loading the samples on a SDS-polyacrylamide gel. While bromphenol blue was used as sample indicator dye, Glycerol increased the weight of the sample in order to keep it in the loading pockets reducing outspilling and loss of protein during loading procedure.

2.5.2 Verifying the genotype in N-cad+/- / N-cad-/- ES cell lines

For verifying the genotype in N-cad +/- and N-cad -/- lines, a Western blot was performed. Therefore 12 days cultured EBs in the last differentiation step (in NB medium) were collected using a cell scraper. After 30 minutes incubation in 0,3 ml RIPA buffer at 37°C they were homogenized by two needles with different tip openings fixed to a syringe. The protein concentration was determined and 1µg/µl of protein was applied to the SDS-polyacrylamide gel. As control a brain of a P6 mouse was homogenized and determined according to procedures described before (1µg/µl). All samples were prepared for SDS-PAGE by adding 2x Laemmli buffer/ β-mercaptoethanol (60µl) and TRIS-buffer (50mM, pH 7,5; concentration according to final concentration of 1µg/µl), vortexing and boiling them for 5 minutes at 100°C.

2.5.3 Detection of proteins in tissue homogenates using Western blot

2.5.3.1 Separation of proteins by SDS-polyacrylamide gel electrophoresis
(Laemmli, 1970)

Via the SDS-PAGE proteins of different sizes can be separated. Depending on the size various concentrations of acrylamide/bisacrylamide in the resolving gel, which accounts for the lower and main part of the gel, should be used. Activated acrylamide starts to form

quickly long chain polymers which are cross-linked by bisacrylamide resulting in polymerized meshed gels. It is considered that with increasing the percentage of acrylamide/bisacrylamide, the pores size of the gel mesh decreases. Accordingly a high concentration should be chosen for small proteins, a smaller one for large proteins. Therefore three different concentrations were applied in this work. In order to verify the genotype of N-cad +/- and N-cad -/- lines (N-cadherin: 135 kDa) which included the comparison with a loading control (Actin: 42 kDa) a 12 % gel was prepared. For the coimmunoprecipitation experiments two different concentrations were used, 8 % for the immunoprecipitation of N-cadherin (135 kDa) and the coimmunoprecipitation of pan-TrK (140 kDa) and 10 % for the coimmunoprecipitation of p75^{NTR} (75 kDa). The stacking gel cast over the resolving gel is a large pore gel of 4 %. Together with the fact, that this gel has also a lower pH than the resolving gel, these conditions are responsible for the right conductivity and therefore a thin and equal starting zone of all proteins. Ammonium persulfate and TEMED served as catalysts for polyacrylamide gel polymerization and were added as last compounds to the gel-mix, before it was poured. An electric field was applied across the gel making the negatively charged proteins migrate away from the upper negative cathode towards the positive anode at the bottom. The voltage was set to 60 V for the stacking gel and to 120 V for the resolution gel. Thereby smaller proteins migrate much faster than larger ones, facing reduced resistance due to the pores of the gel. This results in the separation of proteins regarding their size, which can be determined due to the loading of a marker running along with the proteins.

2.5.3.2 Electrophoretic transfer

After the proteins had been separated via the SDS-PAGE by their size they got transferred to a nitrocellulose membrane. Therefore the gel was first placed on the membrane. Both were wrapped with one filter paper (Whatman) and additionally 1 sponge (Bio-Rad) on both sides each. The entire stack got placed into a transfer chamber connected to a power supply. Via the application of 90 V for 2,5 hours the proteins got pulled from the gel onto the membrane without loosing their separation. Through reciprocal actions (hydrophobic and charged interactions) the proteins bound to the membrane enabling to analyze them.

2.5.3.3 Immunological detection of proteins on nitrocellulose membrane

To approve the presence of specific proteins immunological detection via protein-specific antibodies was used. As the nitrocellulose membrane has been depicted based on its ability of protein binding, first unspecific binding had to be blocked. After washing the membrane for 5 minutes in TBS-T, it was incubated in 5 % skimmed milk reconstituted in TBS-T for 30 minutes under constant agitation. All unspecific binding sites got saturated, so that the later applied antibody could only attach on the binding sites of the specific proteins. Tween-20 as component of TBS-T serves hereby as detergent. The membrane was transferred into a 50 ml Falcon-tube containing 15 ml of the primary antibody and incubated at 4°C under constant rotation overnight. Washing of the membrane for 6 times (each 12 minutes) with TBS-T removed all unbound primary antibody, so that subsequently the membrane could be incubated with a fluorescent labelled secondary antibody coupled with an near-infrared dye for 2 hours (constant agitation, light protection). Another washing procedure (6 times, 12 minutes each) eliminated all leftovers of the secondary antibody and the membranes were ready for the detection of the probes. Using the odyssey infrared imaging system equipped with a photosensoric scanner and appropriate emission filters (LI-COR Biosciences; Nebraska, USA) the detected proteins were visualized and an image of the Western blot was taken. The IRDye800CW coupled to the secondary antibody has an excitation wavelength of 778 nm and an emission wavelength of 795 nm.

2.6 Analysis and statistical evaluation

2.6.1 Analysis of electrophysiological recordings

For quantitative analysis of postsynaptic miniature-currents (amplitudes, frequencies, rise and decay times) the programs Minianalysis (Synaptosoft) and Sigmaplot 9.0 (Jandel Scientific) were used. All detection values were automatically preset by taking the AMPA receptor-mediated EPSC suggestion parameters corresponding to typical properties included in the program, which could be manually modified for correct calculation. The area under the curve value threshold ($2\mu m^2$) and the amplitude threshold (5pA, modified) were restrictive factors to distinguish signals from noise peaks. Rise time, decay time and amplitude were automatically calculated according to figure 2.9, setting points for calculating the baseline, the

maximal amplitude, rise and decay times. The rise time was calculated as the interval between 10% and 90% of the maximal amplitude.
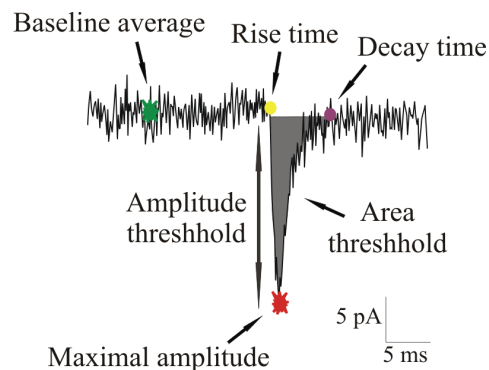

Figure 2.9 Automated detection of AMPA receptor mediated mEPSCs by Minianalysis.
Single AMPA receptor mediated mEPSC and the most important parameters for its detection.

Amplitudes and failure rates of evoked autaptic AMPA receptor-mediated currents as well as maximal amplitudes and decay constants (τ) of evoked NMDA receptor-mediated currents were analyzed using Clampfit 9.0 (Axon, Molecular Devices) and Sigmaplot 9.0. Maximal amplitudes were calculated in Clampfit using two cursors. Progressive blocks of NMDA receptor-mediated currents (MK801) and corresponding τ-values were obtained by bi- or monoexponentiell fits performed in Sigmaplot.

2.6.2 Digital image processing and analysis

Analyses of images were performed via MetaMorph, MetaVue 7.6.3 software, AutoDeblur (Visitron Systems), Microsoft Excel and Sigmaplot 9.0. To analyze length and branching points of neuronal processes 2D images were taken. Regarding all other imaging experiments 3D Z-stack images (images along the z-axis perpendicular to the image plane) with 1µm depth and adjustable top and bottom levels were taken using the motorization of the microscope.

2.6.2.1 Analysis of 2D-images

To reconstruct neuronal processes fluorescent images were loaded in Metavue. After calibration of the images, all processes were traced using a polynomic region tool creating a mask of all dendrites and the axon. The length was measured automatically, while the branch tip number was counted manually. All further analysis was made using Sigmaplot.

[65]

2.6.2.2 Analysis of 3D Z-stack images

All analysis involving the processing of Z-stack images were performed offline in Metamorph. The following operations were applied in order to remove background noise and enable quantitative measurements.

2.6.2.2.1 3D deconvolution of Z-stack images

The deconvolution operation was performed using the AutoDeblur software. The purpose of this method is to create sharpened images of out-of-focus point sources of light that occur in 3D images throughout multiple confocal planes (z-stacks), thus improving the signal-to-noise ratio. The basis of the deconvolution principle is that the aperture of every lens is finite. The collected light is spherical aberrated, meaning that not the entire emitted light from one point source of light can be collected. These points rather appear as complex double-coned 3D shapes. The deconvolution algorithm basically reverses this optical distortion along the pathway a point source of light takes. Hereby a main step is to define how much out-of-focus light is expected as characterized by the mathematical function describing the spread of light emanating from a point (point-spread function, PSF). The result will be an undistorted 3D image, redistributing the out-of-focus light to the point of origin.

Defining the true PSF is impossible, due to for example axis aberrations of objectives, but the software algorithm that forms the basis of the deconvolution theoretically calculates an approximation to it. The AutoDeblur software uses the most common and complete suite of 3D algorithms, which describe the imaging process on a microscope. The simplest formula involves three variables, the **PSF(X,Y,Z),** the information derived from the original 3D image **B(X,Y,Z),** and the actual distribution of light in the 3D image **S(X,Y,Z)**. The variables B and PSF are mostly known or can be calculated, the finding of S is described as the deconvolution. Their relation is generally accepted as

$$\textbf{B(X,Y,Z)= S(X,Y,Z)©PSF(X,Y,Z).}$$

© is understood as the mathematical convolution function describing contrary to the deconvolution function the degree of blurring of the original image (figure 2.10). Depending on the properties of the used lens, a sharp image appears as convoluted blurry image with the shape of the lens. Reversing this, the actual sharp image can be obtained by deconvolution of

[66]

the blurry image using the properties of the point-spread function. The deconvolution function detects the edges of point sources of light in the original image, centers the PSFs at each point and sums the contributions of all shifted PSFs up.
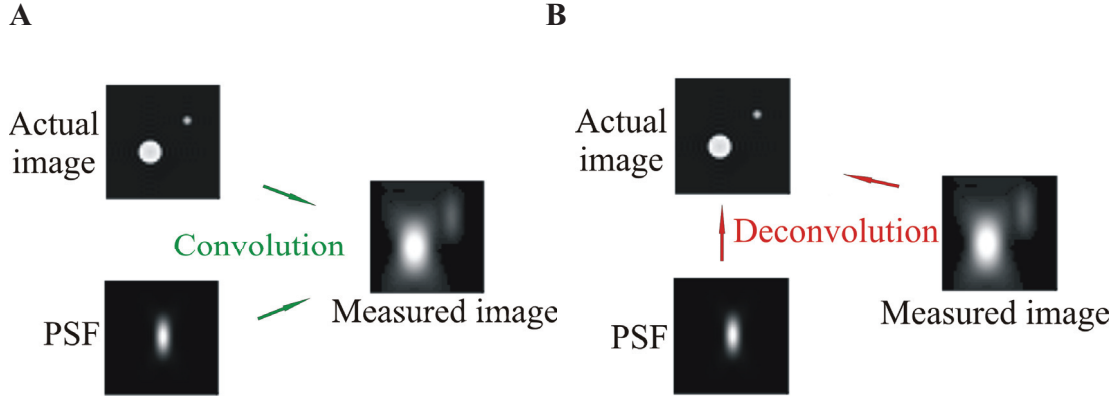

Figure 2.10. Illustration of convolution and deconvolution processes.
(Modified after http://en.wikipedia.org/wiki/File:Convolution_Illustrated_eng.png)
A The convolution function describes the blurring of an image. **B** Deconvoultion reverses the process of optical distortion.

In this work a special deconvolution algorithm, the Blind Deconvolution algorithm, has been used. This function considers PSF to be unknown, making it necessary to systematically try different possible PSFs and detect whether the image has improved. This application of various iterations of the algorithm helps avoiding unrealistic solutions. The only informations are hereby the technical ones about the used objective and the information derived from the original image (**B**). During a single iteration first **PSF** gets assumed, whereby then **S** that could have caused **B** can be estimated. A second calculation starting the other way round follows. Based on the estimated **S, PSF** that could have caused **B** can be deduced. These two steps are repeated in 10 iterations creating the final restored image of the formerly out-of-focus point sources of light.

All deconvolved images were further processed by creating a maximum intensity image. Therefore the maximum image tool takes the maximum value of intensity for each pixel location over all various images in the z-axis and creates from these values a new image.

2.6.2.2.2 Autothreshold operation of maximum images

The autothreshold function was used to differentiate between signal and noise. In order to simplify measurements for all further operations not the entire images were analyzed, but

regions of proximal dendrites were cut from it and further processed. The autothreshold function distinguishes between signal and noise using the histogram distribution of all pixels. Three steps define thereby background or signal. First the largest peak with a width based on noise in the histogram is considered to represent the background. Based on this the local minimum, which is defined as being the trough between background and object level gets determined. The third step then calculates the number of pixels selected. Are less than 1% of the pixels above the threshold, an earlier peak gets defined as background peak and the largest peak is considered to be the signal peak. If no earlier peak can be found, all pixels higher than 2x standard deviation are considered to derive from the signal. Pixels above the threshold appear as coloured objects on black background.

2.6.2.2.3 Low-pass filter operation

The low-pass filter was applied to obtain a correction of single pixels lying above the threshold and therefore appear to be signal, but originally derive from background noise. The principle of a low pass filter is to let elements with low frequencies below their cutoff frequency pass, while high frequencies above this limit are attenuated. The high frequency details of an image such as the perturbing single noise pixels are characterized through lots of abrupt tonal transition changes from pixel to pixel. For every pixel the filter operation calculates the average intensity of a defined region surrounding (3 pixels x 3 pixels) and centers it on the pixel. By this the edges of every pixel get blurry resulting in a smoothed image, in which every pixel is modified depending on the neighbor pixels. Accordingly single pixels without any neighboring pixels being within the threshold are removed.

2.6.2.2.4 Density and Colocalization Analysis

To define the puncta to be counted and further analysed, the region tool "create regions around objects" was applied to the lowpass images. The tool automatically draws a region of interest around all previously thresholded and filtered clusters. These regions were considered as puncta. In order to analyze the colocalization of two puncta the fluorescent images of both signals were merged. A puncta was considered colocalized as long as at least 1 pixel of the created regions belonging to the two fluorescent signals was overlapping.

2.6.2.2.5 Analysis of mean area and mean intensity

For the automated measurement of mean area and intensity of immunocytochemically stained VAMP2 puncta the lowpass filtered images including previously described defined regions of interests were further processed. Therefore the integrated morphometry analysis command combined with classifier filters restricting the measurement to clusters bigger than 8 pixels was used. The detection of the mean intensity required a background subtraction. This demanded the definition of a ~200 pixel big region outside the signal, from which the mean intensity was measured and later subtracted from the analyzed pixels. All values were logged via Microsoft Excel and further processed in Sigmaplot.

2.6.3 Analysis of biochemical experiments

The visualisation of fluorescently labelled protein bands on Western blots was done using the Odyssey infrared imaging system (LI-COR Bioscience). Therefore secondary antibodies were tagged with near-infrared fluorophores that could be detected by a fluorescence detection channel.

2.6.4 Statistical evaluation

For statistical analysis and illustration all data were imported into Sigmaplot 9.0. Statistical evaluation of mean value and standard error (shown as error bars) were made by using Sigmaplot 9.0. The significance was ascertained via Student`s t-test for two groups of values or one-way ANOVA for three groups. A difference was considered significant from $p < 0,05$ (*=$p < 0,05$; **= $p < 0,01$). Figures were further processed in CorelDRAW Graphics Suite 12.0.

3. Results

3.1 Functional properties of glutamatergic synapses with an asymmetric N-cadherin expression

Classical cadherins, such as N-cadherin, are thought to be pivotal for the proper wiring of the CNS. Especially N-cadherin has come under scrutiny as a recognition molecule due to its strong homophilic binding properties. Accordingly, an asymmetric "mis-match" expression of N-cadherin might lead to an elimination of inappropriate connections, which is a common step in defining synaptic circuits. In the first instance general properties of synapses with an asymmetric expression of N-cadherin were studied. Therefore, an assay system had to be created in which N-cadherin expression is restricted to only one side of the synapse. Previous data using chimeric cultures suggested no strong functional alterations when N-cadherin was present only presynaptically (Jüngling, 2006, effects on short-term synaptic plasticity), so that this study refers to asymmetric expression as synapses in which N-cadherin expression is limited to the postsynaptic side. As the elimination of synapses rather than their formation was in the focus of the study, mature ES cell-derived neurons at 11-19 DIV (in later experiments also at 7-22 DIV) have been evaluated. N-cadherin expression in mature neurons is restricted to excitatory synapses (Benson and Tanaka, 1998). Hence, inhibitory synapses were blocked by the addition of Gabazine and were not studied.

3.1.1 Generation of an asymmetric N-cadherin expression

To obtain asymmetric expression of N-cadherin at individual synapses, (postsynaptic only), N-cadherin deficient (Ncad-/-) neurons derived from embryonic stem cells were grown on glial microislands (10-20 neurons/island) and postsynaptically transfected with N-cadherin. Due to the use of the Lipofectamine technique, which has a very low efficacy, only one neuron per island was transfected. This neuron could be specifically defined as the postsynaptic N-cadherin expressing cell, while all other neurons on the island were N-cadherin deficient presynaptic cells (see fig. 3.2A). For visualizing the N-cadherin transfected neurons cotransfection with EGFP was used. Via the comparison with neurons postsynaptically solely transfected with EGFP, the influence of asymmetrically expressed N-

cadherin on synaptic transmission should be figured out. The time point of transfection was at 9-11 DIV; all analysis was carried out 2-8 days later.

3.1.1.1 Characterization of N-cadherin deficient (Ncad-/-) neurons

Before establishing the N-cadherin mis-match system, the ES cell-derived N-cadherin deficient neurons were characterized. Two N-cadherin heterozygous ES cell-derived lines (Ncad+/-) were used as control, as all have a similar genetic background due to their isolation from littermate blastocysts (Moore et al., 1999). Their level of N-cadherin expression has been shown to be similar to wildtype cells (Ncad+/+; Jüngling et al., 2006). Both Ncad+/- lines displayed distinct karyotypes (XX, XY); the Ncad-/- line had an XX-karyotype. For verifying the genotype in all three lines ES cell-derived embryoid bodies (EBs) were allowed to grow for 12 days and analyzed via Western blot analysis. The expression of N-cadherin in both Ncad+/- lines was confirmed, while N-cadherin expression was completely missing in the Ncad-/- line (Fig. 3.1A). This result could be approved by immunocytochemical stainings against N-cadherin of Ncad+/- and Ncad-/- ES cell-derived neurons, respectively. Whereas N-cadherin, corresponding to its synaptic expression, was evidently detectable in a punctate appearance (green signal, Oregon green) in Ncad+/- neurons (n=30), no N-cadherin staining could be obtained in Ncad-/- neurons (n=24) (Fig. 3.1C). Both genotypes expressed the synaptic marker VAMP2 (Synaptobrevin2; Fig. 3.1C; red signal, Cy3), which was colocalized with the N-cadherin puncta in Ncad+/- neurons (Fig.3.1C, for detailed analysis see Fig. 3.3B). As expected from staining presynaptic vesicle clusters, VAMP2 had a punctate distribution. Moreover, similar morphologies of the ES cell-derived neurons with distinct genotypes were evident in phasecontrast images at 12 DIV (Fig. 3.1B).
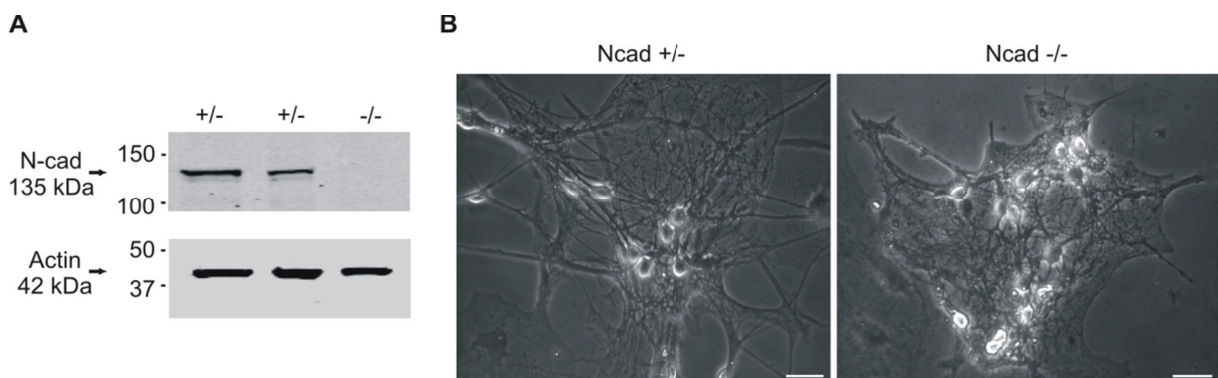
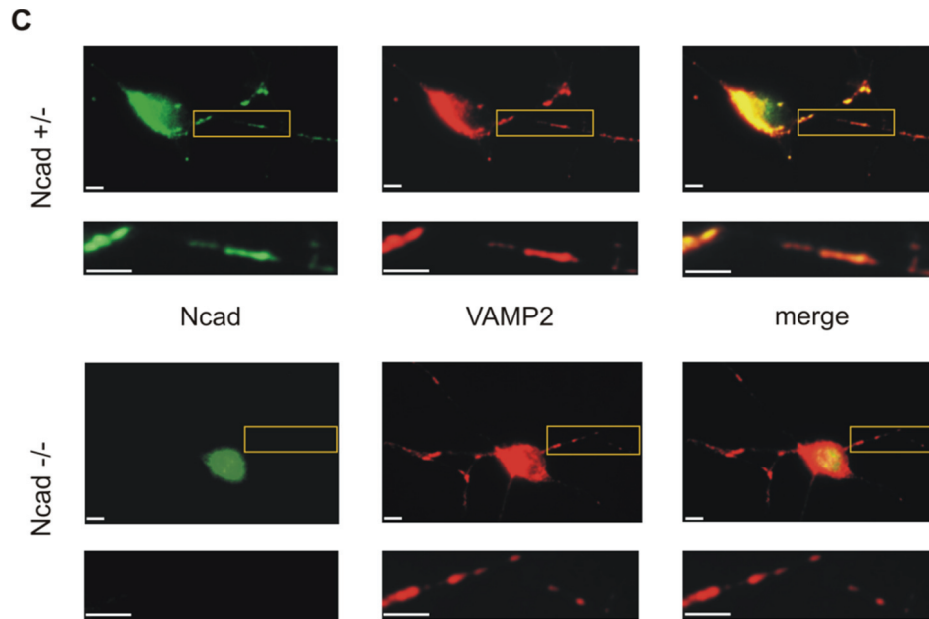**Figure 3.1 Characterization of Ncad+/- and Ncad-/- ES cell-derived neurons.**
A Western-blot analysis of Ncad+/- and Ncad-/- EBs. The N-cadherin band was visible in the Ncad+/- lines at 135 kDa, the loading control (Actin) in all lines at 42 kDa. Karyotyping (from left): XX, XY, XX. **B** Phasecontrast images of Ncad+/- and Ncad-/- neurons cultivated on glial microislands at 12 DIV (Scale bars: 30 µm). **C** Immunocytochemical stainings of Ncad+/- (XY-line) and Ncad-/- neurons cultivated on glial microislands from N-cadherin and VAMP2 (Synaptobrevin2) at 12 DIV. Boxed areas are magnified below the corresponding images. (Scale bars: 5µm).

3.1.1.2 Morpohological characterization of Ncad-/- neurons transfected with N-cadherin

In order to create an asymmetric expression of N-cadherin at synapses, Ncad-/- neurons were cotransfected with N-cadherin/EGFP and with EGFP alone (control), respectively. Due to the use of a glial microisland system in combination with a Lipofectamine-mediated transfection, N-cadherin expression was restricted to one (postsynaptic) neuron of the small network. All presynaptic neurons present on the same glial microisland lacked N-cadherin expression (Fig.3.2A). Comparable morphologies with processes characteristic for neurons were revealed for the transfected neurons by phasecontrast as well as fluorescence images (Fig. 3.2B). By tracing all dendrites of the transfected neurons a quantitative measurement of the dendritic branching was made. The total dendritic branch length showed no significant difference between Ncad-/- neurons transfected only with EGFP (499.0 ± 140,8µm; n = 23) as compared to Ncad-/- neurons transfected with EGFP + N-cadherin (439,1 ± 136,7µm; n = 21). Another measure, representing the complexity of the arborization, is the branch tip number, which was determined by counting of all branch endings (for detailed description see Fig. 3.20E). Similar to the total dendritic branch length no significant difference in branch tip number of the N-

cadherin transfected neurons was found (Fig. 3.2C; EGFP: 9,4 ± 3,0, n= 23; EGFP + Ncadherin: 12,6 ± 5,5, n= 21).
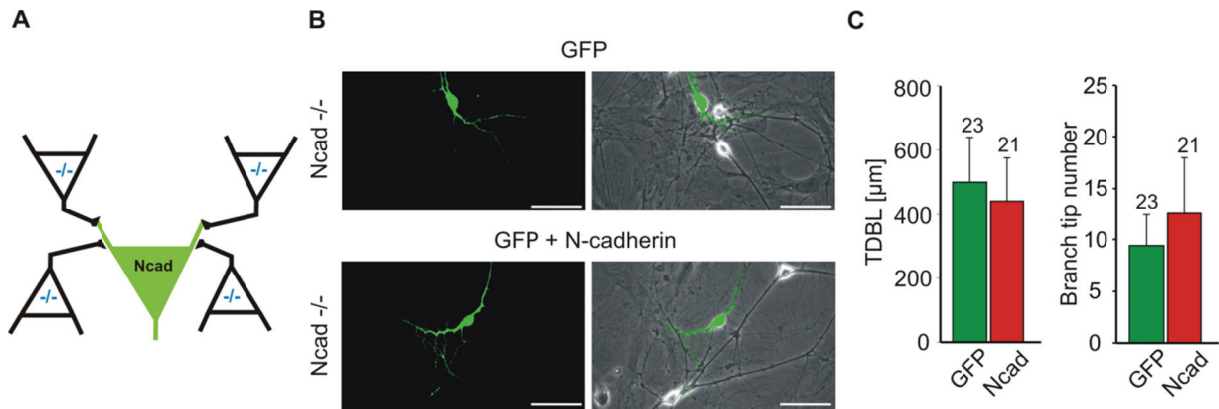

Figure 3.2 Morphological characterization of Ncad-/- neurons with an asymmetric N-cadherin expression.
A Scheme of the established system for analyzing asymmetric N-cadherin expression. Single (postsynaptic) Ncad-/- neurons on glia microislands were transfected with N-cadherin, whereas presynaptic neurons lacked N-cadherin. **B** Fluorescence and phasecontrast images of Ncad-/- neurons 2 days after transfection with EGFP and EGFP+N-cadherin, respectively, showing similar morphologies. **C** Quantitative analysis of the total dendritic branch length (TDBL) and the branch tip number of transfected Ncad-/- neurons. (n= number of dendrites; scale bars: 30 μm; error bars represent s.e.m.).
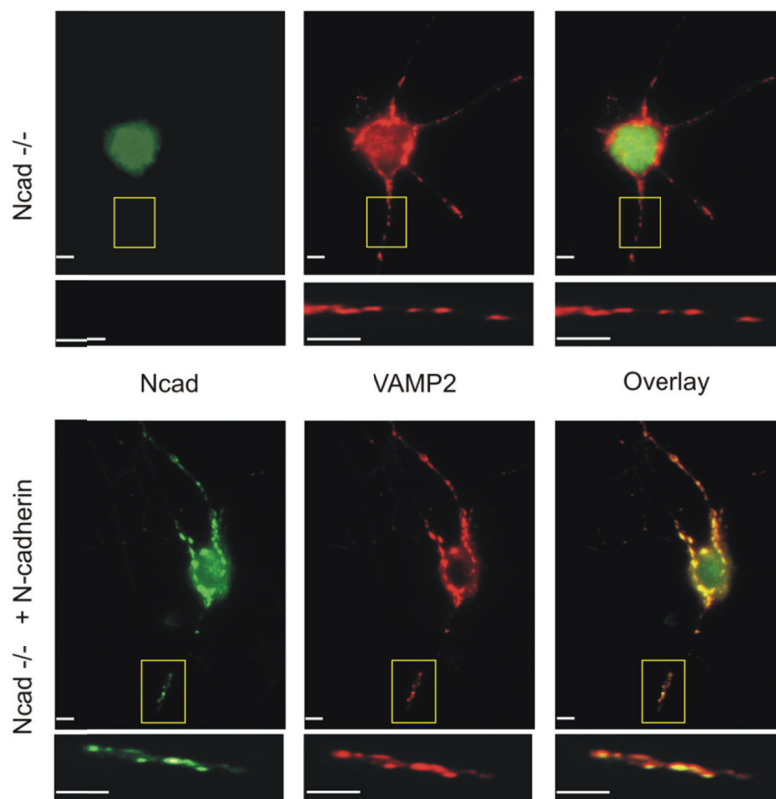
3.1.1.3 Verification of a physiological synaptic localization of expressed N-cadherin

The majority of VAMP2, a synaptic vesicle-associated protein, is suggested to be confined to synaptic boutons (Pennuto et al., 2003). Therefore, the localization of presynaptic vesicle accumulations and corresponding synaptic sites can be determined by immunocytochemical labeling of VAMP2. In order to verify a synaptic localization of the expressed N-cadherin in transfected Ncad-/- neurons, immunocytochemical costainings against VAMP2 (red signal, Cy3) and N-cadherin (green signal, Oregon green) were performed. Untransfected Ncad-/- neurons and Ncad+/- neurons served thereby as control (see Fig. 3C; Fig. 3.3). In order to ensure giving the N-cadherin a sufficient period of time for expression, experiments were carried out 2 and 7/8 days after transfection, respectively. The localization of expressed N-cadherin was studied for both time points. In untransfected Ncad-/- neurons a specific synaptic staining against N-cadherin was completely absent, while VAMP2-positive puncta were nicely distributed along soma and dendrites (Fig. 3.3A). Contrary, Ncad-/- neurons transfected with N-cadherin showed both, N-cadherin and VAMP2-positive puncta, on the soma and dendritic processes (Fig 3.3A). Quantitative analysis of the N-cadherin/VAMP2
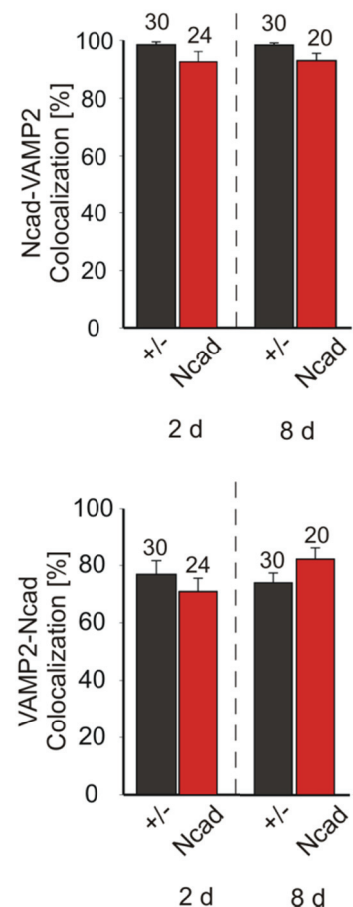
puncta colocalization (N-cadherin puncta overlapping with VAMP2), by which the proportion of N-cadherin expression at synaptic sites is described, revealed a correct synaptic localization of expressed N-cadherin similar to the synaptic localization of N-cadherin in Ncad+/- neurons (Fig. 3.3B; Ncad+/-: 2 days after transfection with EGFP 98,6 ± 1,0 %, 8 days after transfection with EGFP 98,5 ± 0,8 %, n=30 for both time points; Ncad-/-: 2 days after transfection with N-cadherin 92,6 ± 3,6 %, 8 days after transfection with N-cadherin 93,0 ± 2,6 %, n=24 for 2d, n= 20 for 8d). The fraction of synapses in which expressed N-cadherin was present is represented by the VAMP2 puncta overlapping with N-cadherin puncta (VAMP2/Ncad colocalization; Fig 3.3B; Ncad+/-: 2 days after transfection with EGFP 76,9 ± 4,8 %, 8 days after transfection with EGFP 74,1 ± 3,4 %, n=30 for both time points; Ncad-/-: 2 days after transfection with N-cadherin 71,0 ± 4,7 %, 8 days after transfection with N-cadherin 82,1 ± 3,9 %, n=24 for 2d, n= 20 for 8d). As the N-cadherin expression in mature cultured neurons has been described to be restricted to glutamatergic synapses (Benson and Tanaka, 1998), the synaptic sites (VAMP2 puncta) missing an colocalization with N-cadherin might represent GABAergic synapses.

Figure 3.3 Validation of the synaptic localization of expressed N-cadherin in Ncad-/- neurons.

A Immunocytochemical stainings against N-cadherin and VAMP2 of Ncad-/- neurons with and without transfection of N-cadherin at 12 DIV (2 days after transfection). Boxed areas mark dendritic segments magnified below (Scale bars = 5µm). **B** Colocalization analysis of N-cadherin and VAMP2 puncta revealed a localization of expressed N-cadherin at synaptic sites 2 and 8 days after transfection. (n= number of cells; error bars represent s.e.m.).

3.1.2 Effects of asymmetrically expressed N-cadherin on functional synaptic transmission

N-cadherin was shown to be essential for numerous synaptic functions. N-cadherin blocking experiments of using antibodies, dominant negative forms of N-cadherin, blocking peptides or N-cadherin deficient ES cell-derived neurons demonstrated its importance in modulating pre- and postsynaptic specializations and functions (Togashi et al., 2002; Murase et al., 2002; Bamji et al., 2003; Bozdagi et al., 2004; Jüngling et al., 2006; Saglietti et al, 2007). To examine to which extent synaptic function is affected by an asymmetric expression of N-cadherin, Ncad-/- neurons derived from embryonic stem cells or cortical Ncad+/+ neurons were transfected at 9-11 DIV with N-cadherin/EGFP or EGFP and analyzed 2 days later using electrophysiological recording.

3.1.2.1 Analysis of AMPA receptor-mediated miniature postsynaptic currents (mEPSCs)

In order to address experimentally the functional properties of synapses with asymmetric N-cadherin expression miniature EPSCs were recorded (-60 mV holding potential; 2,5 mM extracellular Ca^{2+} concentration). As spontaneous AMPA receptor-mediated miniature EPSCs (mEPSCs) are supposed to result from the release of single presynaptic vesicles, their analysis gives information about various synaptic properties. One aspect defining the frequency, with which the AMPA receptor-mediated mEPSCs appear, is the presynaptic vesicle release probability. Thereby the number of presynaptic vesicles, the density of Ca^{2+}-channels and the intracellular Ca^{2+} concentration can be decisive. In addition to this, the number of presynaptic terminals contacting the postsynaptic neuron, which increases with the maturational stage of the neuronal network, is a factor that affects the AMPA receptor-mediated mEPSC frequency. Furthermore, changes in the mEPSC amplitude indicate postsynaptic alterations, e.g. less AMPA receptors incorporated in the postsynaptic membrane resulting in a smaller amplitude. Moreover, the kinetics of the AMPA receptor-mediated mEPSCs, described by rise time and

decay time, are significant criteria in describing synaptic function. The concentration of transmitter in the synaptic cleft as well as their diffusion out of the synaptic cleft can be pivotal. Additionally, the properties of the postsynaptic receptors are crucial. The kinetics as well as the amplitude of the detected AMPA receptor-mediated mEPSCs were automatically analyzed by the minianalyis program. As rise time the time from 10-90 % of the maximal amplitude was defined.

The first observation, 2 days after inducing a mis-match expression of N-cadherin, that was evident by recording AMPA receptor-mediated mEPSCs was a still functioning synaptic transmission. To confirm whether the detected events were mediated by AMPA receptors, DNQX, a specific AMPA receptor antagonist, was applied at the end of the recording. A complete blockade of the AMPA receptor-mediated mEPSCs was observed (Fig. 3.4A). Strikingly, as illustrated by the example currents, the synaptic transmission seemed to be strongly impaired. The quantitative analysis revealed a significantly reduced frequency of mEPSCs (Fig. 3.4A,B; EGFP: $0,55 \pm 0,17$ Hz, n= 25; EGFP + N-cadherin: $0,09 \pm 0,03$ Hz, n= 20; p = 0,017). Interestingly, the quantitative analysis of the mean amplitude (EGFP: $12,8 \pm 0,8$ pA n= 20; EGFP + N-cadherin: $13,4 \pm 1,1$ pA, n= 11) as well as of the mean rise time (EGFP: $1,33 \pm 0,08$ ms n= 20; EGFP + N-cadherin: $1,28 \pm 0,11$ ms, n= 11) and the mean decay time (EGFP: $2,30 \pm 0,14$ ms n= 20; EGFP + N-cadherin: $2,13 \pm 0,17$ ms, n= 11) showed no significant alterations upon asymmetric expression of N-cadherin (Fig. 3.4B). Together, these results indicate a strong impairment of synaptic transmission in case N-cadherin is expressed asymmetrically at the postsynaptic side. The defect seems to be presynaptic, because the amplitude of the AMPA receptor-mediated mEPSCs was unaltered. Both, presynaptic functional defects or a reduced synaptic density might account for the observed change. As the dysfunction of synapes is thought to precede elimination processes, the detected defective synaptic transmission might subsequently lead to the elimination of synapses.
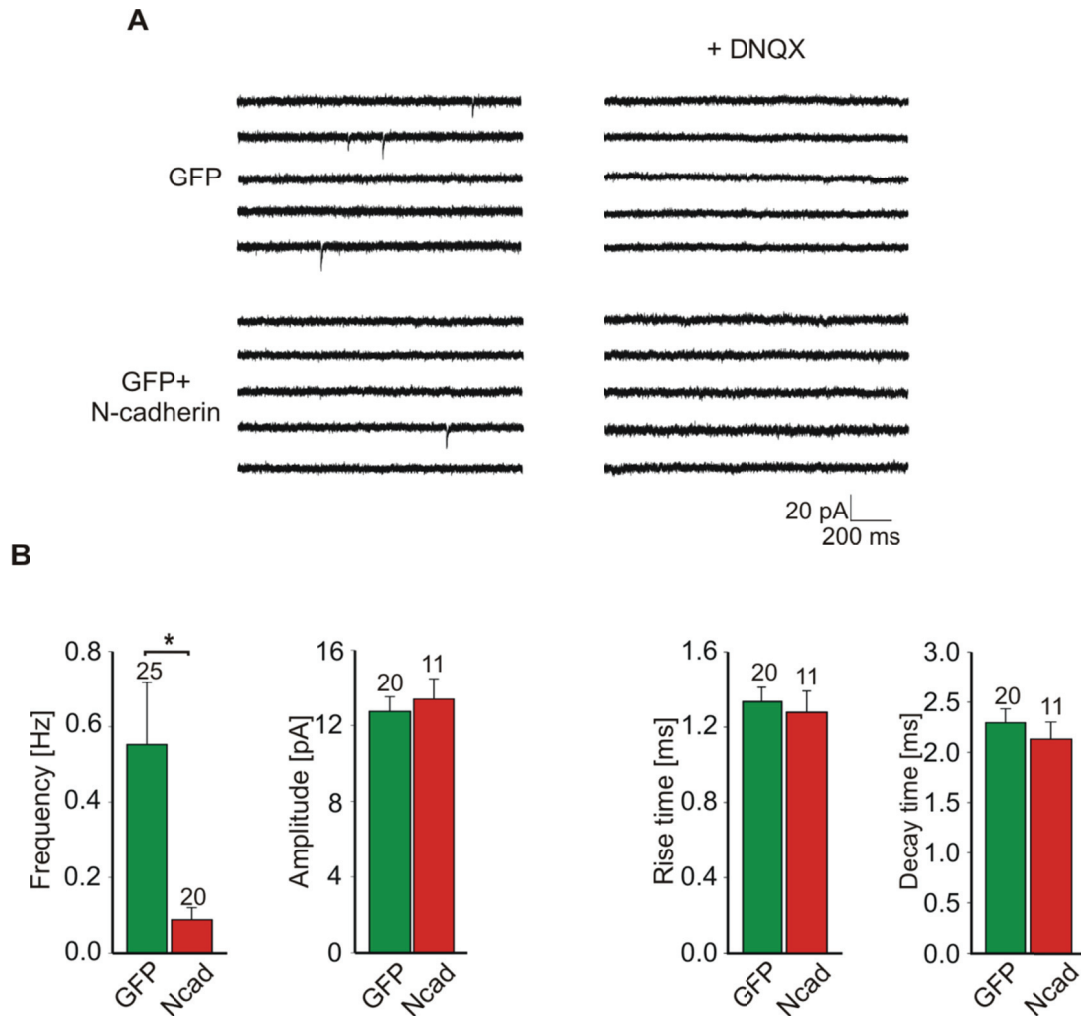
Figure 3.4 Asymmetric expression of N-cadherin at synapses leads to a strong impairment of synaptic transmission.
A Sample traces of AMPA receptor-mediated mEPSCs recorded from Ncad-/- neurons 2 days after the transfection with EGFP or EGFP + N-cadherin. mEPSCs were blocked by application of DNQX (10μM). **B** Quantitative analysis of mean frequency, mean amplitude, mean rise and decay time revealed significant defects in synaptic transmission. (Error bars represent s.e.m.; unpaired *t*-test; n= number of recorded cells; * p < 0,05).

3.1.2.2 Analysis of autaptic connections

The culture system used in this study for analyzing the asymmetric expression of N-cadherin is not only able to serve for examining the N-cadherin mis-match. Moreover, it bears at the same time an intrinsic control, because N-cadherin transfected Ncad-/- neurons express N-cadherin pre- and postsynaptically. Accordingly, the autaptic connections of these transfected neurons are not asymmetric in respect to N-cadherin expression, but express N-cadherin pre- and postsynaptically. In order to address this, an analysis of autaptic connections in Ncad-/- neurons transfected with N-cadherin was carried out via electrophysiological recordings. Depolarization of the soma by 20 mV (pulses of 1 ms duration, 10 s interstimulus interval)

through the patch pipette evoked the generation of action potentials at the axon hillock (Na^+ currents at the voltage clamped soma), which triggered after conduction along the axon the presynaptic vesicle release machinery. The released neurotransmitter induced postsynaptic, autaptic currents, which could be measured through the same patch pipette that injected the pulses (Fig. 3.5A).

Because not every neuron developed autaptic connections the probability for AMPA receptor-mediated autaptic connections was rather low and found to be around 40 % in both transfection conditions (Fig 3.5B; EGFP: 41,4 %, n= 29 ; EGFP + N-cadherin: 40,7 %, n=27). Autaptic currents were rather small, so that an extracellular solution with increased Ca^{2+} concentration had to be used to enhance the autaptic currents. As expected the mean amplitude of the autaptic responses was not significantly different in N-cadherin expressing Ncad-/- neurons compared to EGFP expressing controls. In EGFP transfected neurons the mean amplitude was 144,6 ± 55,0 pA, while the mean amplitude in EGFP + N-cadherin transfected neurons was 175,4 ± 60,1 pA (Fig. 3.5B). A pulse that was not able to induce an autaptic response was defined as "failure", which nevertheless contributed to the mean amplitude. Failures occur, when no vesicles are released, although an action potential reached the presynaptic terminal, reflecting the presynaptic vesicle release probability. The rate of failures was also not significantly different (Fig. 3.5B; EGFP: 28,9 ± 9,4 %; EGFP + N-cadherin: 30,0 ±11,4 %). In summary, these results confirm that the transfection of Ncad-/- neurons with N-cadherin in glial microisland cultures is resulting in an asymmetric expression of N-cadherin at the majority of synapses; autapses appear not to have a big impact on the system.
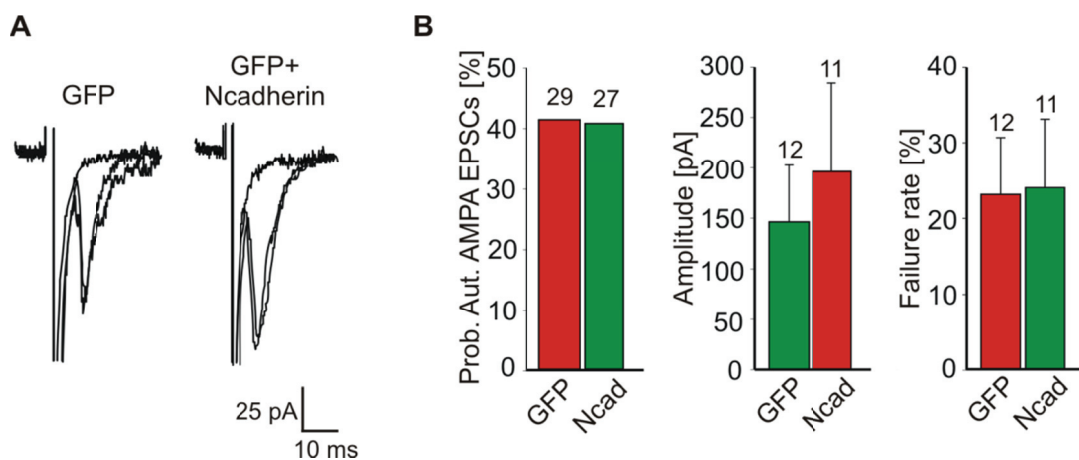

Figure 3.5 Evoked AMPA receptor-mediated autaptic currents revealed unaltered autaptic transmission in N-cadherin expressing Ncad-/- neurons.
A Representative examples of evoked AMPA receptor-mediated autaptic currents 2 days after the transfection of Ncad-/- neurons with EGFP or EGFP + N-cadherin. Voltage-dependent Na^+ currents

are truncated. **B** Quantitative analysis of probability of autapse formation, mean amplitude and failure rate of autaptic AMPA-EPSCs confirmed unaltered autaptic transmission. (Error bars represent s.e.m.; n= number of recorded cells).

3.1.2.3 Analysis of AMPA receptor-mediated mEPSCs at synapses with a quantitatively asymmetric expression of N-cadherin

An asymmetric expression of N-cadherin at individual synapses can be a qualitative mis-match with an absence of N-cadherin at the presynaptic and its presence at the postsynaptic side. Moreover, different levels of N-cadherin expression pre- and postsynaptically represent a quantitative mis-match of N-cadherin expression. To address, whether there is a need for a qualitative mis-match or whether a quantitative mis-match is already sufficient to affect the efficacy of synaptic transmission, cortical neurons (N-cadherin +/+) were cultured on glial microislands and transfected with N-cadherin similar to 3.1.2.1. This resulted in one transfected neuron (postsynaptic) overexpressing N-cadherin, while all surrounding presynaptic neurons expressed N-cadherin at the endogenous level. To examine this quantitative mis-match, electrophysiological recordings of AMPA receptor-mediated mEPSCs were performed. AMPA receptor-mediated mEPSCs were completely blocked by the application of DNQX (10μM) (Fig. 3.6A). The quantitative analysis of AMPA mEPSCs revealed no significant changes (Fig. 3.6B). The mean frequency of AMPA mEPSCs in neurons transfected with EGFP + N-cadherin (2,72 ± 0,76 Hz; n= 18) was not significantly changed as compared to the mean frequency in EGFP transfected neurons (2,01 ± 0,48 Hz; n= 18). Likewise the amplitude of the events in EGFP + N-cadherin transfected neurons (15,18 ± 1,2 pA; n= 16) was not significantly altered compared to the control EGFP transfected neurons (12,39 ± 1,11 pA; n= 17). Furthermore the kinetics of AMPA mEPSCs were similar in both conditions (Rise time: EGFP: 1,96 ± 0,11 ms, n= 17; EGFP + N-cadherin: 1,78 ± 0,16 ms, n= 16; Decay time: EGFP: 4,54 ± 0,49 ms, n= 17, EGFP + N-cadherin: 3,7 ± 0,38ms; n= 16). Taken together, these results indicate the requirement for a qualitative mis-match of N-cadherin expression at individual synapses to observe an impairment of synaptic transmission.
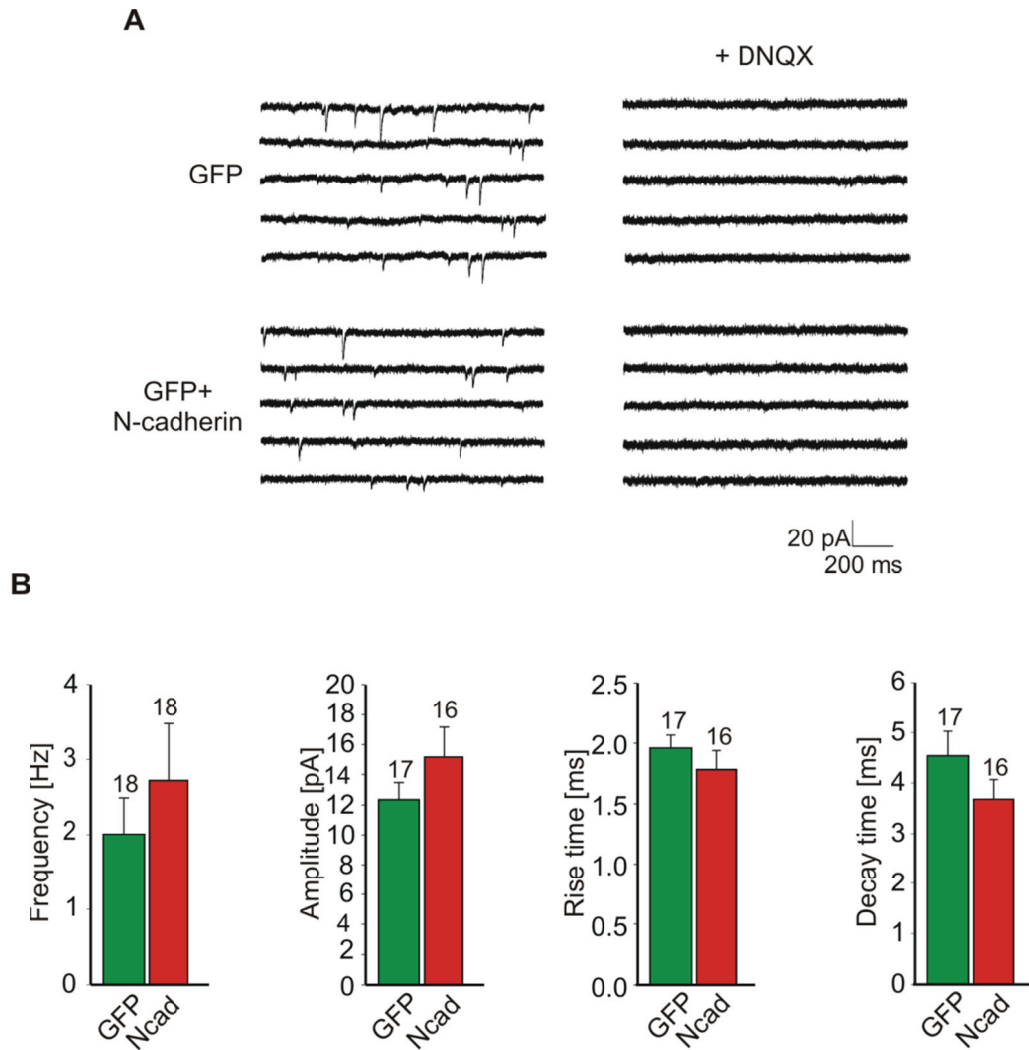
Figure 3.6 Analysis of a quantitative asymmetric expression of N-cadherin.
A Sample traces of AMPA receptor-mediated mEPSCs recorded from cortical N-cadherin wildtype neurons 2 days after the transfection with EGFP or EGFP + N-cadherin. mEPSCs were blocked by application of DNQX. **B** No significant alterations in the mean frequency, mean amplitude, mean rise and mean decay time were observed. (Error bars represent s.e.m.; n= number of recorded cells).

3.2 Molecular interaction partners potentially cooperating with asymmetrically expressed N-cadherin

The molecular interaction partners mediating mechanistically the effects of asymmetrically expressed N-cadherin are, of course, of major interest. To begin to address this open question, electrophysiological as well as biochemical approaches were performed. All electrophysiology was carried out on ES cell-derived Ncad-/- and Ncad+/- neurons, respectively, transfected at 9-11 DIV and analyzed 2 days later. Biochemical experiments were done on P6 brains of N-cadherin +/+ mice (C57/bl6 line).

3.2.1 Role of other classical cadherins

Pre- and postsynaptically localized N-cadherin molecules are especially characterized through strong homophilic binding to each other. However, heterophilic interactions with other cadherins have been described (Shan et al., 2000; Prakasam, 2006). As in the N-cadherin mismatch system used in this study the postsynaptically expressed N-cadherin is not able to have an interaction with presynaptic N-cadherin, it stands to reason that binding to another classical cadherin mediates the impairment of synaptic transmission. The HAV as well as the flanking INP-motif in the EC1 domain of N-cadherin are supposed to be key structures for the interaction with other cadherins (Blaschuk et al., 1990; Doherty et al., 1991; Williams et al., 2000). To address this, two distinct N-cadherin peptide antagonists mimicking the HAV or the INP motif (100µg/ml; Williams et al., 2000; Poskanzer et al., 2003) of N-cadherin were applied directly after transfection of Ncad-/- neurons with EGFP or EGFP + N-cadherin. Hence, the binding site for other cadherin molecules was blocked, the potential signaling pathway interrupted and the impairment of synaptic transmission might have been rescued. 2 days after transfection and application of the distinct N-cadherin antagonists AMPA receptor-mediated mEPSCs were recorded. As controls served the addition of corresponding scrambled peptides to neurons either transfected with EGFP or EGFP + N-cadherin.

As the example currents in Fig. 3.7 indicate, addition of the 16mer long HAV antagonistic peptide to neurons transfected with EGFP + N-cadherin did not show a rescue of the impaired synaptic transmission as compared to control experiments, in which a scrambled peptide (scr) was either added to neurons transfected with EGFP or to neurons transfected with EGFP + N-cadherin (Fig. 3.7A). The mean frequency of AMPA mEPSCs in Ncad-/- neurons transfected with EGFP + N-cadherin and incubated with the HAV peptide was $0,18 \pm 0,05$ Hz (n= 26) ,and thus significantly reduced as compared to the mean frequency of neurons transfected with EGFP and treated with a scrambled peptide ($0,46 \pm 0,11$ Hz; n= 19; p= 0,007). In addition, no alterations could be observed compared to the mean frequency of AMPA-mEPSCs in Ncad-/- neurons transfected with EGFP + N-cadherin and treated with scrambled peptide (Fig. 3.7B; $0,21 \pm 0,06$ Hz, n= 22). The comparison of the mean frequency of Ncad-/- neurons transfected with EGFP + N-cadherin/scr peptide and of Ncad-/- neurons transfected with EGFP/scr peptide showed a significant reduction (p= 0,017). Furthermore, all three conditions showed neither in the quantitative comparison of the mean amplitude (EGFP/scr: $12,6 \pm 0,6$ pA, n= 16; EGFP + N-cadherin/scr: $15,4 \pm 1,4$ pA, n= 17; EGFP + N-cadherin/HAV: $12,8 \pm 0,8$ pA, n= 23) nor of the rise time (EGFP/scr: $1,44 \pm 0,12$ ms, n= 16;

EGFP + N-cadherin/scr: 1,59 ± 0,12 ms, n= 17; EGFP + N-cadherin/HAV: 2,11 ± 0,70 ms, n= 23) nor of the decay time (EGFP/scr: 3,0 ± 0,32 ms, n= 16; EGFP + N-cadherin/scr: 3,36 ± 0,25 ms, n= 17; EGFP + N-cadherin/HAV: 2,89 ± 0,22 ms, n= 23) any significant differences (Fig. 3.7B).

Likewise, the addition of the 7mer INP peptide did not have a rescue effect on the impairment of synaptic transmission. The mean frequency of AMPA EPSCs in Ncad-/- neurons transfected with EGFP + N-cadherin and incubated with the INP peptide was 0,12 ± 0,05 Hz (n=19), and thus similar to the frequency of AMPA EPSCs in Ncad-/- neurons transfected with EGFP + N-cadherin and treated with the scrambled peptide (Fig. 3.7C; 0,14 ± 0,07 Hz, n= 20). Both conditions were significantly different to the mean frequency of AMPA EPSCs in Ncad-/- neurons transfected with EGFP and treated with the scrambled peptide (0,44 ± 0,14Hz, n= 17; p= 0,013 to EGFP + N-cadherin/INP; p= 0,018 to EGFP + N-cadherin/scr). Again the quantitative analysis of the mean amplitude (EGFP/scr: 10,9 ± 0,9 pA, n= 14; EGFP + N-cadherin/scr: 12,3 ± 1,4 pA, n= 9; EGFP + N-cadherin/INP: 12,9 ± 1,3 pA, n= 12), the rise time (EGFP/scr: 1,78 ± 0,13 ms, n= 14; EGFP + N-cadherin/scr: 1,74 ± 0,11 ms, n= 9; EGFP + N-cadherin/INP: 1,72 ± 0,20 ms, n= 12) and the decay time (EGFP/scr: 3,58 ± 0,38 ms, n= 14; EGFP + N-cadherin/scr: 4,65 ± 1,01 ms, n= 9; EGFP + N-cadherin/INP: 3,42 ± 0,59 ms, n= 12) did not show any significant changes (Fig. 3.7C).
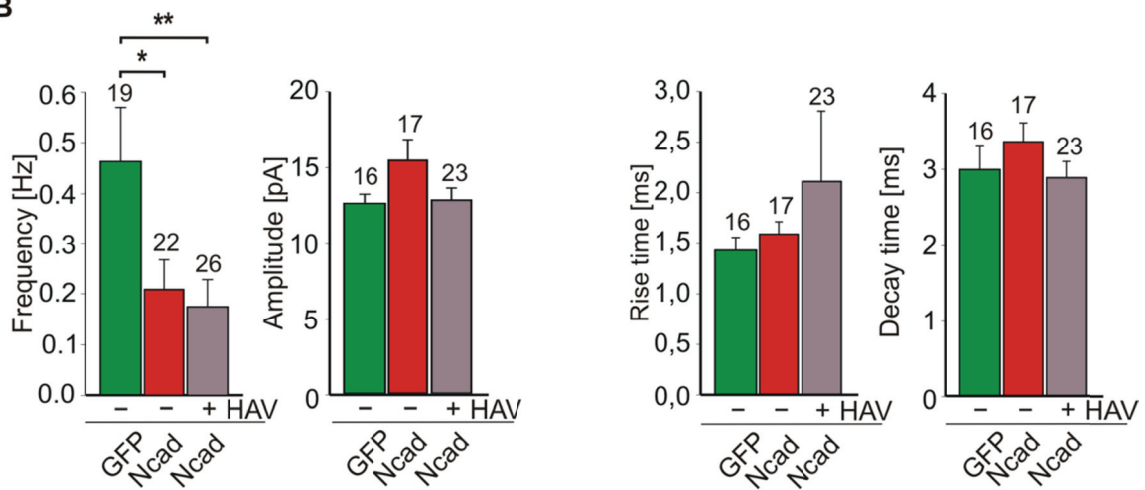
These results demonstrate that a blockade of the cadherin binding site on two distinct locations fails to rescue the defective synaptic function. This further indicates the lack of a potential interaction of asymmetrically expressed N-cadherin with other classical cadherins.
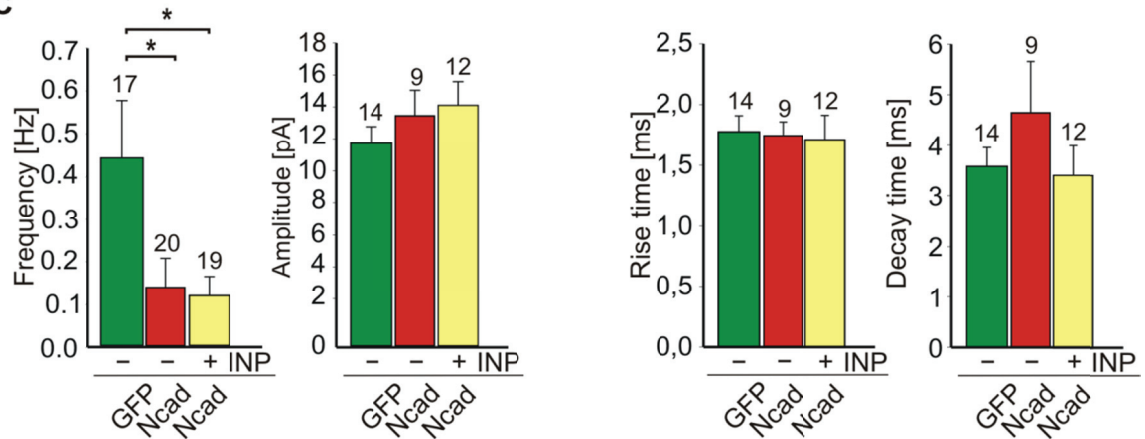
A

B

C

[83]
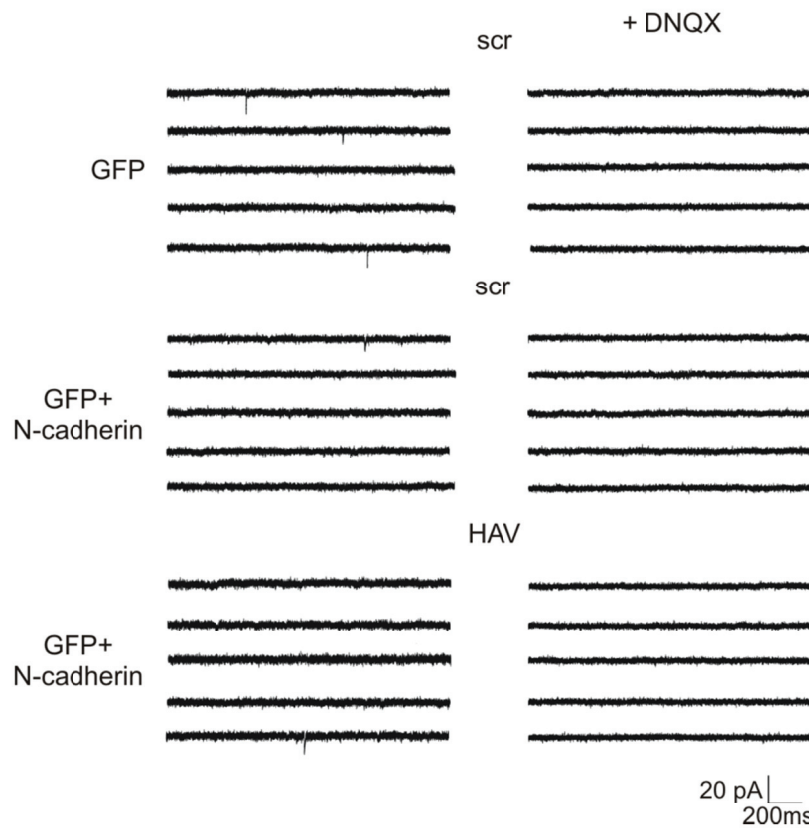
Figure 3.7 Impairing synaptic function does not require binding to other classical cadherins.
A Sample traces of AMPA receptor-mediated mEPSCs recorded from Ncad-/- neurons 2 days after transfection with EGFP or EGFP + N-cadherin and the application of various antagonistic peptides (HAV and corresponding scrambled peptide; 100 µg/ml). mEPSCs were blocked by application of DNQX. Example currents for INP peptide application not shown. **B,C** Quantitative analysis of mean frequency, mean amplitude, mean rise and mean decay time of AMPA EPSCs in HAV (B) or INP (C) treated neurons revealed no cooperation of expressed N-cadherin with other classical cadherins in impairing synaptic transmission. (Error bars represent s.e.m.; n= number of recorded cells; One-way ANOVA; * p < 0,05; ** p < 0,01).

3.2.2 Potential role of the BDNF/TrkB/p75 system

The neurotrophic factor BDNF is known to strongly potentiate synaptic activity by modulating presynaptic function (Lessmann et al, 1994; Schuman, 1999; Kafitz et al., 1999; Li et al., 1998; Bolton et al., 2000; Marty et al., 2000). TrkB was also demonstrated to negatively act on synaptic transmission as well as on synapse number in case a balance between BDNF and its non-liganded receptor TrkB is not given (Klau et al., 2003). This effect was shown to be reversible by addition of BDNF. Taken together, all these experiments gave raise to the idea that the BDNF/TrkB/p75^{NTR} system might be involved in the effects of asymmetric expression of N-cadherin.

3.2.2.1 BDNF rescues defective synaptic transmission triggered by asymmetrically expressed N-cadherin

To gain further insights into the mechanism for impaired synaptic function mediated by asymmetrically expressed N-cadherin, BDNF (100 ng/ml) as a general enhancer of synaptic activity was applied directly after the transfection of ES cell-derived Ncad-/- neurons with EGFP and EGFP + N-cadherin, respectively. 2 days later AMPA receptor-mediated mEPSCs as measure for synaptic transmission were recorded. A corresponding vehicle (0,1 % BSA) was applied to Ncad-/- neurons either transfected with EGFP or EGFP + N-cadherin as control.

Interestingly, in contrast to the application of the N-cadherin antagonists an intriguing change was observed (Fig 3.8A). The mean frequency of AMPA mEPSCs in Ncad-/- neurons transfected with EGFP + N-cadherin and treated with BDNF (0,22 ± 0,06 Hz, n= 18) did not show any significant difference compared to the mean frequency of neurons transfected with EGFP and incubated with the vehicle (0,20 ± 0,06Hz, n=19), indicating a rescue effect triggered by BDNF. At the same time, by comparing the mean frequency of AMPA EPSCs in

Ncad-/- neurons transfected with EGFP + N-cadherin and treated with the vehicle (0,06 ± 0,02; n= 21) with that of Ncad-/- neurons transfected with EGFP and incubated with the vehicle, a significant reduction of the mean frequency of AMPA mEPSCs triggered by asymmetrically expressed N-cadherin was confirmed (p= 0,023). Likewise a significant increase in the mean frequency between neurons transfected with EGFP and incubated with the vehicle, and neurons transfected with EGFP + N-cadherin and treated with BDNF (p= 0,049) was found. The mean amplitude (EGFP/vehicle: 10,7 ± 0,8 pA, n= 11; EGFP + N-cadherin/vehicle: 12,4 ± 0,9 pA, n= 13; EGFP + N-cadherin/BDNF: 12,0 ± 0,6 pA, n= 15) as well as the mean rise time (EGFP/vehicle: 1,54 ± 0,18 ms, n= 11; EGFP + N-cadherin/vehicle: 1,42 ± 0,13 ms, n= 13; EGFP + N-cadherin/BDNF: 1,49 ± 0,12 ms, n= 15) and decay time (EGFP/vehicle: 3,43 ± 0,7 ms, n= 11; EGFP + N-cadherin/vehicle: 2,92 ± 0,26 ms, n= 13; EGFP + N-cadherin/BDNF: 3,4 ± 0,57 ms, n= 15) were not significantly altered in all three conditions (Fig. 3.8B). Together, the application of BDNF was demonstrated to be a potential factor to rescue the malfunctioning synaptic transmission as result of asymmetric expression of N-cadherin.
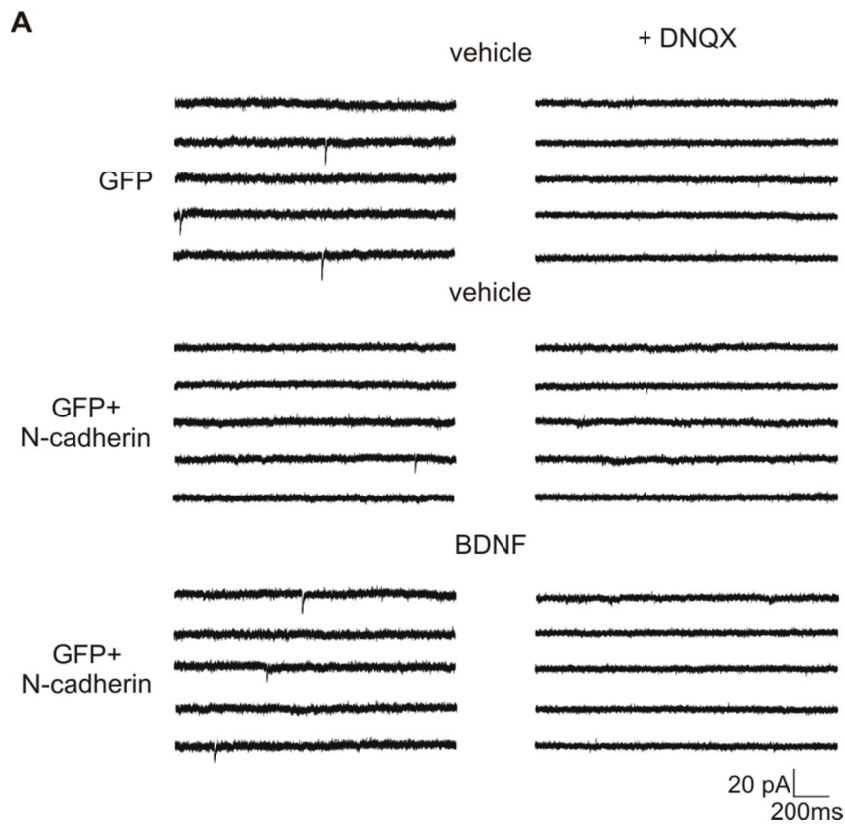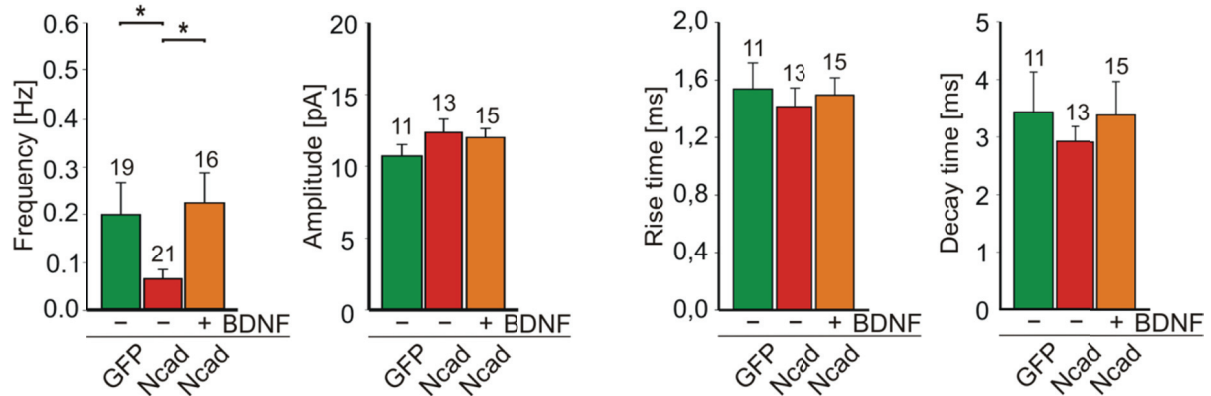
B

Figure 3.8 Application of BDNF rescued impaired synaptic function.
A Representative traces of AMPA receptor-mediated mEPSCs recorded 2 days after the transfection with EGFP or EGFP + N-cadherin and the application of BDNF or a vehicle. All events were blocked by addition of DNQX. **B** Quantification of mean frequency, mean amplitude, mean rise and mean decay time. An involvement of the BDNF/TrkB/p75[NTR] system in the molecular pathway triggered by the asymmetric expression of N-cadherin appears conceivable. (Error bars represent s.e.m.; n= number of recorded cells; One-way ANOVA; * p < 0,05).

3.2.2.2 Analysis of an interaction of N-cadherin and the BDNF/TrkB/ p75[NTR] system

It has been suggested that a general link between homophilically interacting N-cadherin and BDNF function might exist. An indirect linkage between presynaptic N-cadherin and BDNF through a BDNF/TrkB-mediated phosphorylation of β-catenin, disruption of the β-catenin/N-cadherin complex and resultant dispersal of presynaptic vesicles has been hypothesized to modulate synaptic function (Bamji et al., 2006). Moreover, axon growth and branching were found to be triggered by the BDNF/TrkB/β-catenin interplay (David et al., 2008).

To address this ES cell-derived Ncad-/- neurons as well as ES cell-derived neurons expressing N-cadherin (Ncad+/-) were incubated for 2 days with BDNF (100 ng/ml) or a vehicle as control. For ensuring similar experimental conditions as in 3.2.2.1 neurons were transfected with EGFP. To detect a BDNF-mediated potentiation as described in the literature, AMPA receptor-mediated mEPSCs from transfected neurons were recorded (Fig. 3.9A). Indeed, in control neurons (Ncad+/-) the mean frequency of AMPA mEPSCs was significantly increased by the addition of BDNF (0,76 ± 0,21 Hz, n= 21) as compared to the application of the vehicle (0,18 ± 0,04 Hz, n= 22) (Fig 3.9B; p= 0,008). This highly significant increase in AMPA mEPSC frequency was not observed anymore in the absence of N-cadherin in the Ncad-/- neurons (vehicle: 0,2 ± 0,07 Hz, n= 19; BDNF: 0,19 ± 0,05 Hz, n= 24). The application of BDNF did not alter the mean amplitude of AMPA mEPSCs in Ncad+/- neurons (Fig. 3.9B; vehicle: 13,7 ± 2,1 pA, n=, 19; BDNF: 14,2 ± 1,3 n=20), in contrast to what has

been reported from other groups (Lu et al., 2007; Gottmann et al., 2009; Biggs et al., 2010). BDNF had no effect on the mean amplitude in Ncad-/- neurons as well (Fig 3.9B; vehicle: $10,7 \pm 0,8$, n= 11; BDNF: $12,6 \pm 1,7$, n= 18). Likewise the quantification of the mean rise and decay times did not reveal significant changes, neither in Ncad+/- (Fig 3.9B; rise time: vehicle: $1,53 \pm 0,12$ ms, n= 19; BDNF: $1,44 \pm 0,10$ ms, n= 20; decay time: vehicle: $4,36 \pm 0,59$ ms, n= 19; BDNF: $2,83 \pm 0,30$ ms, n= 20) nor in Ncad-/- neurons (Fig 3.9B; rise time: vehicle: $1,54 \pm 0,18$ ms, n= 11; BDNF: $1,55 \pm 0,12$ ms, n= 18; decay time: vehicle: $3,43 \pm 0,7$ ms, n= 11; BDNF: $2,78 \pm 0,28$ ms, n= 18). Together, these results indicate that BDNF can exert a potentiation of synaptic activity only if N-cadherin is present.

In a second, biochemical approach to study a potential cross-linking between postsynaptic N-cadherin and the BDNF/TrkB/p75^{NTR} system co-immunoprecipitation was performed. Brain lysates from P6 mice were precipitated using an N-cadherin antibody. As control preimmune serum (IgG) was applied instead of the N-cadherin antibody. In order to detect co-precipitated proteins (TrkB, p75^{NTR}) within the precipitated complexes, antibodies against TrkB and p75^{NTR} were used, respectively. To increase the probability of finding an N-cadherin/TrkB/p75^{NTR} interaction, one approach involved the application of TrkB receptor bodies (TrkB/Fc; 1µg/ml), scavenging extracellular BDNF. Immunoprecipitates were separated by SDS-page and subsequently probed by immunoblotting using an N-cadherin antibody for precipitation control or pan-Trk and p75 antibodies, respectively (Fig 3.9C). While the precipitation control was successfully performed (Fig. 3.9C left), a co-immunoprecipitation of TrkB or p75^{NTR} was not detectable (Fig. 3.9C right). As expected no signals were detected in the IgG controls. These results were reproduced in three independent experiments.

In summary, the above described results demonstrate a cooperation of homophilically interacting N-cadherin and the BDNF/TrkB/p75 system (Fig 3.9A,B). However, a direct interaction of N-cadherin and TrkB or p75^{NTR} that might be involved in the mechanism triggered by asymmetrically expressed N-cadherin could not be demonstrated.
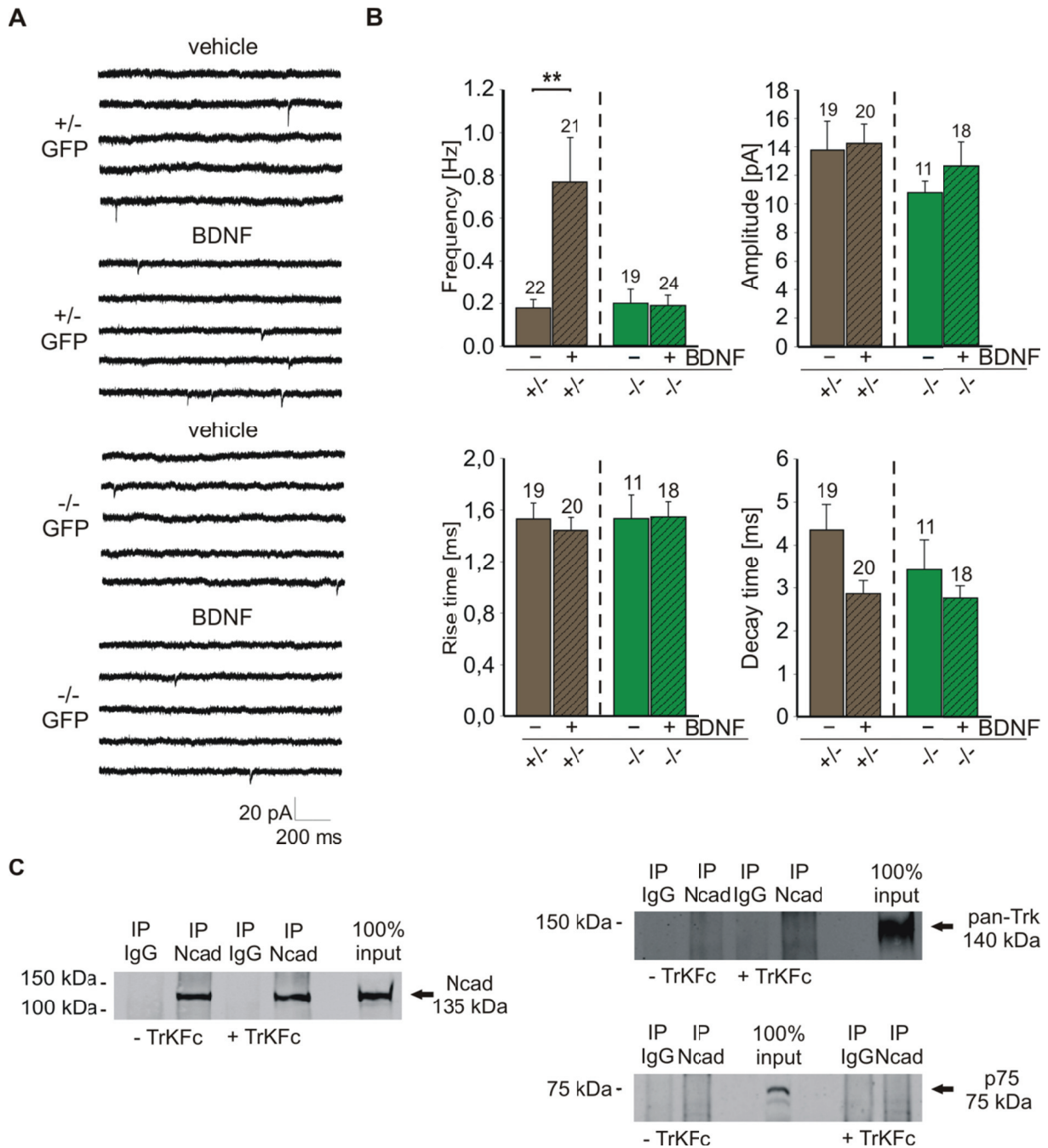
Figure 3.9 BDNF-induced potentiation of synaptic activity requires N-cadherin function.
A AMPA receptor-mediated mEPSCs recorded from Ncad+/- or Ncad-/- neurons 2 days after transfection with EGFP and application of BDNF or a vehicle (100ng/ml; pharmacological block by DNQX not shown). **B** Quantification of the mean frequency, mean amplitude, mean rise and mean decay time of AMPA mEPSCs in Ncad+/- and Ncad-/- neurons treated with BDNF or vehicle. (Error bars represent s.e.m.; n= number of recorded cells; One-way ANOVA; ** $p < 0,01$). **C** Western blot analysis of immunoprecipitations with a N-cadherin specific antibody for precipitation control (left blot) and pan-Trk as well as p75[NTR] antibodies (right blots) for the detection of TrkB and p75[NTR] in the precipitation complex. No co-immunoprecipitation of Trk and p75[NTR] was detectable. No bands were observed in the pre-immuneserume (IgG) control.

3.3 Induction of synapse elimination by asymmetrically expressed N-cadherin

The elimination of synapses is a very common process during the developmental fine-tuning of the nervous system. Studies at the neuromuscular junction gained insights into it, as during embryogenesis muscle fibers are innervated by multiple motor axons, from which most are eliminated until one axon per fiber remains (Lichtman and Colman, 2000).

The above results demonstrated that an asymmetric expression of N-cadherin leads to functional defects in synaptic transmission, which might be caused by presynaptic defects in the release machinery or by alterations in the synapse density. As such functional defects are thought to be the first steps in the elimination of synapses (Colman et al., 1997; Lichtman and Colman, 2000), the following experiments addressed changes in synapse density and morphology. Imaging experiments involving a labeling of synapses and of neuronal processes with specific markers were performed at distinct maturational stages. To gain insights into morphological changes at the time point of disordered synaptic transmission and subsequently thereafter, experiments were carried out 2 and 7/8 days after transfection.

3.3.1 Role of asymmetrically expressed N-cadherin at an early maturational stage

2 days after inducing an asymmetric expression of N-cadherin at 9-11 DIV a defective synaptic transmission was found. To examine whether at this time point functional presynaptic defects or a reduced synaptic density account for this defect, ES cell-derived Ncad-/- neurons were transfected at 9-11 DIV with EGFP or EGFP + N-cadherin. 2 days after the transfection an immunocytochemical staining against VAMP2, labeling all presynaptic vesicle accumulations, was performed. Via counting of VAMP2 puncta on proximal dendrites of transfected neurons (considered as synaptic puncta; red signal, Cy3), the density of synapses made on the transfected neurons could be determined 2 days after transfection. No significant change in synapse density was observed (Fig 3.10B; EGFP: 5,5 ± 0,6 pcta/30µm dendrite, n=19; EGFP + N-cadherin: 4,7 ± 0,7 pcta/30µm dendrite, n= 12). Thus, a defect in the presynaptic vesicle release machinery is at this early time point responsible for an alleviated synaptic transmission. As presynaptic defects lead to synapse elimination, the experiment was repeated 8 days after transfection at 17-19 DIV (Fig 3.10A). In fact, the

VAMP2 density at this time point (Fig 3.10B) revealed a significantly reduced synapse number (p= 0,003) in Ncad-/- neurons transfected with EGFP + N-cadherin (7,1 ± 0,5 pcta/30µm dendrite, n= 18) compared to the control transfected with EGFP (9,2 ± 0,4 pcta/30µm dendrite, n= 22).

Taken together, 2 days after the induction of a N-cadherin mis-match, presynaptic defects led to disordered synaptic transmission without any consequences for synapse number. Subsequently thereafter, these defects seemed to initiate a reduction of synaptic contacts made onto the neurons expressing N-cadherin asymmetrically.
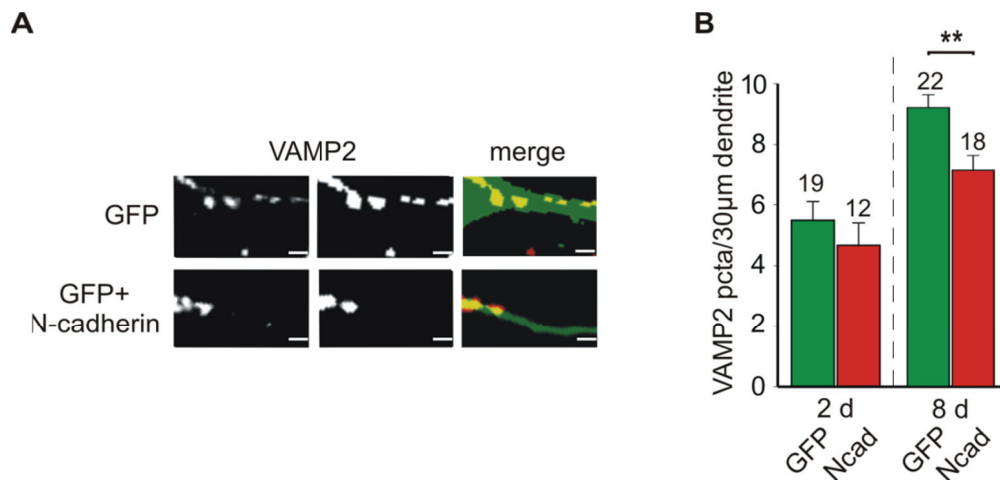

Figure 3.10 Asymmetric N-cadherin expression mediates a decrease in synapse number at an early maturational stage.
A Original (left), thresholded (middle) and thresholded merged images with EGFP fluorescence (right) from immunocytochemical stainings against VAMP2 8 days after the transfection with EGFP or EGFP + N-cadherin (DIV 17; scale bars = 2,5 µm).
B Quantitative analysis of the VAMP2 puncta per 30µm dendrite confirmed a, 8 days after the induction of an asymmetric N-cadherin expression, reduced number of synapses. 2 days after transfection a defect in the presynaptic release machinery without reduced synapse number was found. (n= number of cells; error bars represent s.e.m.; unpaired t-test; ** p < 0,01).

3.3.2 Role of asymmetrically expressed N-cadherin at a late maturational stage

Although the synapse number was reduced compared to controls in the above described experiments, the number of synapses was not decreased below the level of synapses measured 2 days after transfection. Hence, the previous experiment does not clearly reveal an elimination of synapses, because the generation of new synapses could have been affected, as the experiments were carried out on neuronal networks in which still a lot of synapses form. To demonstrate synapse elimination, a more detailed analysis at a later maturational stage was

performed. In this phase most of the synapses in the network have already been formed, which makes an elimination of synapses detectable.

Therefore, ES cell-derived Ncad-/- neurons were transfected with N-cadherin + PSD-95-GFP at 14 DIV and immunocytochemical stained against VAMP2 2 and 8 days later, respectively. As control served ES cell-derived Ncad-/- neurons solely transfected with PSD-95-GFP. This resulted in a labeling of all postsynaptic glutamatergic sites of a transfected neuron asymmetrically expressing N-cadherin via PSD-95-GFP (green signal), while all presynaptic sites on this neuron were marked using the immunocytochemical reaction against VAMP2 (Fig. 3.11; Alexa Flour 350, for better visualization depicted in red).

As shown in figure 3.5, the rate of autapses in the used culture system is relatively low. To ensure analyzing an elimination of synapses without a falsification through autaptic connections, the experiment was engineered to enable the distinction between autapses and synapses. Therefore, the above described Ncad-/- neurons were additionally transfected with DsRed2-VAMP2, labeling all presynaptic vesicle accumulations that arose from autaptic connections. Colocalizations showing all three labels (PSD-95-GFP, DsRed2-VAMP2, VAMP2 stained) were considered as autapses; colocalizations exhibiting only the presence of expressed PSD-95-GFP and stained VAMP2 were regarded as synapses.

3.3.2.1 Analysis of synaptic contacts made on Ncad-/- neurons expressing N-cadherin

As experienced from the experiments in 3.3.1, a loss of synapses made on Ncad-/- neurons expressing N-cadherin appears to take more than 2 days. Hence, the analysis was performed 2 and 8 days after the transfection, respectively. Proximal dendrites of transfected neurons (Fig. 3.11A,B) were selected and analyzed subsequently by image processing with respect to puncta number and colocalization (Fig. 3.11C,D).
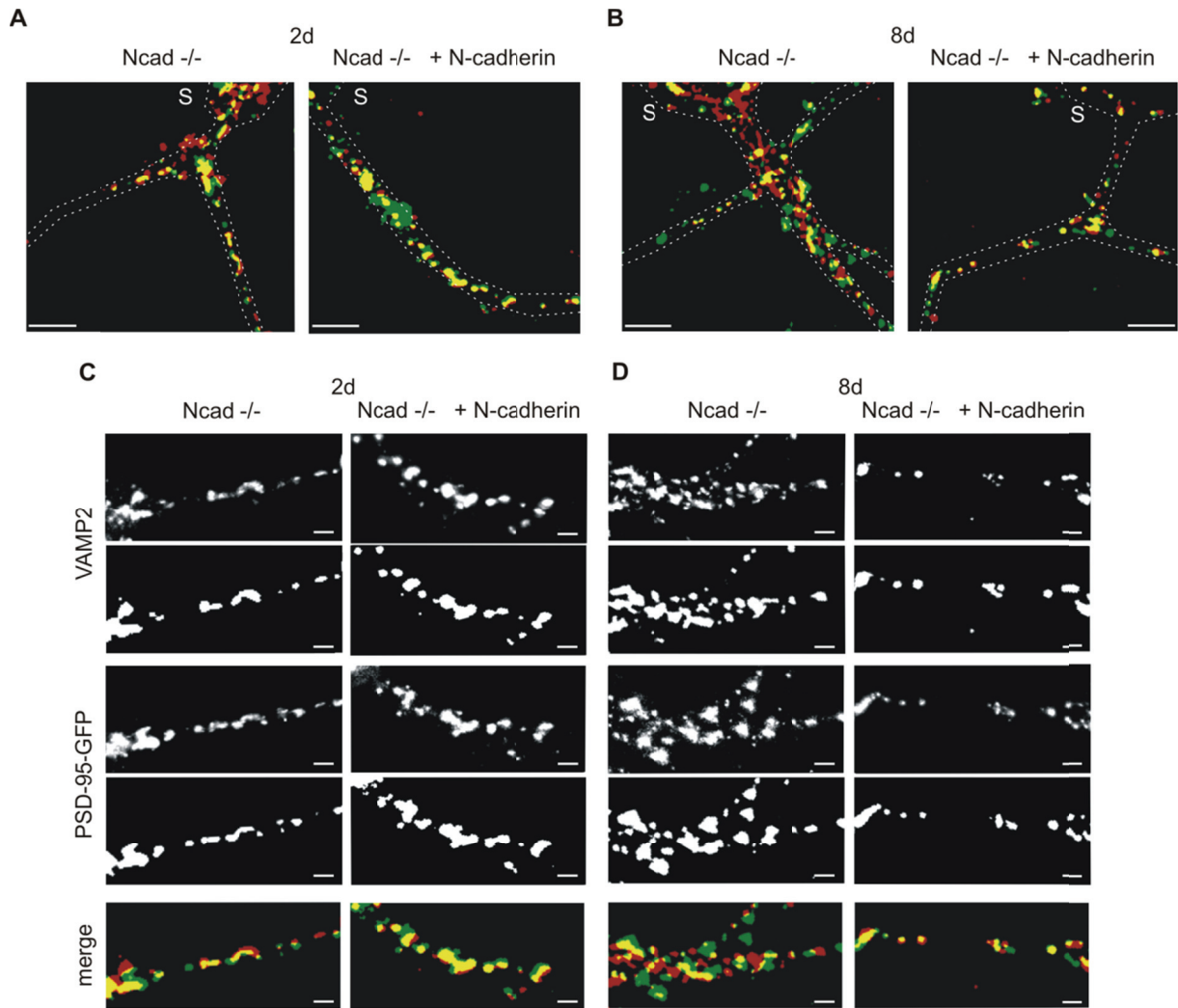
Figure 3.11 Asymmetric N-cadherin expression: Analysis of synapse number and morphology at a late maturational stage.
A,B Example fluorescence images of Ncad-/- neurons 2 (A) or 8 (B) days after transfection with PSD-95-GFP + DsRED2-VAMP2 or PSD-95-GFP + DsRED2-VAMP2 + N-cadherin (PSD-95-GFP: green signal) and immunocytochemical staining against VAMP2 (red signal) at DIV 16 and DIV22, respectively. □S□ represents the location of the cell soma (Scale bars: 10µm) **C,D** Original (upper), thresholded (lower) and corresponding images of dendritic segments showing VAMP2 puncta (immunostaining) and PSD-95 puncta (PSD-95-GFP expression) (Scale bars: 2,5µm). Bottom panel shows merged thresholded images. VAMP2 (red), PSD-95 (green). The corresponding DsRED2-VAMP2 signal is shown in figure 3.13.

To quantify synaptic density and morphology, all immunocytochemical stained VAMP2 puncta on transfected dendrites were counted and analyzed with regard to mean density, mean area and mean intensity. Similar to the results described in 3.3.1, 2 days after induction of a N-cadherin mis-match no significant difference in the VAMP2 puncta density could be observed (Fig 3.12A; PSD-95-GFP + DsRed2-VAMP2: 8,9 ± 0,9 pcta/30µm dendrite, n= 17; PSD-95-GFP + DsRed2-VAMP2 + N-cadherin: 8,6 ± 0,8 pcta/30µm dendrite, n= 18). In contrast, 8 days after transfection the asymmetric expression of N-cadherin resulted in a

highly significant (p< 0,001) reduction of the VAMP2 puncta density (5,9 ± 0,4 pcta/30μm dendrite, n= 27) as compared to control (9,9 ± 0,7 pcta/30μm dendrite, n= 26; Fig. 3.12A). Unexpectedly, the mean area of the VAMP2 puncta was significantly increased 2 days after transfection (PSD-95-GFP + DsRed2-VAMP2: 0,52 ± 0,05 μm^2, n= 17; PSD-95-GFP + DsRed2-VAMP2 + N-cadherin: 0,91 ± 0,11 μm^2, n= 18; p= 0,004), while being not significantly altered 8 days after transfection (PSD-95-GFP + DsRed2-VAMP2: 0,99 ± 0,07 μm^2, n= 17; PSD-95-GFP + DsRed2-VAMP2 + N-cadherin: 1,25 ± 0,12 μm^2, n= 18; Fig. 3.12B). The mean intensity did not show any significant alterations, neither 2 nor 8 days after transfection (Fig. 3.12C; 2d: PSD-95-GFP + DsRed2-VAMP2: 1198,0 ± 132,1 A.U., n= 17; PSD-95-GFP + DsRed2-VAMP2 + N-cadherin: 1339, 1 ± 141,0 A.U., n= 18; 8d: PSD-95-GFP + DsRed2-VAMP2: 1623, 3 ± 147,4 A.U., n= 26; PSD-95-GFP + DsRed2-VAMP2 + N-cadherin: 1838,8 ± 142,9 A.U., n= 27)

As the variable expression level of the PSD-95-GFP construct influences the morphological properties of individual PSD-95 puncta, the analysis of PSD-95-GFP puncta was restricted to the puncta density. PSD-95-GFP puncta density was not significantly altered 2 days after transfection (PSD-95-GFP + DsRed2-VAMP2: 9,0 ± 0,8 pcta/30μm dendrite, n= 17; PSD-95-GFP + DsRed2-VAMP2 + N-cadherin: 8,5 ± 0,8 pcta/30μm dendrite, n= 18), but significantly decreased 8 days after transfection (PSD-95-GFP + DsRed2-VAMP2: 9,4 ± 0,5 pcta/30μm dendrite, n= 26; PSD-95-GFP + DsRed2-VAMP2 + N-cadherin: 7,2 ± 0,4 pcta/30μm dendrite, n= 27; p< 0,001; Fig. 3.12D).

In case VAMP2 and PSD-95-GFP puncta were exclusively (i.e. without a DsRed2-VAMP2 signal) colocalizing with each other, the puncta were considered as synaptic puncta. These were analyzed regarding mean density, mean area and mean intensity of the VAMP2 puncta and are depicted normalized to the control values. The density of synaptic VAMP2 puncta of Ncad-/- neurons asymmetrically expressing N-cadherin was unaffected 2 days after transfection (PSD-95-GFP + DsRed2-VAMP2 + N-cadherin: 128,9 ± 23,8 %, n= 18), but in line with the above described results significantly reduced 8 days after transfection (PSD-95-GFP + DsRed2-VAMP2 + N-cadherin: 76,1 ± 6,6 %, n= 27; p= 0,041) (Fig. 3.12E). Interestingly, the mean area of the synaptic VAMP2 puncta was at both time points significantly increased (Fig 3.12F; 2d: PSD-95-GFP + DsRed2-VAMP2 + N-cadherin: 187,7 ± 24,0 %, n= 18, p= 0,004; 8d: PSD-95-GFP + DsRed2-VAMP2 + N-cadherin: 136,1 ± 12,8 %, n= 27; p= 0,019). The mean intensity of the synaptic VAMP2 puncta showed no significant changes neither 2 days (PSD-95-GFP + DsRed2-VAMP2 + N-cadherin: 105,8 ±

14,0 %., n= 18) nor 8 days after transfection (PSD-95-GFP + DsRed2-VAMP2 + N-cadherin: 114,6 ± 9,7 %., n= 27) (Fig. 3.12G).

In summary, these results confirm a loss of synaptic contacts due to the asymmetric expression of N-cadherin at a late maturational stage 8 days after transfection, but not 2 days after transfection. As the number of synapses at 8 days after transfection was found to be below the level of synapses detected at 2 days after the transfection, this loss appears to be the result of synapse elimination. Accordingly, the effect of asymmetric expression of N-cadherin 8 days after transfection at an early maturational stage (3.3.1) might be likewise considered an elimination of synapses rather than a defect in the formation of new ones.
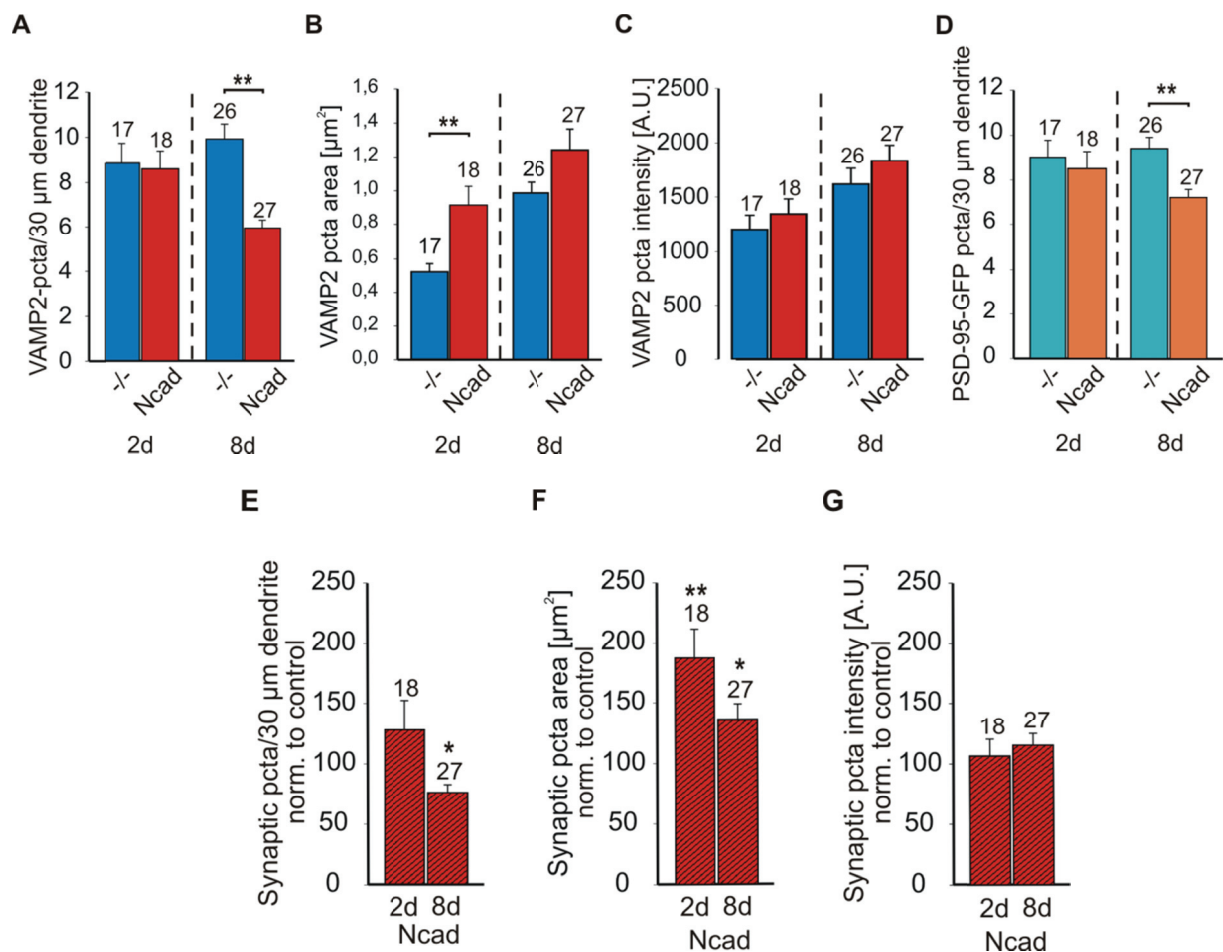

Figure 3.12 Asymmetric N-cadherin expression resulted in synapse elimination and changes in synapse morphology at a late maturational stage.
A-C Quantitative analysis of VAMP2 puncta (immunocytochemical staining) showed a reduced density 8 days after transfection, with no changes 2 days after transfection (A). Interestingly, the mean area of VAMP2 puncta was significantly increased 2 days after transfection (B), while the mean intensity was unaltered at both time points (C). **D** In line with a loss of VAMP2 puncta, the number of PSD-95-GFP puncta was significantly reduced 8 days after transfection. **E-G** The distinction between synapses and autapses revealed a loss of synaptic VAMP2 puncta 8 days after transfection (E), accompanied by a significant increase in their mean area 2 and 8 days after transfection (F). The mean

intensity of the synaptic VAMP2 puncta was unaltered (G). Data were normalized to control values. (n= number of cells; error bars represent s.e.m.; unpaired *t*-test; * p < 0,05; ** p < 0,01).

3.3.2.2 Analysis of autaptic contacts made on Ncad-/- neurons expressing N-cadherin

For the purpose of distinction between autapses and synapses the Ncad-/- neurons had been transfected with DsRed2-VAMP2 in addition to the transfection with PSD-95-GFP and N-cadherin (Fig. 3.13A,B). The number of DsRed2-VAMP2 puncta in Ncad-/- neurons expressing N-cadherin (2d: 2,5 ± 0,6 pcta/30μm dendrite, n= 18; 8d: 0,9 ± 0,2 pcta/30μm dendrite, n= 27) did not show significant differences as compared to control (Fig. 3.13C; 2d: 4,0 ± 1,0 pcta/30μm dendrite, n= 17; 8d: 1,5 ± 0,3 pcta/30μm dendrite, n= 26). DsRed2-VAMP2 puncta colocalized with PSD-95-GFP puncta were considered as autapses. To compare the density of autapses in Ncad-/- neurons expressing N-cadherin at 2d and at 8d after transfection, autapse numbers were normalized to Ncad-/- control neurons (Fig. 3.13D; 2d: PSD-95-GFP + DsRed2-VAMP2 + N-cadherin: 61,2 ± 16,5 %, n= 18; 8d: PSD-95-GFP + DsRed2-VAMP2 + N-cadherin: 53,6 ± 12,2 %, n= 27). No significant elimination of autapses upon expression of N-cadherin was observed. Similar to other studies (Cobb et al., 1997; Lübke et al., 1997), the overall number of autaptic puncta was rather low and a further developmental reduction of autapses was observed.

This was in line with the experiments described in 3.1.2.2 as the rate of autapses in early phase maturation stages seemed to be slightly higher.
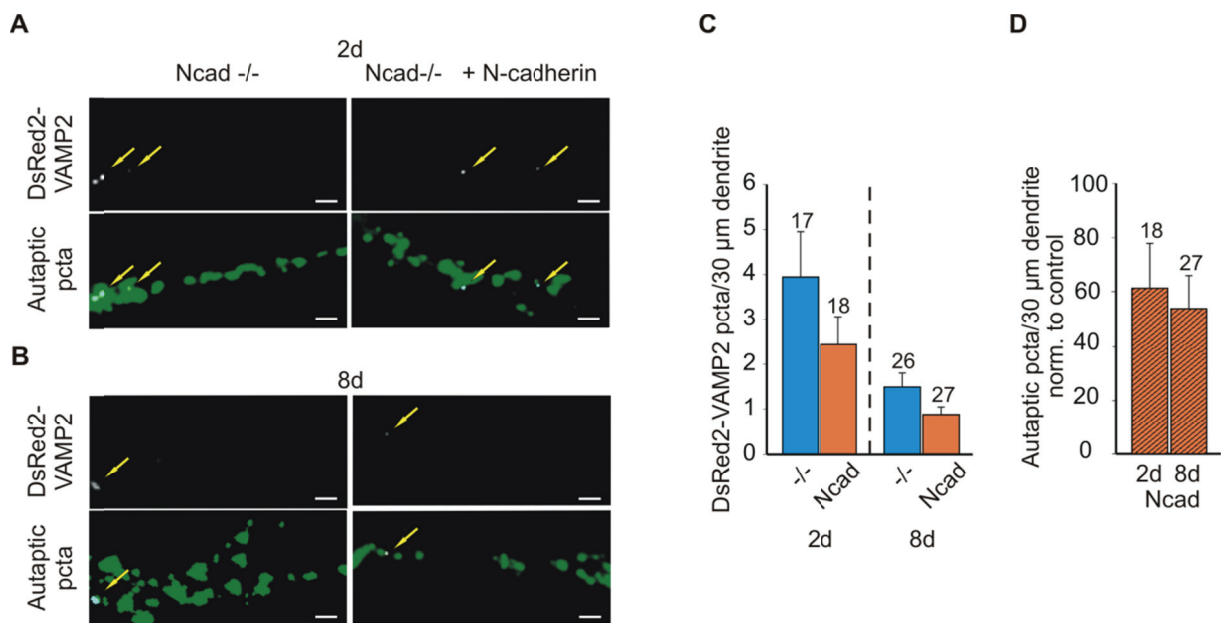
Figure 3.13 Analysis of autapse number at a late maturational stage.
A,B Original DsRed2-VAMP2 and merged (with PSD-95-GFP signal) fluorescence images of Ncad-/-
neurons 2 (A) or 8 (B) days after transfection with PSD-95-GFP + DsRED2-VAMP2 or PSD-95-GFP
+ DsRed2-VAMP2 + N-cadherin (immunocytochemical staining for VAMP2 see figure 3.11).
Dendritic segments corresponding to the images in figure 3.11 are depicted. DsRed2-VAMP2 signal
(white signal) is indicated by yellow arrows. (Scale bars: 2,5µm). **C** Quantitative analysis of the
DsRed2-VAMP2 puncta per 30 µm dendrite revealed no significant alteration in the number of
autapses upon N-cadherin expression. **D** Normalized (to control) density of autapses (DsRed2-
VAMP2 puncta colocalized with PSD-95-GFP puncta) 2d and 8d after transfection with N-cadherin.
(n= number of cells; Error bars represent s.e.m.).

3.3.3 Role of asymmetrically expressed N-cadherin in axon and dendrite retraction

Synapse elimination is accompanied by subsequent retraction of the axon from the synaptic
site. To address this, conditional N-cadherin knockout neurons (Ncad-flox) instead of ES-cell
derived Ncad-/- neurons were used. The Ncad-flox mice (Kostetskii et al., 2005) feature an
insertion of lox-p sites flanking exon 1 of the N-cadherin gene. A Cre-mediated excisive
recombination at the lox-p sites results in the inactivation of the N-cadherin gene. To attain
Cre-mediated recombination Ncad-flox neurons were cultured on glial microislands and
transfected with a CreGFP-vector. By this means the transfected presynaptic neuron is
deficient for N-cadherin, while all surrounding postsynaptic neurons express N-cadherin,
enabling an analysis of a potential axon retraction that is induced by the asymmetric
expression of N-cadherin. The advantage of this assay was that the axon of the transfected
presynaptic neuron can be specifically visualized. For the purpose of visualizing the
transfected neuron including all processes a cotransfection with EGFP was performed. As
control Ncad-flox neurons were solely transfected with EGFP. 2 or 7 days after transfection
the processes of the transfected neurons were imaged.

3.3.3.1 Morphological analysis of Ncad-flox neurons asymmetrically expressing N-cadherin

Because the study of the elimination of synapses due to asymmetric expression of N-cadherin
was a central aim of this work, the analysis of mature neurons was indispensable. To examine
axon retraction single Ncad-flox neurons were transfected at DIV7 with Cre-GFP and
analyzed at DIV14. An analysis of even more mature stages was hindered due to massive
growth and arborization of the axon.

To ensure that a retraction of axons takes place rather than a disturbed growth, the length of axonal processes was first determined at the time point at which the Cre-mediated knock out of N-cadherin was done later (DIV7). Hence, Ncad-flox neurons were transfected with EGFP or EGFP + CreGFP at DIV5 and analyzed at DIV7 (Fig. 3.14). As the examples show, neurons of either condition appeared similar in their morphology.
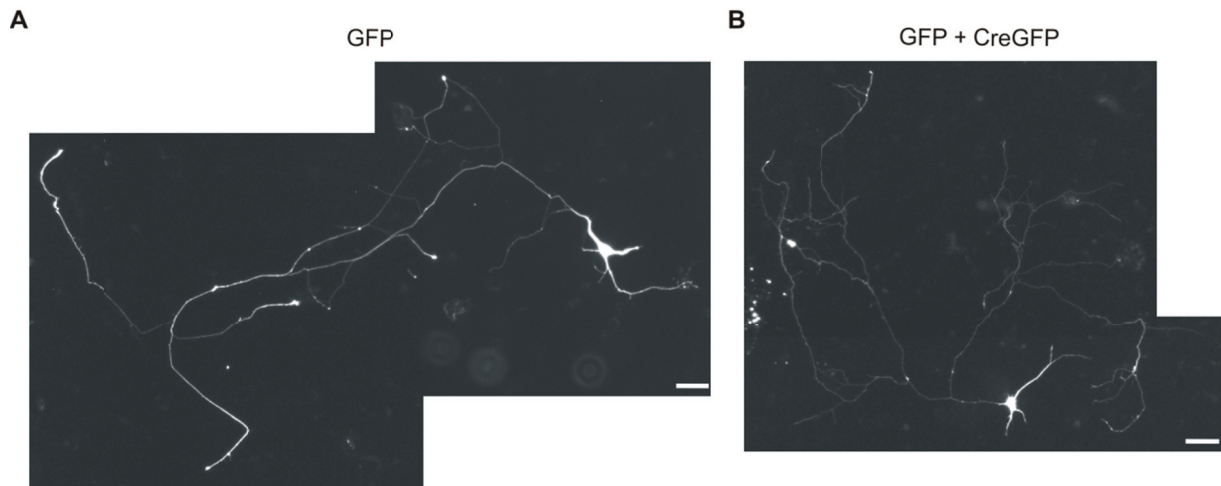

Figure 3.14 Morphological analysis of immature Ncad-flox neurons transfected with Cre-GFP.
A-B Example images of cultured Ncad-flox neurons 2 days after transfection (DIV5) with EGFP (A) or EGFP + CreGFP (B) at DIV 7. (Scale bars= 10µm).

The main focus of experiments was on neurons in a more mature state. Hence, Ncad-flox neurons were transfected with EGFP or EGFP/CreGFP at 7 DIV and analyzed at 14 DIV. The above described experiments (3.3.1; 3.3.2) had demonstrated that 7 days can be assumed to be a sufficient time span for retraction of the axon. Already a morphological examination of neurons in both conditions revealed a strikingly reduced axonal arborization in neurons with asymmetric N-cadherin expression (Fig.3.15).
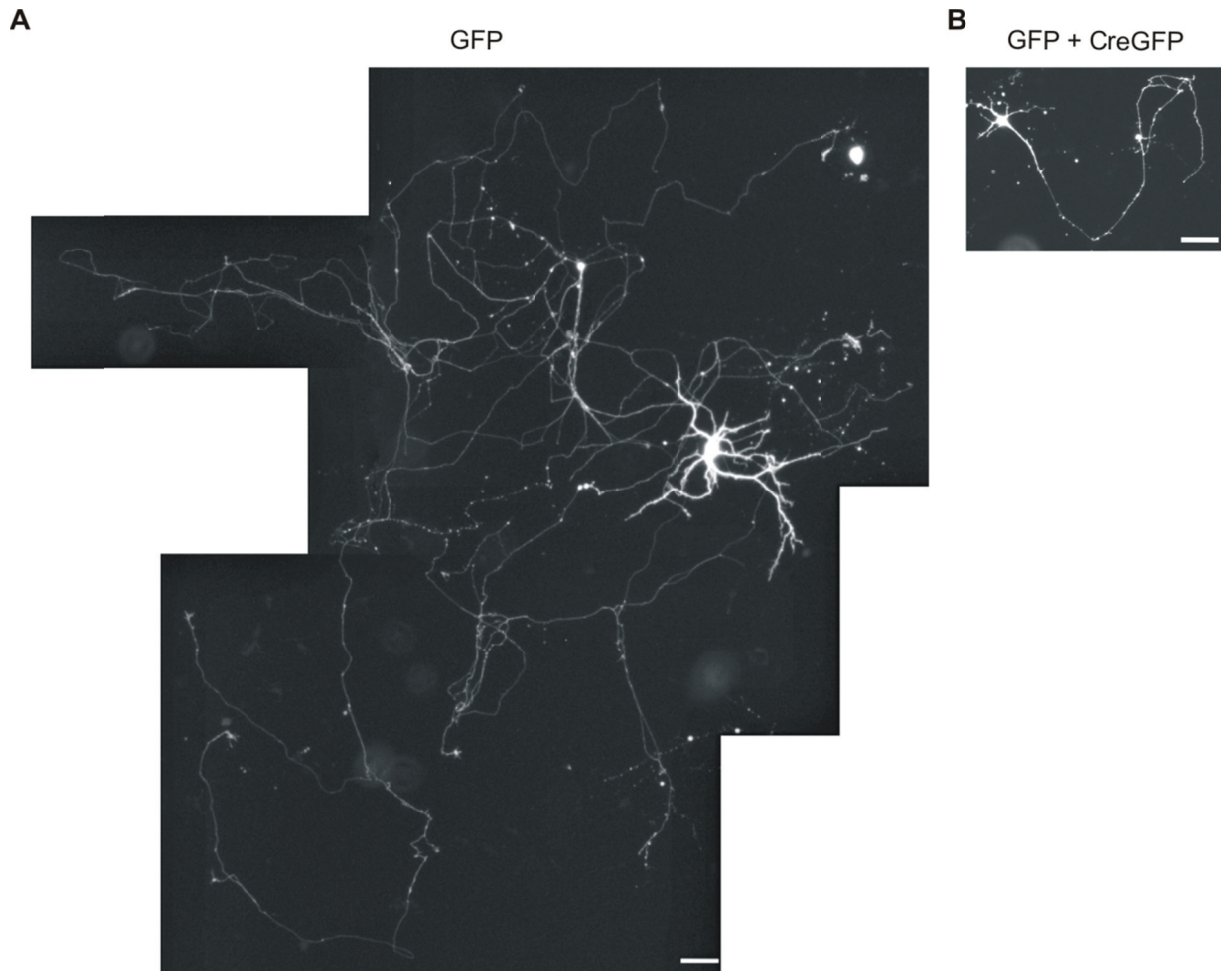
A GFP

B GFP + CreGFP

Figure 3.15 Morphological analysis of mature Ncad-flox neurons transfected by Cre-GFP.
A-B Example images of cultured Ncad-flox neurons 7 days after transfection (DIV7) with EGFP (A) or EGFP + CreGFP (B) at DIV 14. (Scale bars= 10µm).

Another important control is to examine Ncad+/+ neurons and their behavior in terms of axonal growth and arborization. By this experiment any side-effect induced by transfection with the Cre-vector can be excluded. For that purpose cortical neurons from Ncad+/+ mice (Ncad non-flox, C57/bl6) were cultured similar to Ncad-flox neurons on glial microislands. To enable a direct comparison Ncad+/- neurons were transfected with EGFP or EGFP + CreGFP at DIV 7 and imaged at DIV14. As expected, the morphological examination exhibited no obvious differences between both conditions (Fig. 3.16).
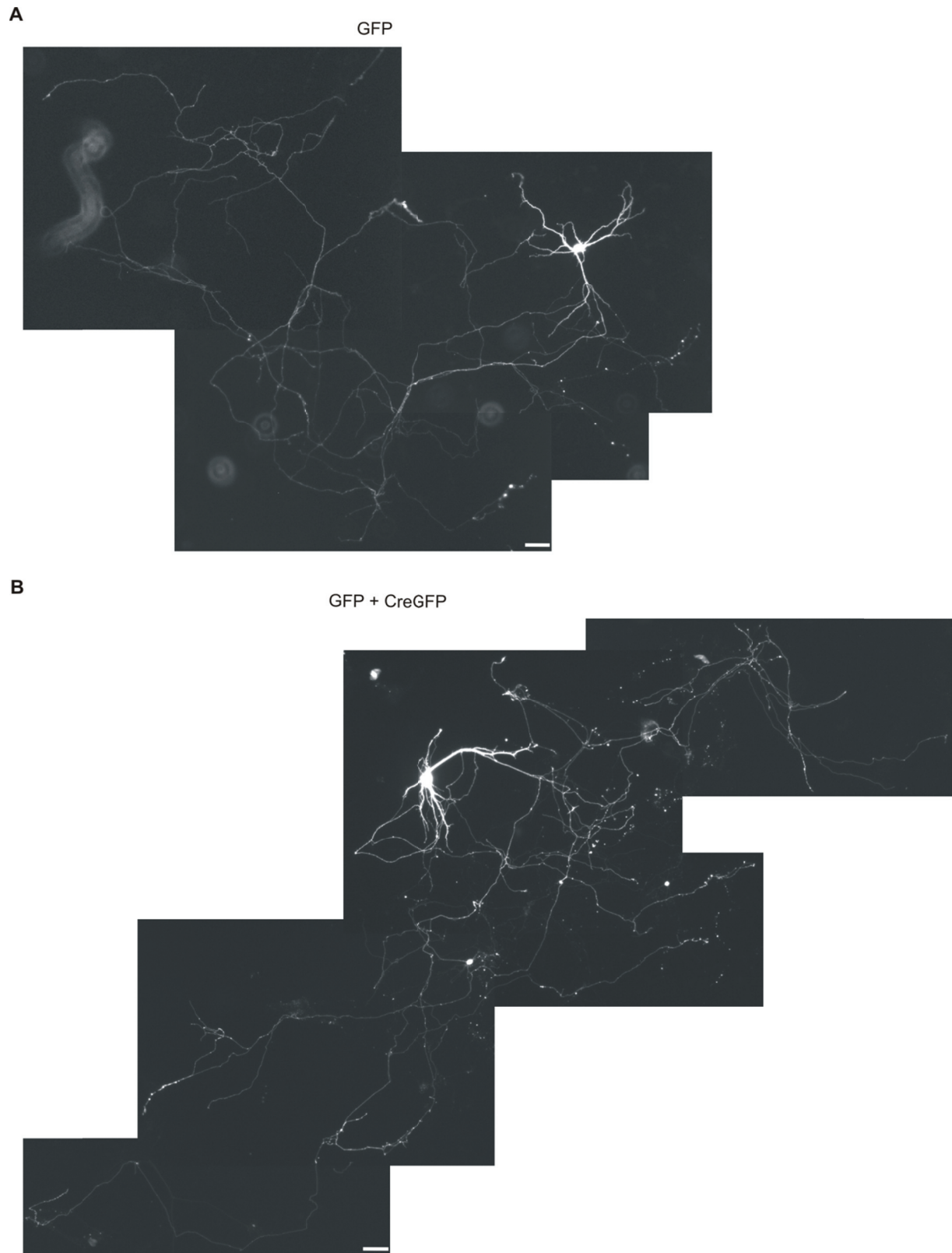
A

GFP

B

GFP + CreGFP

Figure 3.16 Morphological analysis of mature Ncad wildtype (non-flox) neurons transfected with EGFP or EGFP + CreGFP.
A-B Example images of cultured Ncad wildtype (non-flox) neurons 7 days after transfection (DIV7) with EGFP (A) or EGFP + CreGFP (B) at DIV 14. (Scale bars= 10µm).

3.3.3.2 Quantitative analysis of the axonal branch length in Ncad-flox neurons asymmetrically expressing N-cadherin

All neurons obtained in the three independent experiments described in 3.3.3.1 were qualitatively analyzed concerning their morphological properties. All axonal processes were reconstructed and traced in order to examine in the first instance the total axon branch length. Axonal processes were identified by their smaller caliber compared to dendrites and by tracing them back to the soma from the distal end parts.

At DIV7, 2 days after transfection the total axonal branch length (TABL; Fig. 3.17A) was unaltered in Ncad-flox neurons transfected with EGFP + CreGFP ($2026,8 \pm 261,2$ µm , n= 26) compared to the EGFP transfected control ($1967,5 \pm 308,8$ µm , n= 23). In contrast 7 days after transfection at 14DIV the axons of Ncad-flox neurons transfected with EGFP + CreGFP were significantly shorter (Fig. 3.17B; $980,2 \pm 301,4$ µm, n= 22; $p < 0,001$) as the axons of the control ($5167,4 \pm 600,3$ µm , n= 28). As expected, the axons of Ncad non-flox neurons transfected with EGFP + CreGFP at 7 DIV were unaltered (Fig. 3.17C; EGFP: $6836,8 \pm 1565,2$ µm, n= 10) as compared to control (EGFP + CreGFP: $6846,3 \pm 1631,6$ µm, n= 10). To ensure that the above described significant reduction represents axon retraction, an evaluation of the TABL with time in culture was performed. According to the physiological growth of the axon with maturation, a significant increase in the TABL of control Ncad-flox neurons from 7DIV (Fig. 3.17D; 2 days after transfection; $1967,5 \pm 308,8$ µm, n=23) to 14DIV (7 days after transfection; $5167,4 \pm 600,3$ µm , n= 28; $p < 0,001$) was observed. In contrast, due to prolonged asymmetric expression of N-cadherin, Ncad-flox neurons transfected with EGFP + CreGFP revealed a significant reduction of the TABL (2 days after transfection: $2026,8 \pm 261,2$ µm , n= 26; 7 days after transfection: $980,2 \pm 301,4$ µm, n= 22; $p = 0,001$) .

Intriguingly, in line with the elimination of synapses, these results indicate an axon retraction rather than a disturbed growth by an asymmetric expression of N-cadherin.
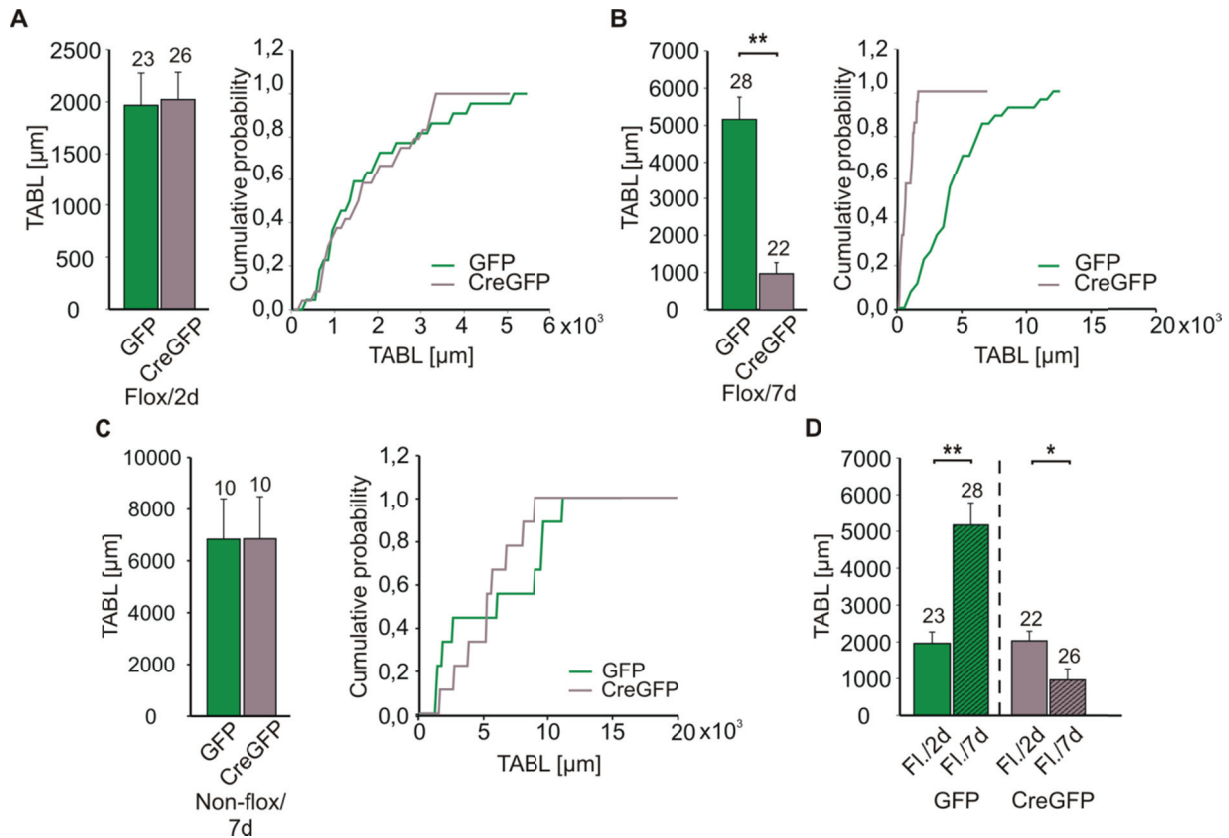
Figure 3.17 Asymmetric expression of N-cadherin resulted in axonal retraction.
A,B Quantification of the total axonal branch length (TABL) in Ncad-flox neurons after transfection with EGFP or EGFP + CreGFP revealed a Cre-induced reduction of axonal processes 7 days after transfection. (A) Transfection at DIV5; analysis 2d later. (B) Transfection at DIV7; analysis 7d later. **C** Analysis of the TABL of Ncad wildtype (non-flox) neurons 7 days after transfection with EGFP or EGFP + CreGFP revealed no alterations as a result of transfection with the Cre-vector. **D** Comparison of the TABL changes over time demonstrated axonal growth in controls (left) and axonal retraction after a mis-match of N-cadherin (right) has been induced. (Fl./2d= DIV7; Fl./7d= DIV14; Error bars represent s.e.m.; n= number of cells; unpaired *t*-test; * p < 0,05; ** p < 0,01).

3.3.3.3 Analysis of the axonal arborization in Ncad-flox neurons asymmetrically expressing N-cadherin

To gain more insight into the morphology of the retracted axons the branch tip number, as measure for the complexity of arborization, was additionally analyzed. As illustrated in figure 3.18E the branch tip number represents the counting of all tips of the individual axon branches. According to the quantifications of the TABL, 2 days after transfection (DIV5) of Ncad-flox neurons the quantitative analysis showed no significant alterations with Cre-GFP expression (Fig. 3.18A; EGFP: 33,5 ± 5,7, n= 23; EGFP + CreGFP: 35,5 ± 4,3, n= 26). In line with the findings described in 3.3.3.2, the branch tip number of Ncad-flox neurons 7 days after transfection (DIV7) with EGFP + CreGFP (Fig. 3.18B; 14,2 ± 2,5, n= 22; p< 0,001) was highly significant reduced as compared to the EGFP expressing control (57,6 ± 6,7, n= 28).

As expected, the branch tip number remained unaltered in Ncad wildtype (non-flox) neurons 7 days after the transfection (DIV7) (Fig. 3.18C; EGFP: 95,1 ± 19,5, n= 10; EGFP + CreGFP: 88,7 ± 16,0, n= 10). Again consistent with the results in 3.3.3.2, the comparison of changes with time in culture showed a significant developmental increase in control EGFP expressing neurons (Fig. 3.18D; 2 days after transfection: 33,5 ± 5,7, n= 23; 7 days after transfection: 57,6 ± 6,7, n= 28; p= 0,010) as well as a significant reduction of the branch tip number in Ncad-flox neurons 7 days after transfection with EGFP + CreGFP (2 days after transfection: 35,5 ± 4,3, n= 26; 7 days after transfection: 14,2 ± 2,5, n= 22; p< 0,001).

Together, these results confirm the reduced axonal retraction found in 3.3.3.2, as also the axonal branching appears to be reduced by prolonged asymmetric expression of N-cadherin.
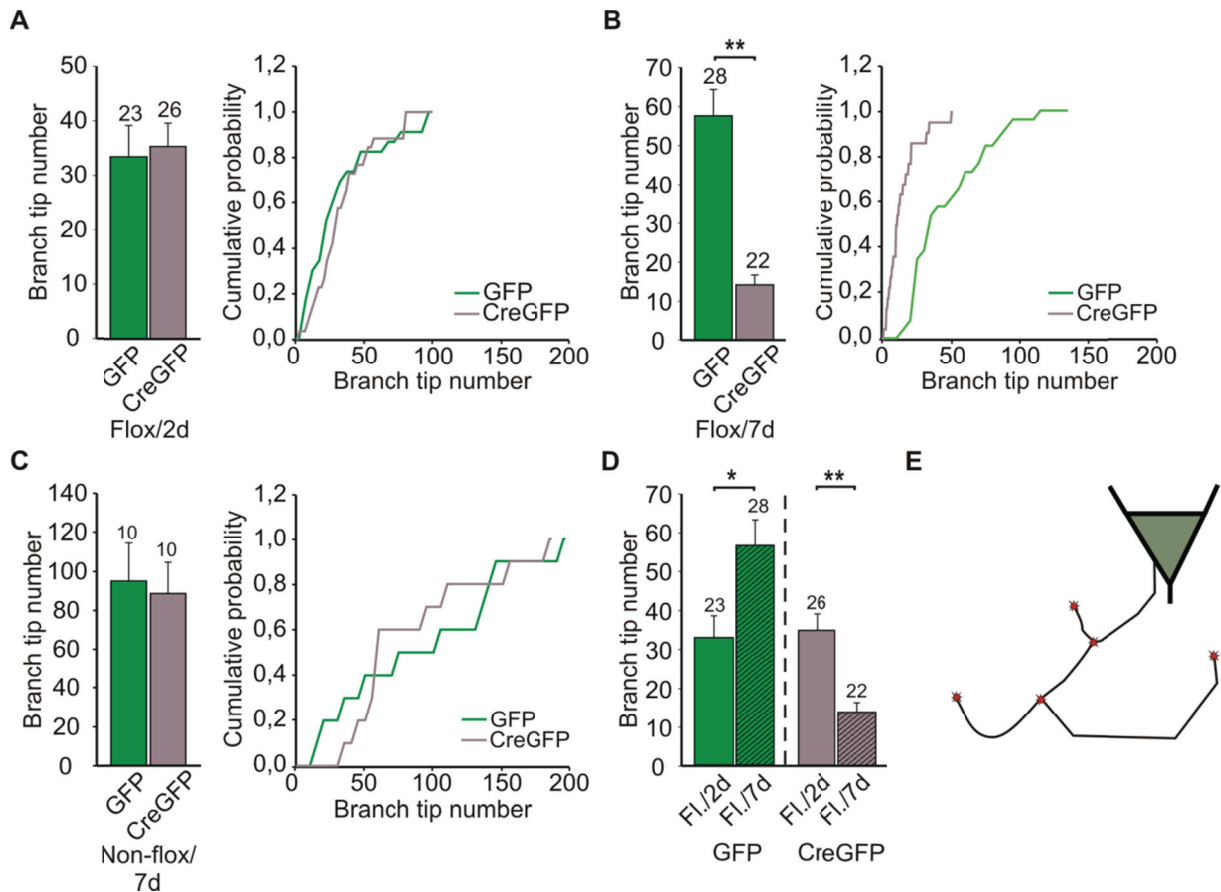

Figure 3.18 Asymmetric expression of N-cadherin resulted in reduced axonal branching.
A,B Quantitative analysis of the axonal branch tip number in Ncad-flox neurons after transfection with EGFP or EGFP + CreGFP demonstrated a disoturbed branching 7 days after transfection. (A) Transfection at 5DIV; analysis 2 days later. (B) Transfection at 7DIV; analysis 7d later **C** The axonal branch tip number in Ncad wildtype (non-flox) neurons 7 days after transfection with EGFP or EGFP + CreGFP remained unaltered. **D** With prolonged asymmetric expression of N-cadherin the branching complexity was reduced (right). With time in culture branching complexity increased in control neurons (left). **E** Scheme illustrating axonal branch tip number. (Fl./2d= DIV7; **F**l./7d= DIV14; Error bars represent s.e.m.; n= number of cells; unpaired *t*-test; * p < 0,05; ** p < 0,01).

3.3.3.4 Analysis of the dendritic branch length in Ncad-flox neurons upon conditional N-cadherin knockout

A N-cadherin-dependent neuron-neuron interaction was found to be required for the maintenance of activity-induced dendrite growth (Tan et al., 2010). The dendrites of Ncad-flox neurons transfected with EGFP + CreGFP are characterized through a presynaptic expression of N-cadherin and a postsynaptic absence. Although preliminary data (Jüngling et al., 2006) describe no obvious changes in the basic function of synapses with this specific N-cadherin mis-match, the consequences for the morphology of the dendritic compartment were evaluated in the following part of this work.

First the total dendritic branch length (TDBL) was analyzed. Thereby, 2 days after transfection (DIV5) with EGFP + CreGFP (Fig. 3.19A; 465,6 ± 63,8 µm, n= 26) no significant alterations were observed as compared to the control (454,1 ± 56,5 µm, n= 23). Giving the knockout of N-cadherin more time to operate, the TDBL was significantly reduced in Ncad-flox neurons 7 days after transfection (DIV7) with EGFP + CreGFP (Fig. 3.19B; 295,7 ± 32,8 µm, n= 22; p= 0,001) in comparison to the control (730,3 ± 108,4 µm, n= 28). The Ncad wildtype (non-flox) neurons revealed no significant alterations 7 days after the transfection (DIV7) with EGFP or EGFP + CreGFP (Fig. 3.19C; EGFP: 878,2 ± 120,3 µm, n= 10; EGFP + CreGFP: 955,9 ± 168,4 µm, n= 10). With time in culture the TDBL was found to be significantly increased in control EGFP expressing neurons (Fig. 3.19D; 2 days after transfection (DIV7): 454,1 ± 56,5 µm, n= 23; 7 days after transfection (DIV14): 730,3 ± 108,4 µm, n= 28; p= 0,039). The analogous comparison with knockout of N-cadherin revealed a highly significant reduction of the TDBL 7 days after transfection with EGFP + CreGFP (Fig. 3.19D; 2 days after transfection (DIV7): 465,6 ± 63,8 µm, n= 26; 7 days after transfection (DIV14): 295,7 ± 32,8 µm, n= 22; p= 0,030).

As expected an efficient N-cadherin-mediated neuron-neuron interaction appeared to be essential for dendritic arborization.
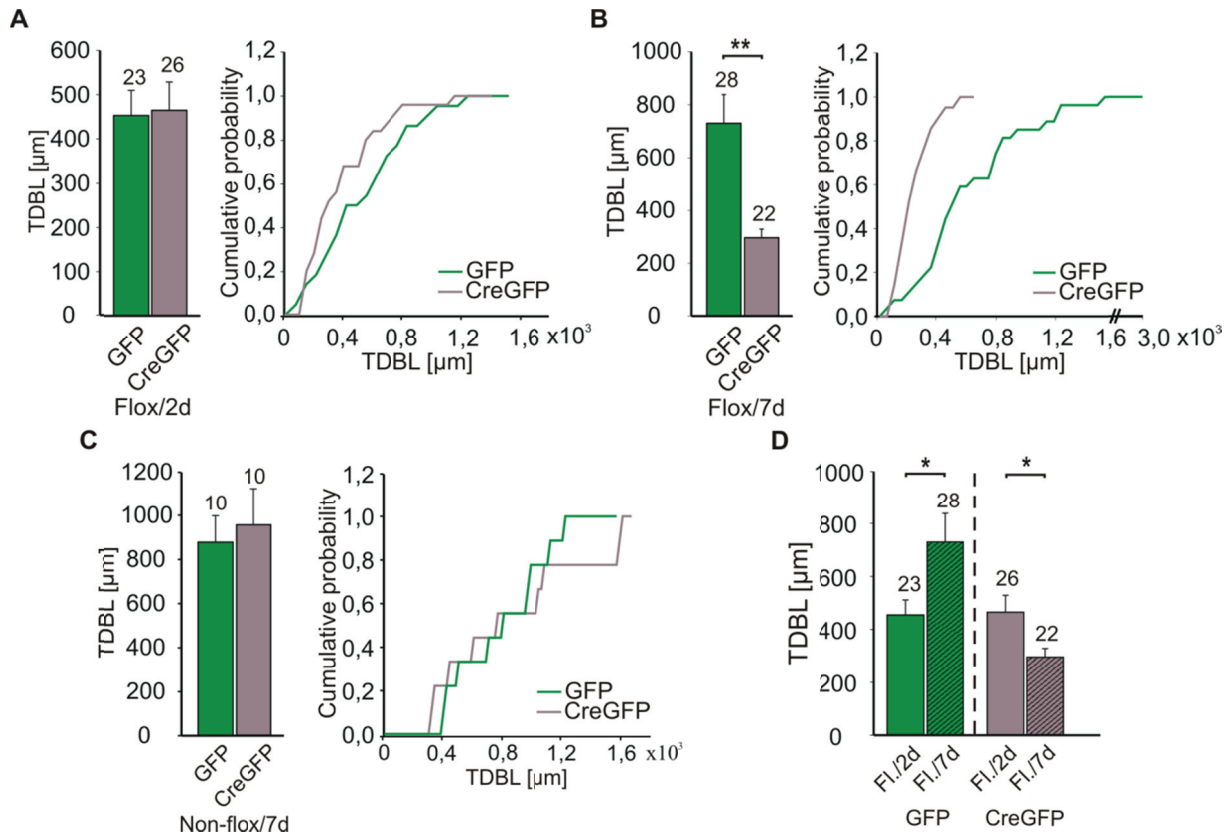
Figure 3.19 Postsynaptic knockout of N-cadherin at synapses with presynaptically expressed N-cadherin resulted in dendrite retraction.
A,B Analysis of the total dendritic branch length (TABL) in Ncad-flox neurons after postsynaptic, Cre-mediated knockout of N-cadherin revealed a reduction of dendritic processes 7 days after transfection. (A) Transfection at 5DIV; analysis 2 days later. (B) Transfection at 7DIV; analysis 7d later **C** Quantification of the TDBL of Ncad wildtype (non-flox) neurons 7 days after transfection (DIV7) with EGFP or EGFP + CreGFP confirmed no alterations by the Cre-vector. **D** Comparison of the TDBL over time demonstrated dendrite retraction upon postsynaptic knockout of N-cadherin (right) and dendrite growth in control (left). (Fl./2d= DIV7; Fl./7d= DIV14; Error bars represent s.e.m.; n= number of cells; unpaired *t*-test; * p < 0,05; ** p < 0,01).

3.3.3.5 Analysis of the dendritic arborization in Ncad-flox neurons upon conditional N-cadherin knockout

According to the evaluation of axonal changes, the complexity of dendritic arborization was also analyzed. As depicted in figure 3.20E all tips of dendritic branch segments were counted and compared. Similar to the TDBL, no significant changes in the branch tip number of Ncad-flox neurons transfected with EGFP + CreGFP (Fig. 3.20A; 24,4 ± 2,7, n= 26) were observed at 7DIV 2 days after transfection (DIV5) compared to the EGFP expressing control (21,5 ± 2,6, n= 23). 7 days after transfection (DIV7) at 14 DIV the branch tip number of Ncad-flox neurons transfected with EGFP + CreGFP (Fig. 3.20B; 12,1 ± 1,4, n=22; p< 0,001) was significantly reduced as compared to Ncad-flox neurons solely transfected with EGFP (24,1 ±

2,4, n= 28). As expected, Ncad wildtype (non-flox) neurons exhibited no significant alterations 7 days after transfection (DIV7) at 14 DIV with EGFP or EGFP + CreGFP (Fig. 3.20C EGFP: 33,3 ± 6,2, n=10; EGFP + CreGFP: 31,4 ± 5,5, n= 10). Comparing changes with time in culture, the branch tip number of control neurons 2 days after transfection (DIV5) at 7DIV was unaltered compared to the branch tip number 7 days after transfection (DIV7) at 14DIV (Fig. 3.20D; 2 days after transfection: 21,5 ± 2,6, n= 23; 7 days after transfection: 24,1 ± 2,4, n= 28). However, the branch tip number of Ncad-flox neurons transfected with EGFP + CreGFP was significantly decreased with time in culture (2 days after transfection: 24,4 ± 2,7, n= 26; 7 days after transfection: 12,1 ± 1,4, n=22; p< 0,001).

Together, these results indicate that a postsynaptic knockout of N-cadherin has influences on the dendritic arborization by reducing dendrite length as well as branching complexity.
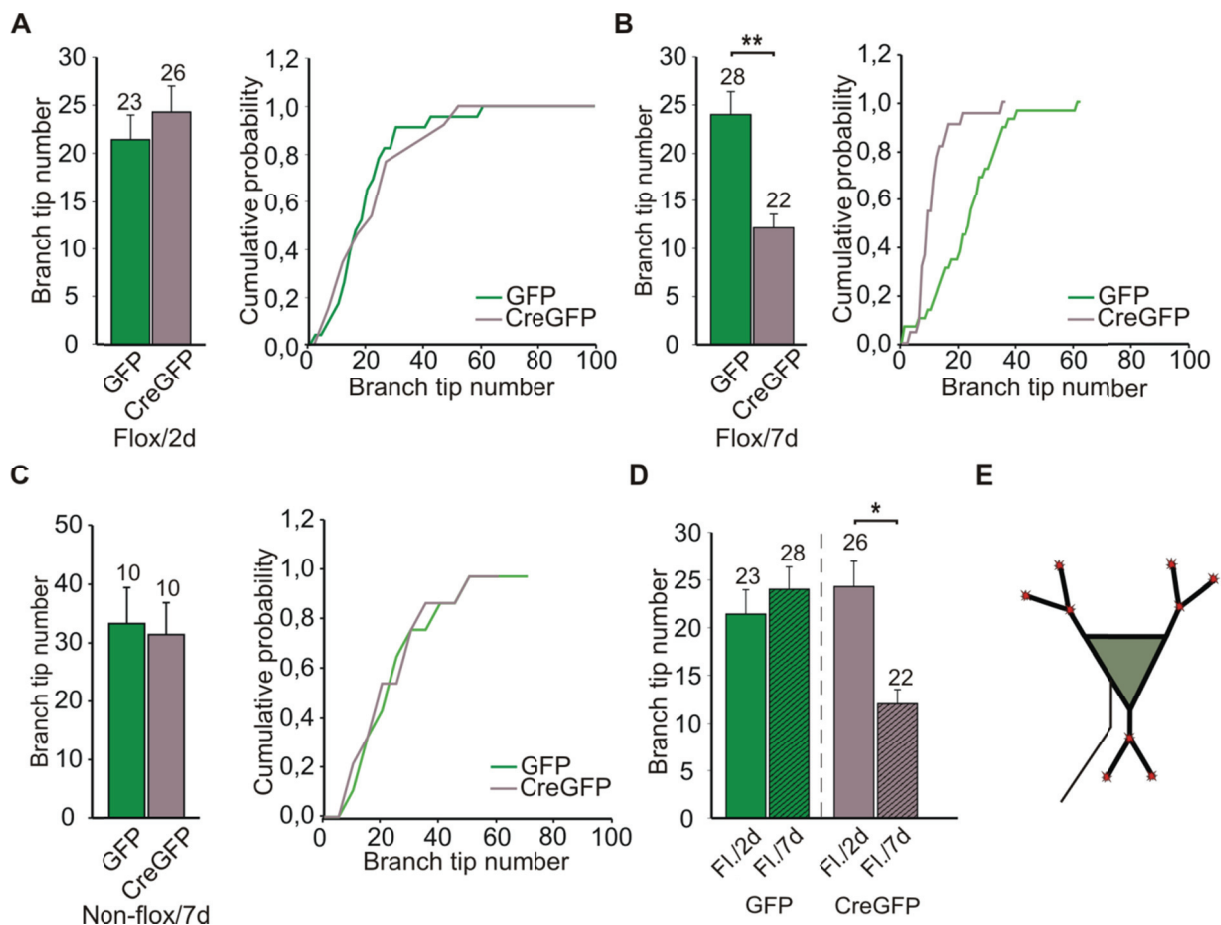
Figure 3.20 Postsynaptic knockout of N-cadherin at synapses with presynaptically expressed N-cadherin impairs dendrite arborization.
A,B Quantification of the dendritic branch tip number in Ncad-flox neurons revealed reduced arborization 7 days after transfection with EGFP or EGFP + CreGFP. (A) Transfection at 5DIV; analysis 2 days later. (B) Transfection at 7DIV; analysis 7d later **C** Ncad wildtype (non-flox) neurons showed no alterations in the dendritic branch tip number 7 days after transfection with EGFP or EGFP + CreGFP. **D** The complexity of branching was reduced upon postsynaptic knockout of N-cadherin.

E Scheme illustrating branch tip number. (Fl./2d= DIV7; Fl./7d= DIV14; Error bars represent s.e.m.; n= number of cells; unpaired *t*-test; * p < 0,05; ** p < 0,01).

3.4 Requirement of N-cadherin for neuroligin1-mediated regulation of synaptic function

The following set of data was obtained within the framework of a study (Stan et al., 2010), investigating the cooperation of N-cadherin and neuroligin in important regulatory processes during synapse formation. Experiments analyzing morphological and molecular properties demonstrated that presynaptic vesicle accumulation depends on an interaction between both adhesion molecule systems. The following electrophysiological approaches were performed to gain insight into the role of the cooperation of N-cadherin and neuroligin1 at the functional level. As neuroligin1 was found to be exclusively expressed at glutamatergic synapses (Song et al., 1999), all GABAergic synaptic activity was blocked by the addition of Gabazine.

3.4.1 Effects of neuroligin1 on AMPA receptor-mediated mEPSCs

Neuroligin1 is well known to induce pre - and postsynaptic specializations (Scheiffele et al., 2000; Graf et al., 2004; Chih et al., 2005). As shown by several groups the overexpression of neuroligin1 induces presynaptic vesicle clustering as well as an increase in the frequency of AMPA receptor-mediated mEPSCs. In order to confirm these results with the neuronal cultures used in this study, cortical neurons were cultured on Poly-L-ornithin-(PO)-coated culture dishes and transfected with neuroligin1 fused to EGFP for enabling visualization (Nlg1-GFP). Neurons solely transfected with EGFP served as control. The neurons overexpressing neuroligin1-GFP were analyzed by recording AMPA receptor-mediated mEPSCs at 12-14DIV (2 days after transfection). A physiological concentration of extracellular Ca^{2+} (2,5 mM) was used (Fig. 3.21A). Under this condition, the overexpression of neuroligin1-GFP resulted as expected in a significantly increased frequency of AMPA receptor-mediated mEPSCs (Fig. 3.21C; 1,45 ± 0,53 Hz, n= 22, p= 0,029) as compared to control (0,26 ± 0,12 Hz , n= 24). In contrast to what has been observed by other groups no significant changes in the amplitude (EGFP: 14,3 ± 1,5 pA, n= 11; Nlg1-GFP: 16,1 ± 2,2 pA, n= 14) could be obtained. Likewise, the kinetics of the AMPA receptor-mediated mEPSCs were not altered (Rise time: EGFP: 1,55 ± 0,22 ms, n=11; Nlg1-GFP: 1,74 ± 0,11 ms, n= 14; decay time: EGFP: 3,74 ± 0,61 ms, n= 11; Nlg1-GFP: 3,69 ± 0,25 ms, n= 14). Several factors

might account for the obtained results. Given that the mEPSC amplitude is not altered, changes at the postsynaptic AMPA receptors can be excluded. In line with other studies, alterations in the presynaptic vesicle release as well as an induction of synapse formation might be presumed. Thereby, the vesicle release probability is limited by the extracellular Ca^{2+} concentration. By increasing the extracellular Ca^{2+} to 5 mM, vesicle release probability gets maximal and cannot be further increased by Nlg1. In fact, the quantitative analysis of AMPA mEPSCs recorded at 5 mM Ca^{2+} (Fig. 3.21B) did not show a significant increase in the mean frequency in Nlg1-GFP transfected neurons (Fig. 3.21C; 0,67 ± 0,35 Hz, n= 12) as compared to control (0,63 ± 0,36 Hz, n= 15). As expected, the mean amplitude (EGFP: 13,5 ± 1,1 pA, n= 10; Nlg1-GFP: 11, 4 ± 1,1 pA, n= 9) as well as the mean rise time (EGFP: 2,00 ± 0,15 ms, n= 10, Nlg1-GFP: 2,15 ± 0,22 ms, n= 9) and mean decay time (EGFP: 3,86 ± 0,61 ms, n= 10; Nlg1-GFP: 4,91 ± 1,09 ms, n= 9) remained also unaltered (Fig. 3.21C).

In line with other studies, these results demonstrated a neuroligin1-mediated regulation of synaptic transmission. Moreover, neuroligin1 might modulate the presynaptic vesicle release properties.

[107]
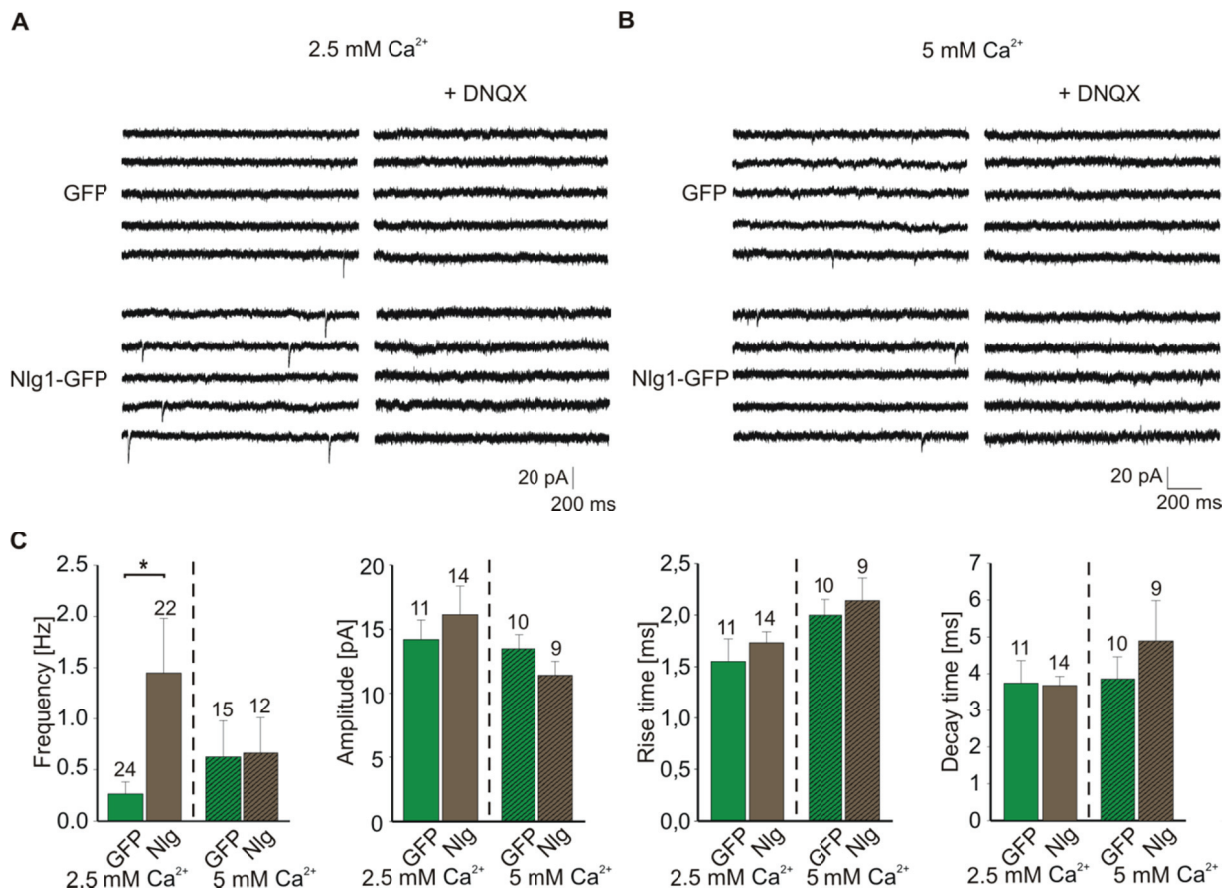
Figure 3.21 Overexpression of neuroligin1-GFP enhanced spontaneous synaptic vesicle release.

A,B Sample traces of AMPA receptor-mediated mEPSCs recorded at 2.5 mM (A) or 5 mM extracellular Ca^{2+} concentration (B) extracellular from cortical neurons transfected with Nlg1-GFP or EGFP. AMPA mEPSCs were blocked by DNQX (10 μM) **C** Quantification of the mean frequencies, mean amplitudes and kinetics of the AMPA receptor-mediated mEPSCs under physiological conditions (2,5 mM Ca^{2+}) revealed an increased synaptic activity by overexpression of neuroligin1. Neuroligin1 failed to increase synaptic activity under 5 mM Ca^{2+}, thus indicating an involvement of presynaptic vesicle release modifications. (Error bars represent s.e.m.; n= number of cells; unpaired *t*-test; * p < 0,05).

3.4.2 Role of N-cadherin in neuroligin1- mediated enhancement of synaptic vesicle release

A role of neuroligin1 in inducing presynaptic vesicle clustering is well described and was confirmed by Stan et al., 2010. Beyond that, the authors demonstrated a dependence of this neuroligin1 action on N-cadherin function. In order to analyze that issue for functional synaptic transmission, electrophysiological recordings were performed. Thereby loss-of-function experiments for N-cadherin were combined with the overexpression of neuroligin1. Primary cultured cortical neurons were cotransfected with Nlg1-GFP and a truncated form of N-cadherin, lacking most of the extracellular domain (Ncad-ΔE). This represents a dominant-negative version of N-cadherin replacing endogenous N-cadherin at the synapse in a competitive manner (Fujimori and Takeichi, 1993; Riehl et al., 1996). Transfections with EGFP and Nlg1-GFP served as control for the neuroligin-mediated effect on synaptic function. Neurons transfected with EGFP + Ncad-ΔE were compared with neurons transfected with Nlg1-GFP + Ncad-ΔE (Fig. 3.22).

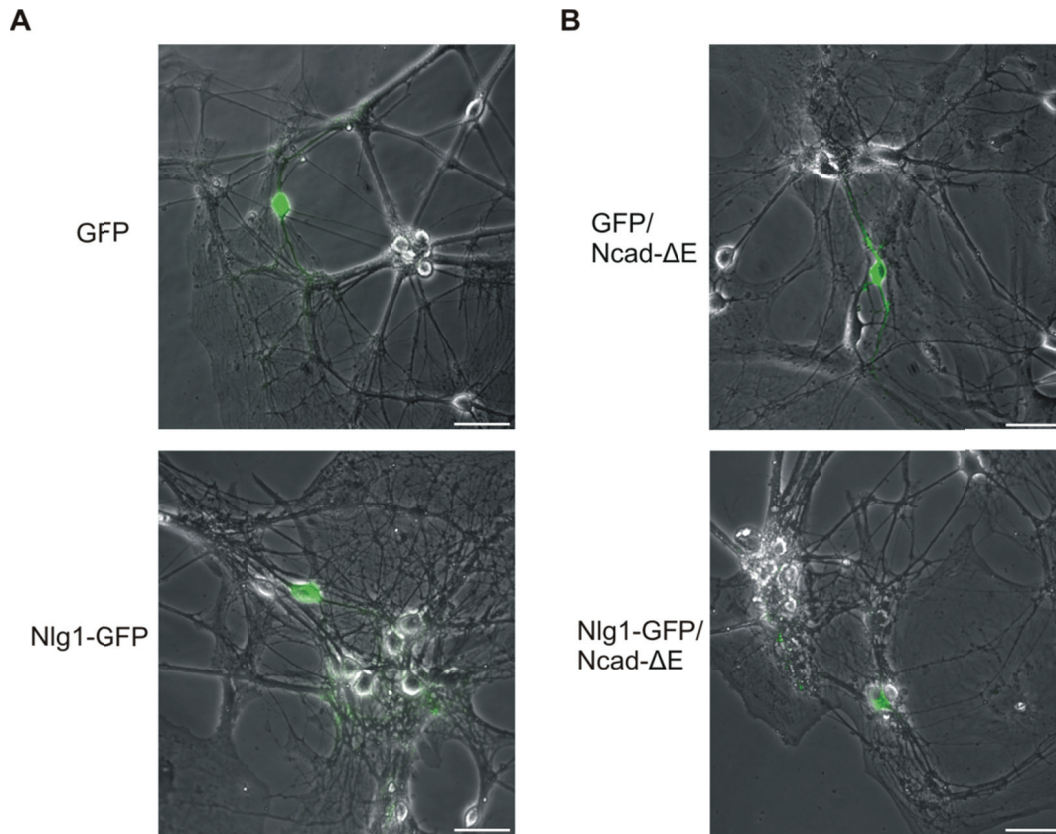**A**

GFP

Nlg1-GFP

B

GFP/
Ncad-ΔE

Nlg1-GFP/
Ncad-ΔE

Figure 3.22 Experimental approach for analyzing the dependence of the neuroligin1-mediated enhancement of synaptic vesicle release on N-cadherin.

A Example images of cortical neurons at 12 DIV transfected with EGFP or Nlg1-GFP as control for neuroligin1-mediated effect (Scale bars= 10μm). **B** Example images of cortical neurons transfected with EGFP + Ncad-ΔE or Nlg1-GFP + Ncad-ΔE. (Scale bars= 10μm).

3.4.2.1 N-cadherin function is required for neuroligin1 induced enhancement of AMPA receptor-mediated mEPSCs

To gain insight into the necessity of N-cadherin function for neuroligin1 activity, spontaneous AMPA receptor-mediated mEPSCs were recorded from cortical neurons transfected (10-12 DIV) with EGFP or Nlg1-GFP/EGFP + Ncad-ΔE or Nlg1-GFP + Ncad-ΔE at 12-14 DIV (Fig. 3.23A,B). All recordings were carried out under physiological conditions (2,5 mM Ca^{2+}; -60 mV holding potential) 2 days after transfection. As already described in 3.4.1 in control cortical neurons the overexpression of Nlg1-GFP resulted in a significant increase in the mean frequency of AMPA mEPSCs (Fig. 3.23C; 1,45 ± 0,53 Hz, n= 22, p= 0,029) as compared to control (0,26 ± 0,12 Hz , n= 24). Most strikingly, this neuroligin1-mediated enhancement was completely abolished upon expression of Nlg1-GFP in neurons cotransfected with Ncad-ΔE (Fig. 3.23C; EGFP: 0,21 ± 0,06 Hz, n= 23; Nlg1-GFP: 0,22 ± 0,07 Hz, n= 18). In both cases no changes in the mean amplitudes (EGFP: 14,3 ± 1,5 pA, n= 11, Nlg1-GFP: 16,1 ± 2,2 pA,

n= 14; EGFP + Ncad-ΔE: 12,9 ± 1,0 pA, n= 15, Nlg1-GFP + Ncad-ΔE: 15,5 ± 2,8 pA, n= 10) and in the kinetics (Rise time: EGFP: 1,55 ± 0,22 ms, n=11, Nlg1-GFP: 1,74 ± 0,11 ms, n= 14; EGFP + Ncad-ΔE: 2.13 ± 0,14 ms, n= 15, Nlg1-GFP + Ncad-ΔE: 2,15 ± 0,23 ms, n=10; decay time: EGFP: 3,74 ± 0,61 ms, n= 11, Nlg1-GFP: 3,69 ± 0,25 ms, n= 14; EGFP + Ncad-ΔE: 4,88 ± 0,45 ms, n= 15, Nlg1-GFP + Ncad-ΔE: 5,16 ± 0,86 ms, n= 10) were observed (Fig. 3.23C).

These results strenghten the morphological findings described by Stan et al., 2010 of a requirement of N-cadherin for neuroligin1 activity also at the functional level.
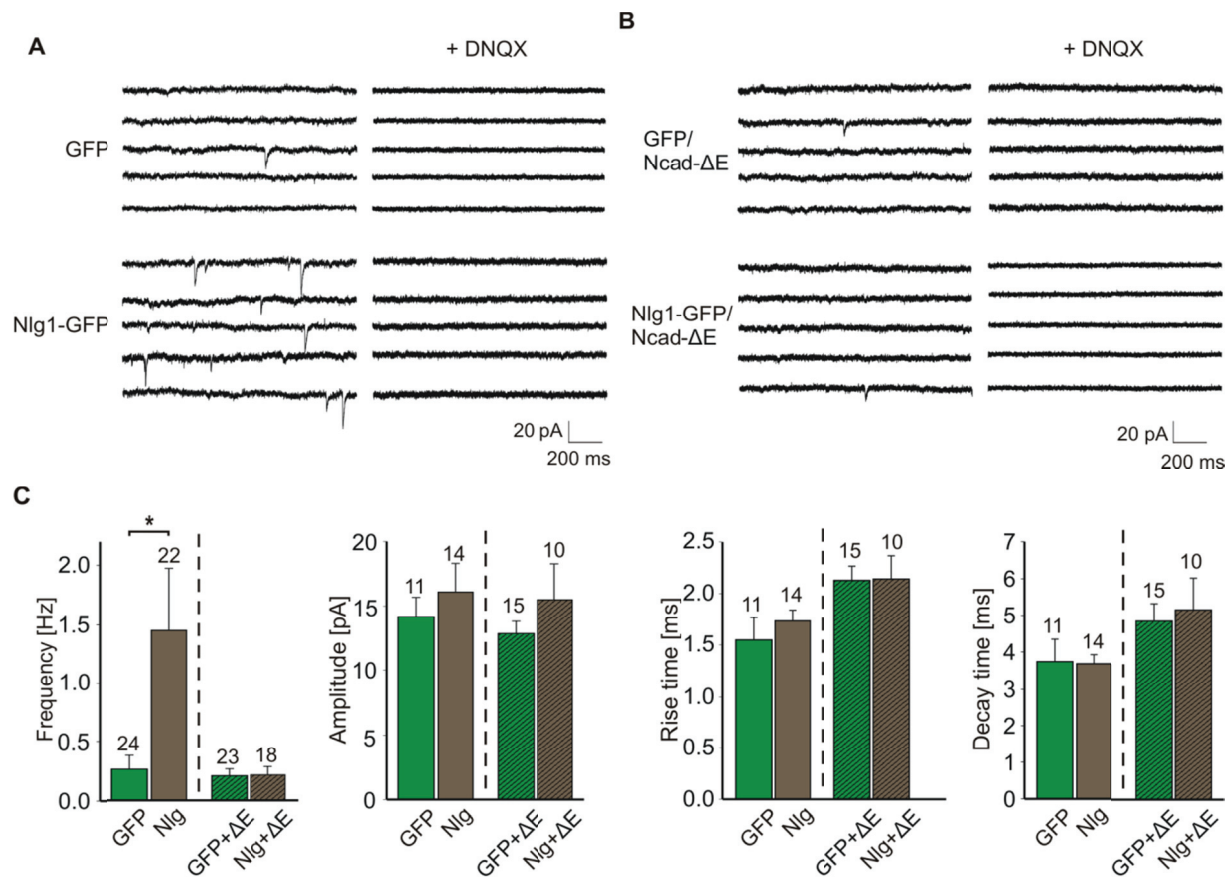
Figure 3.23 N-cadherin function is essential for neuroligin1-induced enhancement of synaptic activity in cortical neurons.
A-B Representative traces of AMPA receptor-mediated mEPSCs recorded after transfection with EGFP or Nlg1-GFP (A) and EGFP + Ncad-ΔE or Nlg1-GFP + Ncad-ΔE (B). AMPA mEPSCs were blocked by DNQX (10 μM). **C** Quantitative analysis of mean frequency, mean amplitude, mean rise and mean decay time revealed a cooperation of the neuroligin1 and the N-cadherin systems in regulating synaptic function. (Error bars represent s.e.m.; n= number of cells; unpaired *t*-test; * p < 0,05).

The majority of the experiments performed by Stan et al., 2010 were carried out on Ncad-/- neurons derived from embryonic stem cells. To examine the N-cadherin/neuroligin1

cooperation in ES cell-derived neurons the above described experiments were repeated. Hence, ES cell-derived Ncad-/- neurons were transfected (DIV 10-12) with EGFP or Nlg1-GFP and spontaneous AMPA receptor-mediated mEPSCs were recorded at 12-14 DIV (Fig. 3.24A). As control Ncad+/- ES cell-derived neurons were transfected with EGFP or Nlg1-GFP (Fig. 3.24B). As expected, the overexpression of Nlg1-GFP in Ncad+/- neurons enhanced the mean frequency of AMPA mEPSCs significantly (Fig. 3.24C; 0,92 ± 0,37 Hz, n= 24; p= 0,048) as compared to control (0,28 ± 0,07 Hz, n= 35). No changes in the mean amplitude (EGFP: 14,1 ± 0,8 pA, n= 30; Nlg1-GFP: 12,5 ± 0,8 pA, n= 23), rise time (EGFP: 1,51 0,1 ms, n= 30; Nlg1-GFP: 1,63 ± 0,07 ms, n= 23) or decay time (EGFP: 3,58 ± 0,32 ms, n= 30; Nlg1-GFP: 3,21 ± 0,18 ms, n= 23) were observed (Fig. 3.24C). Intriguingly, in the absence of N-cadherin neuroligin1 failed to enhance synaptic transmission as revealed by the quantification of the mean frequency of AMPA mEPSCs in Ncad-/- neurons (Fig. 3.24C; EGFP: 0,27 ± 0,07 Hz, n= 28; Nlg1-GFP: 0,42 ± 0,18 Hz, n= 25). The mean amplitude (EGFP: 15,8 ± 1,5 pA, n= 18; Nlg1-GFP: 14,8 ± 1,1 pA, n=10), the mean rise time (EGFP: 1,48 ± 0,16 ms, n= 18; Nlg1-GFP: 1,69 ± 0,25 ms, n= 10) and the mean decay time (EGFP: 3,10 ± 0,31 ms, n= 18; Nlg1-GFP: 2,85 ± 0,19 ms, n= 10) remained unaltered.

Together, these results indicate the necessity of N-cadherin expression for neuroligin1-induced enhancement of synaptic transmission also in ES cell-derived neurons.
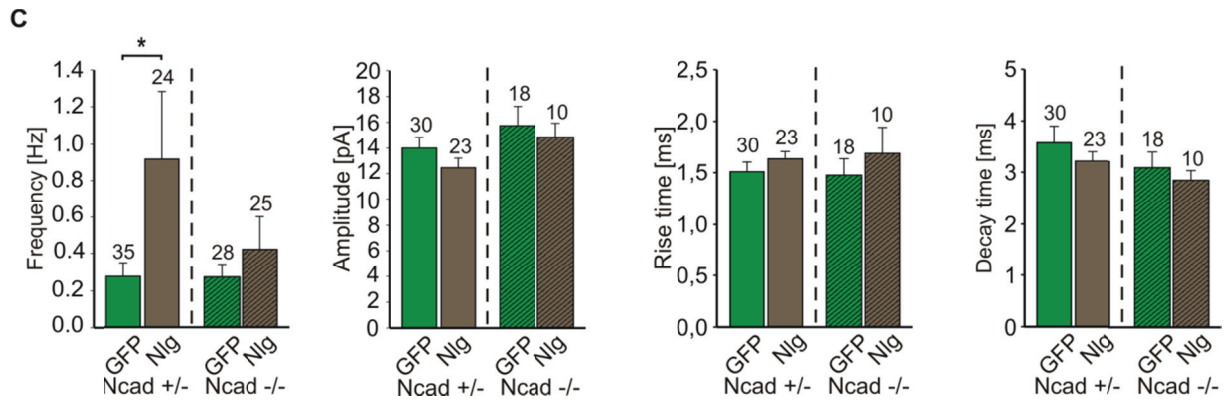
C
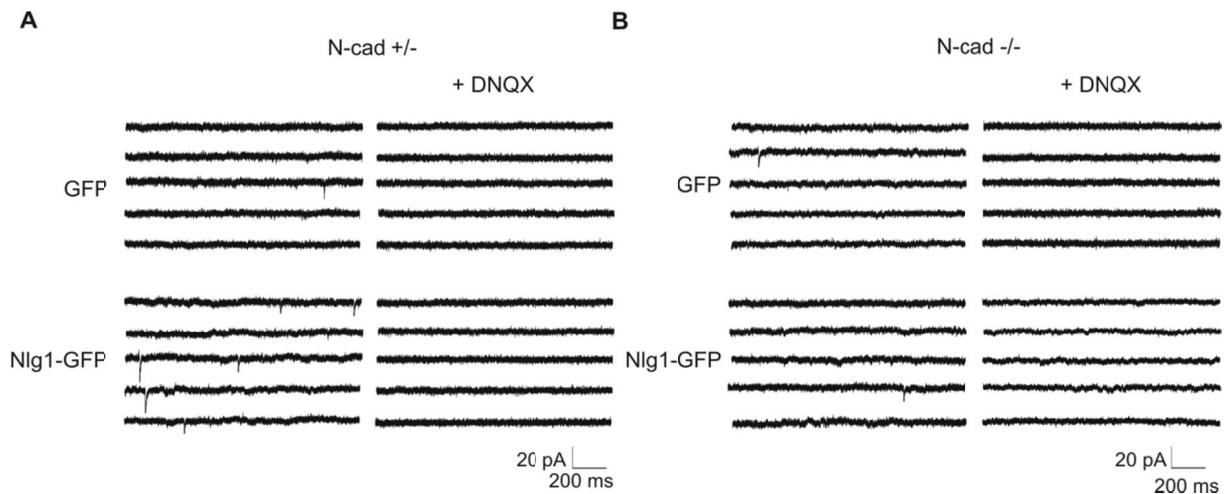
Figure 3.24 Neuroligin1-induced enhancement of synaptic transmission is dependent on N-cadherin expression in ES cell-derived neurons.
A,B Sample traces of AMPA receptor-mediated mEPSCs recorded in ES cell-derived Ncad+/- (A) or Ncad-/- (B) neurons transfected with EGFP or Nlg1-GFP. AMPA mEPSCs were blocked by DNQX (10 μM). **C** Quantitative analysis of the mean frequency, the mean amplitude, mean rise and mena decay time of AMPA mEPSCs. Depending on N-cadherin, neuroligin triggered synaptic function also in ES cell-derived neurons. (Error bars represent s.e.m.; n= number of cells; unpaired *t*-test; * p < 0,05).

3.4.2.2 N-cadherin function is required for neuroligin1-induced enhancement of release probability

Neuroligin1 has been shown to enhance presynaptic vesicle release probability. To show this neuroligin1-induced enhancement is dependent on N-cadherin function primary cultured cortical neurons were transfected (DIV 10-12) with EGFP or Nlg1-GFP or EGFP + Ncad-ΔE or Nlg1-GFP + Ncad-ΔE. At 12-14 DIV evoked (extracellular stimulation) NMDA receptor-mediated EPSCs were recorded in Mg^{2+} free extracellular solution at 2,5 mM Ca^{2+} and -70 mV holding potential and subsequently exposed to MK-801 (20 μM), a channel activity-dependent antagonist of NMDA receptors (Fig. 3.25). The higher the release probability, the faster is the blockade of NMDA receptor-mediated EPSCs by MK-801. Thus, the kinetics of the progressive MK-801 block shed light on the presynaptic release probability.
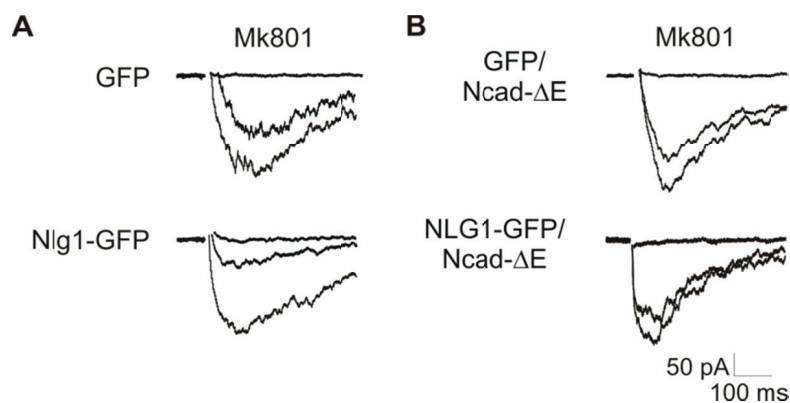
Figure 3.25 MK-801 (20 µM) block of evoked NMDA receptor-mediated EPSCs in neurons transfected with EGFP, Nlg1-GFP, EGFP + Ncad-ΔE or Nlg1-GFP + Ncad-ΔE.
A,B Samples of the progressive, MK-801 block of evoked NMDA receptor-mediated EPSCs in cortical neurons transfected (10-12 DIV) with EGFP, Nlg1-GFP, EGFP + Ncad-ΔE or Nlg1-GFP + Ncad-ΔE at 12-14 DIV. In each case, the first, the 8th and the final response after addition of MK-801 are depicted.

As qualitative measure for the progressive MK-801 block, τ values, representing the number of stimuli until the EPSC amplitude reached 37 % of its initial value, were determined. Comparison of the block kinetics in neurons transfected with EGFP or EGFP + Ncad-ΔE revealed (Fig. 3.26A) that the loss of N-cadherin function has no significant effect on the decay (Fig. 3.26B; EGFP: 33,6 ± 9,2 stimuli, n= 5; EGFP + Ncad-ΔE: 21,3 ± 10,2 stimuli, n= 4). In contrast, the kinetics of the MK-801 block in neurons transfected with EGFP (33,6 ± 9,2 stimuli, n= 5) and neurons transfected with Nlg1-GFP (8,2 ± 2,1 stimuli, n= 6) were significantly different (Fig. 3.26C,D; p= 0,016), indicating an increased release probability upon neuroligin1 expression. As expected, in the absence of N-cadherin function this acceleration of the MK-801 block was completely abolished (Fig 3.26C,D; EGFP + Ncad-ΔE: 21,3 ± 10,2 stimuli, n= 4; Nlg1-GFP + Ncad-ΔE: 17,8 ± 4,4 stimuli, n= 5.).

In summary, these results demonstrate the ability of neuroligin1 to enhance presynaptic release probabilityand its dependence on N-cadherin function.
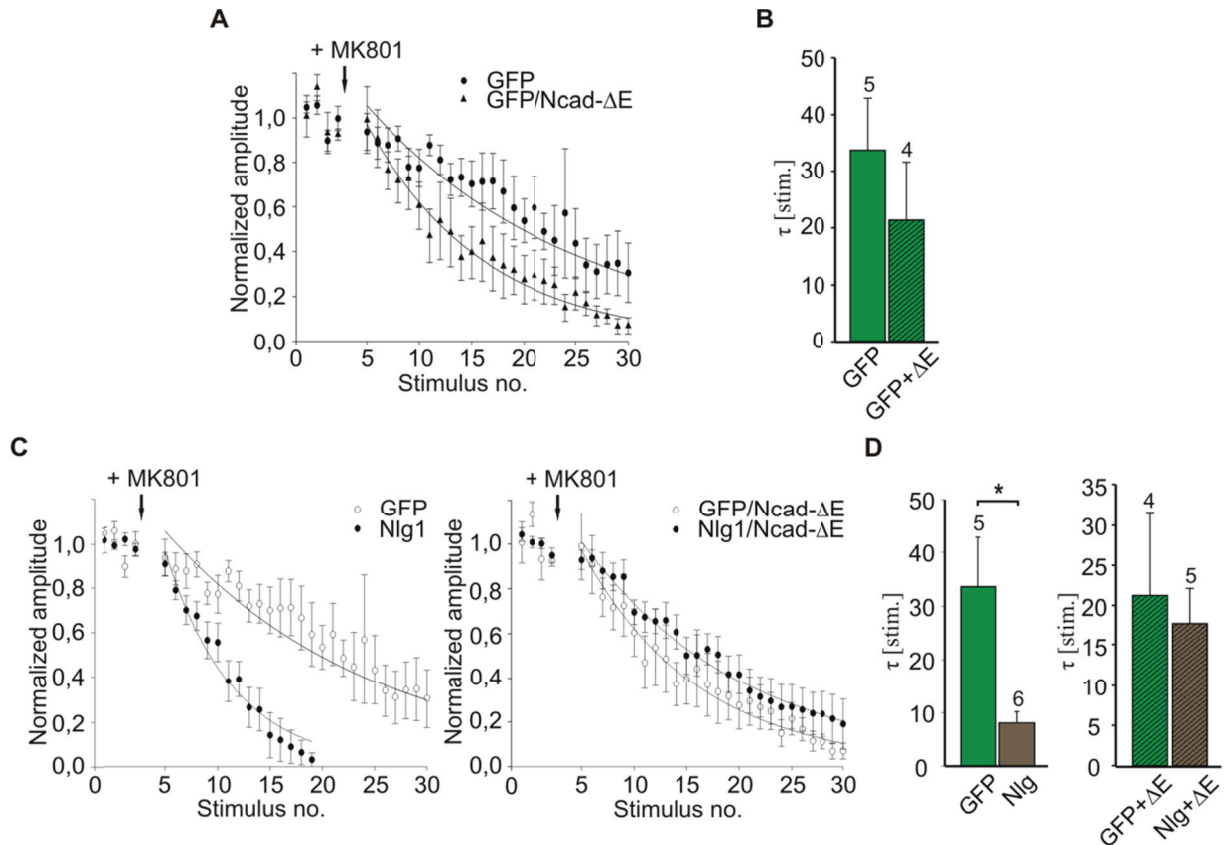
Figure 3.26 Neuroligin1-induced enhancement of presynaptic release probability is dependent on N-cadherin function.

A,B Quantitative analysis of the decay of NMDA receptor-mediated EPSCs by MK-801 block in neurons transfected with EGFP or EGFP + Ncad-ΔE revealing no alterations due to the loss of N-cadherin function. Due to the inability of making a proper fit of the MK-801 block in one of the neurons transfected with EGFP + Ncad-ΔE, the number of cells is 5 in the cumulative plot (A), while the bar chart (B) shows the mean τ of 4 cells. **C,D** Quantifications of the MK-801 block of NMDA receptor-mediated EPSC in neurons transfected with EGFP or Nlg1-GFP and in neurons transfected with EGFP + Ncad-ΔE or Nlg1-GFP + Ncad-ΔE. While neuroligin1 was able to enhance presynaptic vesicle release in the presence of N-cadherin function, this effect was abolished in its absence. (C) Cumulative plot of MK-801 block, (D) Bar chart of mean τ. (Error bars represent s.e.m.; n= number of cells; unpaired *t*-test; * p < 0,05).

4. Discussion

4.1 Characterization of a cell culture system enabling the analysis of an asymmetric expression of N-cadherin

Major goal of this study was to examine an asymmetric expression of N-cadherin on the level of individual synapses and its consequences for synapse function and elimination. Asymmetric expression of synaptic proteins has also been used in other studies (Dityatev et al., 2000; Klau et al., 2001; Hanson and Madison, 2007). To obtain asymmetrical expression the presence of N-cadherin had to be diminished at one side and assured on the other side of the synaptic cleft. Knockout approaches for N-cadherin have been commonly used. Conventional knockout mice were found to be unsuitable for analyzing N-cadherin, as the embryos died in a very early embryonic stage (E10) because of abnormalities in the development of myocardial tissue (Radice et al., 1997). Recently generated conditional knockout mice exhibited completely randomized organization of the cerebral cortex (Kadowaki et al., 2007), which makes them likewise improper to use for specific analysis. Especially an analysis of N-cadherin function in vivo, important to show the physiological relevance, turned out to be rather challenging. Other approaches involving the use of a dominant negative form of N-cadherin (Bamji et al., 1998; Togashi et al., 2002; Bozdagi et al., 2004; Abe et al., 2004) or N-cadherin blocking antibodies (Bozdagi et al., 2000; Poskanzer et al., 2003) shed more light on the function of N-cadherin. However, the dominant negative form of N-cadherin competes, in addition to endogenous N-cadherin, also with the other classical cadherins (e.g. E-cadherin) present at synaptic junctions. Thus, an analysis of putative roles of N-cadherin is rather unspecific.

In order to circumvent these issues, in this study N-cadherin deficient neurons (Fig. 3.1) were derived from embryonic stem cells in vitro (Moore et al., 1999). A commonly used technique to promote the differentiation of embryonic stem cells to neuronal cells is the addition of retinoic acid (Jones-Villeneuve et al., 1982; Strübing et al., 1995; Bain et al, 1996). Thereby, neurons have been observed to differentiate during 48 hours after exposure with it (Jones-Villeneuve et al., 1982). In this context it could be shown that upon differentiation of neuronal cells, neurogenic precursors with properties of radial glia cells are induced (Glaser and Brüstle, 2005). Similarly, the induction of neurons and glial cells from human umbilical cord-derived hematopoietic stem cells has been described to be initiated by retinoic acid in vitro

(Jang et al., 2004). In vivo, retinoic acid, found to be site-specific synthesized by enzymes (Denisenko-Nehrbass et al., 2000), was demonstrated to play pivotal roles in neuroprotection and especially cortical neuron generation by directly binding to target genes after entering the nucleus (Duester et al., 2009; Lee et al., 2009). Furthermore, the cellular reactions after spinal cord injury are accompanied by local synthesis of it (Schrage et al., 2006). Anterior-posterior neural development as well as neuronal population size also at late stages of neural circuit formation were demonstrated to be dependent on retinoic acid (Schubert et al., 2004; Hägglund et al., 2006; Siegenthaler et al., 2009; Duester, 2009). To purify neuronal cells out of the ES cell-derived material, subsequently to differentiation L1-immunoisolation was performed, using L1-antibodies selectively binding to neurons (Jüngling et al., 2003).

In order to obtain synapses with an asymmetric expression of N-cadherin, Ncad-/- neurons derived from embryonic stem cells and cultured as neuronal networks of 10-20 neurons on glial microislands were transfected with N-cadherin. The physiological localization of the transfected N-cadherin could be verified by immunocytochemical stainings against N-cadherin and VAMP2 as presynaptic marker and colocalization analysis of both proteins in Ncad+/- neurons or Ncad-/- neurons transfected with N-cadherin (Fig. 3.3). Moreover, almost all expressed N-cadherin was found to be localized at synaptic sites. N-cadherin puncta not being associated with VAMP2 might represent transport vesicles containing N-cadherin on their way to synapses. However, not all VAMP2 labeled presynaptic accumulations were colocalized with N-cadherin (~ 30 %), indicating the presence of synapses without N-cadherin expression. As N-cadherin expression was shown to be restricted to excitatory synapses at mature stages (Benson and Tanaka, 1998), these non-colocalizing puncta might represent inhibitory GABAergic synapses. For transfecting the neurons the lipofectamine technique, which features an efficiency less than 1 %, has been chosen. Thus, at most one neuron per network was transfected, which could be defined as postsynaptic, N-cadherin expressing cell, surrounded by presynaptic neurons lacking N-cadherin expression. An analysis of synapses displaying this specific mis-match expression of N-cadherin was enabled. Furthermore, the observed effects of asymmetrically expressed N-cadherin could be demonstrated as being specific, as the analysis of the autaptic connections of the transfected neuron, symmetrically expressing N-cadherin, revealed unaltered properties (Fig. 3.5; Fig. 3.13). Autaptic connections in slice cultures were proven to be comparable to synapses concerning their functional properties (Feldmeyer et al., 2002; Silver et al., 2003). A developmental decrease of autapses was observed according to what has been described by other groups (Fig. 3.13).

Moreover, their presence seems to be cell-type specific; pyramidal neurons exhibit autapses only to a small degree and especially inhibitory neurons displayed many of them (Tamás et al., 1997; Lübke et al., 1997).

Glutamatergic synapses expressing N-cadherin at the presynaptic side and lacking N-cadherin at the postsynaptic side have been shown to be largely unaltered in basic synaptic functions (Jüngling et al., 2006). Therefore, this study focused on an asymmetric expression of N-cadherin consisting of presynaptic absence and postsynaptic expression of N-cadherin.

4.2 Effects of asymmetrically expressed N-cadherin on synapse function

The role of N-cadherin in synaptic function is thought to be widespread. Experiments using a dominant negative form of N-cadherin in order to block its function suggested that N-cadherin is important for synaptic transmission at mature stages (10-20 DIV), as electrophysiological recordings demonstrated a significantly reduced frequency of AMPA receptor-mediated miniature EPSCs (Bozdagi et al., 2004). Other studies revealed an impairment of AMPA receptor-mediated mEPSCs only under the conditions of increased synaptic activity by examining N-cadherin deficient neurons derived from ES cells at 10-14 DIV (Jüngling et al., 2006). Furthermore, short-term plasticity of evoked EPSCs was dramatically altered in these neurons, exhibiting an enhanced depression. Moreover, an impaired refill of the readily releasable pool of vesicles in mature neurons (10-14 DIV) as well as a disturbed accumulation of presynaptic vesicles in immature neurons (6-7 DIV) was observed in the absence of N-cadherin, supporting the idea of N-cadherin regulates presynaptic processes (Jüngling et al., 2006; Stan et al., 2010). Interestingly, it could be demonstrated that the postsynaptic N-cadherin modulates presynaptic function via a transsynaptic mechanism (Jüngling et al., 2006), cooperating putatively via the postsynaptically localized S-SCAM with the neuroligin1/β-neurexin adhesion system (Stan et al., 2010).

In addition to these results, also the asymmetric expression of N-cadherin with N-cadherin present only postsynaptically was found to impair synaptic function. Ncad-/- neurons were postsynaptically transfected with N-cadherin at 9-11 DIV and AMPA receptor-mediated mEPSCs were recorded 2 days later (Fig. 3.4). Strikingly, the mean frequency of these spontaneous events was significantly reduced, while all other analyzed parameters such as amplitude and kinetics were unaffected. Considering an AMPA receptor-mediated mEPSC as

being the result of the fusion of a single presynaptic vesicle, an alteration in the density of postsynaptic transmitter receptors would entail reduced ion channels, leading to a smaller amplitude of the mEPSC. As the amplitude of the detected AMPA receptor-mediated mEPSCs did not show alterations, the asymmetrically (postsynaptic) expressed N-cadherin is putatively not acting via postsynaptic modulations, but rather by controlling presynaptic processes or by eliminating the synaptic input. To address this issue, immunocytochemical stainings of postsynaptically transfected Ncad-/- neurons against VAMP2 were performed exactly at the time point when AMPA receptor-mediated mEPSCs had been recorded (Fig. 3.10). According to the current view VAMP2, as part of the SNARE-complex enabling the exocytosis of vesicles, was found to be specifically associated with presynaptic vesicles of neurons and represents therefore a proper candidate as marker for presynaptic vesicle accumulations. Thereby, the synaptic localization of VAMP2 was validated as it could be detected apposed to simultaneously labeled postsynaptic compartments (PSD-95-GFP; Fig. 3.12). The determination of presynaptic vesicle accumulations made on the postsynaptically N-cadherin expressing neuron revealed no alterations at the time point when AMPA receptor-mediated mEPSCs had been recorded, thus confirming presynaptic defects in the vesicle release impairing synaptic function. Because of its presynaptic effects, the postsynaptically expressed N-cadherin is presumably acting via a retrograde transsynaptic mechanism.

In order to reveal that the impaired synaptic function can be attributed to the asymmetric expression of N-cadherin, an additional experiment dealt with neurons displaying only a quantitative mis-match regarding N-cadherin expression. For this, wildtype cortical neurons were cultured on glial microislands and postsynaptically transfected with N-cadherin at 9-11 DIV. By this means the transfected neuron exhibited an overexpression of N-cadherin, while all presynaptic neurons only expressed the endogenous level of N-cadherin. The fact that a transient or permanent shift in the expression of a protein is able to modulate synaptic function has already been described. The N-CAM homologue Fascillin II for example, which controls the fasciculation and axonal pathfinding at the neuromuscular junction (Lin et al., 1994), was shown to exhibit dramatic shifts in the target selection, contact stability and synapse formation depending on its expression (Schuster et al., 1996; Davis et al., 1997). In addition, other adhesion molecules, such as neuroligin1 have been demonstrated to trigger synapse formation when being overexpressed and led to a loss of synapses when being down-regulated (Chih et al., 2005; Stan et al., 2010). However, a quantitative shift in the level of N-cadherin expression was not found to result in altered synaptic transmission (Fig. 3.6). Thus,

the direct comparison of qualitative vs. quantitative asymmetric expression of N-cadherin suggests that postsynaptic N-cadherin impairs synaptic function transsynaptically only in response to the complete loss of presynaptic N-cadherin.

4.2.1 Classical cadherins as potential interaction partners of asymmetrically expressed N-cadherin

As presynaptic N-cadherin as interaction partner can be definitely excluded, the question arises, with which protein the postsynaptic N-cadherin cooperates to transsynaptically mediate impaired synaptic vesicle release. Although N-cadherin is mainly described to exhibit homophilic interactions, heterophilic interactions with other classical cadherins have been observed. Bead aggregation assays and qualitative force measurements demonstrated potential interactions between N-cadherin and E (epithelial)-cadherin or N-cadherin and C-cadherin, although these interactions have not been shown to be relevant in vivo (Prakasam, 2006). Furthermore, functional cis-dimers consisting of N-cadherin and R (retinal)-cadherin have been detected (Shan et al., 2000). Thereby, the extracellular domain of N-cadherin seems to be pivotal as the N-cadherin binding motif, containing as key structure the HAV motif, was described to be arranged in the EC1 domain of the extracellular region (Shapiro et al., 1995; Tamura et al., 1998; Wiliams et al., 2000). Moreover, the amino acids immediately flanking the HAV motif (INP motif) were proposed to be decisive for the unique character of the N-cadherin binding domain (Nose et al., 1990; Williams et al., 2000). Peptides synthesized specifically against these two motifs have been demonstrated to be potent antagonists for N-cadherin dimerization and adhesion (Myatani et al., 1989; Williams et al., 2000). Furthermore, a peptide mimetic of the corresponding INP motif in R-cadherin likewise inhibited N-cadherin function (Williams et al., 2000), thus showing, that the use of these specific antagonists is also blocking the interactions between N-cadherin and other classical cadherins. Taking advantage of this fact, in two independent experiments either a 16mer peptide containing the HAV motif (HAV) or a 7mer peptide comprising the INP motif (INP) were added to the Ncad-/- neurons subsequently after postsynaptic transfection with N-cadherin at 9-11 DIV (Fig. 3.7). By this means a putative interaction between the postsynaptic N-cadherin and a presynaptic classical cadherin, such as E-cadherin, would have been interrupted via the occupancy of the N-cadherin binding site. Accordingly, the signaling cascade inducing a defect in synaptic transmission would have not been initiated, thus resulting in unaltered synaptic function. To test for this, two days after transfection and

application of the N-cadherin antagonists, AMPA receptor-mediated mEPSCs were recorded. As control the experiments were repeated with N-cadherin asymmetrically expressed or completely absent in the presence of corresponding scrambled peptides, having no effect on the binding site of N-cadherin. The quantification of these experiments evidently showed that synaptic transmission in either case, in the presence of HAV or INP, was still altered and impaired. Obviously, neither HAV nor INP were able to interrupt any signaling cascade, so that a cooperation of the postsynaptic N-cadherin with another classical cadherin can be excluded as initiator of an alleviated synaptic activity.

4.2.2 Analysis of BDNF/TrkB/p75^{NTR} as potential interaction partners of asymmetrically expressed N-cadherin

The above described results indicate that other proteins different from classical cadherins might serve as cooperation partners of N-cadherin in modulating synapse function. A connection between the BDNF/TrkB/p75^{NTR} system and the N-cadherin/β-catenin system was suggested by experiments in hippocampal neurons demonstrating that the binding of BDNF to its receptor tropomyosin receptor kinase B (TrkB) initiated subsequently the tyrosine phosphorylation of β-catenin (Bamji et al., 2006; David et al., 2008) and resulted in the dissociation of the N-cadherin/β-catenin complex (Bamji et al., 2006). Consequently, the presynaptic vesicles, known to be localized and clustered by the cooperation of N-cadherin and β-catenin (Bamji et al., 2003; Stan et al., 2010), were found to disperse in the perisynaptic regions (Bamji et al., 2006). These processes have been described to be rapid, probably due to the internalization of TrkB or its deactivation by tyrosine phosphatases. However, a long-term treatment with BDNF was shown to induce synapse formation (Leßmann et al., 1994; Levine et al., 1995; Vicario-Abejon et al., 1998; Bamji et al., 2006), maybe due to the reallocation of the dispersed vesicles at newly formed presynaptic sites. Moreover, BDNF is inducing pre- and postsynaptic maturation as well as the potentiation of synaptic activity, dependent on presynaptic processes (Bolton et al., 2000; Marty et al., 2000; Li et al., 1998).

Interestingly, BDNF does not only have promoting effects on synapse number and function, but induces apoptosis, when Trk-signaling is absent (Casaccia-Bonnefil et al., 1996; Frade et al., 1996; Bamji et al., 1998). In this case BDNF signaling is proposed to be mediated by its second receptor p75^{NTR}. p75^{NTR} is able to bind at RhoA (Yamashita et al., 1999), which results in RhoA inactivation by hydrolysis when BDNF is complexed and RhoA activation in the absence of the ligand (Yamashita et al., 1999). RhoGTPases are proposed to be pivotal in

actin organization and vesicle clustering. Their inactivation in vitro mimicked the effect of neurotrophins by increasing the rate of neurite elongation, while mice carrying a gene mutation in p75[NTR] showed a retarded axon growth (Yamashita et al., 1999). Most intriguingly, RhoGTPases were also shown to affect cadherin stability and clustering by interacting indirectly with p120-catenin (Noren et al., 2003; Reynolds et al., 2004), binding to N-cadherin at the juxtamembrane domain. Furthermore, the indirect modulation of Rho by N-cadherin/p120-catenin is supposed to determine actin polymerization making p120-catenin pivotal in adjusting the strength of cadherin-mediated adhesion (Ohkubo and Ozawa, 1999; Thoreson et al., 2000; Wildenberg et al., 2006). p120-catenin, which is recruited to the membrane by binding to N-cadherin (Noren et al., 2003), recruits the protein p190RhoGAP upon activation by Rac (Nimnual et al., 2003). Through a direct interaction of p120-catenin and p190RhoGAP, Rho is subsequently inactivated by the hydrolysis of RhoGTP to RhoGDP (Niessen and Yap, 2006, Wildenberg et al., 2006), thus enabling actin regulation. In addition, the accumulation of RhoA is thought to be dependent on N-cadherin (Taulet et al., 2009). Accordingly, the indirect p75[NTR]-mediated modulation of the actin assembly and growth cone motility in a ligand-dependent fashion might potentially involve N-cadherin/p120-catenin signaling.

Similarly, BDNF interactions with truncated forms of the TrkB receptors have been shown to have a dominant negative effect on BDNF signaling (Eide et al., 1996), showing that BDNF is not only characterized by its cell promoting functions.

The decision for supporting cell survival or cell death seems to be dependent on the ratio of TrkB and BDNF, as the overexpression of full-length TrkB receptors resulted in a reduced activity of glutamatergic synapses accompanied by a reduction in synapse number. These experiments indicated a possible ligand-independent mechanism (Klau et al., 2001). Considering the presynaptic N-cadherin being the ligand for the postsynaptic N-cadherin these findings are somewhat analogous to what has been described in this study. In vivo, the down-regulation might be induced by BDNF itself, limiting its own promoting efficacy (Chen and Weber, 2004).

As described in the literature, the acute application of BDNF has been found to enhance synaptic transmission (Jovanovic et al., 2000). In order to identify a role of BDNF/TrkB/p75[NTR] in the process of impaired synaptic function when N-cadherin is expressed asymmetrically, BDNF was applied to Ncad-/- neurons subsequently to transfection with N-cadherin at 9-11 DIV. A vehicle was added to Ncad-/- neurons only transfected with

EGFP or postsynaptically cotransfected with N-cadherin and 2 days later AMPA receptor-mediated mEPSCs were recorded. Interestingly, the impairment induced by an asymmetric expression of N-cadherin could be completely reverted by the addition of BDNF, indicating an involvement of the BDNF/TrkB/p75^{NTR} system. To gain more insight, the general necessity of N-cadherin signaling for BDNF-mediated potentiation was tested. Taking advantage of BDNF being able to potentiate synaptic activity, Ncad+/- neurons were treated with BDNF or a vehicle and AMPA receptor-mediated mEPSC were recorded (Fig. 3.9). As expected, the application of BDNF enhanced synaptic transmission, demonstrated by a 4-fold increase in the mean frequency of AMPA mEPSCs. Repeating this experiment using Ncad-/- neurons revealed that the absence of N-cadherin prevented the potentiating effect of BDNF. Accordingly, a requirement of N-cadherin for BDNF function can be suggested. Moreover, an interaction between N-cadherin and TrkB or p75^{NTR} might be conceivable. To test for this, cell lysates from P6 mouse brains were immunoprecipitated using an antibody against N-cadherin (Fig. 3.9). At this time point of development, N-cadherin has been demonstrated to colocalize with pre- and postsynaptic markers (Redies and Takeichi, 1993; Huntley and Benson, 1999). By the immunoprecipitation not only N-cadherin, but rather N-cadherin and associated proteins are purified from the homogenate. In order to detect co-immunoprecipitated TrkB or p75^{NTR} in the protein complex pulled down together with N-cadherin, a pan-Trk as well as a p75^{NTR} antibody was used for immunological identification. Unfortunately, most of the various tested TrkB antibodies showed unspecific bands and thus were unsuitable (data not shown). Although the control homogenates demonstrated specificity for the used antibodies, none of the coimmunoprecipitation approaches could indicate a direct binding between N-cadherin and Trk, or N-cadherin and p75^{NTR}.

As described above, this interaction might be carried out indirectly involving p120-catenin or other associated proteins. Another putative signaling pathway might include β-catenin, as a direct interaction between TrkB and β-catenin was validated by co-immunprecipitation in hippocampal neurons (David et al., 2008). Furthermore, as the connection between two proteins has to be quite stable to be detected by co-immunoprecipitation, the interaction between N-cadherin and TrkB/p75^{NTR} might simply be not strong enough. Moreover, this specific condition for enabling detection of an interaction might require other biochemical methods or optimized experimental protocols. In addition to the co-immunoprecipitation method there are many other techniques such as affinity chromatography or the yeast-two-hybrid assay known to analyze the linkage between two proteins. The most important reason to choose the co-immunoprecipitation method is the fact that thereby an interaction in the

physiological environment of the cell membrane is tested. On the other hand, the observed "rescue" of impaired synaptic function after application of BDNF might represent an induction of autaptic activity, which would have been not distinguishable from synaptic activity by analyzing the mean frequency of AMPA receptor-mediated mEPSCs. Thus, a cooperation of N-cadherin and BDNF/TrkB/p75^{NTR} in some synaptic processes is likely, but whether this interaction is representing the molecular mechanism underlying the defects in synaptic transmission triggered by the asymmetric expression of N-cadherin remains unclear.

N-cadherin was found to interact with various other proteins that might play a role in the mechanism studied in this work. For example, the fibroblast growth factor receptors (FGFR) contain a HAV sequence that has been proposed to interact with the EC4 domain of the extracellular region of N-cadherin (Doherty and Walsh, 1996). Similar to the neurotrophins, fibroblast growth factors (FGFs) as the ligands of the FGFR perform diverse functions in cell migration and differentiation. Especially, FGFR1 and FGFR2 have been found to be essential for a normal number of excitatory neurons in the cortex (Stevens et al., 2010).

Besides a presynaptic modulation, a postsynaptic regulation is conceivable. For example, interaction between the N-cadherin and the AMPA receptor subunit GRIA2 has been verified as cis- or trans interaction shown via co-immunoprecipitation (Saglietti et al., 2007). N-cadherin was thereby supposed to regulate GRIA2 recruitment to the membrane and lateral diffusion, processes being important in triggering pre- and postsynaptic development as well as function. Furthermore, interplay of N-cadherin and the AMPA receptor subunit GRIA1 was reported (Nuriya and Huganir, 2006). As putative link between AMPA receptors and N-cadherin serves the glutamate receptor-interacting protein1 (GRIP1) and the AMPA receptor-binding protein (ABP), which was found to bind GRIA2 and GRIA3 AMPAR subunits through its PSD-95-discs large-zona occludens-1 (PDZ)-binding domains (Dong et al., 1997; Srivastava et al., 1998). The linkage to N-cadherin is established via GRIP1/ABP binding to neural plakophilin-related armprotein (NPRAP; δ-catenin), which is connected to the juxtamembrane domain of N-cadherin (Silverman et al., 2007). Especially AMPA receptor trafficking seems to be regulated by δ-catenin (Ochiishi et al., 2008). β-catenin, complexed with N-cadherin, was furthermore observed to bind to GRIP1 (Song and Gelmann, 2005). A postsynaptic modulation triggered by asymmetric expression of N-cadherin might result in the silencing of these synapses, usually accompanied by a degradation of AMPA receptors. Silent synapses usually occur during immature stages, although active synapses can be silenced by activity during the entire lifetime (Faber et al., 1991; Malenka and Nicoll, 1997;

Costanzo et al., 2000; Voronin and Cherubini, 2004). The stimulation of silent synapses does not evoke EPSCs, which would be consistent with the findings of this study, a reduced frequency and unaltered amplitude of AMPA receptor-mediated mEPSCs. However, the application of BDNF was reported to stabilize silent synapses on neuromuscular junctions (Kwon and Gurney, 1996).

A stimulation or enhancement of NMDA receptors was shown to suppress the expression of N-cadherin as well as the N-cadherin/β-catenin interaction This leads to increased neuronal death, probably initiated by NMDA receptor induced cleavage of N-cadherin by ADAM10 or PS1/γ-secretase (Uemura et al., 2006; Jang et al., 2009).

The observed consequences for synaptic transmission when N-cadherin is expressed asymmetrically might not necessarily require a direct interaction partner. Moreover, unspecific mechanisms involving the diffusion of postsynaptic N-cadherin away from the synaptic site may result in the withdrawal of other associated proteins, such as neuroligin1 or AMPA receptors, leading to a malfunctioning synapse. Interestingly, δ-catenin, as described above to link N-cadherin and AMPA receptors, was also shown to bind PSD-95, providing a link to neuroligin1. The endocytosis of N-cadherin is suggested to be driven by growth factor signaling or NMDA receptor activity (Tai et al., 2007; Delva and Kowalczyk, 2009). Interestingly, S-SCAM, mediating the linkage between N-cadherin and neuroligin1, was shown to interact also with NMDA receptors (Hirao et al., 1998).

4.3 Role of asymmetrically expressed N-cadherin in synapse elimination

For many years N-cadherin has been discussed to play a pivotal role in target recognition, essential for the specific wiring of the CNS. Accordingly, the expression of N-cadherin in pre- and postsynaptic membranes and especially their strong homophilic binding to each other were supposed to constitute a molecular code on the cell surface to connect appropriate axonal growth cones from the presynaptic and filopodial contact sites from the postsynaptic neuron. By N-cadherin function-blocking experiments it has been demonstrated that the axon guidance is extensively disturbed without N-cadherin being functional, as axons from the thalamus did not target in layer IV of the cortex, but instead grew further until layer II/III (Riehl et al., 1996; Huntley and Benson, 1999; Poskanzer et al., 2003). Furthermore, the

expression of N-cadherin, found to occur in neuron-type specific patterns, supports this hypothesis of N-cadherin expression being a code on specific neuronal subtypes (Redies et al., 1993; Fannon and Colman, 1996, Benson and Tanaka, 1998). Moreover, a role of Drosophila N-cadherin in target recognition was demonstrated in the visual system of flies, where N-cadherin serves as attractive mediator between photoreceptor axons (R1-6) and their targets (L1-5) (Prakash et al., 2005). Similarly to N-cadherin, the kin-of-irregular-chiasm-C-roughest-(kirrel)-proteins, belonging to the immunoglobulin superfamily of transmembrane proteins and especially found to be expressed in the pancreas and the nervous system, are proposed to mediate synaptic target selection of afferents by homophilic adhesion, while the surface expression of other proteins, such as ephrin-A2/A5 and ephA5 provokes axon repulsion (Sanes and Yamagata, 2009).

In addition to specific synapse formation, the elimination of inappropriate synapses is a decisive step in matching appropriate neurons together. The formation of synapses as well as their elimination are crucial processes mediated by certain cues that occur during the entire lifetime and enable via this fine-tuning of existing neuronal networks learning and memory. The use of inappropriate synaptic partners as intermediate targets was additionally reported (for review see Sanes and Yamagata, 2009). As the expression of N-cadherin has been found to be very dynamic (Delva and Kowalczyk, 2009) and to occur in mature stages, a role for N-cadherin and its binding properties might also exist in the process of synapse elimination.

Manifold molecular cues for both, synapse formation and elimination, have been found. The exact process of competitive synapse elimination is still not completely understood, but a combination of patterned neuronal activity and molecular cues is supposed to be pivotal. Asynchronous firing patterns are thereby believed to be one trigger (for review see Lichtman and Colman, 2000). However, an inhibition of global activity is insufficient to disrupt central synapse organization (Harms and Craig, 2005). Especially adhesion molecules and neurotrophic factors such as BDNF might be important as supportive molecular cues and a role of their degradation by local proteases or the ubiquitin-mediated protein degradation is discussed (Zoubine et al., 1996). Most recent studies are furthermore suggesting that mechanical tension within axons is important for proper presynaptic vesicle accumulation and ultimately for synapse elimination or maintenance (Siechen et al., 2009). Using axotomy these authors observed the disappearance of vesicle clusters, which could be restored by the artificial application of tension. A proposal that axons are under intrinsic tension, controlled by an axon-internal tension sensing mechanism, was put forward (Engerer and Sigrist, 2009).

DISCUSSION

Several neuronal subnetworks were shown to refine their connections by specific elimination. Thalamocortical axons disconnect from the visual cortical layer IV cells, climbing fibers in the cerebellum disconnect from Purkinje cells and in the autonomic ganglia preganglion neurons in the CNS are specifically eliminated from ganglion cells (for review see Lichtman and Colman, 2000). Specific synapse elimination was particularly well studied at the neuromuscular junction. At birth each muscle fiber possesses a specific region where acetylcholine receptors are highly concentrated and multiple motor axons target. Completed 15-20 days after birth (Zoubine et al., 1996), these axons are stepwise specifically eliminated until one innervating axon remains. Another often discussed in vivo example for specific elimination is given by the ocular dominance, describing the regulation of the inputs from the eyes on specific regions (ocular dominance columns) of the visual cortex. Axons from the retinal ganglion cells (RGCs) from distinct subareas of the retina project after crossing the optic chiasm on the lateral geniculate nucleus (LGN) in eye-specific layers. This segregation is maintained in the projection of the LGN to the visual cortical layer IV, forming there the ocular dominance columns, which correspond to eye or retinal location. Experiments testing a monocular eye closure during the first postnatal months demonstrated a decreased number of neurons driven by the closed eye and an increased number of neurons activated by the open eye, revealing that synaptic connections with a low activity have been eliminated (for review see Katz and Crowley, 2002). Furthermore, it has been reported that dorsal LGN neurons are multiple innervated during the first postnatal weeks, but by the third postnatal week only one or two inputs from RGC axons remain (Hooks and Chen, 2006).

Numerous proteins have been found to directly or under specific conditions support synapse disassembly or prevent synapse assembly. As mentioned above the imbalance of TrkB and BDNF might be one of these mechanisms (Klau et al., 2001). At the neuromuscular junction balanced ratios of TrkB and BDNF were proposed to oppose the protein kinase C (PKC)-mediated depression of acetylcholine (ACh) release, leading to synapse elimination and axon retraction (Tomás et al., 2010). Furthermore, the cadherin-superfamily member Celsr3 was demonstrated to be a key player in axonal path formation. Major bundles were found to be completely defective in mice with a constitutive mutation of Celsr3 (Zhou et al., 2009). Celsr 2 and Celsr3 were also observed to impair ependymal ciliogenesis, causing a lethal hydrocephalus, when being knocked-out (Tissir et al., 2010). By combining loss-of-function and gain-of function experiments Parkin, an ubiquitin ligase mediating the transfer of ubiquitin onto diverse proteins, was likewise shown to negatively regulate excitatory synapse numbers and their strength (Helton et al., 2008).

Recently, the classical complement cascade has been reported to mediate synapse elimination. Thereby, C1q as initiating protein coats dead cells, debris or pathogens and induces a protease cascade, resulting in the deposition of the downstream complement protein C3. Activated C3 fragments (C3b and iC3b) trigger cell or debris elimination by directly activating C3 receptors of macrophages or microglia, thus leading to elimination via phagocytosis, or by initiating cell lysis via the formation of a lytic membrane attack complex. C1q expression throughout the immature CNS was shown to be induced by immature astrocytes. In adult stages the expression of Cq1 is usually downregulated. In glaucoma, an eye disease characterized by the massive death of RGCs leading to irreversible loss-of-vision, C1q gets upregulated. Furthermore, synapse elimination was defect in mice lacking C1q or C3 expresssion (Stevens et al., 2007). Intriguingly, in the same experiments BDNF was found to prevent synapse elimination.

In C.elegans, wnt proteins, which are secreted glycoproteins activating numerous signaling pathways after binding to receptors of the frizzled (fz) family or to complexes consisting of fz and LDL receptor-related proteins 5/6 (LRP5/6), were proven to be able to function as anti-synaptogenic signals by inhibiting presynaptic assembly. The wnt lin-44 localizes the lin-17/Fz receptor by signaling involving egl-20 and dsh-1/Dishevelled to a distinct region of the motor neuron DA9 axon. This specific region of the DA9 axon is supposed to be an asymmetric domain lacking presynaptic terminals. Consequently, the overexpression of lin-44/wnt in adjacent cells resulted in a lin-17/fz localization within the DA9 axon and the inhibition of presynaptic assembly. Accordingly, disruption of this pathway was described to be characterized by synapse formation (Klassen and Shen, 2007). Moreover, by utilization of loss-of function and gain-of-function experiments the axon guidance cue UNC-6/netrin was reported to segregate proteins specific for presynaptic differentiation from the dendrite of the DA9 neuron by signaling through its receptor UNC-5, thus showing that both lin-44/wnt and UNC-6/netrin exclude presynaptic components from the DA9 motor neuron by acting on different regions. In addition, UNC-6/netrin expression was able to rescue the misallocation defect in lin-44/wnt and lin-17/fz mutants, demonstrating that the features are interchangeable, but transduced through different receptors (Poon et al., 2008). Similarly, synaptogenesis-1 (RSY-1) was found to antagonize presynaptic assembly in C.elegans (Patel and Shen, 2009). Interestingly, in the canonical pathway, wnts, binding to the LRP5 receptors, are initiating after accumulation of β-catenin in the cytoplasm the recruitment of the axin/Frat1/adenomatous polyposis coli protein (APC)/glycogen synthase kinase 3/ β-catenin complex to the cytoplasmatic tail of the LRP. By this means several parts of the complex

disassemble, which results in a decreased phosphorylation of β-catenin. As a consequence β-catenin is stabilized and subsequently translocated to the nucleus, where it activates the transcription of specific target genes (Haÿ et al., 2009). N-cadherin interacts directly with β-catenin when being unphosphorylated, thus putatively being indirectly involved in wnt signaling. Moreover, a direct interaction of N-cadherin with the wnt receptor LRP5 and axin in osteoblasts was shown to occur via the cytoplasmatic tail of LRP5. Thereby, the overexpression of N-cadherin stabilized N-cadherin/LRP5 interaction, leading to an increased β-catenin ubiquitination and hence resulted in a decreased gene expression in response to wnt, thus impairing osteoblast function and bone formation. Accordingly, a block of N-cadherin led to increased gene expression, evidently demonstrating N-cadherin as negative modulator of cell function also in extraneuronal systems (Haÿ et al., 2009). Furthermore, p120-catenin, directly connected to N-cadherin, was shown to interact with the transcription factor Kaiso, proposed to act as transcriptional repressor (Anastasiadis and Reynolds, 2000).

More evidence, that N-cadherin might be involved in synapse formation/elimination came up by function blocking experiments using the expression of a dominant negative N-cadherin construct in immature and mature neuronal cultures, resulting in a reduced density of presynaptic boutons and a corresponding reduction of PSD-95 puncta (Togashi et al., 2002). However, because this type of inhibition affects all cadherins and furthermore, this phenomenon could not be completely reproduced by other groups using a dominant negative form of N-cadherin (Bozdagi et al., 2004), the specific role for N-cadherin remained elusive. Moreover, experiments using mature ES cell-derived neurons deficient for N-cadherin did not reveal a reduction in synapse number (Jüngling et al., 2006). In addition, synaptic activity has been described to modify the conformational state of N-cadherin (Tanaka et al., 2000). Furthermore, impairment of N-cadherin led to the inhibition of LTP induction (Tang et al., 1998), implying a synaptic activity-dependence for the stability of N-cadherin-mediated adhesion.

By blocking or removing N-cadherin from the pre- as well as the postsynaptic side all the above described experiments did not take into consideration that N-cadherin is characterized through its homophilic binding and that the exact pre/postsynaptic combination of function block may decide over synapse maintenance or elimination. An asymmetric expression of N-cadherin as described in 4.1 might be crucial. A precursor for the elimination of a synapse is the alleviation of the synaptic transmission. Accordingly, the strongly impaired presynaptic release of vesicles due to the asymmetric expression of N-cadherin found in this study might reflect a first step in the disassembly of these improper synapses. To address this,

immunocytochemical stainings of Ncad-/- neurons postsynaptically transfected with N-cadherin against VAMP2 as presynaptic marker described in 4.2 were repeated after a longer time period of asymmetric N-cadherin expression (Fig. 3.10). Indeed, under this condition a significant loss of VAMP2 puncta was observed. However, as these experiments were performed in a developmental stage where still synapses form an elimination of synapses could not be definitely observed. Beyond that, the decrease of VAMP2 puncta might have resulted from an inability to generate new synapses. To precisely demonstrate a role for asymmetrically expressed N-cadherin in synapse elimination, a modified experiment was carried out at a more mature stage, where most of the synapses have already been formed. Therefore, Ncad-/- neurons were transfected with N-cadherin, PSD-95-GFP and DsRed-VAMP2 at 14 DIV and immunocytochemically stained against VAMP2 2 and 8 days later, respectively (Fig. 3.11). By this means, all pre- (DsRed-VAMP2) as well as all postsynaptic (PSD-95-GFP) compartments of the N-cadherin expressing cell were labeled. A colocalization of these two signals was considered to represent an autaptic connection. Immunocytochemical staining of all, autaptic and synaptic, presynaptic boutons via VAMP2 enabled additionally the analysis of synapses. These were characterized through a colocalization of PSD-95-GFP puncta with only immunocytochemically stained VAMP2 puncta. 2 days after transfection no changes in the density of the synapses could be observed, but intriguingly the area of the synaptic VAMP2 puncta showed an almost 2-fold increase (Fig. 3.12). This enhancement might represent a dispersal of presynaptic vesicles in advance of synapse elimination or be a compensatory mechanism to maintain alleviated synapses. In fact, 8 days after transfection an elimination of synapses was revealed, demonstrating that this process indeed requires a longer time period. Supporting the hypothesis that compensatory mechanisms are involved, the alteration of the VAMP2 puncta area was observed to occur to a lesser extent at this late time point. Consistent with this idea is the observation that in different neuronal systems the elimination of specific axons resulted in an elaboration of additional synapses by the remaining axons (e.g. ocular dominance see above; for review see Lichtman and Colman, 2000).

Selective synapse disassembly is accompanied by a retraction of the neuronal processes as a critical step during neurodevelopment and synapse remodeling (Purves et al., 1986; Lichtman and Colman, 2000). The regulation of actin is supposed to be important (Zhang and Benson, 2001; Colicos et al., 2001; Zito et al., 2004), although the dependence of synaptic stability on actin seems to be reduced in mature stages (Zhang and Benson, 2001). Actin polymerization and depolymerization is regulated rapidly not only by other proteins, but also in response to

the synaptic activity, in line with potentiation or depotentiation induced by NMDA receptor activity (Okamoto et al., 2004). Thus indicates that for the regulation of synapse coordination in addition to presynaptic vesicle release retrograde mechanisms might be important. In order to induce axon retraction, the stability of the synapse has to be reduced. N-cadherin, as an important adhesion molecule, was shown to be bidirectionally regulated via the actin cytoskeleton by interactions with α- and p120-catenin, to some extent by indirectly modulating proteins belonging to the Rho-family of GTPases (Reynolds et al., 2007; Tan et al., 2010). Thereby, the p120-catenin-mediated inactivation of Rho enables actin interaction via α-catenin. Interestingly, wnt/Fz signaling is supposed to be involved in the activation of Rho GTPases (Lai et al., 2009). Furthermore, the modifier of cell adhesion (MOCA), a presenilin binding protein, is implicated in axonal degradation by influencing an enzyme (p21-activated kinase) directly downstream to Rac1 (Chen et al., 2009). As Rac1 initiates p120-catenin-mediated inactivation of Rho (described above), N-cadherin might be indirectly involved here.

In order to monitor, whether additionally axon retraction occurs when N-cadherin is expressed asymmetrically, the experimental system used had to be modified, so that the axons exhibited absence of N-cadherin presynaptically and expression postsynaptically. To address this issue, Ncad-flox neurons were cultured on glial microislands and transfected with CreGFP. By this means, the transfected neurons lack N-cadherin at all their presynaptic boutons, while all surrounding postsynaptic neurons express endogenous levels of N-cadherin. Consistent with the observed synapse elimination also a retraction of axonal processes as well as a reduction in their arborization complexity in mature neurons could be demonstrated to occur several days after induction of the asymmetrical N-cadherin expression (Fig. 3.17; fig. 3.18).

By blocking the homophilic interaction of pre- and postsynaptic N-cadherin in immature neurons using a soluble N-cadherin ectodomain corresponding to the EC1 region, N-cadherin was found not only to be pivotal in axon growth and specificity, but in addition an N-cadherin-mediated neuron interaction in activity-dependent dendrite arborization was uncovered (Tan et al., 2010). Although the dendrites in this work are characterized by N-cadherin being presynaptically expressed and postsynaptically absent, an analysis of the dendrite length and arborization revealed likewise a retraction of the dendrites due to the mis-match of N-cadherin also in mature neurons (Fig. 3.19; Fig. 3.20).

In summary, the described results evidently demonstrate that the asymmetric expression of N-cadherin is impairing synaptic transmission, which leads subsequently to an elimination of these alleviated synapses, accompanied by axonal and dendritic retraction. On the basis of

these findings, a model is proposed that suggests that N-cadherin when being symmetrically expressed is pivotal for synapse formation, but in contrast when being asymmetrically expressed is crucial for synapse elimination (Fig. 5.1).
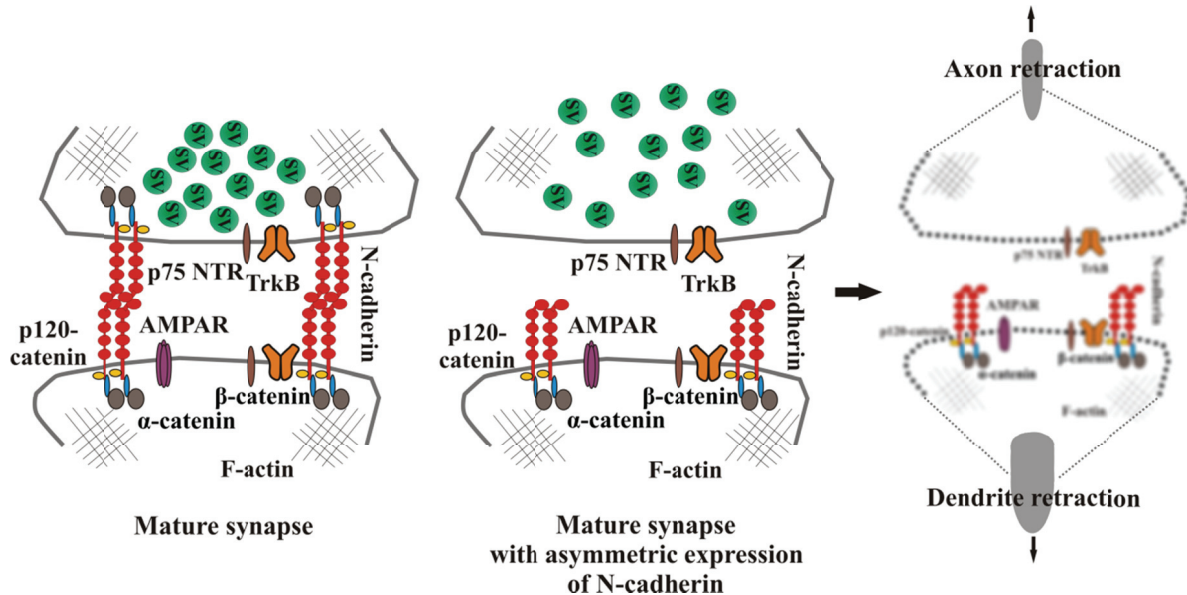

Figure 4.1: The consequences of asymmetrically expressed N-cadherin for synapse function and stability.
When N-cadherin is symmetrically expressed, the synapse is stabilized by the adhesive properties of N-cadherin and its intracellular linkage via α-, β-, and p120-catenin to F-actin. Upon asymmetric expression of N-cadherin, release of presynaptic vesicles (SV) is impaired, accompanied by a dispersal of vesicles. Which role AMPA receptors (AMPAR) or TrkB and p75^{NTR} play remains to be elucidated. Ultimately synapse elimination occurs and axons as well as dendrites disconnect and retract.

In vivo, the situation described in the model assuming asymmetric N-cadherin expression to be pivotal in synapse elimination might occur amongst others between cortical layer V neurons and neurons in the superior colliculus. During early development (late fetal to early postnatal stages) axons from cortical layer V neurons extend a common set of axon collaterals to target neurons in the superior colliculus. Subsequently, in the second to third postnatal week axons originating in the motor cortical layer V disconnect specifically from the target neurons in the superior colliculus, while axons send out from the visual cortical layer V remain stable (O`Leary and Koester, 1993). In line with the discussed findings in cell culture, preliminary in situ hybridization data (C. Redies, personal communication) confirm the expression of N-cadherin at P12 in the optic nerve layer, one of seven distinct fibrous and cellular layers of the superior colliculus, where axons from the visual area of the cortical layer V in immature as well as adult stages target. Consistent with this, the expression of N-cadherin in the motor cortical layer V was strongly reduced, thus realizing an in vivo situation

in which N-cadherin is expressed only postsynaptically and on top of that, axons are selectively eliminated. However, evidence for N-cadherin expression was similarly missing in the visual area of the cortical layer V, thus raising the question how axons manage to circumvent synapse elimination. Interestingly, BDNF expression, tightly regulated by neuronal activity, is low in developing regions of the CNS, but increases at mature stages (Maisonpierre et al., 1990). Most intriguingly, BDNF can be distributed along the axon in retro- (Ma et al., 1998) and anterograde (Zhou and Rush, 1996; Altar et al., 1997) direction. In line with the results of this study, BDNF injections into the superior colliculus of hamsters in neonatal stages, where the death rate of retinal ganglion cells is the greatest, resulted in a significant reduction of cell damage (Ma et al., 1998). These findings indicate a pivotal role for retrogradely transported BDNF in triggering RGC survival as well as in the maintenance of polysynaptic projections from the RGC to the superior colliculus.

Based on this and the findings described in the present study an in vivo experiment, involving the injection of Cre-recombinase into the superior colliculus of newly born Ncad-flox mice, which should result in the abolishment of the asymmetric expression of N-cadherin at synapses between the superior colliculus and the cortical layer V neurons, would be of interest.

4.4 Role of N-cadherin in neuroligin1-induced enhancement of synaptic activity

The pivotal roles of N-cadherin and neuroligin1 in regulating synapse function are well described. Demonstrated by numerous loss-of-function approaches, especially presynaptic processes are known to be determined by the expression and functionality of both adhesion molecules and downstream signaling proteins.

F-actin, surrounding presynaptic vesicle clusters, is thereby proposed to be crucial for multiple steps of the vesicle cycling (Morales et al., 2000; Shupliakov, 2002; Sabaka and Neher, 2003). For example, it has been demonstrated to tether vesicles of the reserve pool to regions adjacent to the vesicles of the readily releasable pool (Pieriebone et al., 1995). Furthermore, during synaptic activity actin is recruited from adjacent axonal regions to the presynaptic terminal, thus indicating a role in presynaptic vesicle accumulation and release (Sankaranarayanan et al., 2003). However, the actin dependence of synaptic vesicle scaffolding was demonstrated to be reduced at mature synapses (Zhang and Benson, 2001),

indicating a role in organizing the bouton rather than in regulating the vesicle cycling (Dunaevsky and Connor, 2000). Additionally, the cooperation of adhesion molecules and actin was proposed to be involved in synaptic plasticity processes (Benson et al., 2000).

N-cadherin function involves the interaction with β- and α-catenin. Via a direct connection to β-catenin, N-cadherin is indirectly interacting with α-catenin, providing a link to the actin cytoskeleton. This and the fact that N-cadherin is localized adjacent to active zones (Uchida et al, 1996) gave rise to its function in coordinating presynaptic vesicle clustering, as demonstrated using N-cadherin deficient neurons (Stan et al., 2010). A knock-out approach of β-catenin function supports this, as the synaptic vesicles were found to be diffusely localized (Biederer et al., 2002; Bamji et al., 2003). However, a knock-out of α-catenin showed controversy results, as the synaptic vesicles were localized in an unaltered manner (Togashi et al., 2002; Abe et al., 2004). Furthermore, Rac and Rho, two GTPases, are known to control actin polymerization (Goodwin and Yap, 2004; Reynolds et al., 2007). Moreover, the direct connection of N-cadherin to p120-catenin at the juxtamembrane domain is supposed to be decisive for this. Accordingly, similar to β-catenin deficient neurons, experiments involving a knockout of p120-catenin demonstrated a disturbed presynaptic vesicle clustering (Elia et al., 2006).

The role of postsynaptic neuroligin1 in presynaptic processes is based on its heterophilic interaction with presynaptically localized β-neurexin. Both proteins contain PDZ-binding motifs in the cytoplasmatic region enabling the interaction with other intracellular proteins containing PDZ-domains. Thereby, especially the membrane-associated guanylate kinase homologue (MAGUK) CASK is a promising candidate for mediating the interaction between β-neurexin and actin (Mukherjee et al., 2008; Biederer and Südhof, 2001). Similar to other intracellular proteins containing a PDZ domain, CASK is proposed to be a key player in organizing pre- and postsynaptic terminals. As β-catenin likewise contains a PDZ-binding motif, an interaction of N-cadherin with CASK might be conceivable. CASK on its own part is associated with multiple other proteins (e.g. MINT, VELI), that are putatively involved in the regulation of presynaptic processes as well (Butz et al., 1998).

The overexpression of neuroligin1 in non-neuronal cell was shown to trigger presynaptic vesicle clustering in contacting axons (Scheiffele et al., 2000). Likewise neuroligin1 was shown to mediate presynaptic maturation in cultured hippocampal neurons. In line with this presynaptic boutons from neuroligin1 knockout mice remained immature (Wittenmayer et al., 2009) Contrary to the observed role in accumulating presynaptic vesicles, a similar effect of

N-cadherin could not be demonstrated (Scheiffele et al., 2000), thus making it likely that N-cadherin not directly affects presynaptic vesicle clustering, but rather indirectly through the cooperation with another molecule.

The cooperation of N-cadherin with neuroligin1 was analyzed using ES cell-derived Ncad-/- neurons (Stan et al., 2010). Combined with a gain-of-function approach targeting neuroligin1 it was demonstrated by live cell imaging that the neuroligin1 triggered accumulation of presynaptic vesicles is dependent on N-cadherin. Mechanistically, N-cadherin and neuroligin1 were found to be linked by a postsynaptic scaffolding protein interconnecting neuroligin1 and β-catenin via its PDZ-domains. Multiple actions, such as morphology, number and type of synapse were already found to be regulated by a linkage of adhesion molecules to scaffolding proteins (Prange et al., 2004). For example, the presence of PSD-95 restricts neuroligin1 to induce excitatory synapses. The scaffolding protein S-SCAM was identified as the adaptor between N-cadherin and neuroligin1, which was experimentally proven by different S-SCAM mutants and an RNAi-mediated knockdown of all S-SCAM isoforms (Stan et al., 2010). As the number of postsynaptically localized neuroligin1 clusters was reduced in the absence of N-cadherin and the colocalization of neuroligin1 with N-cadherin in the absence of S-SCAM function was impaired, N-cadherin-mediated synaptic targeting as well as functional activation of neuroligin1 might be crucial to initiate presynaptic vesicle clustering. In line with this are observations from other studies claiming β-catenin to initiate the recruitment of S-SCAM (Nishimura et al., 2002), while S-SCAM on its own was shown to recruit neuroligin1 (Dresbach et al., 2004, Iida et al., 2004). Experiments in hippocampal slices verified the relevance of the N-cadherin/neuroligin1 cooperation in organotypic networks (Stan et al., 2010). Taken together, these results show the requirement of N-cadherin function for neuroligin1-mediated transsynaptic processes. Thereby, N-cadherin is proposed to regulate the synaptic targeting of neuroligin1 via S-SCAM.

Analysis of the functional aspects of the cooperation of N-cadherin and neuroligin1 in inducing presynaptic vesicle clustering was performed in this work. A measure for functional properties is the examination of synaptic transmission by means of electrophysiological recordings. As neuroligin1 was shown to be exclusively expressed at glutamatergic synapses (Song et al., 1999), the analysis was restricted to these, while GABAergic activity was blocked pharmacologically. Inspired by previous studies describing neuroligin1 to induce an enhancement of spontaneous mEPSCs (Levinson et al., 2005), it was overexpressed in cortical

neurons cultured on glial micro islands and analyzed regarding AMPA receptor-mediated mEPSCs. The analysis shown in figure 3.21 indeed demonstrated the ability of neuroligin1 to induce an increase in the frequency of AMPA mEPSCs. Experiments using a concentration of extracellular Ca^{2+} (5mM; Fig. 3.21) strongly stimulating presynaptic vesicle release allowed the suggestion of a presynaptic mechanism forming the basis of neuroligin1 action. In order to demonstrate a cooperation of N-cadherin and neuroligin1 also in functional synaptic transmission a gain-of-function approach targeting neuroligin1 and a loss-of-function approach targeting N-cadherin were combined by simultaneously overexpressing neuroligin1 and blocking N-cadherin function by co-expressing a dominant negative form of N-cadherin (Fig. 3.23). This mutant form, lacking a large part of the extracellular domain, is integrated into the membrane similar to endogenous N-cadherin, competing with it for intracellular effectors such as catenins (Riehl et al., 1996). As the described interaction of N-cadherin with the catenins is essential, a proper function of N-cadherin is inhibited. To follow up an interaction of both adhesion molecules likewise in ES cell-derived knockout neurons, the experiments were repeated using ES cell-derived Ncad+/- and Ncad-/- neurons, respectively (Fig. 3.24). Intriguingly, both approaches revealed the same result. While in the presence and functionality of N-cadherin a neuroligin1-induced enhancement of synaptic activity was observed, neuroligin1 failed to increase the frequency of AMPA receptor-mediated mEPSCs in the absence of N-cadherin itself or its function. Two aspects may account for an altered frequency of the spontaneous mEPSCs: a modulation in the presynaptic release properties, reflecting amongst others changes in the presynaptic vesicle accumulation, or an altered synaptic density.

In order to confirm a cooperation of both adhesion molecules in the modulation of presynaptic vesicle release, the effect of neuroligin1 on the progressive block of NMDA receptor-mediated EPSCs in cortical neurons was examined with N-cadherin function inhibited. NMDA receptor-mediated PSCs have been described to be affected by neuroligin1 expression. Experiments using either a dominant negative form of neuroligin1 or neuroligin1 knockout mice demonstrated a reduction in these postsynaptic currents (Nam and Chen, 2005; Jung et al., 2010). Furthermore, the recruitment of NMDA receptors is seemingly promoted by neuroligin, probably via the interaction with PSD-95 (Fu et al., 2003). The use of MK801 results in a block of NMDA receptor-mediated EPSCs in an activity-dependent manner, reflecting presynaptic release probability. As expected from an increase in release probability the EPSCs in neuroligin1 overexpressing cortical neurons were blocked after much less stimuli as in the control. Strikingly, in the absence of N-cadherin function (Ncad-ΔE

expression) the kinetics of the MK-801 block were unaltered. In line with the results describing a cooperation of N-cadherin and neuroligin1 in presynaptic vesicle clustering, the analogous necessity of N-cadherin function for neuroligin1-induced modulation of synaptic function could be demonstrated. Via this interaction synapse maturation and cell recognition might be mechanistically coupled.

The observation that synapses are usually equipped with at least one cadherin-like adhesion molecule and at least one immunoglobulin family member (Yamada et al., 2003), suggests other interactions among adhesion molecules, that might be linked by scaffolding proteins as well. Especially the induction of presynaptic vesicle clustering in GABAergic synapses may be regulated in this manner. As in mature stages neuroligin1 and N-cadherin were shown to be exclusively expressed at excitatory synapses, putative candidates might be other neuroligin isoforms found to be expressed at inhibitory synapses. Furthermore, the restricted expression pattern of both adhesion molecules raises a potential for cooperations of other adhesion molecules at synapses, where N-cadherin or neuroligin1 are absent.

5. References

Abe K, Chisaka O, Van Roy F, Takeichi M (2004). Stability of dendritic spines and synaptic contacts is controlled by α N-catenin. *Nat Neurosci* 7: 357-363.

Aberle H, Butz S, Stappert J, Weissig H, Kemler R, Hoschuetzky H (1994). Assembly of the cadherin-catenin complex in vitro with recombinant proteins. *J Cell Sci* 107: 3655-3663.

Ahmari SE, Buchanan J, Smith SJ (2000). Assembly of presynaptic active zones from cytoplasmatic transport packets. *Nat Neurosci* 3: 445-451.

Altar CA, Cai N, Bliven T, Juhasz M, Conner JM, Acheson AL, Lindsay RM, Wiegand SJ (1997). Anterograde transport of brain-derived neurotrophic factor and ist role in the brain. *Nature* 389: 856-860.

Anastasiadis PZ, Reynolds AB (2000). The p120-catenin family: complex roles in adhesion, signaling and cancer. *J Cell Sci* 113: 1319-1324.

Araç D, Boucard AA, Ozkan E, Strop P, Newell E, Südhof TC, Brunger AT (2007). Structures of neuroligin I and the neuroligin I/neurexin I beta complex reveal specific protein-protein and protein- Ca^{2+} interactions. *Neuron* 56:992-1003.

Ashton AC, Ushkaryov YA (2005). Properties of synaptic vesicle pools in mature central nerve terminals. *J Biol Chem* 280: 37278-37288.

Augustine GJ, Charlton MP, Smith SJ (1987). Calcium action in synaptic transmitter release. *Annu Rev Neurosci* 10: 633-693.

Balsamo J, Arregui C, Leung T, Lilien J (1998). The non-receptor protein tyrosine phosphatase PTP1B binds to the cytoplasmatic domain of N-cadherin and regulates the cadherin-actin linkage. *J Cell Biol* 143: 523-532.

Bagnard D, Lohrum M, Uziel D, Püschel AW, Bolz J (1998). Semaphorins act as attractive and repulsive guidance signals during the development of cortical projections. *Development* 125: 5043-5053.

Bähler M, Greengard P (1987). Synapsin I bundles F-actin in a phosphorylation-dependent manner. *Nature* 326: 704-707.

Bailey CH, Kandel ER (1993). Structural changes accompanying memory storage. *Annu Rev Physiol* 55: 397-426.

Bain G, Ray WJ, Yao M, Gottlieb DI (1996). Retinoic acid promotes neural and represses mesodermal gene expression in mouse embryonic stem cells in culture. *Biochem Biophys Re Commun* 223: 691-694.

REFERENCES

Balice-Gordon RJ, Lichtman JW (1993). In vivo observations of pre- and postsynaptic changes during the transition from multiple to single innervations at developing neuromuscular junctions. *J Neurosci* 13: 834-855.

Bamji SX, Majdan M, Pozniak CD, Belliveau DJ, Aloyz R, Kohn J, Causing CG, Miller FD (1998). The p75 neurotrophin receptor mediates neuronal apoptosis and is essential for naturally occurring sympathetic neuron death. *J Cell Biol* 140: 911-923.

Bamji SX, Shimazu K, Kimes N, Huelsken J, Birchmeier W, Lu B, Reichhardt LF (2003). Role of beta-catenin in synaptic vesicle localization and presynaptic assembly. *Neuron* 40: 719-731.

Bamji SX, Rico B, Kimes N, Reichardt LF (2006). BDNF mobilizes synaptic vesicles and enhances synapse formation by disrupting cadherin-β-catenin interactions. *J Cell Biol* 174: 289-299.

Barth AI, Nathke IS, Nelson WJ (1997). Cadherins, catenins and APC protein: interplay between cytoskeletal complexes and signaling pathways. *Curr Opin Cell Biol.* 9: 683–690.

Bats C, Groc L, Chouquet D (2007). The interaction between stargazing and PSD-95 regulates AMPA receptor surface trafficking. *Neuron* 53: 719-734.

Bekkers JM, Stevens CF (1989). NMDA and non-NMDA receptors are coloalized at individual excitatory synapses in cultured rat hippocampus. *Nature* 341: 230-233.

Ben Fredj N, Burrone J (2009). A resting pool of vesicles is responsible for spontaneous vesicle fusion at the synapse. *Nat neurosci* 12: 751-758.

Benson DL, Tanaka H (1998). N-cadherin redistribution during synaptogenesis in hippocampal neurons. *J Neurosci* 18: 6892-6904.

Ben-Zvi A, Yagil Z, Hagalili Y, Klein H, Lerman O, Behar O (2006). Semaophorins 3A and neurotrophins: a balance between apoptosis and survival signaling in embryonic DRG neurons. *J Neurochem* 96: 585-597.

Betz A, Okamoto M, Benseler F, Brose N (1997). Direct interaction of the rat unc-13 homologue Munc13-1 with the N-terminus of syntaxin. *J Biol Chem* 272: 2520-2526.

Biederer T, Südhof TC (2001). CASK and protein 4.1 support F-actin nucleation on neurexins. *J Biol Chem* 276: 47869-47876.

Biederer T, Sara Y, Mozhayeva M, Atasoy D, Liu X, Kavalali ET, Südhof TC (2002). SynCAM, a synaptic adhesion molecule that drives synapse assembly. *Science* 297: 1525-1531.

Biggs JE, Lu VB, Stebbing MJ, Balasubramanyan S, Smith PA (2010). Is BDNF sufficient for information transfer between microglia and dorsal horn neurons during the onset of central sensitization? *Mol Pain* 6: 44.

REFERENCES

Binder DK, Routbort MJ, Ryan TE, Yancopoulos GD, McNamara JO (1999). Selective inhibition of kindling development by intraventricular administration of TrkB receptor body. *J Neurosci* 19: 1424-1436.

Binder DK, Scharfman HE (2004). Brain-derived neurotrophic factor. *Growth factors* 22: 123-131.

Blaschuk OW, Sullivan R, David S, Pouliot Y (1990). Identification of a cadherin cell adhesion recognition sequence. *Dev Biol* 139: 227-229.

Bliss TV, Collingridge GL (1993). A synaptic model of memory: long-term potentiation in the hippocampus. *Nature* 361: 31-39.

Bock JB, Scheller RH (1999). SNARE proteins mediate lipid bilayer fusion. *Proc Natl Acad Sci* 96: 12227-9.

Bollmann JH, Sakmann B, Borst JG (2000). Calcium sensitivity of glutamate release in a calyx-type terminal. *Science* 289: 953-957.

Bolton MM, Pittman AJ, Lo DC (2000). Brain-derived neurotrophic factor differentially regulates excitatory and inhibitory synaptic transmission in hippocampal cultures. *J Neurosci* 20: 3221-3232.

Bortoletto ZA, Clarke VRJ, Delany CM, Parry MC, Smolders I, Vignes M, Hoo KH, Brinton B, Fantaske R, Ogden A, Gates M, Ornstein PL, Lodge D, Bleakman D, Collingridge, GL (1999). Kainate receptors are involved in synaptic plasticity. *Nature* 402:297-301.

Bozdagi O, Valcin M, Poskanzer K, Tanaka H, Benson DL (2004). Temporally distinct demands for classic cadherins in synpase formation and maturation. *Mol Cell Neurosci* 27: 509-521.

Bozdagi O, Wang XB, Nikitczuk JS, Anderson TR, Bloss EB, Radice GL, Zhou Q, Benson DL, Huntley GW (2010). Persistance of coordinated long-term potentiation and dendritic spine enlargement at mature hippocampal CA1 synapses requires N-cadherin. *J Neurosci* 28: 9984-9989.

Brieher WM, Yap AS, Gumbiner BM (1996). Lateral dimerization is required for the homophilic binding activity of C-cadherin. *J Cell Biol* 135: 487-496.

Brose K, Bland KS, Wang KH, Arnott D, Henzel W, Goodman CS, Tessier-Lavigne M, Kidd T (1999). Slit proteins bind Robo receptors and have an evolutionarily conserved role in repulsive axon guidance. *Cell* 96: 795-806.

Brose N, Rosenmund C, Rettig J (2000). Regulation of transmitter release by Unc-13 and its homologues. *Curr Opin Neurobiol* 10: 303-311.

Butz S, Okamoto M, Südhof TC (1998). A tripartite protein complex with the potential to couple synaptic vesicle exocytosis to cell adhesion in brain. *Cell* 94: 773-782.

REFERENCES

Casaccia-Bonnefil P, Carter BD, Dobrowsky RT, Chao MV (1996). Death of oligodendrocytes mediated by the interaction of nerve growth factor with its receptor p75. *Nature* 383: 716-719.

Chapman ER (2002). Synaptotagmin: a Ca(2+) sensor that triggers exocytosis? *Nat Rev Mol Cell Biol* 3: 498-508.

Chen H, Weber AJ (2004). Brain-derived neurotrophic factor reduces TrkB protein and mRNA in the normal retina and following optic nerve crush in adult rats. *Brain Res* 1011: 99-106.

Chen L, Chetkovich DM, Petralia RS Sweeney NT Kawasaki Y, Wenthold RJ, Bredt DS, Nicoll RA (2000). Stargazin regulates synaptic targeting of AMPA receptors by two distinct mechanisms. *Nature* 408: 936-943.

Chen Q, Peto CA, Shelton GD, Mizisin A, Sawchenko PE, Schubert D (2009). Loss of modifier of cell adhesion reveals a pathway leading to axonal degeneration. *J Neurosci* 29: 118-130.

Chen WG, Chang Q, Lin Y, Meissner A, West AE, Griffith EC, Jaenisch R, Greeberg ME (2003). Depression of BDNF transcription involves calcium-dependent phosphorylation of MeCP2.*Science* 302: 885-889.

Chen YA, Scheller RH (2001). SNARE-mediated membrane fusion. *Nat Rev Mol Cell Biol* 2: 98-106.

Cheng HJ, Nakamoto M, Bergemann AD, Flanagan JG (1995). Complementary gradients in expression and binding of ELF-1 and Mek4 in development of the topographic retinotectal projection map. *Cell* 82: 371-381.

Cheng HJ, Bagri A, Yaron A, Stein E, Pleasure SJ, Tessier-Lavigne M (2001). Plexin-A3 mediates semaphoring signaling and regulates the development of hippocampal axonal projections. *Neuron* 32: 249-263.

Chih B, Engelmann H, Scheiffele P (2005). Control of excitatory and inhibitory synapse formation by neuroligins. *Science* 307: 1324-1328.

Chu Z, Hablitz JJ (2000). Quisqualate induces an inward current via mGluR activation in neocortical pyramidal neurons. *Brain Res* 879: 88-92.

Chubykin AA, Atasoy D, Etherton MR, Brose N, Kavalali ET, Gibson JR, Südhof TC (2007). Activity-dependent validation of excitatory versus inhibitory synapses by neuroligin-I versus neuroligin II. *Neuron* 54: 919-931.

Ciani L, Salinas PC (2005). WNTs in the vertebrate nervous system: from patterning to neuronal connectivity. *Nat Rev Neurosci* 6: 351-362.

Clayton EL, Evans GJ, Cousin MA (2007). Activity-dependent control of bulk endocytosis by protein dephosphorylation in central nerve terminals. *J Physiol* 585: 687-691.

REFERENCES

Cobb SR, Halasy K, Vida K, Nyiri G, Tamás G, Buhl EH, Somogyi P (1997). Synaptic effects of identified interneurons innervating both interneurons and pyramidal cells in the rat hippocampus. *Neuroscience* 79: 629-648.

Colicos MA, Collins BE, Sailor MJ, Goda Y (2001). Remodeling of synaptic actin induced by photoconductive stimulation. *Cell* 107: 605-616.

Colman H, Nabekura J, Lichtman JW (1997). Alterations in synaptic strength preseding axon withdrawal. *Science* 275: 356-361.

Conn PJ, Pin JP (1997). Pharmacology and functions of metabotropic glutamat receptors. *Annu Rev Pharmacol Toxicol* 37: 205-237.

Costanzo EM, Barry JA, Ribchester RR (2000). Competition at silent synapses in reinnervated skeletal muscle. *Nat Neurosci* 3: 694-700.

David MD, Yeramian A, Duňach M, Llovera M, Canti C, Garcia de Herros A, Comella JX, Herreros J (2008). Signalling by neurotrophins and hepatocyte growth factor regulates axon morphogenesis by differential catenin phosphorylation. *J Cell Sci* 121: 2718-2730.

Davis GW, Schuster CM, Goodman CS (1997). Genetic analysis of the mechanisms controlling target selection: target-derived fasciclin II regulates the pattern of synapse formation. *Neuron* 19: 561-573.

Deák F, Shin OH, Tang J, Hanson P, Ubach J, Jahn R, Rizo J, Kavalali ET, Südhof TC (2006). Rabphilin regulates SNARE-dependent repriming of synaptic vesicles for fusion. *EMBO J* 25: 2856-2866.

DeCamilli P, Cameron R, Greengard P (1983). Synapsin I (ProteinI), a nerve terminal-specific Phosphoprotein. I. It`s general distribution in synapses of the central and peripheral nervous system demonstrated by Immunoflourescence in frozen and plastic sections. *J Cell Biol* 96: 1337-1354.

Delva E, Kowalczyk AP (2009). Regulation of cadherin trafficking. *Traffic* 10: 259-267.

Denisenko-Nehrbass NI, Jarvis E, Scharff C, Nottebohm F, Mello CV (2000). Site-specific retinoic acid production in the brain of adult songbirds. *Neuron* 27: 359-370.

Dickson BJ (2002). Molecular mechanisms of axon guidance. *Science* 298: 1959-1964.

Ding M, Chao D, Wang G, Shen K (2007). Spatial regulation of an E3 ubiquitin ligase directs selective synapse elimination. *Science* 317: 947-951.

Dingledine R, Borges K, Bowie D, Traynelis SF (1999). The glutamate receptor ion channels. *Pharmacol Rev* 51: 7-61

Dityatev A, Dityateva G, Schachner M (2000). Synaptic strength as a function of post- versus presynaptic expression of the neural cell adhesion molecule NCAM. *Neuron* 26: 207-217.

REFERENCES

Doherty P, Rowett LH, Moore SE, Mann DA, Walsh FS (1991). Neurite outgrowth in response to transfected N-CAM and N-cadherin reveals fundamental differences in neuronal responsiveness. *Neuron* 6: 247-258.

Doherty P, Walsh FS (1996). CAM-FGF receptor interactions: a model for axonal growth. *Mol Cell Neurosci* 8: 99-111.

Dong H, O`Brien RJ, Fung ET, Lanahan AA, Worley PF, Huganir RL (1997). GRIP: a synaptic PDZ domain-containing protein that interacts with AMPA receptors. *Nature* 386: 279-284.

Dontchev D, Letourneau PC (2002). Nerve growth factor and semaphorin 3A signaling pathways interact in regulating sensory neuronal growth cone motility. *J Neurosci* 22: 6659-6669.

Drees F, Pokutta S, Yamada S, Nelson WJ, Weis WI (2005). α-catenin is a molecular switch taht binds E-cadherin-β-catenin and regulates actin-filament assembly. *Cell* 123: 903-915.

Dresbach T, Neeb A, Meyer G, Gundelfinger ED, Brose N (2004). Synaptic targeting of neuroligin is independent of neurexin and SAP90/PSD-95 binding. *Mol Cell Neurosci* 27: 227-235.

Drescher U, Kremoser C, Handwerker C, Löschinger J, Noda M, Bonhoeffer F (1995). In vitro guidance of retinal ganglion cell axons by RAGS, a 25kDa tectal protein related to ligands for Eph receptor tyrosine kinases. *Cell* 82: 359-370.

Duester G (2008). Retinoic acid synthesis and signaling during early organogenesis. *Cell* 134: 921-931.

Duguay D, Foty RA, Steinberg MS (2003). Cadherin-mediated cell adhesion and tissue segregation: qualitative and quantitative determinants. *Dev Biol* 253: 309-323.

Dunaevsky A, Connor EA (2000). F-actin is concentrated in non-release domains at frog neuromuscular junctions. *J Neurosci* 20: 6007-6012.

Eide FF, Vining ER, Eide BL, Zang K, Wang XY, Reichardt LF (1996). Naturally occurring truncated TrkB receptors have dominant inhibitory effects on Brain-derived neurotrophic factor signaling. *J Neurosci* 16: 3123–3129.

Edmonds B, Gibb AJ, Colquhoun D (1995). Mechanisms of activation of glutamate receptors and time course of excitatory currents. *Annu Rev Physiol* 57: 495-519.

Ehrlich I, Malinow R (2004). Postsynaptic density 95 controls AMPA receptor incorporation during longterm potentiation and experience-driven synaptic plasticity. *J Neurosci* 24: 916-927.

Elia LP, Yamamoto M, Zang K, Reichardt LF (2006). p120 catenin regulates dendritic spine and synapse development through Rho-family GTPases and cadherins. *Neuron* 51:43–56.

REFERENCES

Elias GM, Nicoll RA (2007). Synaptic trafficking of glutamate receptors by MAGUK scaffolding proteins. *Trends Cell Biol* 17: 343-352.

Elste AM and Benson DL (2006). Structural basis for developmentally regulated changes in cadherin function at synapses. *J Comp Neurol* 495: 324-335.

Engerer P, Sigrist SJ (2009). Relax? Don`t do it!-Linking presynaptic vesicle clustering with mechanical tension. *HFSP J* 3: 367-372.

Faber DS, Lin JW, Korn H (1991). Silent synaptic connections and their modifiability. Ann *N Y Acad Sci* 627: 151-164.

Feldmeyer D, Lübke J, Silver RA, Sakmann B (2002). Synaptic connections between layer 4 spiny neurone-layer 2/3 pyramidal cell pairs in juvenile rat barrel cortex: physiology and anatomy of interlaminar signalling within a cortical column. *J Physiol* 538: 803–822.

Ferguson SM, Brasnjo G, Hayashi M, Wölfel M, Collesi C, Giovedi S, Raimondi A, Gong LW, Ariel P, Paradise S (2007). A selective activity-dependent requirement for dynamin I in synaptic vesicle endocytosis. *Science* 316:570-574.

Fernandez I, Arac D, Ubach J, Gerber SH, Shin O, Gao Y, Anderson RG, Südhof TC, Rizo J (2001). Three-dimensional structure of the synaptotagmin 1 C2B-domain: synaptotagmin 1 as a phospholipid binding machine. *Neuron* 32: 1057-1069.

Fernandez-Chacon R, Konigstorfer A, Gerber SH, Garcia J, Matos MF, Stevens CF, Brose N, Rizo J, Rosenmund C, Südhof TC (2001). Synaptotagmin I functions as a calcium regulator of release probability. *Nature* 410: 41-9.

Fields RD (2006). Advances in understanding neuron-glia interactions. *Neuron Glia Biol* 2: 23-26.

Frade JM, Rodríguez-Tébar A, Barde YA (1996). Induction of cell death by endogenous nerve growth factor through its p75 receptor. *Nature* 383: 166-168.

Frerking M, Schmitz D, Zhou Q, Johansen J, Nicoll RA (2001). Kainate receptors depress excitatory synaptic transmission at CA3→CA1 synapses in the hippocampus via a direct presynaptic action. *J Neurosci* 21: 2958-2966.

Forsythe ID, Westbrook GL (1988). Slow excitatory postsynaptic currents mediated by NMDA receptors on cultured mouse central neurons. *J Physiol* 396: 515-534.

Frade JM, Barde YA (1998). Nerve growth factor: two receptors, multiple functions. *Bioessays* 20: 137-145.

Fujimori T, Takeichi M (1993). Disruption of epithelial cell-cell adhesion by exogenous expression of a mutated nonfunctional N-cadherin. *Mol Biol Cell* 4: 37-47.

REFERENCES

Fujita Y, Sasaki T, Fukui K, Kotani H, Kimura T, Hata Y, Sudhof TC, Scheller RH, Takai Y (1995). Phosphorylation of Munc-18/nSec1/rbSec1 by Protein Kinase C. *J Biol Chem* 271: 7265-7268.

Gad H, Löw P, Zotova E, Brodin L, Shupliakov O (1998). Dissociation between Ca^{2+}-triggered synaptic vesicle exocytosis and clathrin-mediated endocytosis at a central synapse. *Neuron* 21: 607-616.

Gandhi SP, Stevens CF (2003). Three modes of synaptic vesicular recycling revealed by single-vesicle imaging. *Nature* 423: 607-613.

Garner CC, Kindler S, Gundelfinger ED (2000). Molecular determinants of presynaptic active zones. *Curr Opin Neurobiol* 10:321-327.

Gasic M, Hollmann M (1992). Molecular neurobiology of glutamate receptors. *Annu Rev Physiol* 54: 507-536.

Geppert M, Goda Y, Hammer RE, Li C, Rosahl TW, Stevens CF, Südhof TC (1994). Synaptotagmin I: a major Ca^{2+} sensor for neurotransmitter release at a central synapse. *Cell* 79: 717-727.

Gerrow K, El-Husseini A (2006). Cell adhesion molecules at the synapse. *Front Biosci* 11: 2400-2419.

Glaser T, Brüstle O (2008). Retinoic acid induction of ES cell-derived neurons: the radial glia connection. *Trends Neurosci* 28: 397-400.

Glass DJ, Bowen DC, Stitt TN, Radziejewski C, Bruno J, Ryan TE, Gies DR, Shah S, Mattson K, Burden SJ, DiStefano PS, Valenzuela DM, DeChiara TM, Yancopoulos GD (1996). Agrin acts via a MuSK receptor complex. *Cell* 85: 513-523.

Goodwin M, Yap AS (2004). Classical cadherin adhesion molecules: coordinating cell adhesion, signaling and the cytoskeleton. *J Mol Histol* 35:839-844.

Goda Y, Davis GW (2003). Mechanisms of synapse assembly and disassembly. *Neuron* 40: 243-264.

Gordon J (1991). Use of vanadate as protein-phosphotyrosine phosphatase inhibitor. *Methods Enzymol* 201: 477-82.

Gottmann K, Pfrieger FW, Lux HD (1994). The formation of glutamatergic synapses in cultured central neurons: selective increase in miniature synaptic currents. *Brain Res Dev Brain Res* 81: 77-88.

Gottmann K, Mittmann T, Leßmann V (2009). BDNF signaling in the formation, maturation and plasticity of glutamatergic and GABAergic synapses. *Exp Brain Res* 199: 203-234.

Graf ER, Zhang X, Jin SX, Linhoff MW, Craig AM (2004). Neurexins induce differentiation of GABA and glutamate postsynaptic specializations via neuroligins. *Cell* 119: 1013-1026.

[144]

REFERENCES

Hägglund M, Berghard A, Strotmann J, Bohm Staffan (2006). Retionoic acid receptor-dependent survival of olfactory sensory neurons in postnatal and adult mice. *J Neurosci* 26: 3281-3291.

Halbleib JM, Nelson WJ (2006). Cadherins in development: cell adhesion, sorting and tissue morphogenesis. *Genes Dev* 20: 3199-3214.

Hanson PI, Heuser JE, Jahn R, 1997. Neurotransmitter release – four years of SNARE complexes. *Curr Opin Neurobiol* 7: 310-315.

Hanson JE, Madison DV (2007). Presynaptic Fmr1 genotype influences the degree of synaptic connectivity in a mosaic mouse model of fragile X syndrome. *J Neurosci* 27: 4014-4018.

Harata N, Pyle JL, Aravanis AM, Mozhayeva M, Kavalali ET, Tsien RW (2001). Limited numbers of recycling vesicles in small CNS nerve terminals: implications for neural signaling and vesicular cycling. *Trends Neurosci* 24: 637-643.

Harata NC, Aravanis AM, Tsien RW (2006). Kiss-and-run and full-collapse fusion as modes of exo-endocytosis in neurosecretion. *J Neurochem* 97: 1546-1570.

Harms KJ, Craig AM (2005). Synapse composition and organization following chronic activity blockade in cultured hippocampal neurons. *J Comp Neurol 490*: 72-84.

Hartmann M, Brigadski T, Erdmann KS, Holtmann B, Sendtner M, Narz F, Leßmann V (2004). Truncated TrkB receptor-induced outgrowth of dendritic filopodia involves the p75 neurotrophinreceptor. *J Cell Sci* 117: 5803-5814.

Haÿ E, Laplantine E, Geoffroy V, Frain M, Kohler T, Müller R, Marie PJ (2009). N-cadherin interacts with axin and LRP5 to negatively regulate wnt/β-catenin signaling, osteoblast function and bone formation. *Mol Cell Biol* 29: 953-964.

He Z, Tessier-Lavigne M (1997). Neuropilin is a receptor for the axonal chemorepellent Semaphorin III. *Cell* 90: 739-751.

Helton TD, Otsuka T, Lee M, Mu Y, Ehlers MD (2008). Pruning and loss of excitatory synapses by the parkin ubiquitin ligase. *Proc Natl Acad Sci* 105: 19492-19497.

Hindges R, McLaughlin T, Genoud N, Henkemeyer M, O`Leary DD (2002). EphB forward signaling controls directional branch extension and arborization required for dorsal-ventral retinotopic mapping. *Neuron* 35: 475-487.

Hollmann M, Maron C, Heinemann S (1994). N-glycosylation site tagging suggests a three transmembrane domain topology for the glutamate receptor GluR1. *Neuron* 13: 13331-1343.

Hong K, Hinck L, Nishiyama M, Poo MM, Tessier-Lavigne M, Stein E (1999). A ligand-gated association between cytoplasmatic domains of UNC5 and DCC family receptors converts netrin-induced growth cone attraction to repulsion. *Cell* 97: 927-941.

REFERENCES

Hooks BM, Chen C (2006). Distinct roles for spontaneous and visual activity in remodeling of the retinogeniculate synapse. *Neuron* 52: 281-291.

Huang EJ, Reichardt LF (2003). Trk receptors: roles in neuronal signal transduction. *Annu Rev Biochem* 72: 609-642.

Huber AB, Kolodkin AL, Ginty DD, Cloutier JF (2003). Signaling at the growth cone: ligand-receptor complexes and the control of axon growth and guidance. *Annu Rev Neurosci* 26: 509-563.

Huntley GW, Benson DL (1999). Neural (N)-cadherin at developing thalamocortical synapses provides an adhesion mechansism for the formation of somatopically organized connections. *J Comp Neurol* 407: 453-471.

Huttner WB, Schiebler W, Greengard P, DeCamilli P (1983). Synapsin I (ProteinI), a nerve terminal-specific Phosphoprotein. III. It`s association with synaptic vesicles studied in a highly purified synaptic vesicle preparation. *J Cell Biol* 96: 1374-1388.

Ichtchenko K, Hata Y, Nguyen T, Ullrich B, Missler M, Moomaw C, Südhof TC (1995). Neuroligin I: a splice site-specific ligand for beta-neurexins. *Cell* 81: 435-443.

Ichtchenko K, Nguyen T, Südhof TC (1996). Structures, alternative splicing and neurexin binding of multiple neuroligins. *J Biol Chem* 271: 2676-2682.

Iida J, Hirabayashi S, Sato Y, Hata Y (2004). Synaptic scaffolding molecule is involved in synaptic clustering of neuroligin. *Mol Cell Neurosci* 27: 497-508.

Irie M, Hata Y, Takeuchi M, Ichtchenko K, Toyoda A, Hirao K, Takai Y, Rosahl TW, Südhof TC (1997). Binding of neuroligins to PSD-95. *Science* 277:1511-1515.

Jang YK, Park JJ, Lee MC, Yoon BH, Yang YS, Yang SE, Kim SU (2004). Retinoic acid-mediated induction of neurons and glial cells from human umbilical cord-derived hematopoietic stem cells. *J Neurosci Res* 75: 573-584.

Jang Y, Jung Y, Lee SH, Moon C, Kim C, Baik EJ (2009). Calpain-mediated N-cadherin proteolytic processing in brain injury. *J Neurosci* 29: 5974-5984.

Jones-Villeneuve EMV, McBurney MW, Rogers KM, Kalnins VI (1982). Retinoic acid induces embryonal carcinoma cells to differentiate into neurons and glial cells. *J Cell Biol* 94: 253- 262.

Jovanovic JN, Czernik AJ, Fienberg AA, Greengard P, Sihra TS (2000). Synapsins as mediators of BDNF-enhanced neurotransmitter release. *Nat Neurosci* 3: 323-329.

Jüngling K, Nägler K, Pfrieger FW, Gottmann K (2003). Purification of embryonic stem cell-derived neurons by immunoisolation. *FASEB* J 14: 2100-2102.

REFERENCES

Jüngling K, Eulenberg V, Moore R, Kemler R, Leßmann V, Gottmann K (2006). N-cadherin transsynaptically regulates short-term plasticity at glutamatergic synapses in embryonic stem cell-derived neurons. *J Neurosci* 26: 6968-6978.

Jung SY, Kim J, Kwon OB, Jung JH, An K, Jeong AY, Lee CY, Choi YB, Bailey CH, Kandel ER, Kim JH (2010). Input-specific synaptic plasticity in the amygdala is regulated by neuroligin I via postsynaptic NMDA receptors. *Proc Natl Acad Sci* 107: 4710-4715.

Kadowaki M, Nakamura S, Machon O, Krauss S, Radice GL, Takeichi M (2007). N-cadherin mediates cortical organization in the mouse brain. *Dev Biol* 304:22-33.

Kafitz KW, Rose CR, Thoenen H, Konnerth A (1999). Neurotrophin-evoked rapid excitation through TrkB receptors. *Nature* 401: 918-921.

Kaplan DR, Miller FD (2000). Neurotrophin signal transduction in the nervous system. *Curr Opin Neurobiol* 10: 381-391.

Katsamba P, Carroll K, Ahlsen G, Bahna F, Vendome J, Posy S, Rajebhosale M, Price S, Jessel TM, Ben-Shaul A, Shapiro L, Honig BH (2009). Linking molecular affinity and cellular specificity in cadherin-mediated adhesion. *Proc Natl Acad Sci* 106: 11894-11599.

Katz LC, Crowley JC (2002). Development of cortical circuits: lessons from ocular dominance columns. *Nat Rev Neurosci* 3: 34-42.

Kemler R, Ozawa M (1989). Uvomorulin-catenin complex: cytoplasmatic anchorage of a Ca^{2+} dependent cell adhesion molecule. *Bioessay* 11: 88-91.

Klassen MP, Shen K (2007). Wnt signaling positions neuromuscular connectivity by inhibiting synapse formation in C. elegans. *Cell* 130: 704-716.

Klau M, Hartmann M, Erdmann KS, Heumann R, Leßmann V (2001). Reduced number of functional glutamatergic synapses in hippocampal neurons overexpressing full-length TrkB receptor. *J Neurosci Res* 66: 327-336.

Knott GW, Quairiaux C, Genoud C, Welker E (2002). Formation of dendritic spines with GABAergic synapses induced by whisker stimulation in adult mice. *Neuron* 34: 265-273.

Ko J, Zhang C, Arac D , Boucard AA, Brunger AT, Südhof TC (2009). Neuroligin I performs neurexin-dependent and neurexin-independent functions in synapse validation. *EMBO J* 28: 3244-3255.

Koch AW, Bozic D, Pertz O, Engel J (1999). Homophilic adhesion by cadherins. *Curr Opin Struct Biol* 9: 275-281.

Koch AW, Farooq A, Shan W, Zeng L, Colman DR, Zhou MM (2004). Structure of the neural (N-) cadherin prodomain reveals a cadherin extracellular domain-like fold without adhesive characteristics. *Structure* 12: 793-805.

REFERENCES

Kochubey O, Majumdar A, Klingauf J (2006). Imaging clathrin dynamics in drosophila melanogaster hemocytes reveals a role for actin in vesicle fission. *Traffic* 7: 1614-1627.

Kolbeck R, Jungbluth S, Barde YA (1994). Characterization of neurotrophin dimmers and monomers. *Eur J Biochem* 225: 995-1003.

Kosik KS, Donahue CP, Israely I, Liu X, Ochiishi T (2005). Delta-catenin at the synaptic-adherens junction. *Trends Cell Biol* 15: 172-178.

Kostetskii I, Li J, Xiong Y, Zhou R, Ferrari VA, Patel VV, Molkentin JD, Radice GL (2005). Induced deletion of the N-cadherin gene in the heart leads to dissolution of the intercalated disc structure. *Circ Res* 96: 346-354.

Kristensen AS, Geballe MT, Snyder JP, Traynelis S (2006). Glutamate receptors: variation in structure-function coupling. *Trends Pharmacol Sci* 27: 65-69.

Kwon YW, Gurney ME (1996). Brain-derived neurotrophic factor transiently stabilizes silent synapses on developing neuromuscular junctions. *J Neurobiol* 29: 503-516.

Laemmli UK (1970). Cleavage of structural proteins during the assembly of the head of bacteriophage T4. *Nature* 227: 680-685.

Lai S, Chien AJ, Moon RT (2009). Wnt/fz signaling and the cytoskeleton: potential roles in tumorigenesis. *Cell Res* 19: 532-545.

Latefi NS, Pedraza L, Schohl A, Li Z, Ruthazer ES (2009). N-cadherin prodomain cleavage regulates synapse formation in vivo. *Dev Neurobiol* 69: 518-529.

Le Bé JV, Markram H (2006). Spontaneous and evoked synaptic rewiring in the neonatal neocortex. *Proc Natl Acad Sci* 103: 13214-13219.

Lee J, Duan W, Mattson MP (2002). Evidence that brain-derived neurotrophic factor is required for basal neurogenesis and mediates, in part, the enhancement of neurogenesis by dietary restriction in the hippocampus of adult mice. *J Neurochem* 82: 1367-1375.

Lee S, Lee B, Lee JW, Lee SK (2009). Retinoid signaling and neurogenin2 function are coupled for the specification of spinal motor neurons through a chromatin modifier CBP. *Neuron* 62: 641-654.

Leßmann V, Gottmann K, Heumann R (1994). BDNF and NT-4/5 enhance glutamatergic synaptic transmission in cultured hippocampal neurons. *Neuroreport* 6: 21-25.

Levine ES, Dreyfus CF, Black IB, Plummer MR (1995). Brain-derived neurotrophic factor rapisly enhances synaptic transmission in hippocampal neurons via postsynaptic tyrosine kinase receptors. *Proc Natl Acad Sci* 92: 8074-8078.

Levinson JN, Chéry N, Huang K, Wong TP, Gerrow K, Kang R, Prange O, Wang YT, El-Husseini A (2005). Neuroligins mediate excitatory and inhibitory synapse formation:

involvement of PSD-95 and neurexin-1 beta in neuroligin-induced synaptic specificity. *J Biol Chem* 280: 17312-17319.

Lewin GR, Barde YA (1996). Physiology of the neurotrophins. *Annu Rev Neurosci* 19: 289-317.

Lewis AK, Bridgman PC (1992). Nerve growth cone lamellipodia contain two populations of actin filaments that differ in organization and polarity. *J Cell Biol* 119: 1219-1243.

Li HS, Chen JH, Wu W, Fagaly T, Zhou L, Yuan W, Dupuis S, Jiang ZH, Nash W, Gick C, Ornitz DM, Wu JY, Rao Y (1999). Vertebrate slit, a secreted ligand for the transmembrane protein roundabout, is a repellent for olfactory bulb axons. *Cell* 96: 807-818.

Li YX, Yu X, Du J, Lester HA, Davidson N, Schuman EM (1998). Expression of a dominant negative TrkB receptor, T1, reveals a requirement for presynaptic signaling in BDFN-induced synaptic potentiation in cultured hippocampal neurons. *Proc Natl Acad Sci* 95: 10884-10889.

Li YX, Zhang Y, Lester HA, Schuman EM, Davidson N (1998). Enhancement of excitatory neurotransmitter release induced by BDNF in cultured hippocampal neurons. *J Neurosci* 18: 10231-10240.

Lichtman JW, Colman H (2000). Synapse elimination and indelible memory. *Neuron* 25: 269-278.

Lin DM, Fetter RD, Kopczynski C, Grenningloh G, Goodman CS (1994). Genetic analysis of Fasciclin II in drosophila: defasciculation, refasciculation and altered fasciculation. *Neuron* 13: 1055-1069.

Lisé MF, El-Husseini A (2006). The neuroligin and neurexin families: from structure to function at the synapse. *Cell Mol Life* Sci 63: 1833-1849.

Llinas R, Gruner JA, Sugimori M, McGuiness TL, Greengard P (1991). Regulation by synapsin I and Ca2+ -calmodulin-dependent protein kinase II of transmitter release in squid giant synapse. *J Physiol* 436: 257-282.

Lodge D, Johnson KM (1990). Noncompetitive excitatory amino acid receptor antagonists. *Trends Pharmacol Sci* 11:81-86.

Lonart G, Südhof TC (2000). Assembly of SNARE core complexes prior to neurotransmitter release sets the readily releasable pool of synaptic vesicles. *J Biol Chem* 275: 27703-27707.

Lu VB, Ballanyi K, Colmers WF, Smith PA (2007). Neuron type-specific effects of brain-derived neurotrophic factor in rat superficial dorsal horn and their relevance to □central sensitization□. *J Physiol* 548: 543-563.

Lübke J, Markram H, Frotscher M, Sakmann B (1997). Frequency and dendritic distribution of autapses established by layer 5 pyramidal neurons in the developing rat neocortex: Comparison with synaptic innervation of adjacent neurons of the same class. *J Neurosci* 16: 3209-3218.

REFERENCES

Nagar B, Overduin M, Ikura M, Rini JM (1996). Structural basis of calcium-induced E-cadherin rigidification and dimerization. *Nature* 380: 360-364.

Nam CI, Chen L (2010). Postsynaptic assembly induced by neurexin-neuroligin interaction and neurotransmitter. *Proc Natl Acad Sci* 102: 6137-6142.

Niethammer M, Kim E, Sheng M (1996). Interaction between the C terminus of NMDA receptor subunits and multiple members of the PSD-95 family of membrane-associated guanylate kinases. *J Neurosci* 16: 2157-2163.

Nuriya M, Huganir RL (2006). Regulation of AMPA receptor trafficking by N-cadherin. *J Neurochem* 97: 652-661.

Ma YT, Hsieh T, Forbes ME, Johnson JE, Frost DO (1998). BDNF injected into the superior colliculus reduces developmental retinal ganglion cell death. *J Neurosci* 18: 2097-2107.

Maisonpierre PC, Belluscio L, Friedman B, Alderson RF, Wiegand SJ, Furth ME, Lindsay RM, Yancopoulos GD (1990). NT-3, BDNF and NGF in the developing rat nervous system: parallel as well as reciprocal patterns of expression. *Neuron* 5: 501-509.

Malenka RC, Nicoll RA (1993). NMDA receptor-dependent synaptic plasticity: multiple forms and mechanisms. *Trends Neurosci* 16: 521-527.

Malenka RC, Nicoll RA (1997). Silent synapses speak up. *Neuron*: 19: 473-476.

Malmivou J, Plonsey R (1995). Bioelectromagnetism. *New York Oxford University Press*.

Martelli AM, Baldini G, Tabellini G, Koticha D, Bareggi R, Baldini G (2000). Rab3A and Rab 3D control the total granule number and the fraction of granules docked at the plasma membrane in PC12 cells. *Traffic* 1: 976-986.

Marty S, Wehrlé R, Sotelo C (2000). Neuronal activity and brain-derived neurotrophic factor regulate the density of inhibitory synapses in organotypic slice cultures of postnatal hippocampus. *J Neurosci* 20: 8087-8095.

McBain C, Dingledine R (1992). Dual-component miniature excitatory synaptic currents in rat hippocampal CA3 pyramidal neurons. *J Neurophysiol* 68: 16-27.

McBain CJ, Mayer ML (1994). N-methyl-D-aspartic acid receptor structure and function. *Physiol Rev* 74: 723-760.

Missler M, Fernandez-Chacon R, Südhof TC (1998). The making of neurexins. *J Neurochem* 71: 1339-1347.

Miyatani S, Shimamura K, Hatta M, Nagafuchi A, Nose A, Matsunaga M, Hatta K, Takeichi M (1989). Neural cadherin: role in selective cell-cell adhesion. *Science* 245: 631-635.

Monyer H, Sprengel R, Schoepfer R, Herb A, Higuchi M, Lomeli H, Burnashev N, Sakman B, Seeburg PH (1992). Heteromeric NMDA receptors: molecular and functional dictinction of subtypes. *Science* 256: 1217-1221.

REFERENCES

Moore R, Radice GL, Dominis M, Kemler R (1999). The generation and in vivo differentiation of murine embryonal stem cells genetically null for either N-cadherin or N-and P-cadherin. *Int J Dev Biol* 43: 831-834.

Morales M, Colicos MA, Goda Y (2000). Actin-dependent regulation of neurotransmitter release at central synapses. *Neuron* 27: 539-550.

Mukherjee K, Sharma M, Urlaub H, Bourenkov GP, Jahn R, Südhof TC, Wahl MC (2008). CASK functions as a Mg^{2+}- independent neurexin kinase. *Cell* 133: 328-339.

Murase S, Mosser E, Schumann EM (2002). Depolarization drives beta-catenin into neuronal spines promoting changes in synaptic structure and function. *Neuron* 35: 91-105.

Nakanishi S (1994). Metabotropic glutamate receptors: synaptic transmission, modulation, and plasticity. *Neuron* 13: 1031-37.

Niessen CM, Yap AS (2006). Another Job for the talented p120-catenin. *Cell* 127: 875-877.

Nimnual AS, Taylor LJ, Bar-Sagi D (2003). Redox-dependent downreulation of Rho by Rac. *Nat Cell Biol* 5: 236-241.

Noren NK, Arthur WT, Burridge K (2003). Cadherin engagement inhibits RhoA via p190RhoGAP. *J Biol Chem* 278: 13615-13618.

Nose A, Tsuji K, Takeichi M (1990). Localization of specificity determining sites in cadherin cell adhesion molecules. *Cell* 61: 147-155.

Nuriya M, Huganir RL (2006). Regulation of AMPA receptor trafficking by N-cadherin. *J Neurochem* 97: 652-661.

Obst-Pernberg K, Medina L, Redies C (2001). Expression of R-cadherin and N-cadherin by cell groups and fiber tracts in the developing mouse forebrain: relation to the formation of functional circuits. *Neuroscience* 3: 505-533.

Ochiishi T, Futai K, Okamoto K, Kameyama K, Kosik KS (2008). Regulation of AMPA receptor trafficking by δ-catenin. *Mol Cell Neurosci* 39: 499-507.

Ohkubo T, Ozawa M (1999). p120(ctn) binds to the membrane-proximal region of the E-cadherin cytoplasmatic domain and is involved in modulation of adhesion activity. *J Biol Chem* 274: 21409-21415.

Okamoto K, Nagai T, Miyawaki A, Hayashi Y (2004). Rapid and persistent modulation of actin dynamics regulates postsynaptic reorganization underlying bidirectional plasticity. *Nat Neurosci* 7: 1104-1112.

O`Leary DDM, Koester SE (1993). Development of projection neuron types, axon pathways and patterned connections of the mammalian cortex. *Neuron* 10: 991-1006.

Ozawa M, Kemler R (1990). Correct proteolytic cleavage is required for the cell adhesive function of uvomorulin. *J Cell Biol* 111: 1645-1650.

REFERENCES

Patel MR, Shen K (2009). RSY-1 is a local inhibitor of presynaptic assembly in C. elegans. *Science* 323: 1500-1503.

Patel SD, Chen CP, Bahna F, Honig B, Shapiro L (2003). Cadherin-mediated cell-cell adhesion: sticking together as a family. *Curr Opin Struct Biol* 13: 690-698.

Patel SD, Ciatto C, Chen CP, Bahna F, Rajebhosale M, Arkus N, Schieren I, Jessel TM, Honig B, Price SR, Shapiro L (2006). Type II cadherin ectodomain structures: implications for classical cadherin specificity. *Cell* 124: 1255-1268.

Pennuto M, Bonanomi D, Benfenati F, Valtorta F (2003). Synaptophysin I controls the targeting of VAMP2/Synaptobrevin II to synaptic vesicles. *Mol Biol Cell* 14:4909-4919.

Pertz O, Bozic D, Koch AW, Fauser C, Brancaccio A, Engel J (1999). A new crystal structure, Ca^{2+} dependence and mutational analysis reveal molecular details of E-cadherin homoassociation. *EMBO* J 18: 1738-1747.

Pfrieger FW, Barres BA (1997). Synaptic efficacy enhanced by glial cells in vitro. *Science* 277: 1684-1687.

Pieribone VA, Shupliakov O, Brodin L, Hilfiker-Rothenfluh S, Czernik AJ, Greengard P (1995). Distinct pools of synaptic vesicles in neurotransmitter release. *Nature* 8: 493-497.

Poskanzer K, Needleman LA, Bozdagi O, Huntley GW (2003). N-cadherin regulates ingrowth and laminar targeting of thalamocortical axons. *J Neurosci* 23: 2294-2305.

Poon VY, Klassen MP, Shen K (2008). UNC-6/netrin and its receptor UNC-5 locally exclude presynaptic components from dendrites. *Nature Lett* 455: 669-674.

Prakasam AK, Maruthamuthu V, Leckband DE (2006). Similarities between heterophilic and homophilic cadherin adhesion. *Proc Natl Acad Sci* 103: 15434-15439.

Prakash S, Caldwell JC, Eberl DF, Clandinin TR (2005). Drosophila N-cadherin mediates an attractive interaction between photoreceptor axons and their targets. *Nat Neurosci* 8: 443-450.

Prange O, Wong TP, Gerrow K, Wang YT, El-Husseini A (2004). A balance between excitatory and inhibitory synapses is controlled by PSD-95 and neuroligin. *Proc Natl Acad Sci* 101: 13915-13920.

Pyle JL, Kavalali ET, Piedras-Renteria ES, Tsien RW (2000). Rapid reuse of readily releasable pool vesicles at hippocampal synapses. *Neuron* 28: 221-231.

Radice GL, Rayburn H, Matsunami H, Knudsen KA, Takeichi M, Hynes RO (1997). Developmental defects in mouse embryos lacking N-cadherin. *Dev Biol* 181: 64-78.

Radziejewski C, Robinson RC, DiStefano PS, Taylor JW (1992). Dimeric structure and conformational stability of brain-derived neurotrophic factor and neurotrophin-3. *Biochemistry* 31: 4431-4436.

REFERENCES

Redies C, Takeichi M (1993). Expression of N-cadherin mRNA during development of the mouse brain. *Dev Dyn* 197: 26-39.

Redies C, Engelhardt K, Takeichi M (1993). Differential expression of N- and R-cadherin in functional neuronal systems and other structures of the devolping chicken brain. *J Comp Neurol* 333: 398-416.

Reichardt LF (2006). Neurotrophin-regulated signaling pathways. *Phil Trans R Soc B* 361: 1545-1564.

Reynolds AB, Carnahan RH (2004). Regulation of cadherin stability and turnover by p120ctn: implications in disease and cancer. *Semin Call Dev Biol* 15: 657-663.

Reynolds AB (2007). p120-catenin: past and present. *Biochim Biophys Acta* 1173: 2-7.

Riehl R, Johnson K, Bradley R, Grunwald GB, Cornel E, Lilienbaum A, Holt CE (1996). Cadherin function is required for axon outgrowth in retinal ganglion cells in vivo. *Neuron* 17: 873-848.

Rizo J, Südhof TC (2002). SNAREs and munc18 in synaptic vesicle fusion. *Nat Rev Neurosci* 3: 641-653.

Rizzoli SO, Betz WJ (2005). Synaptic vesicle pools. *Nat Rev Neurosci* 6: 57-69.

Rodriguez-Tebar A, Dechant G, Barde YA (1990). Binding of brain-derived neurotrophic factor to the nerve growth factor receptor. *Neuron* 4: 487-492.

Rose CR, Blum R, Pichler B, Lepier A, Kafitz KW, Konnerth A (2003). Truncated TrkB-T1 mediates neurotrophin-evoked calcium signaling in glia cells. *Nature* 426: 74-78.

Rosenmund C, Rettig J, Brose N (2003). Molecular mechanisms of active zone function. *Curr Opin in Neurobiol* 13: 1-11.

Ryan TA, Smith SJ (1995). Vesicle pool mobilization during action potential firing at hippocampal synapses. *Neuron* 14: 983-989.

Sabatini BL, Regehr WG (1999). Timing of synaptic transmission. *Annu Rev Physiol* 61: 521-542.

Sabo SL, McAllister AK (2003). Mobility and cycling of synaptic protein-containing vesicles in axonal growth cone filopodia. *Nat Neurosci* 6: 1264-1269.

Saglietti L, Dequidt C, Kamieniarz K, Rousset MC, Valnegri P, Thoumine O, Beretta F, Fagni L, Choquet D, Sala C, Sheng M, Passafaro M (2007). Extracellular interactions between GluR2 and N-cadherin in spine regulation. *Neuron* 54: 461-477.

Sakaba T, Neher E (2003). Involvement of actin polymerization in vesicle recruitment at the calyx of Held synapse. *J Neurosci* 23: 837-846.

REFERENCES

Sambrook J, Russell DW (2000). Molecular cloning: a laboratory manual. *CSHL Press*

Sanes JR, Yamagata M (2009). Many paths to synaptic specificity. *Annu Rev Cell Dev Biol* 25: 161-195.

Sankaranarayanan S, Atluri PP, Ryan TA (2003). Actin has a molecular scaffolding, not propulsive, role in presynaptic function. *Nat Neurosci* 6: 127-135.

Sanson MSP, Usherwood PNR (1990). Single channel studies of glutamate receptors. *Int Rev Neurobiol* 32: 51-106.

Sara Y, Virmani T, Deák F, Liu X, Kavalali T (2005). An isolated pool of vesicles recycles at rest and drive spontaneous neurotransmission. *Neuron* 45: 563-573.

Schaefer AW, Kabir N, Forscher P (2002). Filopodia and actin arcs guide the assembly and transport oft wo populations of microtubules with unique dynamic parameters in neuronal growth cones. *J Cell Biol* 158: 139-152.

Scheiffele P, Fan J, Choih J, Fetter R, Serafini T (2000). Neuroligin expressed in nonneuronal cells triggers presynaptic development in contacting axons. *Cell* 101: 657-669.

Schikorski T, Stevens CF (1997). Quantitative ultrastructural analysis of hippocampal excitatory synapses. *J Neurosci* 17 : 5858-5867.

Schikorski T, Stevens CF (2001). Morphological correlates of functionally defined synaptic vesicle populations. *Nat Neurosci* 4: 391-395.

Schneggenburger R, Neher E (2000). Intracellular calcium dependence of transmitter release rates at a fast central synapse. *Nature* 406: 889-893.

Schnell E, Sizemore M, Karimzadegan S, Chen L Bredt DS, Nicoll RA (2002). Direct interactions between PSD-95 and stargazin control synapstic AMPA receptor number, *Proc Natl Acad Sci* 99: 13902-13907.

Schoepp DD, Jane DE, Monn JA (1999). Pharmalogical agents acting at subtypes of metabotropic glutamate receptors. *Neuropharmacology* 38: 1431-1476.

Schrage K, Koopmans G, Joosten EAJ, Mey J (2006). Macrophages and neurons are targets of retinoic acid siganling after spinal cord contusion injury. *Eur J Neurosci* 23: 285-295.

Schubert M, Holland ND, Escriva H, Holland LZ, Laudet V (2004). Retinoic acid influences anteroposterior positioning of epidermal sensory neurons and their gene expression in a developing chordate (amphioxus). *Proc Natl Acad Sci* 101: 10320-10325.

Schuman EM (1999). Neurotrophin regulation of synaptic transmission. *Curr Opin Neurobiol* 9: 105-109.

Schuster CM, Davis GW, Fetter RD, Goodman CS (1996). Genetic dissection of structural and functional components of synaptic plasticity.I. Fasciclin II controls synaptic stabilization and growth. *Neuron* 17: 641-654.

[154]

REFERENCES

Sebeo J, Hsiao K, Bozdagi O, Dumitriu D, Ge Y, Zhou Q, Benson DL (2009). Requirement for protein synthesis at developing synapses. *J Neurosci* 29: 9778-9993.

Shan W, Yagita Y, Wang Z, Koch A, Fex Svenningsen A, Gruzglin E, Pedraza L, Colman DR (2004). The minimal essential unit for cadherin-mediated intercellular adhesion comprises extracellular domains 1 and 2. *J Biol Chem* 279: 55914-55923.

Shan WS, Tanaka H, Phillips GR, Arndt K, Yoshida M, Colman DR, Shapiro L (2000). Functional cis-heterodimers of N- and R-cadherins. *J Cell Biol* 148: 579-590.

Shelton DL, Sutherland J, Gripp J, Camerato T, Armanini MP, Phillips HS, Carroll K, Spencer SD, Levinson AD (1995). Human trks: molecular cloning, tissue distribution and expression of extracellular domain immunoadhesins. *J Neurosci* 15: 477-491.

Shupliakov O, Bloom O, Gustafsson JS, Kjaerulff O, Low P, Tomilin N, Pieribone VA, Greengard P, Brodin L (2002). Impaired recycling of synaptic vesicles after acute perturbation of the presynaptic actin cytoskeleton. *Proc Natl Acad Sci 99:* 14476-14481.

Siechen S, Yang S, Chiba A, Saif T (2009). Mechanical tension contributes to clustering of neurotransmitter vesicles at presynaptic terminals. *Proc Natl Acad Sci* 106: 12611-12616.

Siegenthaler JA, Ashique AM, Zarbalis K, Patterson KP, Hecht JH, Kane MA, Folias AE, Choe Y, May SR, Kume T, Napoli JL, Peterson AS, Pleasure SJ (2009). Retinoic acid from the meninges regulates cortical neuron generation. *Cell* 139: 597-609.

Silver RA, Lübke J, Sakmann B, Feldmeyer D (2003). High-probability uniquantal transmission at excitatory synapses in barrel cortex. *Science* 302: 1981-1984.

Silverman, Restituito S, Lu W, Lee-Edwards L, Khatri L, Ziff EB (2007). Synaptic anchorage of AMPA receptors by cadherins through neural plakophilin-related arm protein-AMPA receptor-binding protein complexes. *J Neurosci* 27: 8505-8516.

Song JY, Ichtchenko K, Südhof TC, Brose N (1999). Neuroligin I is a postsynaptically cell-adhesion molecule of excitatory synapses. *Proc Natl Acad Sci* 96: 1100-1105.

Song HJ, Poo MM (1999). Signal transduction underlying growth cone guidance by diffusible factors. *Curr Opin Neurobiol* 9: 355-363.

Song L, Gelmann EP (2005). Interaction of β-catenin and TIF2/GRIP1 in transcriptional activation by the androgen receptor. *J Biol Chem* 280: 37853-37867.

Srivastava S, Osten P, Vilim FS, Khatri L, Inman G, States B, Daly C, DeSouza S, Abagyan R, VAltschanoff JG, Weinberg RJ, Ziff EB (1998). Novel anchorage of GluR2/3 to the postsynaptic density by the AMPA receptor-binding protein ABP. *Neuron* 21: 581-591.

Stan A, Pielarski KN, Brigadski T, Wittenmayer N, Federochenko O, Gohla A, Leßmann V, Dresbach T, Gottmann K (2010). Essential cooperation of N-cadherin and neuroligin I in the transsynaptic control of vesicle accumulation. *Proc Natl Acad Sci* 107: 11116-11121.

REFERENCES

Stappert J, Kemler R (1994). A short core region of E-cadherin is essential for catenin binding and is highly phosphorylated. *Cell Adhes Commun* 2: 319-327.

Stein V, House DR, Bredt DS, Nicoll RA (2003). Postsynaptic density-95 mimics and occludes hippocampal long-term potentiation and enhances lomg-term depression. *J Neurosci* 23: 5503-5506.

Stevens B, Allen NJ, Vazquez LE, Howell GR, Christopherson KS, Nouri N, Micheva KD, Mehalow AK, Huberman AD, Stafford B, Sher A, Litke AM, Lambris JD, Smith SJ, John SWM, Barres BA (2007). The classical complement cascade mediates CNS synapse elimination. *Cell* 131: 1164-1178.

Stevens CF, Williams JH (2000). "Kiss and run" exocytosis at hippocampal synapses. *Proc Natl Acad Sci USA* 97: 12828-12833.

Stevens HE, Smith KM, Maragnoli ME, Fagel D, Borok E, Shanabrough M, Horvath TL, Vaccarino FM (2010). FGFR2 is required for the development of the medial prefrontal cortex and its connections with limbic circuits. *J Neurosci* 30: 5590-5602.

Strübing C, Ahnert-Hilger G, Shan J, Wiedenmann B, Hescheler J, Wobus AM (1995). Differentiation of pluripotent embryonic stem cells into the neuronal lineage in vitro gives rise to mature inhibitory and excitatory neurons. *Mech Dev* 53: 275-287.

Sucher NJ, Akbarian S, Chi CL, Leclerc CL, Awobuluyi M, Deitcher DL, Wu MK, Yuan JP, Jones EG, Lipton SA (1995). Developmental and regional expression pattern of a novel NMDA receptor-like subunit (NMDAR-L) in the rodent brain. *J Neurosci* 15: 6509-6520.

Sucher NJ, Awobuluyi M, Choi YB, Lipton SA (1996). NMDA receptors: from genes to channels. *Trends Pharmacol Sci* 17: 348-355.

Südhof TC (1995). The synaptic vesicle cycle: a cascade of protein-protein interactions. *Nature* 375: 645-653.

Südhof TC (2000). The synaptic vesicle revisited. *Neuron* 28: 317-320.

Südhof TC (2004). The synaptic vesicle cycle. *Annu Rev Neurosci* 27; 509-547.

Südhof TC (2008). Neuroligins and neurexins link synaptic function to cognitive disease. *Nature* 455: 903-911.

Tada T, Sheng M (2006). Molecular mechanisms of dendrite spine morphogenesis. *Curr Opin Neurobiol* 16: 95-101.

Tai CY, Mysore SP, Chiu C, Schuman EM (2007). Activity-regulated N-cadherin endocytosis. *Neuron* 54: 771-785.

Takeishi M (1990). Cadherins: a molecular family important in selective cell-cell adhesion. *Annu Rev Biochem* 59: 237-252.

REFERENCES

Tamás G, Buhl EH, Somogyi P (1997). Massive autaptic self-innervation of GABAergic neurons in cat visual cortex. *J Neurosci* 17: 6352-6364.

Tan ZJ, Peng Y, Song HL, Zheng JJ, Yu X (2010). N-cadherin dependent neuron-neuron interaction is required for the maintenance of activity-induced dendrite growth. *Proc Natl Acad Sci* 107: 9873-9878.

Tanaka E, Sabry J (1995). Making the connection: cytoskeletal rearrangements during growth cone guidance. *Cell* 83: 171-176.

Tanaka H, Shan W, Phillips GR, Arndt K, Bozdagi O, Shapiro L, Huntley GW, Benson DL, Colman DR (2000). Molecular modification of N-cadherin in response to synaptic activity. *Neuron* 25: 93-107.

Tang L, Hung CP, Schuman EM (1998). A role for the cadherin family of cell adhesion molecules in hippocampal long-term potentiation. *Neuron* 20: 1165-1175.

Tao X, Finkbeiner S, Arnold DB, Shaywitz AJ, Greenberg ME (1998). Ca^{2+} influx regulates BDNF transcription by a CREB family transcription factor-dependent mechanism. *Neuron* 20: 709-726.

Tao X, West AE, Chen WG, Corfas G, Greenberg ME (2002). A calcium-responsive transcription factor, CaRF, that regulates neuronal activity-dependent expression of BDNF. *Neuron* 33: 383-395.

Tarsa L, Goda Y (2002). Synaptophysin regulates activity-dependent synapse formation in cultured hippocampal neurons. *Proc Natl Acad Sci* 99: 1012-1016.

Taulet N, Comunalse F, Fayard C, Charrasse S, Bodin S, Gauthier-Rouvière C (2009). N-cadherin/p120-catenin association at cell-cell contacts occurs in cholesterol-rich membrane domains and is required for RhoA activation and myogenesis. *J Biol Chem* 284: 23137-23145.

Tessier-Lavigne M, Goodman CS (1996). The molecular biology of axon guidance. *Science* 274: 1123-1133.

Thoreson MA, Anastasiadis PZ, Daniel JM, Ireton RC, Wheelock MJ, Johnson KR, Hummingbird DK, Reynolds AB (2000). Selective uncoupling of p120(ctn) from E-cadherin disrupts strong adhesion. *J Cell Biol* 148: 189-202.

Thoumine O, Lambert M, Mège RM, Chouquet D (2006). Regulation of N-cadherin dynamics at neuronal contacts by ligand binding and cytoskeletal coupling. *Mol Biol Cell* 17: 862-875.

Tissir F, Qu Y, Montcouquiol M, Zhou L, Komat K, Shi D, Fujimori T, Labeau J, Tyteca D, Courtoy P, Poumay Y, Uemura T, Goffinet AM (2010). *Nat Neurosci* 13: 700-707.

Togashi H, Abe K, Mizoguchi A, Takaoka K, Chisaka O, Takeichi M (2002). Cadherin regulates dendritic spine morphogenesis. *Neuron* 35: 77-89.

REFERENCES

Tomás J, Santafé MM, Lanuza MA, Garcia N, Besalduch N, Tomás M (2010). *J Neurosci* advance of print.

Tomschy A, Fauser C, Landwehr R, Engel J (1996). Homophilic adhesion of E-cadherin occurs by a cooperative two-step interaction of n-terminal domains. *EMBO* J 15: 3507-3514.

Trachtenberg JT, Chen BE, Knott GW, Feng G, Sanes JR, Welker E, Svoboda K (2002). Long-term in vivo imaging of experience-dependent synaptic plasticity in adult cortex. *Nature* 420: 788-794.

Tuttle R, O`Leary, DDM (1998). Neurotrophins rapidly modulate growth cone response to the axon guidance molecule collapsing-1. *Mol Cell Neurobiol* 11: 1-8.

Ubach J, Zhang X, Shao X, Südhof TC, Rizo J (1998). Ca^{2+} binding to synaptotagmin: how many Ca^{2+}-ions bind to the tip of a C2-domain? *Embo J* 17: 3921-3930.

Uchida N, Honjo Y, Johnson KR, Wheelock MJ, Takeichi M (1998). The catenin/cadherin adhesion system is localized in synaptic junctions bordering transmitter release zones. *J Cell Biol* 135: 767-779.

Uemura K, Kitagawa N, Kohno R, Kuzuya A, Kageyama T, Chonabayashi K, Shibasaki H, Shimohama S (2003). Presenilin 1 is involved in maturation and trafficking of N-cadherin to the plasma membrane. J Neurosci Res 74: 184-191.

Uemura K, Kihara T, Kuzuya A, Okawa K, Nishimoto T, Ninomiva H, Sugimoto H, Kinoshita A, Shimohama S (2006). Characterization of sequential N-cadherin cleavage by ADAM10 and PS1. *Neurosci Lett* 402: 278-283.

Varoqueaux F, Jamain S, Brose N (2004). Neuroligin 2 is exclusively localized to inhibitory synapses. *Eur J Cell Biol* 83: 449-456.

Varoqueaux F, Aramuni G, Rawson RL, Mohrmann R, Missler M, Gottmann K, Zhang W, Südhof TC, Brose N (2006). Neuroligins determine synapse maturation and function. *Neuron* 51: 741-754.

Vesa J, Kruttgen A, Shooter EM (2000).p75 reduces TrkB tyrosine autophosphorylation in response to brain-derived neurotrophic factor and neurotrophin 4/5. *J Biol Chem* 275: 24414-24420.

Vicario-Abejon C, Collin C, McKay RDG, Segal M (1998). Neurotrophins induce formation of functional excitatory and inhibitory synapses between cultured hippocampal neurons. *J Neurosci* 18: 7256-7271.

Voronin LL, Cherubini E (2004). □Deaf, mute and whispering□ silent synapses: their role in synaptic plasticity. *J Physiol* 557: 3-12.

Waites CL, Craig AM, Garner CC (2005). Mechanisms of vertebrate synaptogenesis. *Annu Rev Neurosci* 28: 251-274.

REFERENCES

Wang KH, Brose K, Arnott D, Kidd T, Goodman CS, Henzel W, Tessier-Lavigne M (1999). Biochemical purification of a mammalian slit protein as a positive regulator of sensory axon elongation and branching. *Cell* 96:771-784

Wang XH, Poo M (1997). Potentiation of developing synapses by postsynaptic release of neurotrophin-4. *Neuron* 19: 825-835.

Wakeham DE, Ybe JA, Brodsky FM, Hwang PK (2000). Molecular structures of proteins involved in vesicle coat formation. *Traffic* 1: 393.

Washbourne P, Bennett JE, McAllister AK (2002). Rapid recruitment of NMDA receptor transport packages to nascent synapses. *Nat Neurosci* 5: 751-759.

Washbourne P, Dityatev A, Scheiffele P, Biederer T, Weiner JA, Christopherson KS, El-Husseini A (2004). Cell adhesion molecules in synapse formation. *J Neurosci* 24: 9244-9249.

Watkins JC, Pook PC, Sunter DC, Davies J, Honore T (1990). Experiments with kainite and quisqualate agonists and antagonists in relation to the sub-classification on □non-NMDA□ receptors. *Adv Exp med Biol* 268: 49-55.

Watkins JC, Jane DE (2006). The glutamate story. *Br J Pharmacol* 147: 100-108.

Whiteheart SW, Rossnagel K, Buhrow SA, Brunner M, Jaenicke R, Rothman JE (1994). N-ethylmaleimide-sensitive fusion protein: a trimeric ATPase whose hydrolysis of ATP is required for membrane fusion. *J Cell Biol* 126: 945-954.

Wildenberg GA, Dohn MR, Carnahan RH, Davis MA, Lobdell NA, Settleman J, Reynolds AB (2006). P120-catenin and p190GAP regulate cell-cell adhesion by coordinating antagonism between Rac and Rho. *Cell* 127: 1027-1039.

Williams EJ, Williams G, Gour B, Blaschuk O, Doherty P (2000). INP, a novel N-cadherin antagonist targeted to the amino acids that flank the HAV motif. *Molecular Cell Neurosci* 15: 456-464.

Wittenmayer N, Körber C, Liu H, Kremer T, Varoqueaux F, Chapman ER, Brose N, Kuner T, Dresbach T (2009). Postsynaptic neuroligin I regulates presynaptic maturation. *Proc Natl Acad Sci* 106: 13564-13569.

Wolfel M, Schneggenburger R (2003). Presynaptic capacitance measurements and Ca^{2+} uncaging reveal submilisecond exocytosis kinetics and characterize the Ca^{2+} sensitivity of vesicle pool depletion at a fast CNS synapse. *J Neurosci* 23: 7059-7068.

Wong JT, Yu WT, O`Connor TP (1997). Transmembrane grasshopper Semaphorin I promotes axon outgrowth in vivo. *Development* 124: 3597-3607.

Xu G, Craig AW, Greer P, Miller M, Anastasiadis PZ, Lilien J, Balsamo J (2004). Continous association of cadherin with β-catenin requires the non-receptor tyrosine-kinase Fer. *J Cell Sci* 117: 3207-3219.

REFERENCES

Yang B, Steegmaier M, Gonzalez LC Jr, Scheller RH (2000). nSec1 binds a closed conformation of syntaxin1A. *J Cell Biol* 148(2): 247-52.

Yamada S, Pokutta S, Drees F, Weis WI, Nelson WJ (2005). Deconstructing the cadherin-catenin-actin complex. *Cell* 123: 889-901.

Yamagata M, Sanes JR, Weiner JA (2003). Synaptic adhesion molecules. *Curr Opin Cell Biol* 15: 621-632.

Yamashita T, Tucker KL, Barde YA (1999). Neurotrophin binding to the p75 receptor modulates Rho activity and axonal outgrowth. *Neuron* 24: 585-593.

Yang J, Siao C, Nagappan G, Marinic T, Jing D, McGrath K, Chen Z, Mark W, Tessarollo L, Lee FS, Lu B, Hempstead BL (2009). Neuronal release of proBDNF. *Nat Neurosci* 12: 113-115.

Zhai RG, Vardinon-Friedman H, Cases-Langhoff C, Becker C, Gundelfinger ED, Ziv NE, Garner CC (2001). Assembling the presynaptic active zone: a characterization of an active one precursor vesicle. *Neuron* 29: 131-143.

Zhou S, Sousa R, Tannery HN, Lafer EM (1992). Characterization of a novel synapse-specific protein. II. cDNA cloning and sequence analysis of the F1-20 protein. *J Neurosci* 12: 2144-2155.

Zhou XF, Rush RA (1996). Endogenous brain-derived neurotrophic factor is anterogradely transported in primary sensory neurons. *Neuroscience* 74: 945-951.

Zito K, Knott G, Shepard GM, Shenolikar S, Svoboda K (2004). Induction of spine growth and synapse formation by regulation of the spine actin cytoskeleton. *Neuron* 44: 321-334.

Ziv NE, Garner CG (2004). Cellular and molecular mechanisms of presynaptic assembly. *Nat Rev Neurosci* 5: 385-399.

Zhou L, Qu Y, Tissir F, Goffinet AM (2009). Role of atypical cadherin Celsr3 during development of the internal capsule. *Cereb Cortex* 19:114-119.

Zoubine MN, Ma JY, Smirnova IV, Citron BA, Festoff BW (1996). A molecular mechanism for synapse elimination: novel inhibition of locally generated thrombin delays synapse loss in neonatal mouse muscle. *Dev Biol* 179: 447-457.

6. Appendix

6.1 Abbreviations

ABP	AMPA receptor-binding protein
Ag	silver
AMPA	α-amino-3-hydroxy-5-methylisoxazol-4-propionacid
ARAC	Cytosin-β-D-arabinofuranosid-hydrochloride
APS	Ammoniumpersulfat
ATP	Adenosine triphosphate
BCA	Bicinchoninic acid
BDNF	Brain-derived neurotrophic factor
BME-medium	Basal medium eagle
BSA	Bovine serum albumine
(X) °C	(X) degree Celsius
Ca^{2+}	Calcium
CAM	Cell adhesion molecule
CaM kinase II	Calcium-calmodulin-dependent proteinkinase II
cAMP	Cyclic adenosine monophosphate
CASK	Calcium/calmodulin-dependent serine protein kinase
CNR	Cadherin-related neuronal receptors
CNS	Central nervous system
CO_2	Carbon dioxide
Cu^{2+}	Copper
DCC-receptor	Deleted-in-colorectal-cancer
DIV	Day in vitro
DMEM	Dulbecco's Modified Eagle's Medium
DMSO	Dimethyl sulfoxide
DNaseI	Desoxyribonuclease I
DNQX	6,7-dinitroquinoxalin-2,3-dion
DsRed	Discosoma sp. red fluorescent protein
E(X)	Embryonic day (X)
EBs	Embryoid bodies
EBSS medium	Earle's balanced salts solution
EC	Extracellular domain
EDTA	Ethylenediamine-tetraacetic acid
EF cells	Embryonic feeder cells
EGTA	Ethylenbis(oxyethylen-nitrilo-)tetraaceticacid
EGFP	Enhanced green fluorescent protein
EPSP	Excitatory postsynaptic potential
ES cells	Embryonic stem cells
F-actin	Filament actin
FCS	Fetal calf serum

APPENDIX

FGF	Fibroblast growth factor
FGFR	Fibroblast growth factor receptors
fz	Frizzled
G-Protein	Guanosinnukeotid-dependent protein
GABA	γ-aminobutanoic acid
GCM	Gli-conditioned medium
GDP	Guanosine diphosphate
GRIA	Glutamate receptor, ionotropic, AMPA
GRIK	Glutamate receptor, ionotropic, kainate
GRIN	Glutamate receptor, ionotropic, N-methyl D-aspartate
GRIP	Glutamate receptor interacting protein
GRM	Glutamate receptor, metabotropic
GTP	Guanosine triphosphate
HEPES	N-2-hydroxyethylpiperazin-N`-2-ethansulfonacid
HSV tk	Herpes simplex virus thymidine kinase
IP3	Inositol-1,4,5-trisphosphate
IPSP	Inhibitory postsynaptic potential
IR	Infrared
K^+	Potassium
kDa	Kilodalton
LB-media	Luria-Bertani media
LIF	Leukemia inhibitory factor
LTD	Long-term depression
LTP	Long-term potentiation
MAGUK	Membrane-associated guanylate kinase
Mg^{2+}	Magnesium
MEM	Minimal essential medium
MK801	Dizocilpine
mESC	Miniature postsynaptic excitatory current
MOCA	Modifier of cell adhesion
n	Number of experiments
Na^+	Sodium
NB-medium	Neurobasal medium
Ncad+/-	N-cadherin heterozygous deletion mutant
Ncad-/-	N-cadherin homozygous deletion mutant
Ncad-flox	N-cadherin floxed mutants
N-CAM	Neural cell adhesion molecule
Neo-casette	Neomycin phosphotransferase expression cassette
NGF	Nerve growth factor
NMDA	N-methyl D-aspartate
NP-40	Nonidet P-40; Igepal
NPRAP	Neural plakophilin-related armprotein
NTF	Neurotrophins
NT	Neurotrophin

[162]

NSF	Soluble N-ethylmaleimide-sensitive-factor
op-amp	Operational amplifier
OTK	Tyrosine-protein kinase-like otk, off-track
P(X)	Postnatal day (X)
PAGE	Polyacrylamide gel electrophorese
PBS	Phosphate buffered saline
PDZ	PSD-95-discs large-zona occludens-1
PKC	Protein kinase C
PO	Poly-L-Ornithine
PSD	Postsynaptic density
PSD-95	Postsynaptic density protein-95
PSF	Point-spread function
PTB	Protein-tyrosine phosphatase
RRP	Readily releasable pool
RIMs	Rab3 interacting molecules
RIPA	Radioimmunoprecipitation assay buffer
scr peptide	Scrambled peptide
SDS	Sodium dodecyl sulfate
SDS	Sodium dodecyl sulfate
SEM	Standard error of means
SNAP	Soluble N-ethylmaleimide-sensitive-factor-attachment-protein
SNAP-25	Soluble N-ethylmaleimide-sensitive-factor-attachment-protein 25
SNARE	Soluble N-ethylmaleimide-sensitive-factor-attachment-protein-receptor-complex
SR-media	Serum replacement media
S-SCAM	Synaptic scaffolding molecule
SV	Synaptic vesicle
SynGAP	Synaptic GTPase activating protein
TARP	Transmembrane AMPA receptor regulatory proteins
TBS-T	Tris-Buffered Saline Tween-20
TEA	Tetraethylammoniumchloride
TEMED	Tetramethylethylendiamin
TRIS	Tris(hydroxymethyl)-aminomethan
TTX	Tetrodotoxin
UV	Ultraviolet
V	Volt
VAMP	Vesicle-associated membrane protein
v-SNARE	vesicle-SNARE

6.2 List of figures

[163]

6.3 Curriculum vitae

Name: Kim Nadine Pielarski

Date of birth: 16.04.1980

Place of birth: Essen, Germany

Marital status: unmarried

2006-2010   PhD at the Institute of Neuro- and Sensory Physiology, University of Düsseldorf

05.2006-10.2006   Research assistant at the Institute of Neuro- and Sensory Physiology, University of Düsseldorf

2006   Graduation as "Diplom-Biologin"; Grade: 1,3

2005-2006   Diploma thesis at the Institute of Neuro- and Sensory Physiology, University of Düsseldorf

1999-2005   Studies of Biology at the University of Düsseldorf

1990-1999   Städtisches Gymnasium Wülfrath

1986-1990   Gemeinschaftsgrundschule Tönisheide, Velbert

6.4 Publications and conferences attended

Pielarski KN, Jüngling K, Gottmann K (article in preparation)

Stan A, Pielarski KN, Brigadski T, Wittenmayer N, Federochenko O, Gohla A, Leßmann V, Dresbach T, Gottmann K (2010). Essential cooperation of N-cadherin and neuroligin I in the transsynaptic control of vesicle accumulation. *Proc Natl Acad Sci* 107: 11116-11121.

Pielarski KN, Jüngling K, Gottmannn K (2008). Impairment of glutamatergic synaptic transmission upon selective postsynaptic expression of N-cadherin. *6th FENS Forum of European Neuroscience Geneva, Switzerland, 2008.*

Pielarski KN, Jüngling K, Gottmann K (2008). Asymmetric expression of N-cadherin impairs glutamatergic synaptic transmission. *87th Annual Meeting of the DPG Köln, Germany, 2008.*

APPENDIX

Pielarski KN, Frank M, Gottmann K (2007). Analysis of γ-protocadherin-deficient synapses in neocortical neurons. *7th NWG meeting of the German Neuroscience society Göttingen, Germany.*

Pielarski KN, Frank M, Gottmann K (2006). Electrophysiological characterization of synapses in γ-protocadherin-deficient neocortical neurons. *5th FENS Forum of European Neuroscience Vienna, Austria, 2006.*

7. Acknowledgements